REGULATION OF SPERM MOTILITY BY CELL – SIGNALLING EVENTS IN HUMAN SPERM

By

COSMAS ACHIKANU EZEKAIBEYA

A thesis submitted to
The University of Birmingham
For the degree of
DOCTOR OF PHILOSOPHY

School of Biosciences
The University of Birmingham
August 2017

ABSTRACT

Ca^{2+} signals from activated Ca^{2+} channels (CatSper) and mobilisation of Ca^{2+} stores regulate human sperm cell behaviour as they ascend the female tract. I investigated the effects on human sperm $[Ca^{2+}]_i$ and behaviour of CatSper channel activation (alkaline pH and progesterone) and Ca^{2+}-store mobilisation (4-aminopyridine, thimerosal) using a fluorescence plate reader and CASA. Extracellular alkalinisation raised pH_i (pHi = 6.9 and 7.2 at pHo7.4 and 8.5 respectively), caused tonic elevation of $[Ca^{2+}]_i$, which was partially inhibited by CatSper block and increased the proportion of hyperactivated cells (from 1.8±0.5 to 10.5±1.6%; n=34, $P=1x10^{-7}$). Progesterone elevated $[Ca^{2+}]_i$ but caused negligible hyperactivation. Co-application of these stimuli revealed little, if any, synergistic interaction. Ca^{2+}-store mobilisation (4-aminopyridine) caused prolonged $[Ca^{2+}]_i$ elevation and was associated with strong hyperactivation. Analysis of $[Ca^{2+}]_i$ and hyperactivation data from 24 different conditions in this study showed a continuous relationship between $[Ca^{2+}]_i$ and hyperactivation. The strong hyperactivating effect of store mobilisation (compared to CatSper activation) may reflect opening of store-operated channels. Human sperm behaviour assessed over a 180 s recording revealed regular 'switching' between progressive and various hyperactivated types. Mobilisation of Ca^{2+} stores potently increased hyperactivated behaviour and suppressed the rate of behavioural switching.

ACKNOWLEDGEMENTS

My enormous hearty gratitude goes to my supervisor, Dr. S.J. Publicover for his unconditional support, valuable guidance, research and character skills that made this thesis possible. I would like to thank Joao of the Cairn research for his technical support during the research work. My thanks go to Timo Strunker of University Hospital Munster, centre for Reproductive Medicine and Andrology, Munster, Germany for providing a novel CatSper inhibitor.

I would also like to thank the donors who provided the samples, which were essential to carry out my research. I would also like to thank School of Biosciences, University of Birmingham for opening their doors and providing resources for continuing the project.

I really appreciate the friendship and support i received from members of our research group and colleagues in the 8th floor, School of Biosciences particularly Elis Nitao, Sarah Costello (Post doc with Steve), Sanjana Pillay, Susane Wijesinghe, Diaa Al-Raawi, Maiss Al-Amere and Rhian Jones. I would also like to heartily thank members of Rhema Faith Church in Birmingham for their loving care to me, particularly my bible study group. Most importantly, I would like to especially thank my wife, Norah Achikanu for permitting me to do this PhD study and standing through for me at home. I would also thank my children Somto, Amara, Chinwem and Eze for their patience with me as they had the 'feeling of my absence' during my study. I am most grateful to members of Lively Seed Assembly in Nigeria for their support to my family. I would also like to thank the administration of Enugu State University of Science and Technology, Enugu, Nigeria for their cooperation during my PhD studies. Thanks to the federal government of Nigeria for three years financial support during my PhD studies.

TABLE OF CONTENTS

LIST OF FIGURES

CHAPTER 1

CHAPTER 2

CHAPTER 3

CHAPTER 4

CHAPTER 5

CHAPTER 6

CHAPTER 7

LIST OF TABLES

LIST OF ABBREVIATIONS

5'AMP	5'adenosine monophosphate
ATP	Adenosine monophosphate
ABHD2	Alpha/beta hydrolase domain containing protein 2
ADA	N-(2-acetamido) iminodiacetic acid
AKAPs	A-kinase anchor proteins
ALH	Amplitude of lateral head displacement
4AP	4-aminopyridine
AR720-F1	Novel catSper inhibitor
ATP	Adenosine triphosphate
AM	Acetoxymethyl
BCECF-AM	2'7'-bis-(2-carboxyethyl)-5-(and-6-)-carboxyfluorescein acetoxymethyl ester
BCF	Beat frequency
BSA	Bovine serum albumin
Ca^{2+}	Calcium ions
$[Ca^{2+}]_i$	Intracellular calcium concentration
Cav	Calcium voltage channel
CABYR	Calcium binding protein
$CaCl.2H_2O$	Calcium chloride dihydrate
cADPR	Cyclic adenosine diphosphate receptor

CaM	Calmodulin
CaMK 11	Calmodulin kinase 11
cAMP	Cyclic adenosine monophosphate
CASA	Computer aided semen analysis
CatSper	Sperm specific cation channel
CatSper β,γ,δ	Auxillary subunits of catsper
CCE	Capacitative Ca^{2+} entry
CD38	Adenine dinucleotide phosphoribosyl cyclase
CICR	Calcium induce calcium release
Cl-	Chloride ion
DMSO	Dimethyl sulfoxide
DNA	Deoxyribonucleic acid
F	Frequency
F_t	Fluorescence intensity at time t
F_{basal}	Mean fluorescence in absence of drug
Fluo-3	1-[2-amino-5-(2,7-dichlooro-6-hydroxy-3-oxy-9-xanthenyl)phenoxyl]-2-(2-amino-5-methylphenoxy) ethane-N,N,N',N'-tetraaceticacid ammonium potassium salt

Fluo4-AM	Glycine,N-[4-[6-[(acetyloxy)methoxy]-2,7difluoro-3-oxo3h-xanthen-9-yl]-2-[2-[2-bis[2-[(acetyloxy)methoxy]-2-oxoethyl]amino]-5-methylphenoxy]ethoxy]phenyl]-N-[2-(acetyloxy)methoxy]-2-oxoethyl](acetyloxy)methyl ester
FF	Follicular fluid
Fura2-AM	5-oxazolecarboxylicacid,2-6-(bis(2-((acetyloxy)methoxy)-2-oxoethyl)amino)-5-methylphenoxy)ethoxy)-2-benzofuranyl)-,(acetyloxy)methyl ester
GPCR	G-protein coupled receptor
H^+	Proton ion channel
HCl	Hydrochloric acid
HCO_3^-	Bicarbonate ion
HEPES	4-(2-hydroxyethyl)-1-piperazineethanesulfonic acid
hFF	Human follicular fluid

Hv1	Proton channel 1
HVA	High voltage-activated channel
HYP7	Hyperactivation sort 7
IAM	Inner acrosomal membrane
IP_3R	Inositol triphosphate
K^+	Potassium ion
KCl	Potassium chloride
Kd	Dissociation constant
KSper	Sperm specific potassium ion channel
LIN	Linearity
LVA	Low voltage-activated channel
MAPKs	Mitogen-activated protein kinases
$MgSO_4 .7H_2O$	Magnesium sulphate heptahydrate
mOsm	Milliosmolarity
mM	Millimolar
Na^+	Sodium ion
NAADP	Nicotinic acid-adenine dinucleotide phosphate
NBC	Sodium bicarbonate exchanger
Na^+- Ca^{2+}	Sodium-calcium ion exchangers
NaCl	Sodium chloride

$NaHCO_3$	Sodium bicarbonate
NaH_2PO_4	Sodium dihydrogen phosphate
NaOH	Sodium hydroxide
Na^+/H^+	Sodium/proton exchanger
Na^+/HCO_3^-	Sodium/bicarbonate ion exchanger
NH_4Cl	Ammonium chloride
nM	Nanomolar
NNC55-0396	Catsper inhibitor
NS	Non- significant
Orai 1	Protein channel
OAM	Outer acrosomal membrane
p	Probability
P4	Progesterone
pHi	Intracellular pH
pHo	pH outside cell
PDE	Phosphodiesterase
PIP_2	Phosphoinositol 4,5-bis phosphate
PKA	Protein kinase A
PTP	Protein tyrosine phosphorylation
PM	Plasma membrane
PMCA4	Plasma membrane calcium –ATPase pump

R^2	Correlation
r-hCG	Recombinant human chorionic gonadotropin
RNE	Redundant nuclear envelope
R_{tot}	Overall mean fluorescence intensity
RyR	Ryanodine receptor
sAC	Soluble adenylyl cyclase
sEBSS	Supplemented Earle's balanced salt solution
SERCA	Sarcoplasmic endoplasmic Ca^{2+} ATPase
Slo1	Voltage operated potassium ion channel
Slo3	Voltage operated potassium ion channel
sHNE	Sperm sodium proton ion exchanger
SOCE	Store operated channel
SPCA1	Secretary pathway Ca^{2+} -ATPase 1
STIM	Stromal interaction molecule
STR	Straightness
T	Period (minutes)

Tm	Thimerosal
TAPS	N-Tris(hydroxymethyl)methyl-3-amino propane sulfonic acid
tmAC	Transmembrane adenylyl cyclase
TPC	Two pore channel
TRPC	Transient receptor potential canonical
µM	Micromolar
VAP	Average path velocity
VCL	Curvilinear velocity
WOB	Wobble
ZP 1-4	Zona pellucida protein 1-4

CHAPTER 1: INTRODUCTION

1.1 Human sperm cell structure

Human spermatozoa are ≈60μm in length (Eisenbach, 1999). It is made up of the head, neck, mid piece and tail (Figure 1.1A). The nucleus carrying the male DNA is covered by nuclear membrane which, after nuclear condensation, extends into the neck as redundant nuclear envelope (Publicover et al., 2007). Anterior to the nucleus, at the apex of the sperm head is the acrosome, an organelle surrounded by an outer and inner membrane. Acrosomal exocytosis, which occurs adjacent to the zona pellucida of the oocyte, releases proteolytic enzymes from the acrosomal lumen and reveals proteins that are required for fusion with the oocyte (Johnson, 2007, Okabe, 2013, Buffone et al., 2014). At the equatorial segment are receptor molecules that enable the sperm to bind to the oocyte plasma membrane while the post acrosomal sheath bears signalling proteins that lead to activation of the oocyte and initiation of zygote development (Sutovsky, 2006). The head is joined to the mid-piece through a connecting piece made up of segmented columns and a dense fibrous structure (Mortimer, 1997, Sutovsky, 2006, Johnson, 2007). Mitochondria are present in the mid-piece as a mitochondrial sheath. These mitochondria are believed to contribute significantly to the supply of adenosine triphosphate (ATP) providing energy for movement of the tail (Sutovsky, 2006, Johnson, 2007, Publicover and Barratt, 2011b, Lishko et al., 2012). The annulus connects the mid-piece to the main part of the tail which is further divided into the principal piece and the end-piece.

Outer dense fibres, providing elasticity, run through the midpiece and principal piece. A protein-rich fibrous sheath is also present in the principal piece, which may provide shape and plane to the flagella beat (Turner, 2005, Freitas et al., 2017). The axoneme runs through the tail and it is made up of A and B subunits of 9 doublets of microtubules and 2 central microtubules connected by radial – spokes. Adjacent doublet microtubules are

joined by nexin an elastic linkage that regulates the peak and trough of flagella bending and permits the microtubules to move smoothly over each other. ATPase complex dynein arms on each of the outer doublets interact with neighbouring doublets to cause relative sliding of the microtubules, generating a wave to propagate along the flagellum (Figure 1.1B) (Mortimer, 1997, Mortimer, 2000, Eddy, 2007, Publicover and Barratt, 2011b). This movement is regulated by calcium ions in association with the central pair tubules and the radial spokes (Smith, 2002, Nakano, 2003). Calmodulin, a calcium sensor and downstream kinases are implicated in this regulation of motility (Smith, 2002, Nomura, 2004). Axoneme bending is also influenced by intracellular pH (Brokaw and Kamiya, 1987, Lishko et al., 2012). When the intracellular pH raises above 7 it promotes dynein activity and flagella beating (Suarez, 2008).

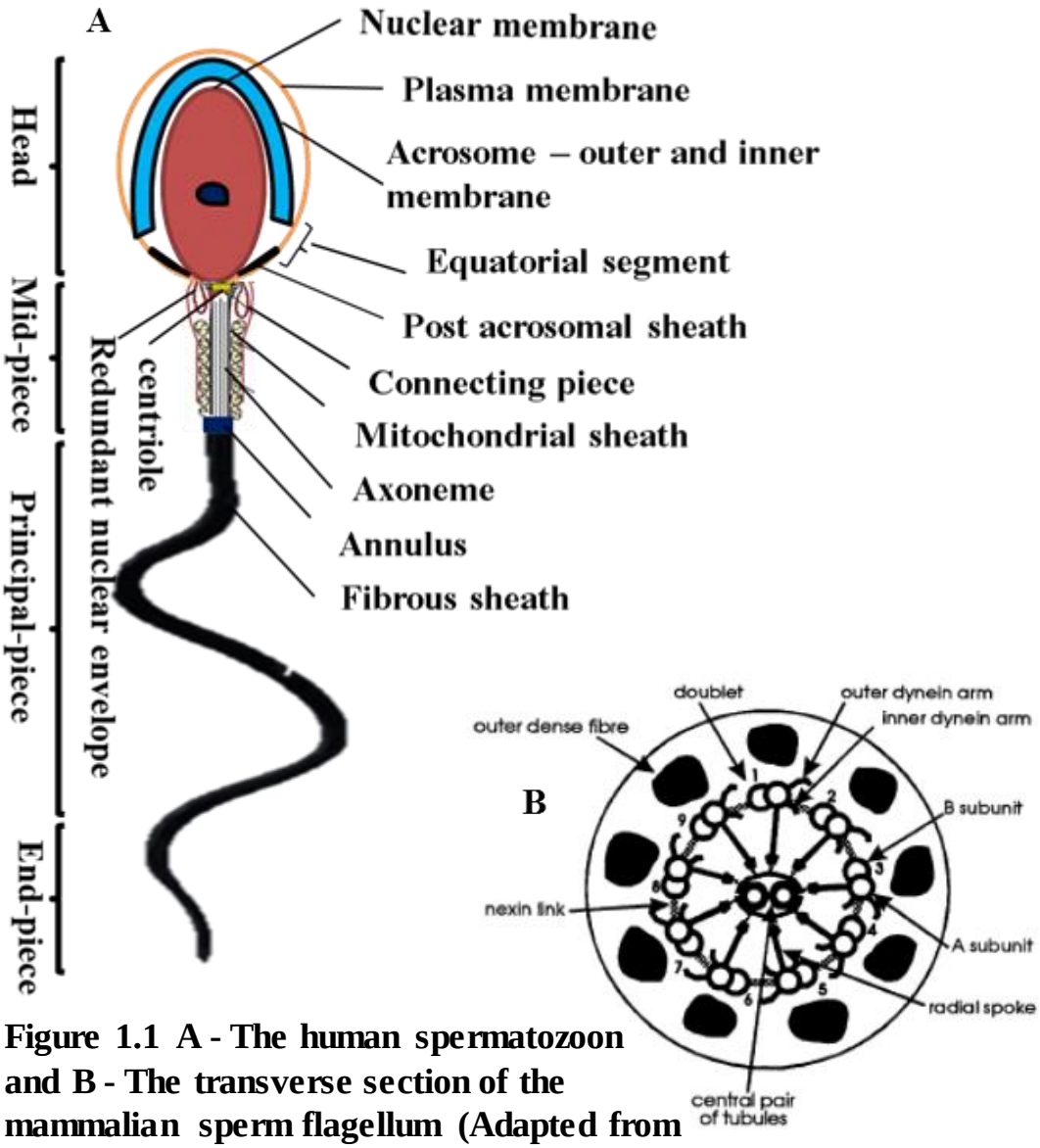

Figure 1.1 A - The human spermatozoon and B - The transverse section of the mammalian sperm flagellum (Adapted from Mortimer, 1997).

1.2 Spermatogenesis

The paired and ovoid shaped testes are made up of clusters of coiled seminiferous tubules, the epididymis and vas deferens as exit duct (Figure 1.2 A). The seminiferous tubule is the site for sperm production. Stem cells (typeA spermatogonia) adjacent to the basement membrane of the tubule undergo mitosis to maintain cell number in spermatogenesis, which is regulated by hypothalamic hormones (Starr, 2012, Sherwood, 2013). Some

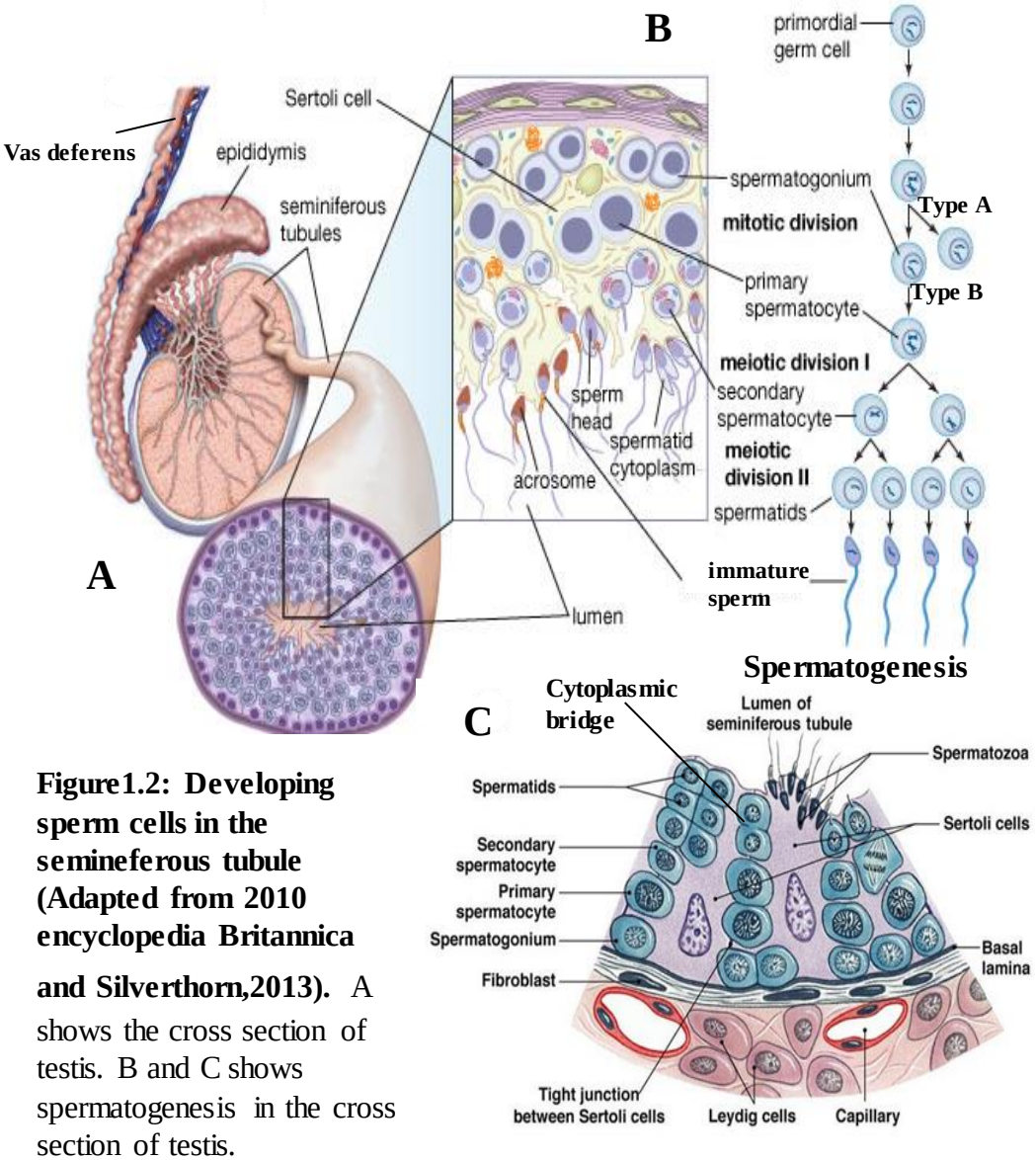

Figure1.2: Developing sperm cells in the semineferous tubule (Adapted from 2010 encyclopedia Britannica and Silverthorn,2013). A shows the cross section of testis. B and C shows spermatogenesis in the cross section of testis.

daughter cells (type B spermatogonia) then undergo mitotic division to produce primary spermatocytes. Primary spermatocytes then undergo meiosis to generate two secondary spermatocytes and subsequently four haploid spermatids (Sherwood, 2013, Silverthorn and Johnson, 2013) (Figure 1.2B). The sertoli cells provide nourishment for the developing sperm and produces hormones like inhibin, enzymes, growth factors and androgen binding protein, leydig cells produces testosterone while the spermatids are linked through the cytoplasmic bridges (Figure 1.2C). Spermiogenesis, which takes place near the tubule lumen, involves a change from round shape to elongated spermatid with definite sperm cell features including loss of cytoplasmic volume and organelle content (Sherwood, 2013). The spermatozoa which are functionally immatured when released into the lumen are carried along by the tubule fluid secreted by Sertoli cells into the epididymis for maturation (Johnson, 2007, Sutovsky, 2006, Cooper and Yeung, 2007). Maturation involves biochemical and physiologic processes that result in changes in the motility and morphology of the sperm preparing it for capacitation during transit in the female tract (Cooper, 2011, Sherwood, 2013, Varner, 2015, Freitas et al., 2017).

1.3 Oogenesis

In female gametogenesis, the germ cell oogonium undergoes mitotic divisions to increase in number and then begins the first step of meiosis (prophase 1) where the germ cell deoxyribonucleic acid (DNA) is duplicated to form the primary oocytes containing 92 chromosomes (Silverthorn and Johnson, 2013). All this happens in the newborn ovaries within the primordial follicle made up of the granulosa cells around the primary oocyte enclosed in a membrane (Starr, 2012). Several biochemical and structural changes are associated with the follicular growth which eventually leads to growth of the oocyte

(Johnson, 2007, Sherwood, 2013). The oocytes then arrest till attainment of puberty, after which some of these oocytes activate each other. Each activated oocyte divides to form a secondary oocyte and first polar body containing 46 chromosomes each. The polar body disintegrates, while each secondary oocyte begins meiosis II, which arrests at metaphase II. When the follicle ruptures in ovulation (by the action of protease enzymes), the fluid carries the cumulus-oocyte complex to the fallopian tubes for fertilisation by a sperm, which will released the oocyte from metaphase II arrest (Johnson, 2007, Sherwood, 2013) (Figure 1.3).

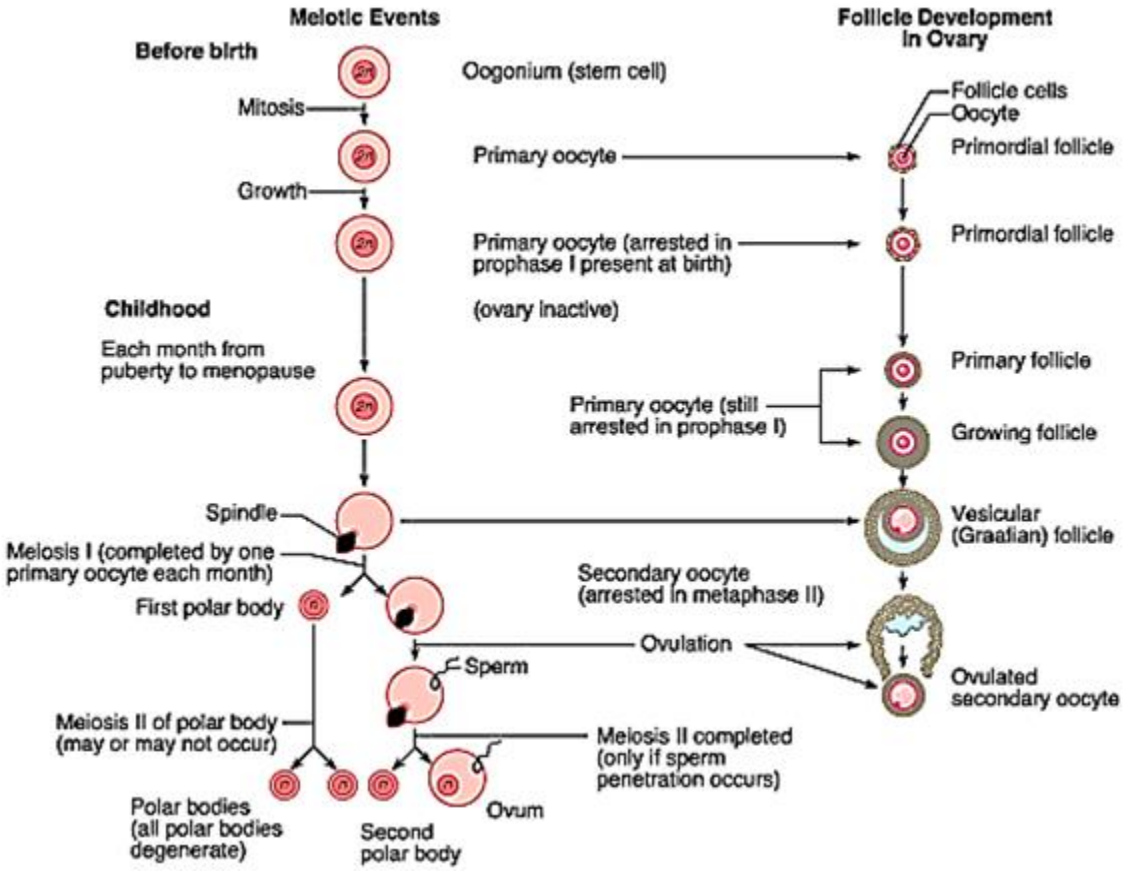

Figure 1.3: Developmental steps of the oogonium in the ovarian follicle (adapted from 2010 encyclopeadia Britannica).

1.4 Sperm transport in female tract

In the human about 2-5mls of semen (Johnson, 2007), which is sperm suspended in seminal plasma, is ejaculated into the female tract; the vagina in human and uterus in the mouse respectively (Eisenbach and Giojalas, 2006). The seminal fluid from the prostate and seminal vesicle provides mucus for lubrication, buffer to neutralise the acidic vaginal fluid, prostaglandins, fructose, citric acid, vitamin C, and carnitine as nutrients and protective chemicals like immunoglobin, lysozyme and antibacterial actions (Silverthorn and Johnson, 2013). Millions of human sperm cells deposited in the vagina have a difficult journey of about 120-160 mm to find and fuse with the egg in the fallopian tube (Eisenbach, 1999, Publicover et al., 2007). One out of the millions fertilise the oocyte and only a few hundred reaches the oviduct (Suarez and Pacey, 2006, Publicover et al., 2007). The progesterone-oestrogen controlled cervix secretes cervical mucous which 'filters' out weak sperm (Suarez and Pacey, 2006, Sherwood, 2013). The number further decreases to a few thousands due to the effect of leucocytes and on reaching the uterus-tubal junction they bind to the epithelium as a storage site (Suarez and Pacey, 2006, Johnson, 2007), waiting for ovulation. The sperm has 5-6 days viability in the female tract (Silverthorn and Johnson, 2013).

1.4.1 **Capacitation**

The idea of mammalian sperm capacitation was conceived in (1951) by Austin and Chang. Freshly ejaculated spermatozoa have activated motility but cannot fertilise the egg. However the sperm acquires the ability as it ascends the female tract by undergoing metabolic and physiological changes called capacitation (Mortimer, 1997). Functional changes that occur during capacitation include the ability to detect and follow a

chemotractant gradient, hyperactivation and ultimately release of the contents of the acrosome (, Kay and Robertson, 1998, Eisenbach and Giojalas, 2006, Publicover et al., 2007, Park et al., 2011, Aitken and Nixon, 2013). Capacitation requires cholesterol, bicarbonate ions and calcium ions and glucose may also be essential (Okabe, 2013). Events occurring in the sperm involve a range of biochemical/physiological processes including elevation of $[Ca^{2+}]_i$ and pH_i, cyclic adenosine monophosphate (cAMP) concentration, activation of protein kinase A, phosphatase activity and flux of K^+ and Cl^- (leading to hyperpolarised membrane potential) (Naz and Rajesh, 2004,Darszon et al., 2011,Chávez et al., 2014, Sati et al., 2014). Molecules absorbed or incorporated into the sperm during maturation in the epididymis may be removed or altered to enhance successful binding to the egg (Ickowicz et al., 2012). Sialidases catalyse the removal of sialic acid from the sperm glycocalyx coatings on the sperm head to enhance binding to the zona pellucida (Ma et al., 2012). In mouse and bovine sperm 20-40% of cells become synchronously capacitated (López-González et al., 2014) while in human sperm only 2-14% capacitate at a time with a duration of 50-240 minutes (Eisenbach, 1999). Only capacitated sperm cell can bind to zona pellucida (Dun et al., 2010). Recently it has been shown that treatment for 10 min with the calcium ionophor A23187 (followed by washing) imparts full fertilising capacity on mouse sperm, apparently circumventing the cyclic adenosine monophosphate- protein kinase- pathway (Tateno et al., 2013).

1.4.1.1 Molecular mechanisms of capacitation

Interplay of soluble adenylyl cyclase, CatSper and associated proteins (ion channels, pumps and exchangers) regulate the process of capacitation in the female tract (Darszon et al., 2011) (Figure 1.4). Exposure of the sperm to increased concentrations of bicarbonate $[HCO_3^-]$, and sodium $[Na^+]$ and decreased potassium $[K^+]$ in the seminal fluid and female

tract activates the sperm. The sodium/bicarbonate (Na^+/HCO_3^-) co –transporter facilitates influx of bicarbonate ions (Lishko et al., 2012, Chávez et al., 2014). This has a number of effects;

(i) activation of the soluble adenylyl cyclase enzyme that catalyses the synthesis of cAMP, a secondary messenger that activates protein kinase A for the phosphorylation of serine and threonine proteins and regulation of the influx of calcium ions (Visconti, 2009a, Darszon et al., 2011);

(ii) alteration of the plasma membrane phospholipids like phospatidylserine and phospatidylethanolamine through the enzyme scramblase (Darszon et al., 2011, Ickowicz et al., 2012, Aitken and Nixon, 2013);

(iii) increase in membrane fluidity which may increase permeability to Ca^{2+} (Aitken and Nixon, 2013);

(iv) increase of intracellular pH due to activity of the membrane sodium/proton (Na^+/H^+) exchanger and removal of zinc from the proton (H^+) channel Hv1 which facilitates H^+ efflux when the cell is in the alkaline environment of the female tract. This channel is lacking in mouse (Lishko et al., 2013, Chávez et al., 2014);

(v) opening of the sperm-specific cation voltage/agonist gated ion channel (CatSper) for influx of calcium ions (Gadella, 2006, Darszon et al., 2011, Ickowicz et al., 2012, Jin and Yang, 2016) into the cytoplasm and

(vi) hyperpolarisation of the membrane potential through activation of K^+ channels (Slo3 in mouse and Slo3 or Slo1 in humans) (Mannowetz et al., 2013, López-González et al., 2014, Mansell et al., 2014, Seifert et al., 2015). Membrane hyperpolarisation in mouse depends primarily on Slo3 (Chávez et al., 2014) and Slo3 null mice express impaired motility and inability to undergo acrosomal reactions (Santi et al., 2010).

Interaction may occur between a number of these physiological processes. For instance, Ca^{2+} influx through CatSper may cause membrane hyperpolarisation due to activation of K^+ channels and consequent K^+ efflux. Hyperpolarisation of the cell membrane may enhance the rise in intracellular pH by increasing the inward driving force for Na^+ thus increasing activity of the sodium/proton (Na^+/H^+) exchanger (Navarro et al., 2007, Chávez et al., 2014). Calcium inhibits the activity of the phosphodiesterase enzyme that breaks down cyclic adenosine monophosphate. These rapidly occurring and interacting physiological events are referred to as the fast signaling events in capacitation and may begin immediately upon exposure of the sperm to bicarbonate and increased extracellular pH (Lishko et al., 2012).

Cholesterol efflux from the membrane is enhanced by binding to serum albumin and this marks the onset of the slow events in capacitation (Visconti, 2009b, Ickowicz et al., 2012). The removal of cholesterol by albumin destabilises the plasma membrane of the sperm cell, increasing the membrane fluidity which enhances the permeability to bicarbonate (HCO_3^-) and Ca^{2+} through the Na^+/HCO_3^- co-transporter and the CatSper channels (Ren, 2010, Darszon et al., 2011), thus increasing their concentrations in the cytoplasm (Visconti, 2009a, Miller, 2015). A time dependent increase in tyrosine phosphorylation of proteins localised primarily to the flagellum is a major late event in capacitation and is associated with acquisition of hyperactivated motility and binding to the zona pellucida, oolemma binding and gamete fusion (Sati et al., 2014). Various events including the increased intracellular bicarbonate concentration mediate this tyrosine phosphorylation through cAMP regulated protein kinases that activates tyrosine kinases indirectly (Naz and Rajesh, 2004, Signorelli et al., 2012, Jin and Yang, 2016). Ion channels, enzymes and

calcium-binding protein (CABYR), a structural protein in the principal piece of human sperm were identified as tyrosine phosphorylated proteins (Ickowicz et al., 2012, Ijiri et al., 2012). The A- kinase anchoring proteins (AKAPs) the scaffold protein required for the organisation and intergrity of the fibrous sheath and the mitogen-activated protein kinases (MAPKs) are implicated in the tyrosine phosphorylation (Naz and Rajesh, 2004, Sutovsky, 2006, Sati et al., 2014).

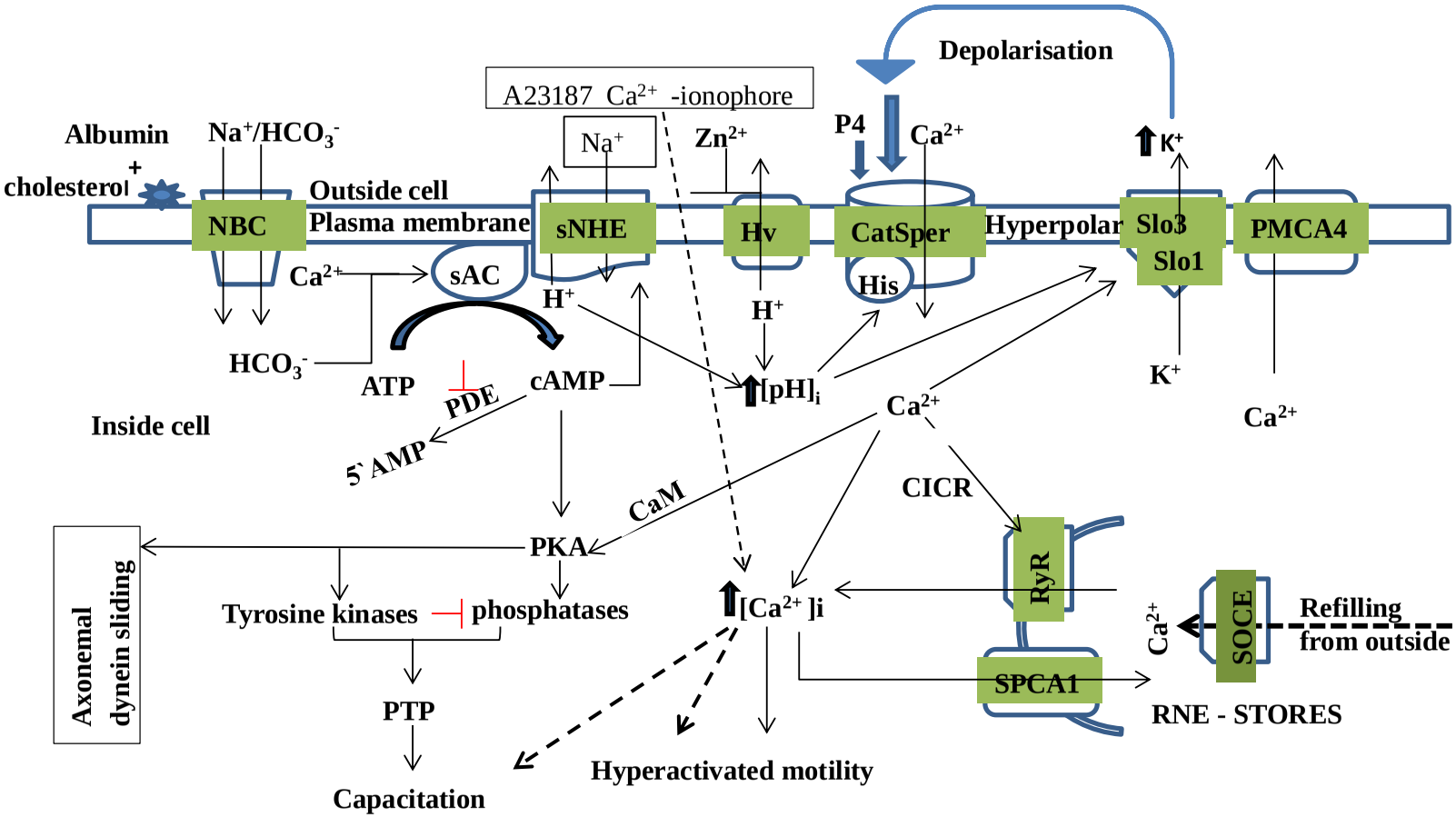

Figure 1.4 :Ca^{2+} signaling for capacitation and hyperactivated motility.
Inter play of several ion channels leading to capacitation via removal of cholesterol ,sAC/cAMP/PKA/tyrosine kinases and hyperactivation via sNHE/Hv/CatSper/slo3/slo1/ agonist/RyR inducing $[Ca^{2+}]_i$. Ca^{2+} ionophore induces capacitation and hyperactivation by increasing $[Ca^{2+}]_i$ only. NBC- sodium/bicarbonate channel, sAC- soluble adenylyl cyclase, cAMP- cyclic adenosine monophosphate, sNHE-sperm sodium/proton ion exchanger, H+ - proton ion channel, CatSper- sperm Ca^{2+} ion channel, Slo3/1-potassium ion channel, PMCA4 – Ca^{2+} ATPase, RyR – ryanodine receptor, SPCA1 – secretory pathway Ca^{2+} ATPase, RNE – redundant nuclear envelope in neck, CICR- calcium induce calcium release, CaM ─ axoneme Calmodulin, SOCE – store operated channel.

1.4.2 Sperm behaviour in the female tract

The human sperm must undergo activation to gain motility that will enable it swim in the female tract and this requires alkalinization of sperm. Upon contact with bicarbonate (HCO_3^-) ions in the seminal fluid and female tract, immotile sperm acquire flagellar movement that is symmetrical, low amplitude and high frequency. This normal swimming behaviour does not require elevated levels of $[Ca^{2+}]i$ and Ca^{2+} that enters the cytoplasm via the alkaline-activated CatSper channel is pumped out by the Ca^{2+}-ATPase (Lishko et al., 2012). Subsequently the sperm must develop hyperactivated motility that is essential for movement along the oviduct and penetration of the zona pellucida (Navarro et al., 2008, Freitas et al., 2017). The process of hyperactivation is believed to be Ca^{2+}-dependent and calaxin, a calcium sensing protein may regulate the activity of dynein motors in the axoneme causing high amplitude assymetric flagellar bendings (called hyperactivation) (Darszon et al., 2011, Mizuno et al., 2012). The patterns of sperm motility characterised *in vitro* include, activated/linear/progressive, hyperactivated-progressive (transitional) and hyperactivate non-progressive patterns (Figure 1.5) (Mortimer, 2000). The hyperactivated type is characterised by two distinct types of high curvature flagellar bending; extreme flagellar bending in the proximal mid piece not propagated that causes the head to produce hatchet- like motion and extreme reverse bending occurring more distally in the mid piece propagated along the flagellum resulting in figure of eight shape (Kay and Robertson, 1998, Mortimer, 2000).

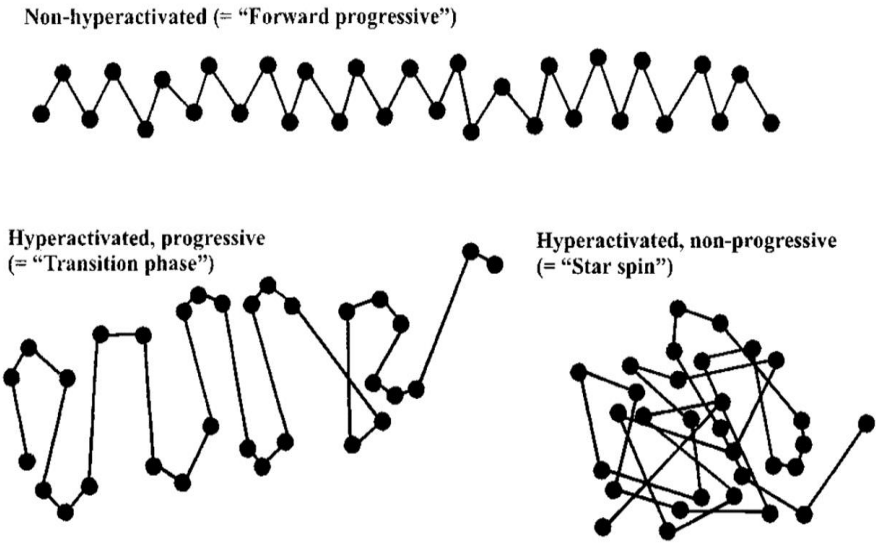

Figure 1.5 : Motility patterns of capacitated human spermatozoa (Adapted from (Mortimer, 2000).

A sub - population of capacitated sperm may show transitions between the low amplitude symmetrical beat pattern to a high amplitude asymmetrical thrashing of the sperm tail (Mortimer, 1997, Aitken and Nixon, 2013, Okabe, 2013). It has been proposed that the hyperactivated flagellar pattern is necessary to penetrate the mucus filled cervix, which thus acts as a filter allowing only the vigorously active cells to pass through (Suarez and Pacey, 2006). Hyperactivated motility is also apparently required for sperm to detach from the oviductal epithelium, escape the entrapment in the highly folded oviduct and penetrate the cumulus mass and zona pellucida surrounding the oocyte (Kay and Robertson, 1998, Suarez and Pacey, 2006, Darszon et al., 2011).

1.4.3 Chemotaxis

Only about 10% of sperm that reach the uterus go on to enter the oviduct (Eisenbach and Giojalas, 2006). In mammals it has been suggested that the ability of the sperm to locate the oocyte is dependent on one or more forms of taxis. Potential mechanisms include a temperature gradient (thermotaxis) towards the ampulla (Boryshpolets et al., 2015), swimming against fluid flow in the oviduct (rheotaxis), which has been demonstrated in sperm of mammals, though not clarified in humans (, Miki and Clapham, 2013, Sugiyama and Chandler, 2014) and following of a chemical gradient (chemotaxis) generated by the oocyte and/or its vestments (Sugiyama and Chandler, 2014). Chemoattractants may modulate the pattern of flagellar movement that guides the sperm to the oocyte (Eisenbach and Giojalas, 2006). Only capacitated sperm (2-12%) are chemoattractant responsive and progesterone, a steroid hormone synthesised by the cumulus mass and the egg, is believed to be a chemoattractant in the picomolar concentration range (Teves et al., 2006). Progesterone may activate chemotaxis through activation of Ca^{2+} channels and release of Ca^{2+} from stores or through a number of other mechanisms including phosphorylation of proteins via protein kinase A or protein kinase G (Teves et al., 2009).

1.4.4 Acrosomal reaction

The capacitated and hyperactivated sperm, on penetrating the viscous-elastic cumulus mass, reach the zona pellucida (ZP), the extracellular coat around the egg and bind to it through a receptor on the anterior region of the head. This induces the fusion of the outer acrosomal membrane with the plasma membrane in the apical region of the sperm head and the release of acrosomal vesicle contents (Publicover et al., 2007, Darszon et al., 2011,

Sosa et al., 2015). Acrosomal swelling is a prerequisite for acrosomal exocytosis. It is reported to be evoked by cAMP after the opening of store-operated calcium channels (Sosa et al., 2016). There are four zona pellucida glycoproteins (ZP 1 -4) in humans and three (ZP 1-3) in mouse respectively (Lefievre et al., 2004). Previously, Mouse ZP3 and human ZP1,3, & 4 were implicated in induction of acrosomal exocytosis as interactive sites (Gupta and Bhandari, 2011). Recently, the human ZP2 with the functional segment residing in the N – terminal region was reported as the site of interaction with the egg (Baibakov et al., 2012, Avella et al, 2015) and that the N – linked glycosylation rather than the ester-link is a requirement for ZP to induce acrosomal reaction (Gupta and Bhandari, 2011, Okabe, 2013, Chiu et al., 2014). However, (Jin et al,2011) reported that most mouse sperm acrosome reacted in the cumulus mass of the oocyte while (Hino et al., 2016) showed that they may have started acrosomal exocytosis before reaching the ampulla region of the oocyte. The acrosome releases proteolytic enzymes (including acrosin) that, in combination with the whiplash propulsion of the hyperactivated tail, enable the sperm to penetrate the zona pellucida (Cooper, 2007, Johnson, 2007, Okabe, 2013). In the perivitelline space between the zona pellucida and the oolemma, the acrosomal reacted sperm cell lies tangential to the oocyte surface for binding and fusion with the oocyte (Johnson, 2007, Okabe, 2013). In humans and mice a folate gylcophospatidylinositol anchored receptor on the egg called Juno was reported to interact with Izumo 1 on the male sperm head for fusion of the sperm and oocyte membranes (Satouh et al., 2012, Bianchi et al., 2014). Acrosomal reaction indicates the completion of capacitation (Okabe, 2013) (Figure 1.6).

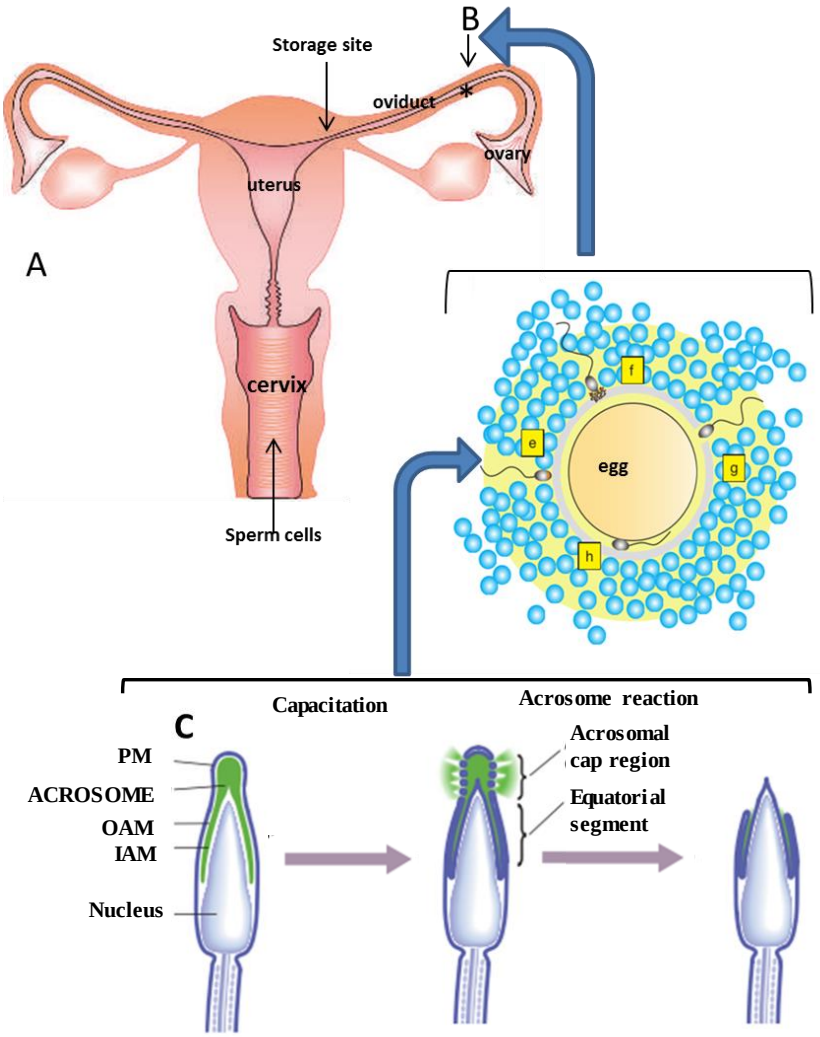

Figure1.6 : Human sperm transport in female tract.

A- the cervical mucus filters off weak sperm from millions deposited in the vagina to thousands. In the uterus leucocytes further decrease sperm number and hundreds are found in the fallopian tubes with only one fertilising the oocyte. Capacitation takes place along the tract. A storage site at the isthmus may temporarily keep the sperm attached to the epithelium waiting for ovulation, hyperactivation detaches them and they are believed to be attracted towards the egg as they swim through the gelatinous isthmus tube. At B, the high pH ampulla region, the sperm encounter the egg which is surrounded by the cumulus mass that produces progesterone in high µM concentration. The hyperactivated sperm swims through the cumulus mass and binds to the zona pellucida (ZP) (e) inducing acrosomal reaction (f) & C – release of the acrosome contents. Then sperm penetrates the ZP (g) and finally fuses with the egg through the izumo-juno sites of sperm & egg (h). PM – Plasmas membrane, OAM – Outer acrosomal membrane, IAM – Inner acrosomal membrane, (Adapted from Publicover et al., 2007 and Okabe 2013).

1.5 Intracellular pH and sperm function

Intracellular pH plays a central role in regulating sperm activities in vertebrates and invertebrates (Lishko et al., 2010, Lishko and Kirichok, 2010, Nishigaki et al., 2014, Varner, 2015, Zhou et al., 2015). Sperm ion channels like CatSper and potassium ion (Slo3) are opened by intracellular pH (Lishko et al., 2012, Nishigaki et al., 2014).

pHi of sperm cells is greatly dependent on the pH of the surrounding medium (pHo). At low epididymal pH (< 6.5) intracellular pH is acid and the axonemal dynein activity is inhibited, making the sperm quiescent (Lishko et al., 2010). The female vaginal pH increases from 4.3 to 7.2 in the presence of seminal plasma after intercourse, alkalinizing the environment and thus enabling spermatozoa to begin swimming. The intracellular (pHi) further rises as the sperm ascend the female reproductive tract but remains lower than pHo. At mid-cycle, when fertility is greatest in humans, the cervical mucus viscosity is lowest and pH increases to 9.0, producing a less stringent barrier to sperm (Lishko et al., 2012). The pH in the female tubular fluid is between 7 and 8 in mice (Navarro et al., 2008). In the rhesus monkey, the pH of oviduct lumen is reported to rise at the time of ovulation from pH 7.3 to pH 7.7 (Maas et al., 1977).

The ion transporters regulating intracellular pH in sperm are mainly the sodium/proton (Na^+/H^+) ion exchanger and the H_V1 proton (H^+) ion channel (Nishigaki et al., 2014). The Na^+/H^+ ion exchanger (sNHE) is sperm specific and of the SLC9C gene family subgroup (Wang et al., 2003). It is made up of 14 transmembrane segments, 4 of which are analogous to voltage-sensing helices of ion channels, and has a long cytoplasmic carboxyl terminus that includes a cyclic nucleotide binding sequence (Harayama, 2013, Nishigaki et al., 2014). sNHE1 was reported in humans and sNHE5 in rats (Woo et al., 2002).

Knockout of sNHE caused infertility in mice (Wang et al., 2003, Chávez et al., 2014). The voltage gated proton channel (H^+) is a homodimer with two proton permeable pores. The channel opens to depolarisation, extracellular proton concentration, the endocannabinoid and amandamide but inhibited by zinc ion (Lishko et al., 2010, DeCoursey, 2013). Both sNHE and H_V1 are localised in the principal piece of the flagellum.

Human and mouse sperm regulate their intracellular pH differently (Nishigaki et al., 2014). In mouse, the high external pH and the high concentration of bicarbonate ions in the female tract probably stimulates the first change in the intracellular pH. Membrane hyperpolarisation drives Na^+ influx that further increase the intracellular pH through the Na^+/H^+ exchanger (Chávez et al., 2014). The principal intracellular pHi ion channel in human is the proton channel (Hv1) which is opened by depolarisation (Lishko et al., 2010). When intracellular pHi increases, CatSper opens allowing influx of calcium ions which may cause hyperactivated motility (Lishko and Kirichok, 2010, Darszon et al., 2011). In sea Urchin, hyperpolarisation raises the intracellular pH through the sNHE mechanism and sNHE may be involved in controlling intracellular Ca^{2+} in humans (Chávez et al., 2014). Intracellular rise in pH is a basic requirement for the zona pellucida – induced acrosome reactions in mammal (Nishigaki et al., 2014).

1.6 Regulation of sperm motility

Both cAMP and Ca^{2+}-signalling pathways play important roles in regulation of motility in mammalian sperm and their signalling pathways interact (Freitas et al., 2017). In sperm cAMP is generated both by the soluble adenylyl cyclase (sAC) and G-protein coupled receptor -regulated transmembrane adenylyl cyclase (tmAC). tmAC is implicated in activating sperm motility through protein phosphorylation (Dey et al., 2014, Shiba and

Inaba, 2014, Teves et al., 2009) but it is likely that subsequent regulation of [cAMP] in the flagellum is achieved primarily through sAC. The fluid of the female reproductive tract is high in bicarbonate (HCO_3^-) ions which are transported into sperm during capacitation (see section 1.4.1.1). Bicarbonate and Ca^{2+} activate sAC which causes an increase in beat frequency (Hess et al., 2005, Xie et al., 2006). In mouse epididymal sperm application of bicarbonate induced Ca^{2+} entry and flagellar beat regulation, increasing frequency but decreasing asymmetry (Wennemuth et al., 2003). Male mice null for the sAC gene are infertile and their sperm lack forward motility (Esposito et al., 2004). sAC - mediated cAMP signalling activates a cascade of reactions through protein kinase A (PKA) found in the fibrous sheath of the principal piece of the sperm flagellum (Burton and McKnight, 2007). In human sperm, the A-kinase anchoring proteins (AKAP3 and AKAP4) are found in the fibrous sheath (Luconi et al., 2011). PKA regulates the frequency of the flagella beating and absence of the catalytic subunit in sperm cells makes them infertile (Skalhegg et al., 2002, Nolan et al., 2004). Addition of phosphate ions on proteins with serine/threonine residues are catalysed by PKA which in turn activates tyrosine kinases for the phosphorylation of amino acid tyrosine residues. Tyrosine phosphorylation is essentially associated with motility of sperm (Bajpai and Doncel, 2003, Burton and McKnight, 2007).

$[Ca^{2+}]_i$ signalling is central to regulation of motility. In demembranated bovine sperm, low $[Ca^{2+}]_i$ (10 – 40 nM) activates sperm motility and causes the sperm flagellum to beat symmetrically but at higher concentration of (100 – 300 nM) the angle of the flagella bending increases and more whip-like movements and more powerful swimming force are produced (Suarez, 2008). When the level of intracellular calcium rises above about 9μM, motility is suppressed and it may be associated with decreased phosphorylation events

(Pereira et al., 2017). Microtubule movement is dynein dependent and Ca^{2+} regulated (Brokaw, 1987, Smith, 2002). Calmodulin (CaM) is a calcium ion detector found in the mammalian sperm axoneme and may regulate sperm motility through protein kinases (including calmodulin kinase II (CaMKII) in mice and calmodulin kinase IV (CaMKIV) in human) and phosphatases (Marín-Briggiler et al., 2005, Schlingmann et al., 2007, Pereira et al., 2017).

pHi is reported to regulate the functions of sperm membrane ion transporters, thus contributing to the control of motility. Increasing the intracellular or extracellular pH enhances $[Ca^{2+}]i$ (Fraire-Zamora and Gonzalez-Martinez, 2004, Marquez and Suarez, 2007, Jin and Yang, 2016) – most likely by activating the sperm-specific Ca^{2+} channel CatSper (see section 1.7.1). CatSper activation and Ca^{2+} store mobilisation both modify sperm behaviour but produce different patterns of motility (Marquez and Suarez, 2007,Qi et al., 2007, Lefievre et al., 2012, Alasmari et al., 2013a). $[Ca^{2+}]_i$ release from the stores is shown to induce hyperactivation and can induce a response even in CatSper deficient sperm (Williams et al., 2015). Failure of Ca^{2+} regulation of sperm motility is implicated in male subfertility (Espino et al., 2009, Smith et al., 2013, Williams et al., 2015).

1.7 The sperm calcium-signalling tool

Compared to somatic cells, the sperm cell is structurally simple with a highly condensed nucleus, no endoplasmic reticulum and transcriptionally silent (Figure 1.7) (Baldi et al., 2002, Publicover et al., 2007). It modulates the functions of already existing proteins through actions of intracellular messengers (Costello et al., 2009, Correia et al., 2015, Freitas et al., 2017). However, (Miller and Ostermeier, 2006, Aquila and De Amicis, 2014) reported the presence of mRNA in mammalian sperm suggesting presence of protein synthesis machinery. Integration of different ion pumps and channels that transverse their plasma and intracellular membranes regulate changes in the $[Ca^{2+}]_i$ and relay discrete information between cells and the environment in cellular processes (Bedu-Addo, 2008) (Figure 1.7). Much of the regulation of sperm function that must occur in the female tract in order to fertilise the egg is controlled by changes in the cAMP, intracellular pHi, membrane voltage and $[Ca^{2+}]_i$ via ion pumps and transporters across the membrane (Darszon et al., 2011). Calcium signalling apparatus (the Ca^{2+} tool kit) found in the head, mid piece and flagellum regulate calcium concentration in the cytoplasm, thus regulating the functions of the sperm (Jimenez-Gonzalez et al., 2006, Ren, 2010, Miller, 2015,) (Figure 1.7A). At rest, calcium concentrations outside and inside the cell is 1-2 mM and 50-100 nM respectively. An increase in intracellular calcium concentration is required for the activation of functions of the spermatozoa expressed during capacitation, hyperactivation and acrosomal reaction (Lishko et al., 2012).

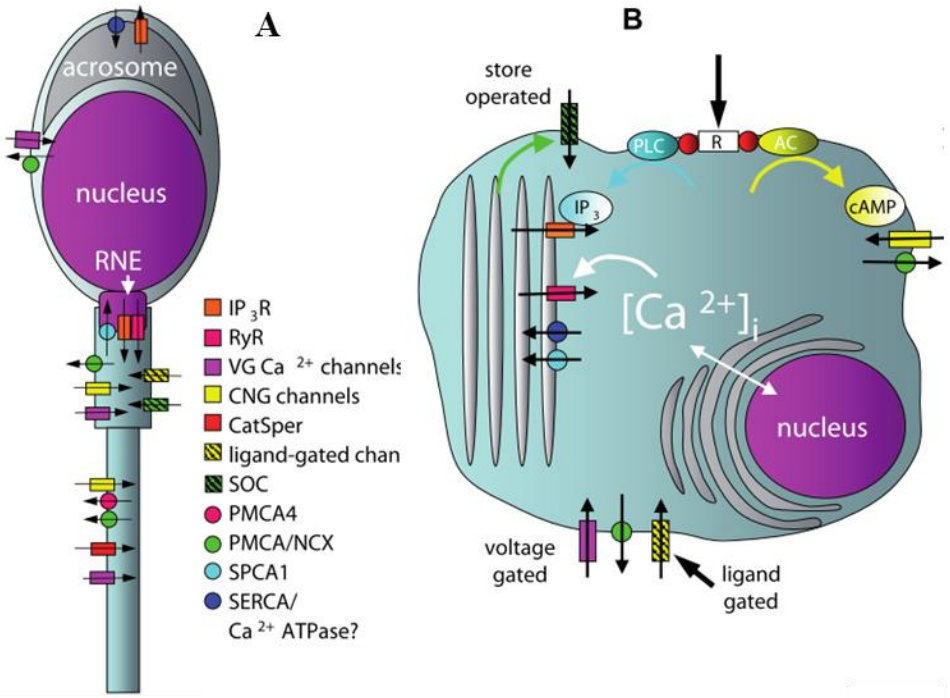

Figure 1.7: Calcium toolkits in somatic and sperm cell . (A) Sperm cell (B) Somatic cell (adapted from (Bedu-Addo, 2008).

1.7.1 Voltage operated calcium channels

The voltage operated calcium channels, which permit Ca^{2+} influx into the cell in response to membrane potential change are of two types; the high voltage activated (HVA) channels with L, N, P, Q and R subtypes that require strong depolarisation to open and the low voltage – activated channel (LVA) or T-type that opens to weaker depolarisation and

inactivate faster (Darszon et al., 2011). Though several Cav proteins were detected in sperm, their functional relevance has not been established (Ren, 2010). Mice null for Cav2.2, Cav2.3 & Cav3.1 were found to be fertile (Lishko et al., 2012). A sperm specific cation channel CatSper was detected in the principal piece of mouse (Quill et al., 2001) sperm/testis showing structural similarity with the Cavs (Ren, 2010, Darszon et al., 2011). CatSper orthologs have been found in humans, chimpanzee, dogs, rat, sea squirt and sea urchin (Navarro et al., 2008, Seifert et al., 2015). CatSper has approximately 50% degree of sequence identity between human and mouse (Ren, 2010), 81% in transmembrane identity and 89% in pore regions (Singh and Rajender, 2015). It has four separate pore-forming subunits (CatSper 1-4), each with 6 transmembrane segments (S1-S6) with intracellular carboxyl and amino terminals. Similarly to voltage-gated channels, the S4 segment of each subunit is a voltage–sensor with charged amino acids (lysine/arginine) spaced at 3 amino acid intervals (Darszon et al., 2011, Singh and Rajender, 2015) that can respond to transmembrane voltage changes to regulate opening and closing of the pore (Navarro et al., 2008). However, though CatSper 1 has the 'normal' complement of six lysine/arginine residues, only four residues are present in CatSper 2 and only two in CatSper 3 & 4 (Singh and Rajender, 2015). This decrease in the charged amino acid residues in CatSper 2-4 reduces the voltage sensitivity of the CatSper heterotetrameric channels (Navarro et al., 2008). Auxiliary CatSper subunits include; CatSper β containing two transmembrane segments with two short cytoplasmic domains and one large extracellular domain, CatSper γ made up of single transmembrane segment with a large extracellular domain and short cytoplasmic tail and CatSper δ having a single transmembrane segment with a large extracellular domain and short cytoplasmic tail (Singh and Rajender, 2015).

CatSper is believed to be the principal pathway for calcium Ca^{2+} entry into the sperm flagellum (Kirichok et al., 2006, Lishko and Kirichok, 2010). Under physiological conditions CatSper is believed to permit significant Ca^{2+} entry but recordings of its activity have relied upon the fact that, in the absence of divalent cations, it is highly permeable to monovalent ions (Darszon et al., 2011, Lishko et al., 2011, Strünker et al., 2011). Much of our understanding of the role of CatSper has been obtained from studies of CatSper null mice. Sperm from these animals undergo tyrosine phosphorylation and acrosome reaction induced by zona pellucida (Xia et al., 2007) but cannot swim up through the oviduct (Miki and Clapham, 2013, Chung et al., 2014) or penetrate the egg coat (, Ren et al., 2001, Quill et al., 2003, Carlson et al., 2005) leading to male infertility (Navarro et al., 2008). (Quill et al., 2003, Qi et al., 2007) observed that CatSper is involved in regulating basal motility. Although the amplitude of flagella bending in a CatSper deficit mice is reduced, application of thimerosal that opens the stores via the inosine triphosphate receptor (IP_3R) could increase the flagella bending to a hyperactivated pattern (Bultynck et al., 2004, Marquez et al., 2007).

Human CatSper is a polymodally gated ion channel. Like mouse CatSper it is regulated by membrane potential (weakly) and intracellular pHi. At pH 7.5, 50% activation of CatSper occurs at +11 mV in mouse but at +85 mV in human (Lishko et al., 2011, Miller, 2015). However, human CatSper is also potently activated by a range of agonists including progesterone, prostaglandin, and many other small organic molecules including synthetic endocrine disrupting chemicals (Lishko et al., 2011, Strünker et al., 2011, Brenker et al., 2012, Alasmari et al., 2013b,Tavares et al., 2013, Schiffer et al., 2014). Cases of infertile men with CatSper 1 & 2 gene mutation(s) have been reported (Hildebrand et al., 2010, Lishko et al., 2012, Jaiswal et al., 2014).

1.7.2 Calcium stores, mobilisation of stores and stores operated channel (SOCS)

The mammalian sperm has at least two Ca^{2+} storage organelles, one in the acrosomal region and another in the sperm neck and midpiece (Costello et al., 2009). Inositol trisphosphate receptors (IP_3R) were detected in the outer membrane of the acrosome and at the sperm neck and anterior mid piece (Jimenez-Gonzalez et al., 2006, Publicover et al., 2007). They are activated by inositol trisphosphate (IP_3) generated at the plasma membrane due to the catalytic action of phospholipase Cδ on phosphoinositol 4,5-bis phosphate (PIP_2) (Bedu-Addo, 2008) activated either through tyrosine kinase coupled receptors or G-protein coupled receptors (GPCR) (Darszon et al., 2011). Calreticulin, a Ca^{2+} binding protein is reported to be present in the acrosome of developing rat sperm and in the acrosomal and neck regions of human and bovine sperm (Bedu-Addo, 2008, Costello et al., 2009).

Ryanodine-receptors (RyRs) have also been detected in the neck region of mature human sperm (Park et al., 2011). RyRs are sensitive to increased $[Ca^{2+}]_i$ and amplify calcium ion signaling by calcium induced calcium release (CICR) (Bedu-Addo, 2008, Darszon et al., 2011). RyRs also opens upon binding of the nucleotide messenger cyclic adenosine diphosphate ribose (cADPR) (Billington et al., 2006, Jimenez-Gonzalez et al., 2006) and nicotinic acid-adenine dinucleotide phosphate (NAADP). These are both products of adenine dinucleotide phosphoribosyl cyclase (CD38), which has been detected in human sperm (Park et al., 2011, Sánchez-Tusie et al., 2014). IP_3 and cADPR normally release Ca^{2+} from storage in the endoplasmic reticulum while NAADP may target acidic calcium store such as the lysosome. A novel NAADP synthase without cyclase activity of CD38 was detected in the sea urchin and human sperm (Sánchez-Tusie et al., 2014) with a two

pore channel (TPC) proposed to be NAADP receptor or calcium ion channel of acidic calcium stores (Arndt et al., 2014).

Efflux of Ca^{2+} from the storage organelles typically activates store operated channels (capacitative calcium entry), which allow Ca^{2+}-influx to sustain the Ca^{2+} signal and refill the store (Jimenez-Gonzalez et al., 2006, Correia et al., 2015). The calcium store membrane sensor molecule STIM (stromal interaction molecule), a channel protein Orai and perhaps transient receptor potential canonical (TRPC) are implicated in this process (Correia et al., 2015). STIM, on sensing the need to refill the calcium organelle, undergoes a conformational change and activates Orai thus opening the membrane ion channel and letting in Ca^{2+} (Jimenez-Gonzalez et al., 2006, Costello et al., 2009, Darszon et al., 2011, Lefievre et al., 2012).

Maintaining resting intracellular level of calcium or pumping calcium back to the store organelles is modulated by energy driven calcium pumps (Ca^{2+} ATPases), Na^{+} - Ca^{2+} and Ca^{2+} /H^{+} exchangers (Jimenez-Gonzalez et al., 2006, Bedu-Addo, 2008, Michelangeli and East, 2011). The calcium pumps include plasma membrane calcium ATPase (PMCA), sarcoplasmic endoplasmic reticulum calcium ATPase 2 (SERCA) and the secretory pathway calcium ATPase 1 (SPCA). PMCA, which exists as four isoforms (PMCA 1-4), is present in sperm and located in the principal piece where it contributes to regulation of motility (Jimenez-Gonzalez et al., 2006). Male mice without PMCA4 were infertile (Lishko et al., 2012). SERCA was detected in the acrosome and mid piece using the specific inhibitor thapsigargin (Rossato et al., 2001) and was found in the human, bovine, and mouse sperm using SERCA antibodies (Lawson et al., 2007). The Secretory pathway calcium ATPase 1 (SPCA1) an intracellular calcium ion pump was stained at the

neck/midpiece in human and sea urchin (Harper and Publicover, 2005). It was observed to interact with the Orai calcium ion channel (Feng et al., 2010).

1.8 Progesterone and sperm function

The oviductal and follicular fluids of the female tract contain biological molecules that are reported to regulate human sperm functions through change in $[Ca^{2+}]_i$ (Baldi et al., 1998, De Jonge, 2005, O'Gorman et al., 2013, Fujinoki et al., 2015). Progesterone (Figure 1.8) is a component of follicular fluid (Aquila and De Amicis, 2014). It is a steroid hormone that can control cell activities through both nuclear (genomic) and membrane receptor (non-genomic) mechanisms (Luconi et al., 2004, Miller et al., 2016). The action of progesterone on human sperm is rapid and clearly non-genomic (Blomberg Jensen and Publicover, 2012). Sperm is reported to have mRNA (Miller and Ostermeier, 2006;). The action of progesterone on human sperm is exerted by activation of CatSper, located in the plasma membrane of the flagellum (Lishko et al., 2011, Strünker et al., 2011, , Sumigama et al., 2015).

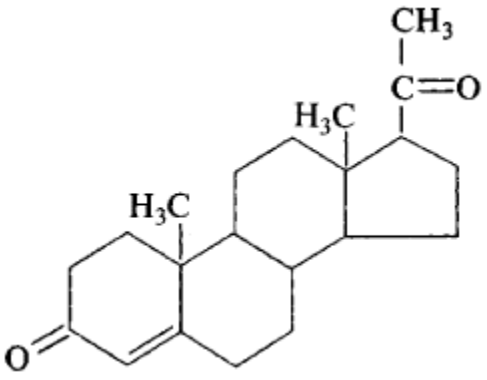

Figure 1.8 : Structure of progesterone

Progesterone, produced by the cells of the cumulus oophorus that surround the egg, is found in micromolar concentrations around the oocyte and due to simple diffusion and flow of oviduct fluid, different gradients of progesterone may be found along the female reproductive tract such that near isthmus, where a sperm storage site may occur, the concentration of progesterone may be in nano molar range (Sagare-Patil et al., 2012, Tamburrino et al., 2014). Progesterone produces a modest increase in hyperactivated motility of human sperm, apparently via activation of CatSper and increased $[Ca^{2+}]_i$ (Baldi et al., 2009, Lishko et al., 2012). This effect requires the presence of extracellular Ca^{2+} and is initiated in the principal piece but is propagated to the head through the midpiece and may be amplified by calcium induced calcium release mechanism from the calcium stores at the sperm neck (Jimenez-Gonzalez et al., 2006, Bedu-Addo et al., 2007, Xia et al., 2007). $[Ca^{2+}]_i$ oscillations may accompany progesterone induced calcium signalling (Harper et al., 2004, Kirkman-Brown et al., 2004) but they do not evoke acrosome reactions (Harper and Publicover, 2005). (Strünker et al., 2011, Tamburrino et al., 2014) reported that the CatSper inhibitors mibefradil and NNC55-0396 inhibited the progesterone induced $[Ca^{2+}]_i$ response showing that progesterone modulates sperm functions by activating CatSper channel activity. Using asthenozoospermic samples, (Tamburrino et al., 2015) provided evidence that progesterone evoked progressive and hyperactivated motility in human sperm are dependent directly on CatSper but acrosome reaction is not.

A second mechanism of non-genomic progesterone action may also occur in human sperm. Whilst low ($\leq$1 μM) concentrations of progesterone affect tyrosine phosphorylation and motility (apparently through CatSper), higher (1-10 μM) concentrations were required to induce acrosomal reactions and modify activity of a number of kinases, phosphatases and

hyperactivation (Sagare-Patil et al., 2012, Sagare-Patil and Modi, 2016). The action of progesterone on CatSper has so far been detected only in primates (humans and macaques) and rodent CatSper has been shown not to be sensitive to progesterone (Lishko et al., 2011, Sumigama et al., 2015, Barón et al., 2016). However, at higher concentration (10-20x those needed with human sperm) effects can be observed. In mouse initiation of acrosome reaction is associated with a temporary rise in $[Ca^{2+}]_i$ in the sperm head (Romarowski et al., 2016) and low concentrations of progesterone induce hyperactivation and tyrosine phosphorylation in hamster sperm (Noguchi et al., 2008).

1.9 4-aminopyridine and sperm function

4-aminopyridine (4AP) is a widely-used, broad-spectrum inhibitor of voltage-sensitive K^+ channels. In neurons, treatment with 4AP (Figure 1.9) prolongs action potentials and thereby potentiates activity of the nervous system (Smith et al., 2000). It is also a weak base that rapidly enters cells and increases pH_i. Entry of 4AP across the plasma membrane is dependent on extracellular pH because increased pH favours the non-ionised form of the molecule that easily crosses the cell membrane. (Stephens et al., 1994).

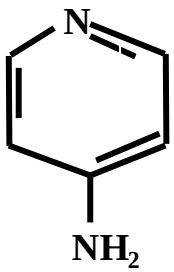

Figure 1.9 : Structure of 4- aminopyridine.

In mammalian sperm 4AP strongly promotes hyperactivated motility (Gu et al., 2004, Barfield et al., 2005, Chang and Suarez, 2011, Alasmari et al., 2013b). Blockade of K^+ channels does not underlie this effect since the sperm potassium ion channel KSper (Slo3) is not sensitive to the drug (Tang et al., 2010). In mouse sperm this effect of 4AP has been interpreted as indirect activation of CatSper due to increasing cytoplasmic pH, causing inflow of Ca^{2+} (Navarro et al., 2007, Chang and Suarez, 2011). However, in experiments on human sperm it was shown that (i) equivalent elevation of pHi with NH_4Cl failed to induced hyperactivation, (Alasmari et al., 2013b). (ii) 4AP increased $[Ca^{2+}]_i$ even in the absence of $[Ca^{2+}]_o$ (Bedu-Ado 2008) and (iii) 4AP increased hyperactivation in sperm from a man who was functionally null for CatSper (Williams et al., 2015). Mobilisation of stored Ca^{2+} by 4AP has been described and characterised in other cell types (Grimaldi, 2001, Bhaskar, 2008, Wu et al., 2009). Since release of stored Ca^{2+} at the sperm neck has been shown to regulate hyperactivated motility of sperm from rodents, bulls and humans (Ho and Suarez, 2001, Ho and Suarez, 2003, Publicover et al., 2007) it appears that 4AP mobilises stored Ca^{2+} in mammalian sperm and this contributes significantly to its effect on hyperactivated motility.

Research aims

Until now there is no drug for treating male infertility. Understanding the molecular works of the human sperm, as it journeys across the female tract, encountering different chemicals that modulate its motility patterns, will help to address subfertility associated with motility. The aim of this work was further to characterise how these cues interact with the sperm, eliciting $[Ca^{2+}]$i signals that produce the required motility types, especially the hyperactivated pattern, at the right time and place. The following specific aims were identified;

(1). How do progesterone (CatSper activator) and 4-Aminopyridine (Ca^{2+} store mobiliser) modify $[Ca^{2+}]_i$ and hyperactivation in human sperm- chapter 3.

(2). How does extracellular pH (and consequent change in pHi) modify responses to progesterone and 4AP – are effects of progesterone and pHi synergistic? –chapters 4 and 6

(3). Are effects of pH on Ca^{2+} signals due to enhanced activity of CatSper - investigated by pharmacological block of CatSper – chapter 5.

(4) How do the interacting effects of pH and calcium mobilising drugs affect sperm behaviour– chapter 7.

CHAPTER 2: MATERIALS AND METHODS

2.1 Materials

2.1.1 Chemicals

All chemicals were from Sigma-Aldrich (Poole, UK) unless stated otherwise. The supplemented Earle's balanced salt solution (sEBSS) contained 1.0167mM NaH_2PO_4, 5.4mM KCl, 0.811mM $MgSO_4.7H_2O$, 5.5mM $C_6H_{12}O_6$, 2.5mM $C_3H_3NaO_3$, 19mM $CH_3CH(OH)$ COONa, 25mM $NaHCO_3$, 1.8mM $CaCl_2.2H_2O$, 15 or 25 mM Hepes (pH 7.4), 0.3% BSA (molecular biological grade; US Biological, SWAMPSCOTT, MA 01907). 25 mM Hepes was normally used for experiments with 4AP because at high doses (2-5 mM) this weak base caused an increase in saline pH of 0.2-0.4 pH units in medium buffered with 15 mM Hepes while 25 mM Hepes reduced this effect by >50%. For pH 8.5 sEBSS, 15 mM Hepes was replaced with 25mM TAPS N-Tris (hydroxymethyl) methyl-3-aminopropanesulfonic acid.

NaCl was used to adjust the osmolality to 291-294 mOsm. pH was corrected using NaOH/HCl if required and checked immediately prior to use. Saline for pHi calibration used the same recipe but were buffered as follows: 15 mM ADA [N – [2 –Acetamido] – 2 – iminodiacetic acid] for pH6.0 and 6.5, 15mM Hepes for pH 7.0, 7.4 and 8.0, 25mM TAPS for pH8.5 and 9.0. pH buffer tablets (Phosphate) of pH 9.2 and 4 for calibrating the pH meter were from Fisher scientific, UK.

The probes for $[Ca^{2+}]_i$ and pHi; fluo-4-AM, fluo5F-AM , fura2-AM and BCECF-AM were obtained from Thermo Fisher Scientific, UK and prepared at concentrations of 0.91 mM, 1.0 mM, 2.0 mM and ≈0.9 mM respectively in DMSO containing 20% Pluronic F-127 (Thermo Fisher) .

Stock solutions of chemicals were as follows: Progesterone (P4) [4-pregnene-3,20-dione] (Sigma, Poole, UK) was dissolved in DMSO at 10mM, 4- aminopyridine (4AP, Sigma, Poole, UK) was dissolved in DMSO at 500mM, 12% triton X–100 was dissolved in saline, NH_4Cl was dissolved in deionised water at 500 mM, thimerosal (Tm) (Mercury – [(o – carboxyphenyl) thio]ethyl sodium salt) was dissolved in deionised water at 100mM, poly-D-Lysine (BD – Biosciences) was made up at 0.001% in deionised water and AR720-F1 (CatSper inhibitor; courtesy Prof. Timo Strunker, University of Munster, Germany) was made up as 30 mM stock in DMSO). All the drugs administered were prepared in saline of pH 7.4 (15mM Hepes or 25mM Hepes) or pH 8.5.

2.1.2 Human follicular fluid (hFF)

Cell-free human follicular fluid was provided courtesy of Prof. C. Barratt, University of Dundee. hFF was obtained in accordance with the Human Fertilization and Embryology Authority (HFEA) Code of Practice (V8) under local ethics approval (13/ES/0091) from the East of Scotland Research Ethics Service REC1. Oocytes (mostly metaphase II) were obtained through transvaginal aspiration 36 hr after administering r-hCG. From the largest follicles recovered non-blood contaminated hFF was centrifuged at 2500 g for 10 minutes, separating the supernatant from the cellular components. The supernatant was the filtered (0.22μm) to ensure removal of any remaining debris and cell-free, supernatant was stored at -20°C.

2.2 Donor recruitment

All the sample donors were recruited in line with the Human Fertilisation and Embryology Authority code of practice at the Department of Biosciences, School Biosciences, University of Birmingham (ERC 07-009 and ERN-12-0570). Six – ten students of 18 – 21

years were donors in this research. We did not store their personal information and their fertility status was not established.

2.3 Experimental Design

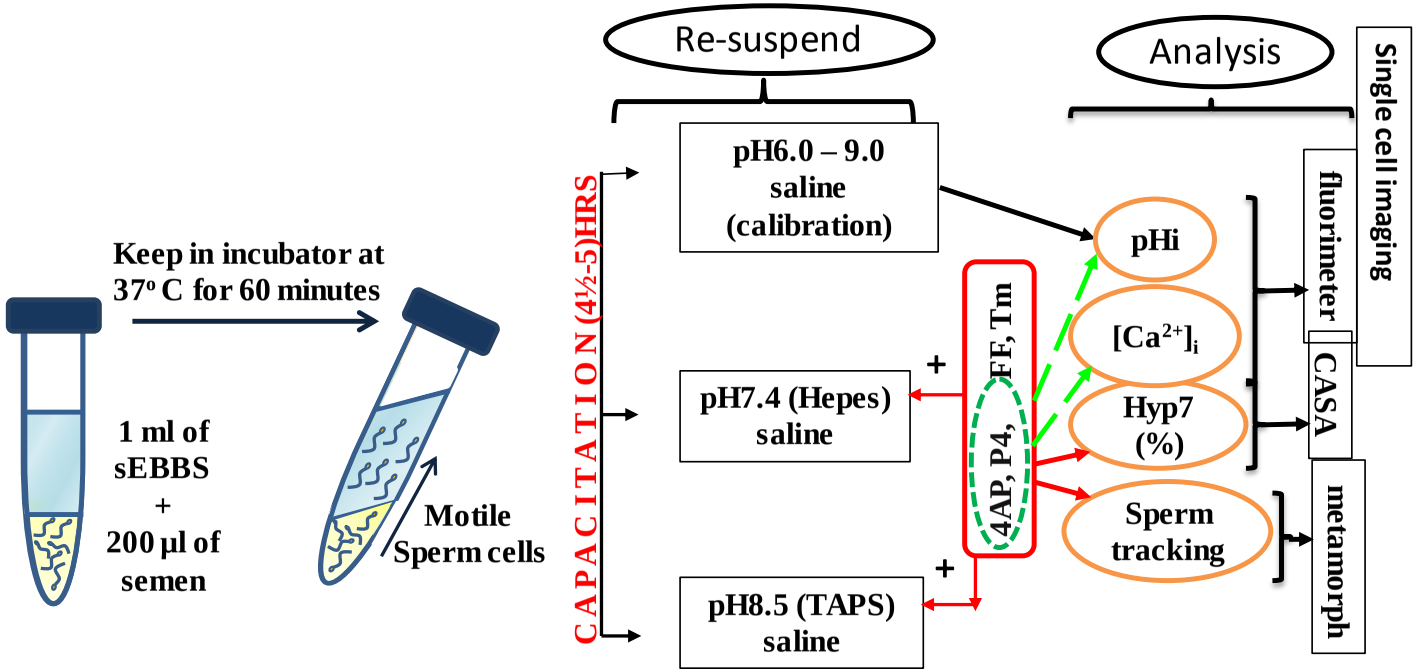

Figure 2: Flow chart of the experimental design. In all analysis, the sperm cells were separated from the semen by swim up method in pH 7.4 saline and capacitated at 6million cells /ml for 4½ - 5hrs at 37° C. The capacitated cells were centrifuged and re-suspended to pH 7.4 and 8.5 saline to determine hyperactivated motility (CASA) and single cell behaviour (metamorph) respectively. Also cells loaded with Ca^{2+} and pHi probes (fluo 4 and BCECF) for 30 minutes were centrifuged and re-suspended into pH 7.4, 8.5 and pH 6.0 – 9.0 for fluorimetry analysis respectively. Perfusion of pH 7.4 and 8.5 saline (in the absence and presence of P4) were used in single cell analysis. 4AP – 4 aminopyridine, FF – follicular fluid, P4 – progesterone and Tm – thimerosal were drugs used.

2.4 Sperm preparation/capacitation

Human ejaculated spermatozoa were collected by masturbation in a sterile 60 ml pot after 2-3 days of sexual abstinence. They were liquefied for 30 minutes at 37º C and the volume was measured. A sample 1µl of the raw semen was diluted in 1:50 with de-ionised water and 10 µl pipetted into the Neubauer haemocytometer (0.100 mm depth), which was viewed using a Nikon eclipse TS 100 microscope to determine the raw concentration of the sperm cells in semen. 5µl of the raw sample was pipetted into the pre-warmed 20µm chamber (Hamilton-Thorn 2X-Cel) and placed on the heated stage of the Olympus CX41 microscope connected to a Hamilton Thorn CEROS computer assisted sperm analysis (CASA) system for determining the proportion of motile, progressively motile and hyperactivated cells.

Motile cells separated by swim up procedure in sEBSS-BSA (0.3%) saline. 1ml of the sEBSS-BSA (0.3%) pH 7.4 saline was pipetted into a 5 ml BD falcon polystyrene round bottom tubes (Corning Science, Mexico) and 200µl of liquefied semen was under-layered in the round bottom falcon tubes. They were placed in the incubator diagonally to create maximum surface area for cells to swim up at 37^0C, 6% CO_2 for 1 hour. The top 0.7 ml of saline, containing the motile fraction of the sperm cells, was then collected from each tube with a 1ml pipette tip into a 15 ml BD falcon polystyrene tube. The final volume of prepared cells was measured and the concentration, motility, progressive motility and hyperactivated motility of swim-up cells were evaluated with the Neubauer haemocytometer/counting chamber and the CASA system respectively. Concentration was adjusted to 6 million cells/ml and cells were placed in 15 ml BD falcon polystyrene tubes

(1-2 ml in each) and left to capacitate for at least 4½ - 5 hours in the incubator at 37^{o}C, 6% CO_2 (Figure 2.0).

2.5 Fluorimetric measurement of changes in $[Ca^{2+}]_i$

Changes in intracellular calcium concentration $[Ca^{2+}]_i$ were measured in cells prepared as described above. In most experiments the cells were loaded with 4.5 μM fluo4-AM (diluted 1/200 from stock, DMSO-0.5%) for 30 minutes in the incubator at 37^{0}C and 5% CO_2, centrifuged (Eppendorf 5417R) twice at 700g for 10 minutes to remove extracellular dye and re-suspended into sEBSS pH7.4. For experiments using fluo5F and fura2 the loading protocol was essentially the same, final dye concentrations being 5 μM and 10 μM respectively.

Aliquots of the re-suspended cells were centrifuged at 1500 g/10 mins and the supernatant analysed for fluorescence for background subtraction from experimental values. 90μl of cell sample was pipetted into the appropriate number of wells in a 96 well micro plates and fluorescence was assessed using a Fluostar Omega, Labtech 96 plate reader (BMG) (Figure 2.2) set at 30°C, plate mode, 490 nm excitation and 530 nm emission wavelengths using top optics and 20% photomultiplier gain and 5s cycle time. In experiments using fura-2, which is ratiometric (takes care of experimental and equipment bias), alternating excitation of 340 nm and 380 nm was applied and emission was measured at 510 nm. For most experiments multiple wells were used, allowing several treatments/doses to be assessed in parallel. After assessing resting fluorescence for 55 seconds (Figure 2.1a,b), agonist/antagonist and vehicle were added to each well, as appropriate, at the times specified in the result chapters. Additions were made with a multi-channel pipette so that dose-effect of agonists and antagonists could be measured in parallel in multiple wells.

Stock solutions of progesterone and 4AP were diluted in sEBBS (pH7.4) to give appropriate final concentrations in the well (0.001, 0.01, 0.1, 1.0, 10, 20 μM and 200, 400, 600, 800, 1000, 2000 and 5000 μM respectively). Additions of other drugs were carried out similarly. Control (vehicle) wells received DMSO equivalent to the highest concentration added to experimental well of (0.2% for progesterone, 1% for 4AP). Fluorescence was then measured in each well, at 5 s intervals, for the next 5 minutes. The sequence (position on the plate) of the different drug doses was varied randomly between repeats.

For determination of $[Ca^{2+}]$i signals at pH 8.5 capacitated sperm cells were loaded with fluo4-AM as described above but when washes to remove extracellular dye were carried out cells were re-suspended into pH 8.5 saline. Progesterone and 4-aminopyridine stocks were diluted in pH 8.5 saline before addition.

The data from the plate reader were exported to Microsoft Excel for analysis. The effects of progesterone and 4-aminopyridine on $[Ca^{2+}]_i$ transient and sustain increments{(Δ mean fluorescence intensity of 300 – 350 seconds} were determined respectively (Figure 2.1a). Also the change in $[Ca^{2+}]_i$ transient and sustain responses to AR720-F1 were determined as in (Figure 2.1b). The resting $[Ca^{2+}]_i$ (F_{basal}) is calculated as the mean for the 55 seconds period before application of agonists while peak fluorescence (F_{peak}) or inhibitory traces ($F_{inhibited)}$ is the mean of 5 values with the maximum or minimum fluorescence intensity in the middle.

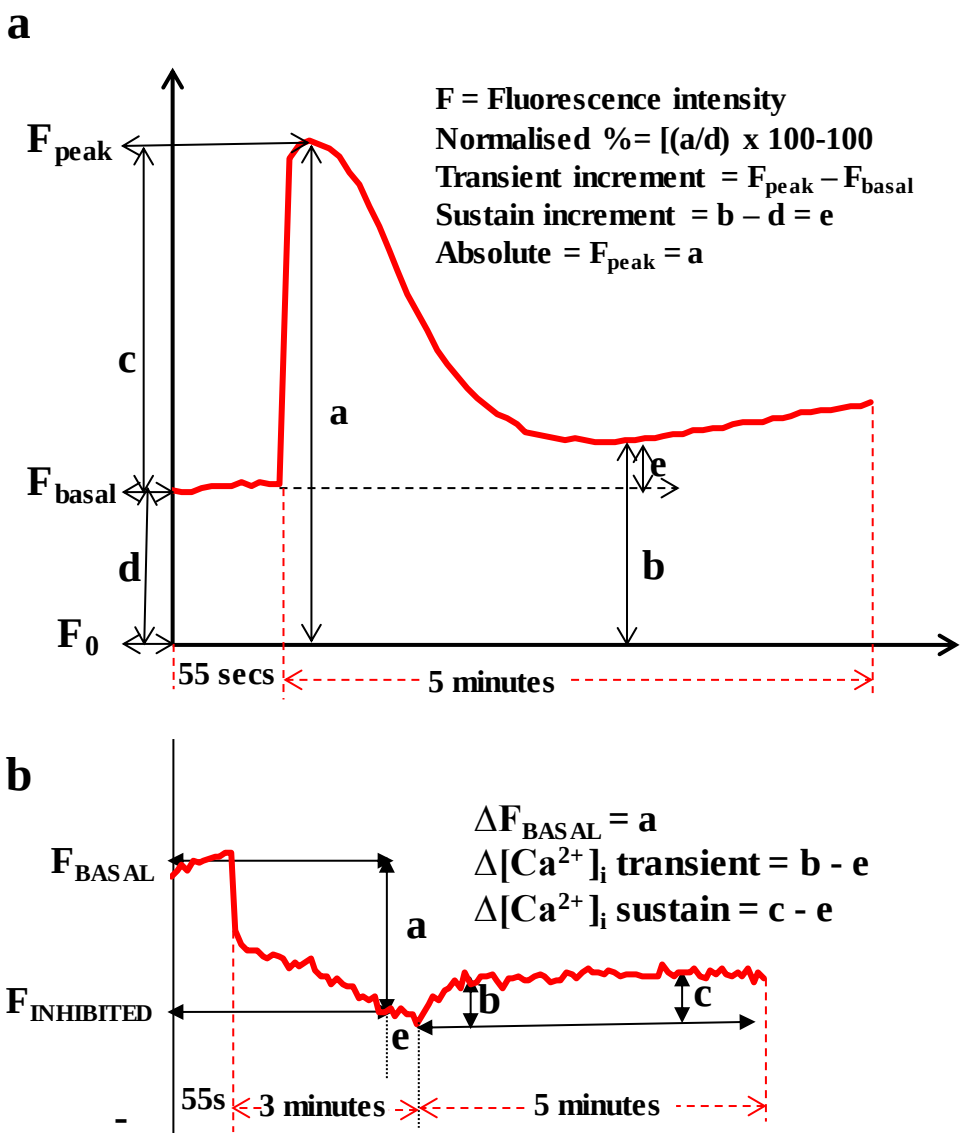

AR720-F1 inhibitory Ca^{2+} signalling

Figure 2.1 : The dimensions of a typical biphasic calcium ion signal. (a) – shows how the transient and sustain increment, absolute and normalised (%) values were obtained. (b) – shows how the inhibitory effect of AR720-F1 on Ca^{2+} signalling at rest, transient and sustained increment were determined.

2.6 Fluorimetric assessment of pHi

3ml aliquots of capacitated cells (6 million/ml) were loaded with 0.45 µM BCECF-AM for 30 minutes in the incubator at 37°C, and 6%CO_2 and washed by centrifugation prior to experimentation as described above for Ca^{2+} dyes. Alternating excitation (440 and 490 nm) was applied and emission was measured at 530 nm and converted to a ratio (490/440) in Excel.

To calibrate the BCECF signal, after washing to remove extracellular dye, 7 aliquots of BCECF-loaded cells were re-suspended in saline buffered at pH 6.0, 6.5, 7.0, 7.4, 8.0. 8.5, 9.0 respectively, (Naz, 2014). Each sample of 99µl was pipetted into a well of a 96 well micro plate and basal fluorescence intensity measured for 60 seconds at 30°C, 20% G (gain), top optics, 7 second cycle time with 100 rpm shaking frequency (double orbital mode). 1µl of 0.12% Triton X-100 was then added to permeabilise the cell membrane making (pHo=pHi) and measurement of BCECF fluorescence was continued for a 5 minutes. Using the BCECF ratio (490/440) at each pH value a sigmoidal calibration curve was constructed. Non-permeabilise sperm cells were treated with 2mM 4AP, (1, 10, 20 µm) P4, 25mM NH_4CL and DMSO (control) to determine their effect on pHi.

Figure 2.2: The fluorescence plate reader connected to a computer system (Fluostar omega,BMG Labtech 96)

2.7Assessment of hyperactivated motility

After capacitation at pH 7.4, aliquots of capacitated sperm cells (6 million cells/ml) were centrifuged (Eppendorf 5702) at 300 g for 5 minutes and re-suspended into sEBSS buffered at saline at either pH 7.4 or 8.5. 100 µl aliquots of the samples were placed in 1.5ml Eppendorf tubes and stimulated with different doses progesterone or 4AP, diluted into saline of the appropriate pH (as described above for fluorimetric experiments). To assess whether effects of 4AP on hyperactivation were due to intracellular alkalinisation the effect of 25mM NH_4Cl was also investigated. Control tubes received vehicle and saline.

5µl of each sperm aliquot was loaded to a pre-warmed 20 µm CASA chamber (Hamilton Thorn 2X-Cel) and placed immediately on the heated stage of the Olympus CX41 microscope with 10x objective connected to a Hamilton Thorn CEROS CASA system (version 14.0) (Figure 2.3A). Kinematic parameters of sperm head movement were assessed 5 minutes after application of the stimulus. The order in which of the effects of different treatments were assessed was randomised in each experiment. 30 video frames were collected at 60 Hz and for each cell in the field of view, a minimum of 13 track points were required for acceptance. At least 200 sperm were tracked (up to 20 fields). Cells were defined as hyperactivated when they satisfied the criteria for sort7 (HYP7), which are VCL (curvilinear velocity - total distance covered by sperm head per unit time) ≥150µm/s, LIN (linearity = straight line velocity/VCL) <50% and ALH (amplitude of lateral movement of the sperm head) ≥7µm (Mortimer, 2000). Other kinematic parameters - VSL (straight line velocity - speed of movement calculated from first and last point on the track, VAP (average path velocity - speed of the sperm head along its average path, BCF (beat cross

frequency - rate at which the sperm head crosses its average path), STR (straightness - degree of curvature in the average path - VSL/VAP) and WOB (wobble – degree of deviation of the sperm head from its average path - VAP/VCL) ; Figure 2.3B) were also collected.

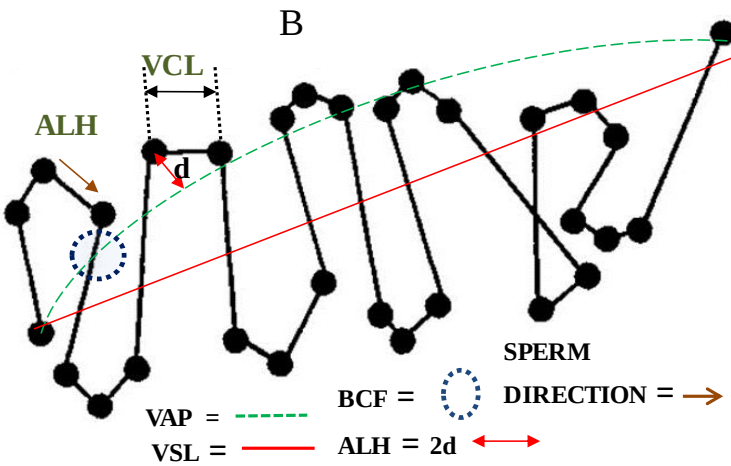

Figure 2.3: A – The Olympus CX41 Microscope connected to Hamilton Thorn CEROS CASA system. B - Kinematic parameters as measured by CASA. VAP is the average path travelled (green dotted lie). VSL is the distance between the first and last point (red line). BCF is the beat cross frequency (blue circle). ALH is the amplitude lateral head displacement and the brown arrow indicates the sperm direction.

2.8. Single-cell imaging of $[Ca^{2+}]_i$

A 200µl aliquot of capacitated cells (3 x 10^6 / ml) was incubated with 5 µM of fluo4-AM for 30 minutes (37°C, 6% CO_2). The cells were transferred to an imaging chamber, the base of which was a coverslip coated with 0.001% poly-D-lysine. After allowing 5-10 minutes for cells to adhere to the coverslip the imaging chamber was attached to the perfusion system on the microscope (Nikon TE300 inverted with 40x oil objective fitted with an Andor Ixon 897E EMCCD camera) and perfused with sEBSS (pH 7.4) to remove unattached cells and excess dye. All experiments were performed at 25 ± 0.5 °C in a continuous flow of sEBSS at pH7.4 or pH8.5, with a perfusion rate of 0.6 ml/minute. Images were captured at 0.2 Hz by iQ3 software (Andor Technology, Belfast, UK) using excitation at 485 nm (LED) and emission at 520 nm. An intial control period was recorded (at least 3 min) before application of any stimuli. There was a delay of ≈60 s between addition of progesterone to the perfusion header and arrival in the imaging chamber. Offline images were analysed by drawing lasso around the head/neck of each sperm in the field of view, the series of image were replayed several times to identify and remove those sperm that moved out of the region of interest or died (fluorescence faded to zero within the duration of experiment). After background correction, fluorescence intensity for each cell was normalised using % change in intensity= $(F_t/F_{basal)}$*100-100), where F_t = fluorescence at time t and F_{basal} = mean fluorescence for the initial recording period before stimulation. With the normalised fluorescence intensity of each cell, an overall mean intensity R_{tot} was calculated and used to plot a mean normalised response for the experiment (Nash et al., 2010).

2.8.1 Analysis of single cell $[Ca^{2+}]_i$ responses

Responses on individual cells were analysed using Microsoft Excel. To assess the effects of alkalinisation and P4- induced Ca^{2+} signalling at pHo 7.4 and 8.5, the amplitude of the transient and sustain fluorescent intensity of each cell was calculated using the average of five points at the peak of the response and in the plateau phase (Figure 2.4a; X and Y respectively). The distribution of response amplitudes and correlation between different components of responses were also assessed using Excel. For some analyses, data on experiments from 3 different donors were combined. The frequency of $[Ca^{2+}]_i$ oscillations under different conditions was assessed by counting the number of oscillations within that period. The mean duration and amplitude of the oscillations were determined as in (Figure 2.4b). The oscillations measured were normally smaller in amplitude than the transient spike.

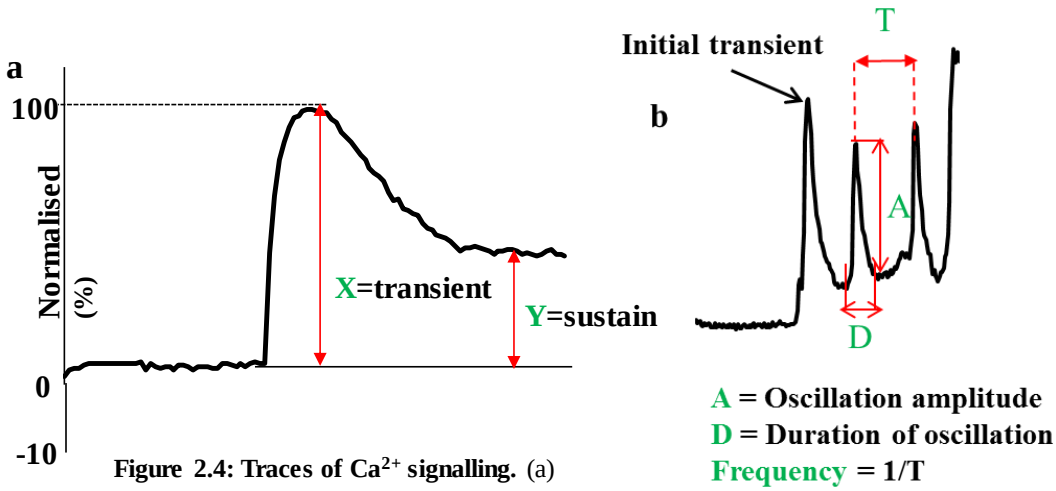

Figure 2.4: Traces of Ca^{2+} signalling. (a) Normalised plot of biphasic Ca^{2+} response from single cell imaging. (b) Dimensions of agonist - induced $[Ca^{2+}]_i$ oscillations identified and labelled visually.

2.9 Long-duration sperm tracking

20 μm observation chambers were constructed using two glass cover slips chamber (22 mm x32 mm, 0.13-0.16 mm thickness (Academy) and 22 mm x50 mm, thickness no. 1.5 (VWR International). 18 -22 μm soda lime glass beads (Cospheric microspheres, Santa Barbara, USA) were dispersed 'thinly' in vacuum grease (Dow-Corning) and small dabs were placed at each corner of the 22 mm x 32 mm coverslip – providing a 20 μm space when the two coverslips were 'glued' together (figure 2.5a). 1.5ml aliquots of the capacitated cells (adjusted to 1.2 x 10^6/ml) samples were placed in Eppendorf tubes at both pHo=7.4 or 8.5 as required. After stimulation (0.3μM progesterone (P4), 1% follicular fluid (FF), 1μM thimerosal (Tm), 2mM 4AP, control for a minute at 37^{o}C), 5μl was loaded into the coverslip chamber and placed immediately on the platform of a thermostatic controller (Warner TC-324B - 36.5°C) on the stage of inverted microscope (Nikon ECLIPSE TE200, Japan) with a 10x phase contrast objective (Plan Flour n.a. 0.3) fitted with a Zyla sCMOS camera (ANDOR ^{TM} Technology, Belfast) and a Prior ProScan II motorised stage (Figure 2.5b).

Images (10,800 frames at 50-55 Hz, 15 ms exposure) were acquired continuously over a period of 180-220 s using Micro manager software v1.4.22 (image 1392 x 1040 pixels, 16 bit dynamic range, camera set for global shuttering). For each recording a randomly selected sperm was followed for 3 minutes, the cell being rapidly re-centred using the motorised stage when it approached the edge of the field of view. Sperm cells that were immotile or had their tails stuck to slides were not used in the analysis. The position of the sperm head was tracked (x,y co-ordinates of sperm head centroid) offline using the multidimensional motion analysis application in the MetaMorph® NX Microscopy Automation & Image Analysis Software (version 2.0 Molecular Devices 2011). The

software was calibrated (0.65μm pixel size) based on the objective (10x) and camera (Zyla) so data imported into Excel was in μm. Tracks (x,y co-ordinates) were 'stitched' together in Excel by compensating the difference in' x' and 'y' after each movement of the stage. Using playback of videos combined with assessment of tracks in Image J, four different types of motility were visually identified - types T1, T2, T3 and T4 – further details are given in section 7.3.2. The data were analysed in Excel using a tracking buffer calibration application (definition of parameters same as CASA but not limited to 30 frame analysis) for generating kinematic parameters and trajectories of the motility patterns. Other analyses (transition rate between motility types and mean time spent per motility type) were calculated in Microsoft Excel.

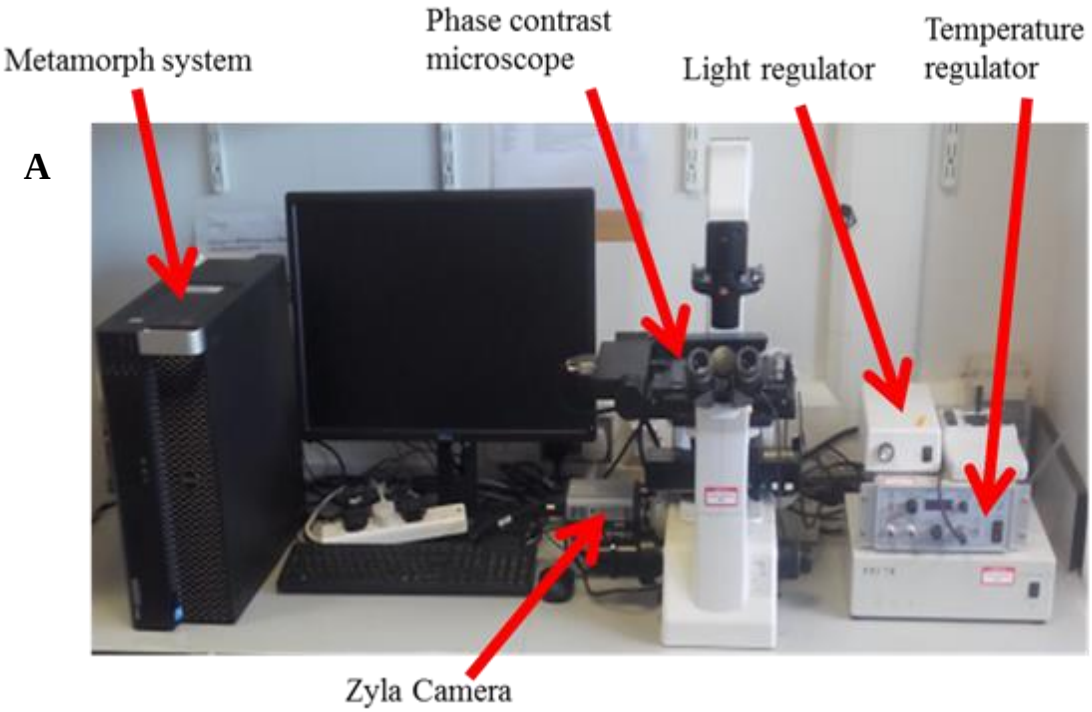

Figure 2.5: A – Sperm tracking system. B – A two glass coverslip chamber of depth 18 - 22µm

2.10 Statistical analysis

The data are presented as mean ± SEM with $P<0.05$ indicative of statistical significance. Microsoft Excel 2010 and Graph Pad Prism^{TM} were used to analyse the data statistically. The normality of data sets was confirmed by comparison of frequency distributions with normal distribution generated from sample mean and standard deviation or by generation of quantile–quantile (Q–Q) plots when possible. Paired t –tests were used to test difference in responses of cells from the same sample to drug and vehicle stimuli and differences in effects of drugs at pHo=7.4 and pHo=8.5. Where multiple comparisons were made the calculated P levels were adjusted using a Holm-Bonferroni sequential correction routine in Microsoft Excel (Gaetano, 2013). One way ANOVA was used to determine the statistical significance of dose-dependence of drug effects on $[Ca^{2+}]_i$ or motility parameters. Unpaired t-test and Holms –Bonferroni sequential calculator were used for the analysis of tracking data in chapter 7.

CHAPTER 3: DOSE EFFECT OF CALCIUM MOBILISING DRUGS ON THE $[Ca^{2+}]_i$ AND SPERM MOTILITY

3.1 Objective

The significance of CatSper in regulation of sperm motility is well established yet the evidence for and characterisation of stimulation of hyperactivated motility by CatSper activation in human sperm is poor. The aim of the experiments reported in this chapter was to characterise and compare effects on $[Ca^{2+}]_i$ and motility of progesterone (CatSper activation) and 4-AP (Ca^{2+} store mobilisation).

3.2 Introduction

In the female tract, progesterone is synthesised by a mass of granulosa cells buried in a gelatinous matrix surrounding the oocyte, and thus the sperm must pass through an area of high [progesterone] as it approaches the oocyte (Lopez-Torres and Chirinos, 2017). Progesterone is a member of the family of reproductive steroid hormones (Johnson, 2007) which classically control activation of biological functions by binding to a nuclear receptor, regulating gene transcription and evoking long-lasting signalling mechanisms (Baldi et al., 2009, Miller et al., 2016). More recently, a range of rapid, non-classical (non-genomic) effects of steroids have been described, which occur through binding of membrane receptor (Losel and Wehling, 2003, Luconi et al., 2004). In human sperm cells, the primary receptor for progesterone appears to be CatSper (the sperm specific cation channel) and its associated proteins in the plasma membrane (Ren, 2010). Activation of CatSper by progesterone, leading to generation of $[Ca^{2+}]_i$ signals (Lishko et al., 2011, Publicover and Barratt, 2011a, Strünker et al., 2011) contributes to regulation of a number of functions of the sperm including chemotaxis, hyperactivation and acrosomal reactions that would enable the sperm carry out its duty of fertilisation (Harper et al., 2004, Publicover et al., 2007, Qi et al., 2007).

Change in $[Ca^{2+}]_i$ regulates flagella beating of sperm (Carlson et al., 2003, Jin and Yang, 2016, Pereira et al., 2017). Hyperactivated movement, which may enable the sperm to swim across the highly visco - elastic surrounding of the oocyte (Suarez, 2008), occurs when $[Ca^{2+}]_i$ is increased (see section 1.6). However, there is some inconsistency in reports of the effect of progesterone on sperm motility (Baldi et al., 2009). (Sagare-Patil et al., 2012) showed that progesterone would dose-dependently evoke hyperactivated motility. In contrast, several groups reported there was little or no significant effect of progesterone on

hyperactivation recorded within a few minutes of stimulation. (Alasmari et al., 2013a, Alasmari et al., 2013b, Luconi et al., 2004, Tamburrino et al., 2014, Wang et al., 2001). Alasmari and colleagues concluded that in a subset of cells Ca^{2+} influx via CatSper may be amplified by calcium- induced calcium released from the Ca^{2+} stores in the neck, leading to effective induction of hyperactivated motility (Alasmari et al., 2013b). 2mM 4AP was reported to induce hyperactivated motility by mobilising the Ca^{2+} stores however it is also suspected to indirectly open CatSper by increasing cytoplasmic pH (Alasmari et al., 2013, Chang and Saurez, 2011).

In this chapter I studied the effects of progesterone, and 4AP, which mobilise stored Ca^{2+} (see section 1.9) on $[Ca^{2+}]_i$ and hyperactivation of human sperm.

3.3 Materials and Methods

3.3.1 Materials

For the Materials section, see Chapter 2.1. 1

Control (absence of drug), progesterone (P4) and 4-aminopyridine (4AP) were used in this experiment.

3.3.2 Methods

3.3.2.1 Donor recruitment

Donor recruitment was conducted as described in Chapter 2.2.

3.3.2.2 Sperm cell preparation

The sperm cells were prepared as explained in Chapter 2.4

3.3.2.3 Measurement of $[Ca^{2+}]_i$ in fluorimeter

The effect of different concentrations of P4 and 4AP were performed as described in Chapter 2.5 (P4, n = 8 and 4AP, n = 6).

3.3.2.4 Measurement of hyperactivated motility in CASA

Assessment of the effect of P4 and 4AP on hyperactivation were performed as described in Chapter 2.7 (P4, n = 21 and 4AP, n = 13)

3.4 Results

3.4.1 Effect of progesterone on the $\Delta[Ca^{2+}]_i$ in human sperm

Stimulation of human sperm with 0.001 – 20 μM doses of progesterone increased $[Ca^{2+}]_i$ in a biphasic manner. At first there was a very quick rise of $[Ca^{2+}]_i$ that peaked at 15seconds and declined within 30-75seconds to a plateau phase (Figure 3.1, panel a).

3.4.1.1 Effect on Δ $[Ca^{2+}]_i$ transient increment

P4 produced a dose - dependent transient phase that was statistically significant to basal fluorescence at doses ≥0.001 μM and saturated at >1 μM (**P < 0.01, ***P > 0.001, n = 8) (Figure 3.1, panel b).

3.4.1.2 Effect on Δ $[Ca^{2+}]_i$ sustained increment

P4 effect on the sustained phase was dose - dependent and statistically significant to basal fluorescence at doses ≥ 0.001 μM and saturated at >1μM (***P < 0.001, n = 8) (Figure 3.1, panel c).

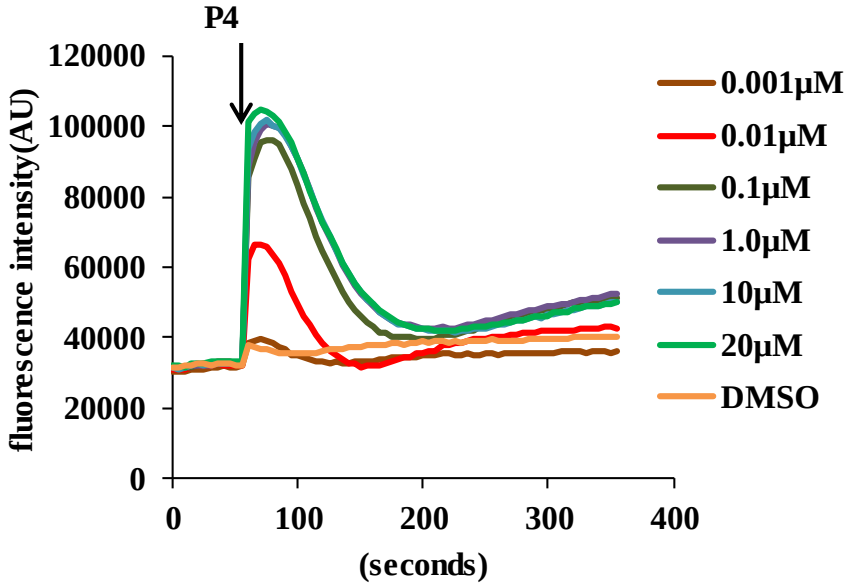
P4
120000
100000
80000
60000
40000
20000
0
fluorescence intensity(AU)
0
100
200
300
400
(seconds)
0.001µM
0.01µM
0.1µM
1.0µM
10µM
20µM
DMSO

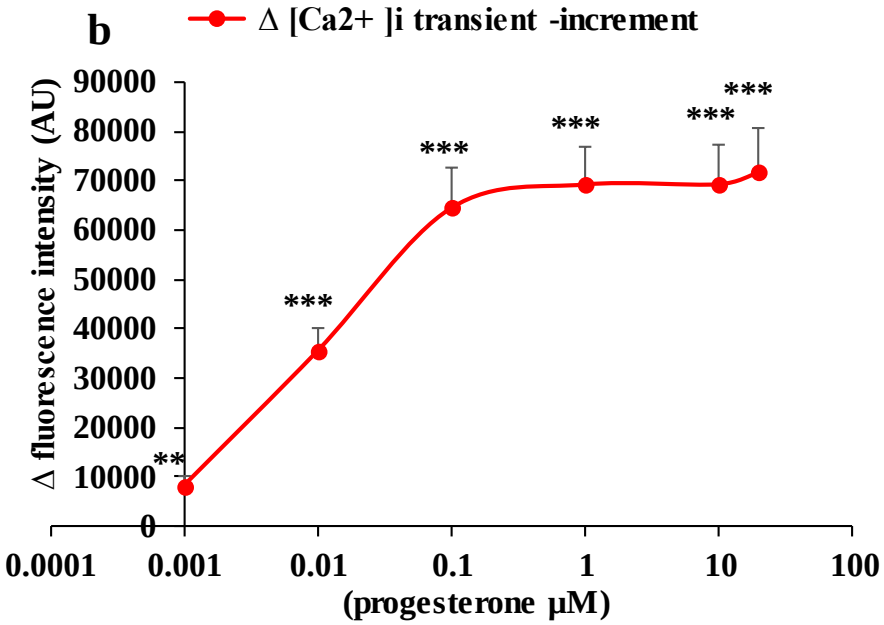
b
Δ [Ca2+]i transient -increment
90000
80000
70000
60000
50000
40000
30000
20000
10000
0
Δ fluorescence intensity (AU)
**
***
***
***
***
***
0.0001
0.001
0.01
0.1
1
10
100
(progesterone µM)

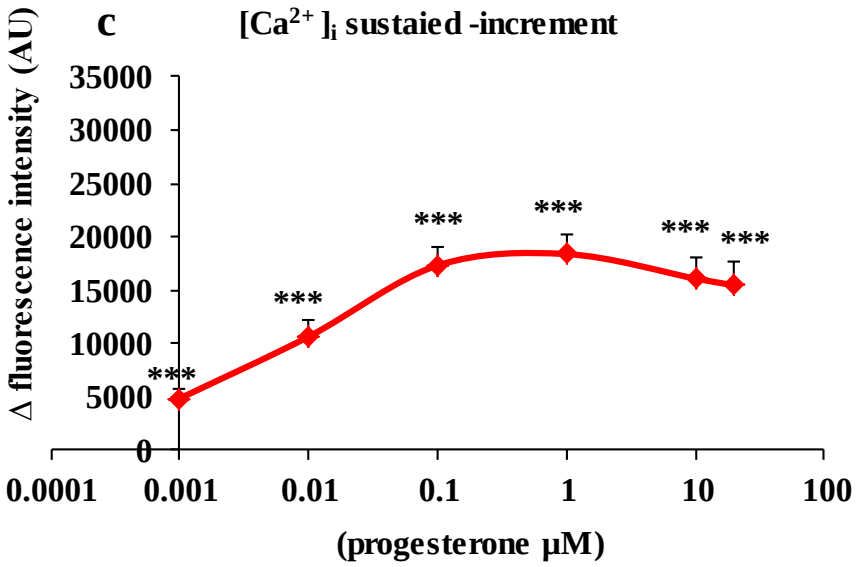

Figure 3.1: Dose effect of progesterone on Δ $[Ca^{2+}]_i$. a- Dose dependent biphasic $[Ca^{2+}]_i$ responses produced by progesterone . b- Progesterone evoked a dose dependent increment in the Δ $[Ca^{2+}]_i$ transient which is significantly different from the basal effect (**P < 0.01, ***P < 0.001, n = 8). c- Dose response induced by progesterone on the Δ $[Ca^{2+}]_i$ sustained increment is significantly different from basal fluorescence (***P < 0.001, n = 8).

3.4.2 Effect of 4-aminopyridine on the Δ $[Ca^{2+}]_i$ in human sperm

Dose effect of 200 - 5000 µM 4-aminopyridine **(**4AP) on human sperm also produced at the beginning a very fast and sudden rise of $[Ca^{2+}]_i$ that reached the peak within the range of 15-25seconds, decayed slowly over a period of 50 – 55 seconds and then plateau (Figure 3.2, panel a).

The two $[Ca^{2+}]_i$ responses are plainly different in shape. P4 induced a transient peak that was greater than that of 4AP and took longer to decay across all the doses while the 4-AP $[Ca^{2+}]_i$ sustained increase was larger than that of P4.

3.4.2.1 Effect on Δ $[Ca^{2+}]_i$ transient increment

The effect of 4AP on transient phase was dose - dependent and significantly different to control at doses ≥ 200 µM (*P < 0.05, **P < 0.01, n = 6) (Figure 3.2, panel b).

3.4.2.2 Effect on Δ $[Ca^{2+}]_i$ sustained increment

The effect of 4AP on sustained phase increased significantly compared to control at ≥ 200 µM (*P < 0.05, n = 6) (Figure 3.2,panel c).

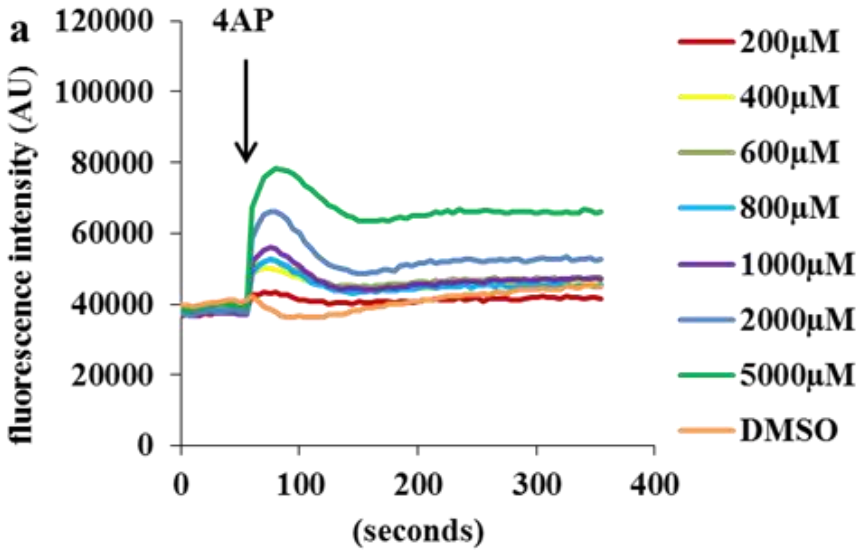

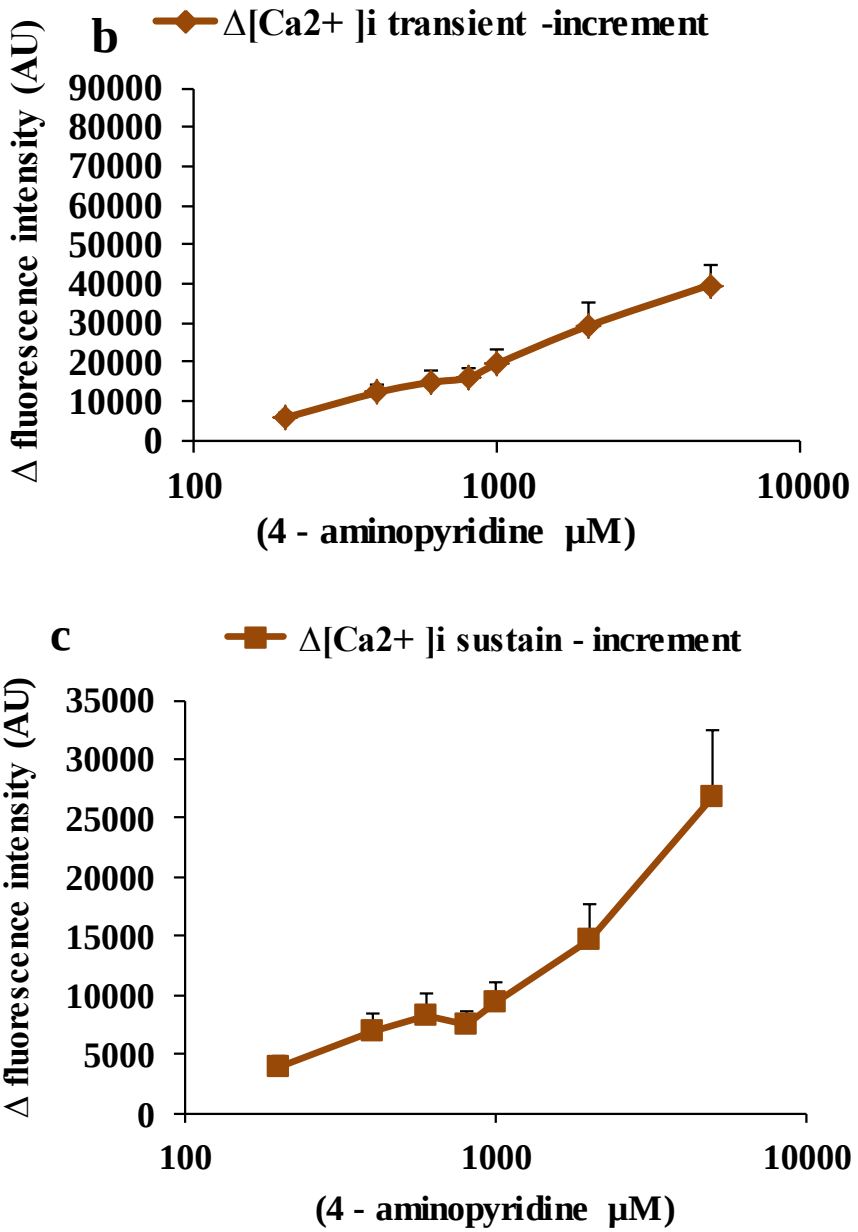

Figure 3.2: 4-aminopyridine induced dose dependent Δ $[Ca^{2+}]_i$. a- Dose dependent biphasic $[Ca^{2+}]_i$ response produced by 4AP. b - The dose dependent transient induced by 4 – aminopyridine was statistically significant compared to the control (*P < 0.05, **P < 0.01, n = 6). c - 4AP induced a dose dependent Δ $[Ca^{2+}]_i$ sustained increment which was significantly different when compared with the control (*P < 0.05, n = 6).

3.4.3 Progesterone and 4 - aminopyridine dose effect on human sperm motility

The effect of different dose of P4 and 4AP on hyperactivated motility(%), its associated kinematic properties and percent frequency distributions were evaluated 5 minutes after stimulation respectively.

3.4.3.1 Progesterone and 4-aminopyridine induced effect on hyperactivated motility

The effect of P4 on hyperactivated motility was evaluated using concentrations of 0.1, 1, 10 and 20 μM. Before stimulation, the proportion of cells with hyperactivated motility was 2.5 ± 0.66% (n = 21). Doses of P4 ≤ 20 μM induced an increase in the proportion of hyperactivated cells when compared with the control (no drug) however it was statistically significant only at doses of 1 and 20 μM (*P < 0.05 , n = 21) (Figure 3.3 panel a). The effect was small (increment of 4-5%) and was not dose-dependent.

The effect of 4AP on hyperactivated motility (%) was evaluated using concentrations between 200 and 5000 μM (Figure 3.3 panel b). 4AP induced a significant change in hyperactivation (%) only at a dose of 5000μM, where HYP (%) increased from 0.54 ± 0.39 to 10.46 ± 2.37 % (**P < 0.01, n = 13, paired t = test) (Figure 3.3 panel b).

4AP produced a clear dose-dependent effect on hyperactivation (%) (***P < 0.001, n = 13).

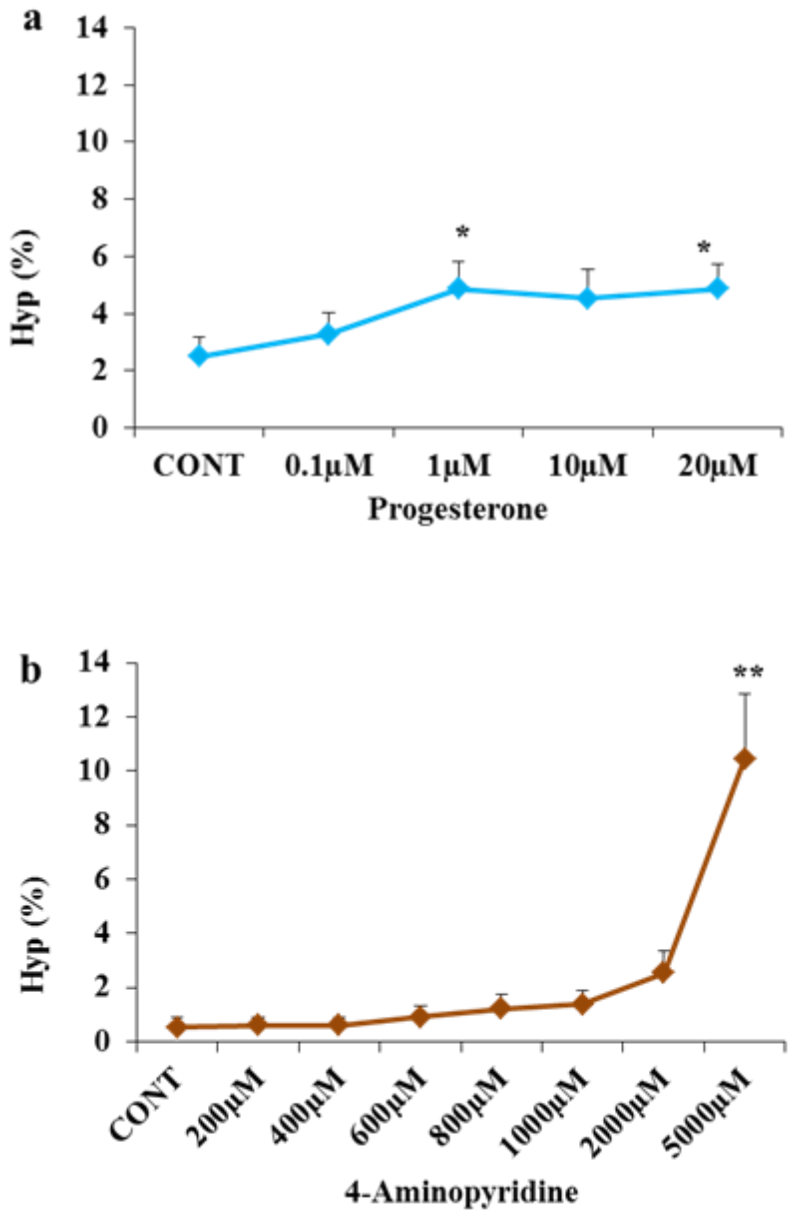

Figure 3.3: Progesterone and 4-aminopyridine induced hyperactivated motility. a-Higher concentrations of P4 at 1 and 20µM produced significant higher percent response on hyperactivation when compared with the control (no drug) (*P < 0.05, n = 21). b- 4AP induced a dose dependent effect on hyperactivated motility. 4-Aminopyridine at dose of 5000µM induced significant increased percent dose effect on hyperactivation when compared with the control (no drug) (*P < 0.01, n = 13).

3.4.3.2 Effects of progesterone and 4-aminopyridine on VCL

Distance covered with time (VCL) was assessed 5 minutes after stimulation with P4. At 20 μM progesterone VCL was significantly increased (*P < 0.05, n = 21, Figure 3.4a) but the effect was small (control=91.10 ± 3.25 μm/s; 20 μM P4= (95.96 ± 3.60 μm/s). Other P4 doses failed significantly to increase VCL (P > 0.05, n= 21). When frequency distributions were plotted the control had a bell-shaped curve with a modal value of 90 um/s (Figure 3.4b yellow plot). Only 1 and 20 μM P4 changed the modal VCL (red and green plots in Figure 3.4b) but at other doses there was a clear fall in the proportion of cells in the modal class and a (dose-dependent) increase in the proportion of cells swimming at high velocity (>150 μm/s) (Figure 3.4b).

In experiments with 4AP, the VCL of control (no drug) was 83.99 ± 3.53 μm/s. 5 minutes after application of 4AP VCL was dose dependently increased (Figure 3.4 panel c), this effect being significant at dose of 5000 μM (***P < 0.001, n = 13) (Figure 3.4 panel c). As with P4 experiments, the frequency distribution for control cells had a bell-shape with a modal value of 90-100 μm/s (E in Figure 3.4d yellow plot). After treatment there was a clear, dose-dependent, rightward shift of the distribution and at 2000 and 5000 μM 4AP, the modal value shifted to ≈110 μm/s (F in Figure 3.4 paneld) and at 5000 μM there was a great increase in the proportion of cells with VCL ≥150 μm/s.

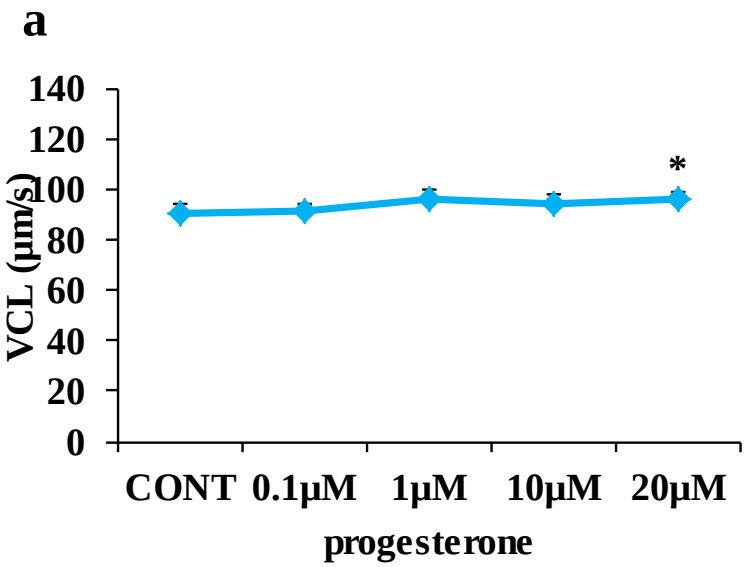
a
140
120
100
80
60
40
20
0
VCL (µm/s)
*
CONT
0.1µM
1µM
10µM
20µM
progesterone

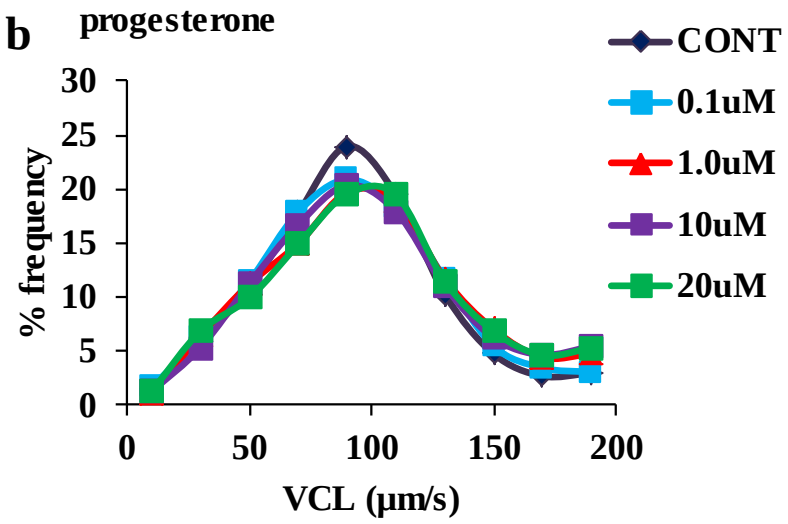
b
progesterone
30
25
20
15
10
5
0
% frequency
0
50
100
150
200
VCL (µm/s)
CONT
0.1uM
1.0uM
10uM
20uM

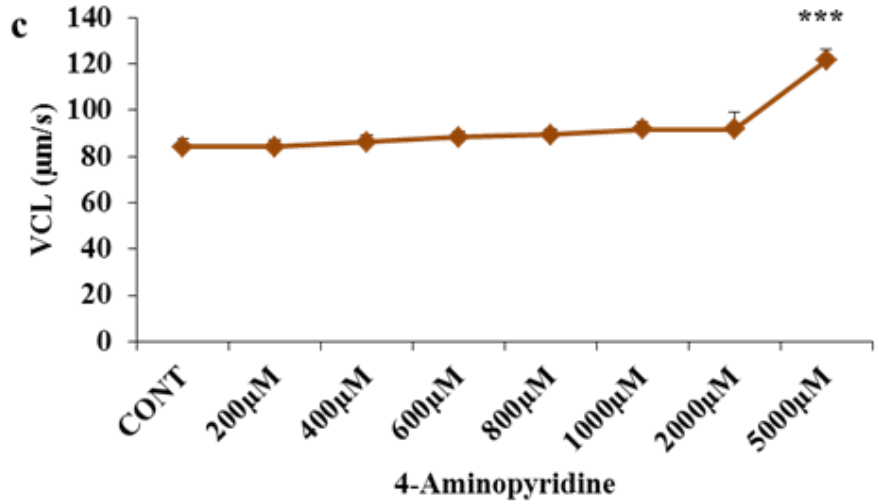

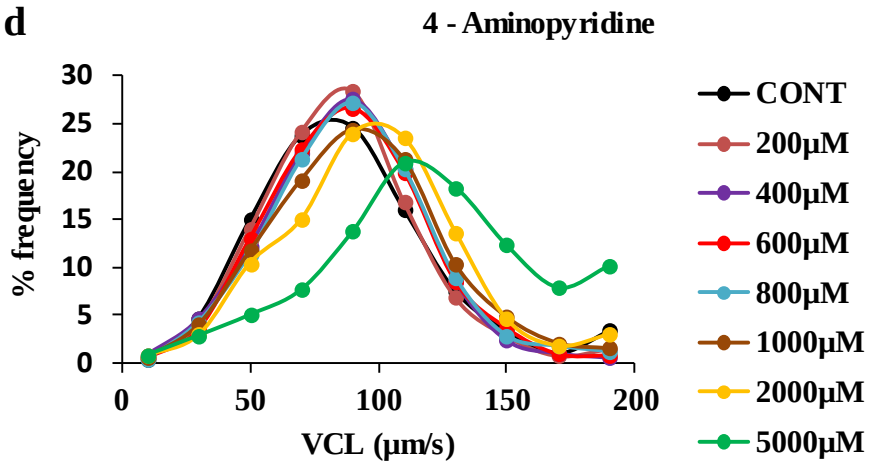

Figure 3.4: Effect of progesterone and 4-aminopyridine in the curvilinear velocity (VCL). a – P4 increases the VCL dose independently. At 20µM the VCL (µm/s) was significantly increased when compared with the control (*P < 0.05, n =21). b – P4 in frequency distribution decreased the population of cells in the modal class when compared the control (n =21) and at 1 and 20µM P4, the VCL was shifted to the right. c – At 5000µM 4AP, the VCL was significantly increased when compared with the control (***P < 0.001, n =13). d – The 4AP dose dependent frequency distribution was shifted to the right and at ≥ 2000 µm the value of VCL in the modal class increased from 90 – 130 µm/s. At 5000µM 4AP, number of cells with VCL ≥ 150 µm/s increased greatly.

3.4.3.3 Effects of progesterone and 4- aminopyridine on ALH

Treatment with progesterone (5 min) caused a small but significant increase in the amplitude of side to side movement of sperm head (ALH) above the control level (3.93 ± 0.10 µm) at all 4 doses used (***P < 0.001, n = 21) but there was no detectable dose-dependent effect (P > 0.05, n = 21, Figure 3.5 panel a). Plotting of frequency distributions showed that though the modal value for ALH was not shifted at any dose, there was a clear change in shape of the distribution due to a shift to the right.

4AP induced a significant change in ALH only at a dose of 5000µM, where ALH increased from 3.74 ± 0.20 to 5.32 ± 0.22 µm (***P < 0.001, n = 13) (Figure 3.5 panel c). Plotting of the frrequency distribution clearly showed this effect , with a strong rightward shift and an increase in the modal value of ALH for 5000 µM (green plot Figure 3.5 panel d).

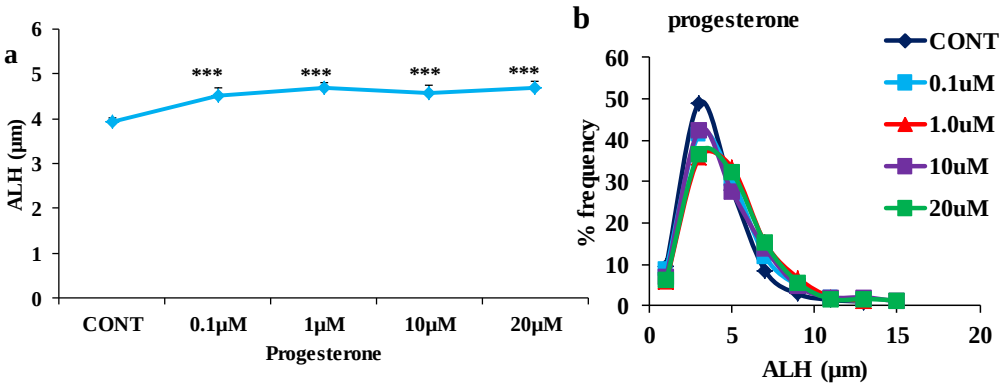

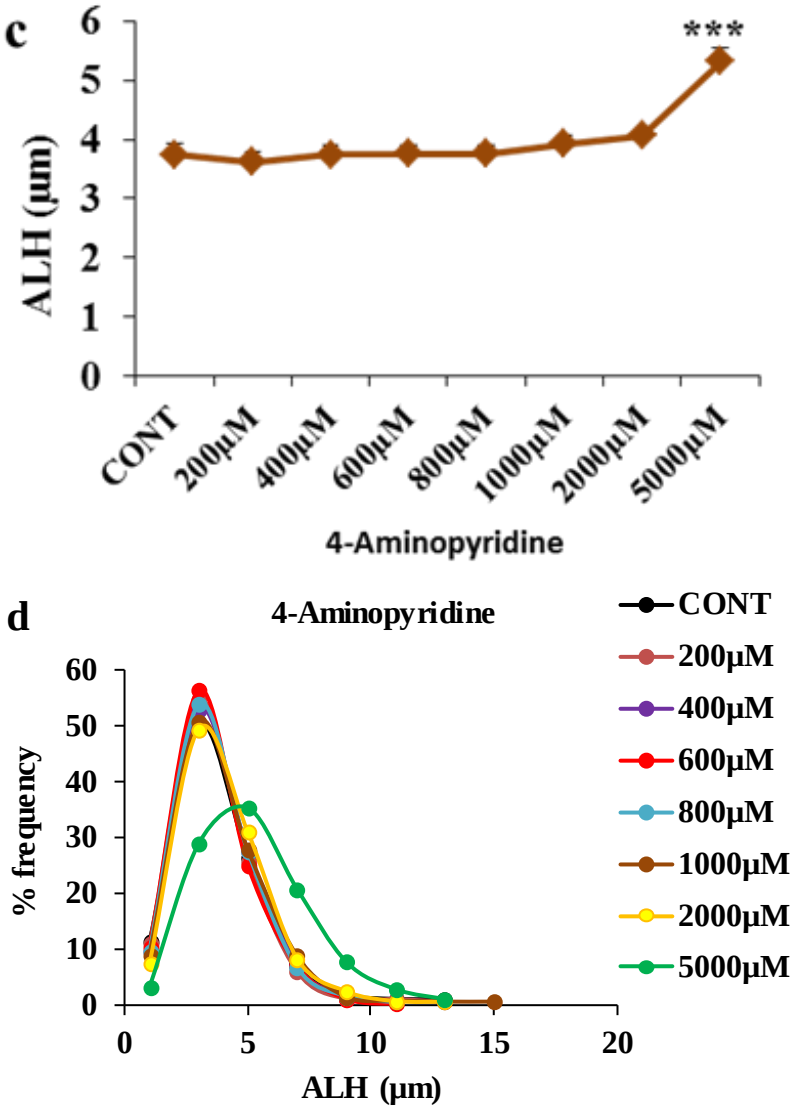

Figure 3.5: Effect of progesterone and 4 – aminopyridine on the amplitude lateral head displacement (ALH). a – P4 increased the ALH significantly in a dose independent manner when compared with the control (***P < 0.001, n =21). b – The frequency distribution shows that P4 decreased the value of the modal class with a slight shift to the right of the distribution. c- Effect of 4AP was dose dependent on ALH and at 5000µM ALH was significantly increased compared to the control (***P < 0.001, n = 13). d- 5000µM (4AP) increased the modal value of ALH by shifting the distribution to the right.

3.4.3.4 Effects of progesterone and 4-aminopyridine on LIN

The mean linearity of the sperm swimming path (LIN) before stimulation was 58.86 ± 1.27% . After 5 minutes of stimulation with P4, LIN was significantly decreased at all doses used ($P<0.001$, n = 21, Figure 3.6 panel a), but there was no discernible dose dependence to this effect. In unstimulated cells the frequency distribution for LIN was broad and apparently bimodal, with peaks at 75% (A in Figure 3.6 panel b) and 55% (B in Figure 3.6 panel b) respectively. On stimulation, with P4 this distribution was shifted to the left and the bimodal distribution was less clear (Figure 3.6b). However in unstimulated cells, 3 separate days distribution for LIN reveal a peak and shoulder suggesting that P4 does not just shift the cells but distribute them between the two peaks in the control (Figure 3.6 panel c).

Treatment with 4AP (5 min) at doses up to 5000 µM had no significant effect on LIN even though there was a clear shift from the basal value of 62.15 ± 2.35% to 57.15 ± 2.16% at 5000 µM ($P > 0.05$, n = 13, Figure 3.6c). Plotting of frequncy distribution for LIN showed a slight increase in the proportion of cell with LIN >80% but strangely at 400µM dose a clear leftward shift occured (purple plot Figure 3.6 panel d).

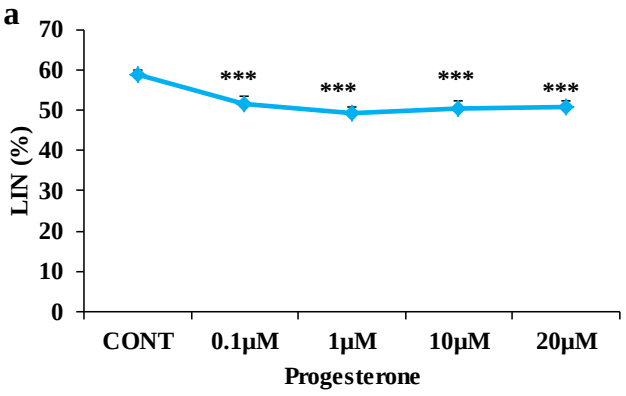

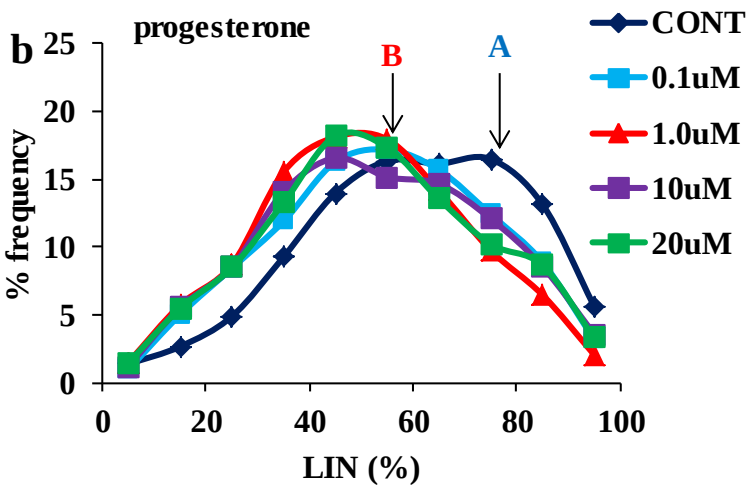
b
progesterone
B
A
CONT
0.1uM
1.0uM
10uM
20uM
% frequency
25
20
15
10
5
0
0
20
40
60
80
100
LIN (%)

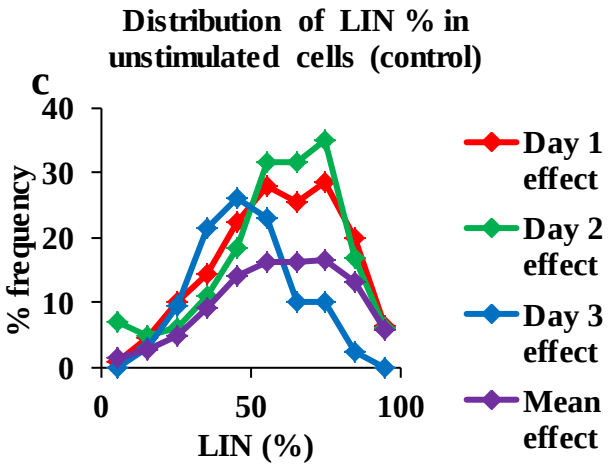
Distribution of LIN % in unstimulated cells (control)
c
% frequency
40
30
20
10
0
0
50
100
LIN (%)
Day 1 effect
Day 2 effect
Day 3 effect
Mean effect

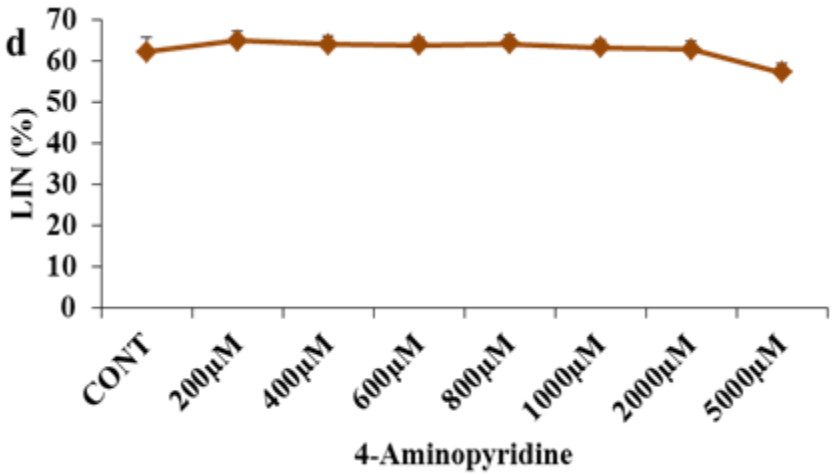
d
LIN (%)
70
60
50
40
30
20
10
0
CONT
200μM
400μM
600μM
800μM
1000μM
2000μM
5000μM
4-Aminopyridine

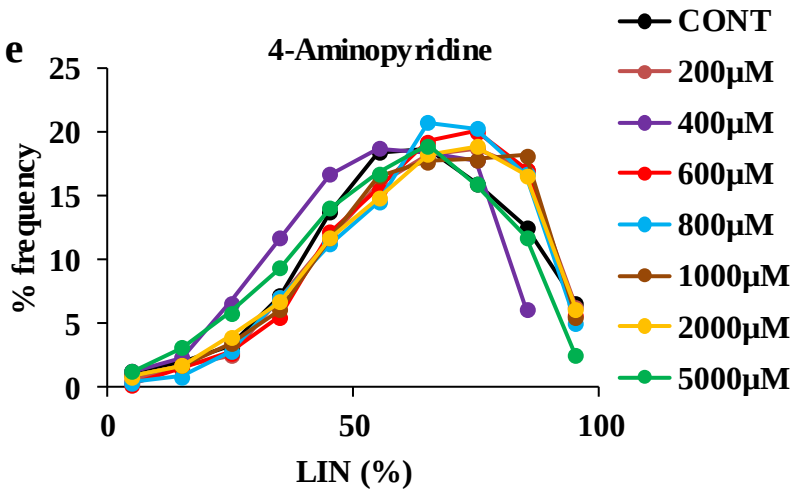

Figure 3.6: Effect of progesterone and 4 – aminopyridine on Linearity (LIN). a shows P4 decreased the % linearity dose independently and statistically significant when compared with control (***P < 0.001, n = 21). b – The frequency distribution of LIN reveals broad and bimodal classes of cells (A and B) in the control. P4 shifted the mean linearity to the left with unclear bimodal class. c –However distribution plots of LIN for 3 separate days shows that the bimodal occurrence is repetitive in daily analysis. d – All the 4AP doses increased the % linearity non – significantly when compared with control (P > 0.05, n = 13). e shows 4AP shifted the LIN distribution to the right increasing the proportion of cells with LIN > 80% but at 0.4µM 4AP, there was a shift to the left.

3.4.3.5 Effects of progesterone and 4-aminopyridine on BCF

Resting beat cross frequency (BCF) was 27.7 ± 0.7 Hz. Exposure to progesterone for 5 min significantly reduced BCF at all 4 concentrations tested (*P < 0.05, **P < 0.01,n = 21, Figure 3.8 panel a) but there was no discernible dose dependence to this effect (P>0.05). Plotting of frequency distributions showed that under resting conditions the BCF distribution had a broad peak which appeared to be bimodal (Figure 3.7 panel b, yellow plot) with peaks at 35 Hz and 18 Hz (marked A and B respectively in Figure 3.7 panel b).

After exposure to P4 this bimodal distribution was still present but cell had shifted from class A to B decreasing mean BCF (Figure 3.7 panel b).

The unstimulated cells had a basal BCF of 23.82 ± 0.85 Hz. Administering with 4AP (5 min) at doses 200 - 5000 µM increased BCF statistically non- significant compared to the basal BCF ($P > 0.05$, $n = 13$, Figure 3.7c) and it was dose - independent. 4AP shifted the modal values of mean BCF to the right with a broad peak in all doses of 4AP (Figure 3.7 panel d).

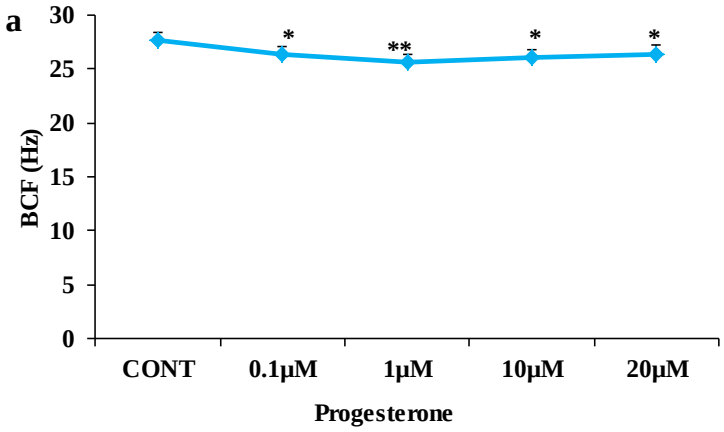

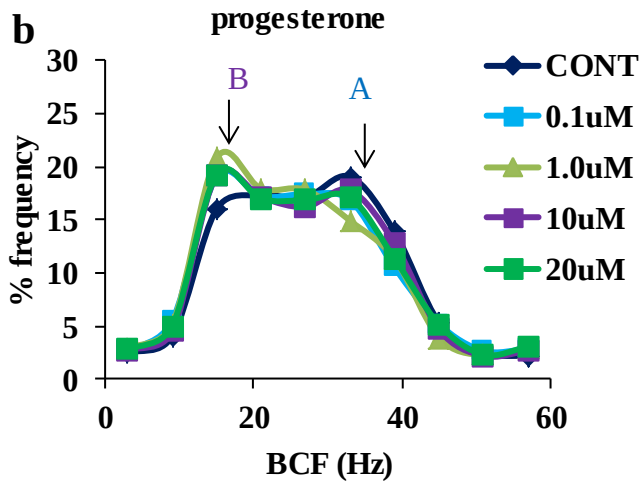

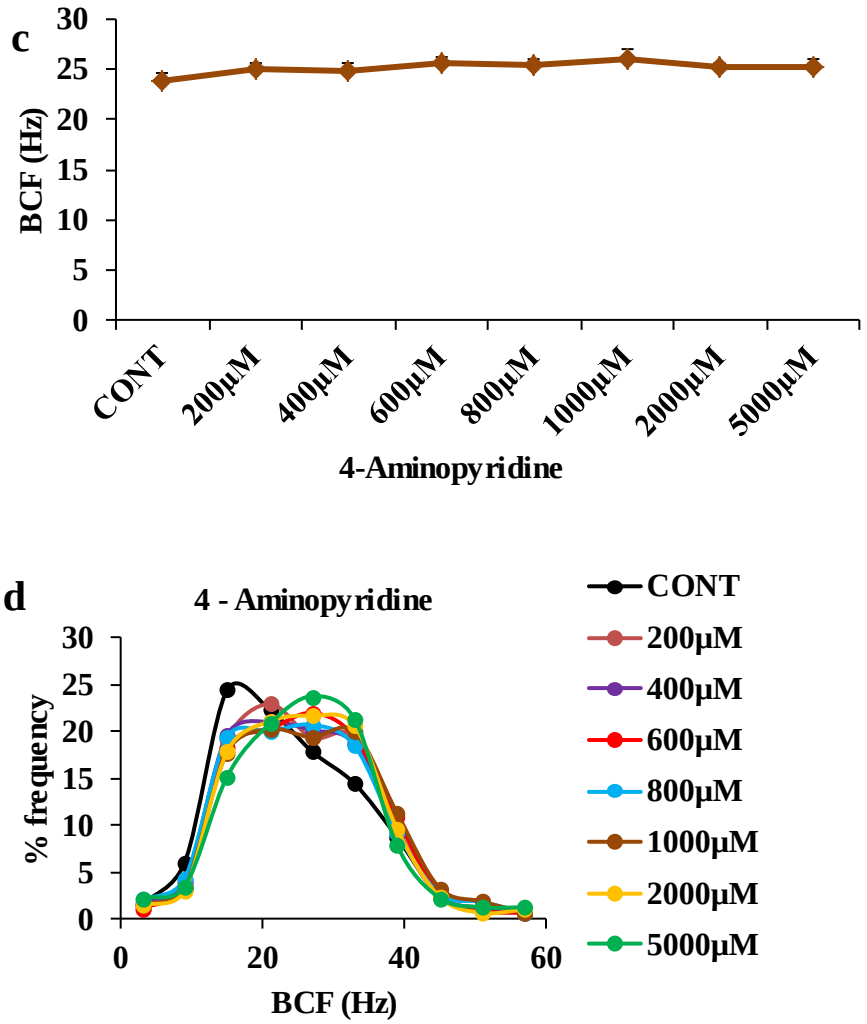

Figure 3.7: Effect of progesterone and 4 - aminopyridine on Beat cross frequency (BCF). a shows P4 significantly decreased the BCF when compared with the control (*P < 0.05, **P < 0.01, n = 21). b shows P4 shifted mean BCF to the left retaining the bimodal distribution of BCF. c - 4AP up to 5000µM increased BCF non - significantly compared to the control (*P < 0.05, n = 13). d - 4AP increased the mean BCF by broadening the modal peaks of BCF and shifting it to the right.

3.5 Key findings

(i) P4 and 4AP induced dose - dependent biphasic elevation of $[Ca^{2+}]_i$.

(ii) The effect of P4 on $[Ca^{2+}]$i saturated at 100 nM but the response to 4AP increased across the range of concentrations used (100 nM – 5 mM).

(iii) The P4-induced $[Ca^{2+}]_i$ transient was greater than that seen with 4AP but 4AP-induced $[Ca^{2+}]_i$ signals decayed only slightly from the initial peak such that the sustained signal was greater than that induced by P4.

(iv) P4 had a small and dose-independent effect on hyperactivation but 4AP caused a dose-dependent increase in hyperactivation across the range of concentrations used.

(v) The effects of 2 mM 4AP on $[Ca^{2+}]_i$ and motility observed were less than previously reported. This may be because in weakly buffered medium (as used previously) 4AP increases pHo, facilitating penetration of the drug into the cytoplasm.

3.6 Discussion

Change in $[Ca^{2+}]_i$ is the pivotal signal involved in activating and sustaining hyperactivated motility (Alasmari et al., 2013a, Suarez, 2008). CatSper in flagellum and calcium stores in the neck/midpiece have been implicated in regulating the $[Ca^{2+}]_i$ for hyperactivated motility (Aitken and McLaughlin, 2007, Carlson et al., 2003, Costello et al., 2009, Ho and Suarez, 2001, Ho et al., 2009). The CASA kinematic parameters that are used to define hyperactivated motility are increased VCL (μm/s) and ALH (μm) and decreased LIN (%) (Mortimer, 2000). In this chapter I investigated the effect of stimulating; (a) the CatSper ion channel in the plasma membrane with progesterone and (b) calcium stores in the neck/midpiece with 4-aminopyridine on $[Ca^{2+}]_i$ and hyperactivated motility.

3.6.1 Progesterone and 4AP-induced $[Ca^{2+}]_i$ signals

The effect of progesterone on $[Ca^{2+}]_i$ was biphasic (consisting of a transient lasting ≈90 s) followed by a plateau phase. Consistent with previous studies, the effect on $[Ca^{2+}]_i$ was dose-dependent (saturating at 0.1-1 μM) and occurred with no discernible delay ((Bedu-Addo et al., 2007, Lishko et al., 2011, Miller et al., 2016, Strünker et al., 2011). This rapid timescale indicates that progesterone acts on the human sperm by interacting with a receptor on the sperm plasma membrane rather than by induction of a second messenger response in the sperm cytoplasm (Lishko et al., 2011, Strünker et al., 2011). The transient rise in $[Ca^{2+}]_i$ induced by progesterone is dependent upon entry of Ca^{2+} through CatSper (Lishko et al., 2011, Strünker et al., 2011) but may be 'amplified' by consequent mobilisation of the stores through the ryanodine receptor in the mid piece/neck (CICR) (Bedu-Addo, 2008, Olson et al., 2010), resulting in tail-to- head $[Ca^{2+}]_i$ propagation in the sperm (Xia et al., 2007). The mechanism by which the initial Ca^{2+} -influx is curtailed is not

clear. The kinetics of the transient are not altered in sperm functionally null for Slo3 (Brown et al., 2016) indicating that activation of Slo3 by Ca^{2+} and consequent hyperpolarisation are not required for this process. Following the $[Ca^{2+}]_i$ transient induced by progesterone there is a Ca^{2+} plateau. This response is also dose-dependent (Harper et al., 2003). This phase may be maintained by a low level of Ca^{2+} influx through CatSper but store-operated Ca^{2+} entry, following Ca^{2+} store mobilisation, has also been proposed (Bedu-Addo, 2008, Costello et al., 2009, Lefievre et al., 2012).

4- aminopyridine also produced a rapid rise in $[Ca^{2+}]_i$ which was biphasic in nature with transient and sustained phase. The effect was clearly dose-dependent, increasing in amplitude over the entire concentration range tested (Figure 3.2 panel a). The nature of this action is less clear than the effect of P4. Though 4AP increases pHi and therefore may activate CatSper (Kirichok et al., 2006, Navarro et al., 2007), its functional effects are far greater than those exerted by a dose of NH_4Cl which induces an equivalent rise in cytoplasmic pH (Alasmari et al., 2013b). It appears that 4AP also releases stored Ca^{2+}, either by activating IP3Rs and/or inhibiting Ca^{2+} store pumps {(Alasmari et al., 2013b, Bhaskar, 2008, Grimaldi, 2001, Wu et al., 2009) see section 1.9} and that this may be responsible for the effects seen (Alasmari et al., 2013b).

3.6.2 Modulation of hyperactivated motility by P4 and 4AP

Progesterone treatment increased the proportion of hyperactivated cells by up to 1.9 fold when compared with the the control, an effect which saturated at ≈1 μM P4. The kinematic parameters VCL, and ALH increased while the LIN and BCF decreased when compared with the control. 4AP was far more effective, increasing the proportion of

hyperactivated cells by nearly 20-fold at the highest dose used (5000 µM), an effect which did not appear to saturate. The robust effect of 5mM 4AP on hyperactivated motility was also reflected in the noticeable changes effected on the frequency distributions of kinematic properties when compared with the control. VCL, ALH and BCF increased while the LIN was decreased concomitantly.

3.6.3 4AP induced change in $[Ca^{2+}]_i$ and hyperactivation is more robust than the progesterone response

Progesterone evokes a large, immediate $[Ca^{2+}]_i$ transient which rapidly dies away and is followed by a relatively modest sustained phase (fig 3.1a, see above). This effect is clearly dose dependent (Figure 3.2a; Figure 3.3a). When motility was assessed (by CASA) ≈5 min after stimulation the effects on hyperactivation were small though significant. P4 is reported to induce hyperactivation by activation of CatSper (Gakamsky et al., 2009, Kilic et al., 2009, Lishko et al., 2011, Servin-Vences et al., 2012) and it is noticeable that the observed effect of P4 on motility saturated at 1 uM, consistent with such a mode of action. However, the effect was modest and it appears that when motility is assessed not immediately (as in the studies cited above) but after decay of the $[Ca^{2+}]_i$ transient, the sustained signal supports only a modest level of hyperactivation.

Though 4AP (at the doses used here) induces a smaller $[Ca^{2+}]_i$ transient than P4, the sustained $[Ca^{2+}]_i$ signal at 5000 nM is clearly larger than that at any of the doses of P4 (compare Figures 3.2 panel c and 3.1 panel c). The ability of 4AP to induce this large sustained $[Ca^{2+}]_i$ rise probably reflects mobilisation of stored Ca^{2+}, leading to activation of SOCE (Lefievre et al., 2012). This large sustained Ca^{2+} signal may be strong enough to activate and maintain a robust level of hyperactivation (Figure 3.4b) and clear changes in

the associated kinematic parameters (Figure 3.5-3.8). A further factor that may contribute to the greater potency of 4AP than P4 as an inducer of hyperactivated motility is site of $[Ca^{2+}]_i$ elevation. The enhanced release of Ca^{2+} followed by SOCE at the sperm neck (where store-operated channels were detected; (Lefievre et al., 2012) will increase $[Ca^{2+}]_i$ in the proximal flagellum where the greatest increase in bending occurs during the transition to hyperactivation.

Though the effects of 4AP are clear, the action at 2000 nM is modest and smaller than that described by (Alasmari et al., 2013b). This may reflects the strong buffering of pHo used in the current experiments (25 mM HEPES), which maintains 4AP in its ionised form and greatly slows entry into the cytoplasm (Stephens et al., 1994). (Alasmari et al., 2013b) allowed the pHo to rise when 4AP was applied, thus increasing influx of the drug. This is addressed in chapter 4 when the effect of manipulating pH is investigated .

CHAPTER 4: EFFECT OF ELEVATED pH ON THE ACTION(S) OF Ca^{2+} MOBILISING DRUGS

4.1 Objective

Cytoplasmic pH is a key regulator of the activity of CatSper, the primary Ca^{2+} channel of human sperm. Previous evidence suggests that pHi of human sperm is sensitive to pHo and that the wide range of pH experienced by sperm in the female tract may have pronounced effects on pHi and on CatSper function. In this chapter the objectives were

i) To investigate the effect pHo on pHi of human sperm prepared in the laboratory.

ii) To compare the effects of progesterone (CatSper activation) and 4AP (Ca^{2+} store mobilisation) on $[Ca^{2+}]_i$ and motility at two different values of pHo (with known effects on pHi).

iii) To determine whether increased pHi interacts synergistically with P4 in activation of CatSper.

4.2 Introduction

As the spermatozoon ascends the female tract, different activity of the sperm is controlled with time and place by biological agonists it encounters (Inaba, 2011, Olson et al., 2010). $[Ca^{2+}]_i$ signalling, which plays a key role in regulation of all the major activities of the sperm, is dependent primarily on the activity of CatSper, a plasma membrane permeable ion channel in the flagellum, and Ca^{2+} stores in the neck/midpiece and acrosome, which contribute to regulation of hyperactivation and acrosome reaction in mammalian sperm (Bedu-Addo, 2008, Costello et al., 2009, Gu et al., 2004) .

CatSper channels are weakly voltage-sensitive but are also activated (in human sperm) by ligands such as progesterone and by increased pH_i (Carlson et al., 2003, Lishko et al., 2011, Quill et al., 2003, Ren et al., 2001). Sperm pHi is sensitive to pHo (Fraire-Zamora and Gonzalez-Martinez, 2004, Marquez and Suarez, 2007, Varner, 2015) and environmental pH within the female tract may therefore contribute significantly to regulation of CatSper activity. In mouse and bovine sperm, it has been shown that elevated pHo results in a rise in pHi and enhanced Ca^{2+} signalling due to CatSper activation (Berridge et al., 2003, Marquez and Suarez, 2007, Qi et al., 2007). Activation of CatSper channels by alkalinisation is thought to be responsible for the influx of $[Ca^{2+}]_i$ during capacitation near the oocyte and probably during binding to the zona pellucida (Xia and Ren, 2009a). Significantly, the pH of cervical mucus and of follicular and oviductal fluids increase during ovulation (Maas et al., 1977, Navarro et al., 2008), cervical mucus changing remarkably from strong acidity to values that may approach 9.0 (Eggert-Kruse et al., 1993). Since, on approaching the oocyte, the sperm encounters micromolar concentrations of P4 (Tamburrino et al., 2014), it appears that the sperm CatSper channel is simultaneously stimulated by increasing pH and by ligand binding. Electrophysiological

studies have shown that both alkalinisation and progesterone activate CatSper by shifting the current-voltage relationship to more negative voltages and it appears that simultaneous stimulation is synergistic, activating the channel to an extent that is greater than the sum of the two effects when applied separately (Lishko et al., 2011) Figure 4.0).

Accumulation and mobilisation of Ca^{2+} stored at the neck region in sperm of rodents, bulls and humans is believed to regulate hyperactivated motility (Costello et al., 2009, Ho and Suarez, 2001, Ho and Suarez, 2003, Marquez and Suarez, 2007, Publicover et al., 2007). $[Ca^{2+}]$i store mobilisation and the activation of store operated channels may cause the periodic bursts of hyperactivation stimulated by chemical cues in the female tract (Machado-Oliveira et al., 2008). 4AP is a weak base which increases sperm cytoplasmic pH and indirectly opens CatSper (Alasmari et al., 2013b, Chang and Suarez, 2011, Navarro et al., 2007), but its ability to mediate hyperactivation apparently depends primarily on mobilising Ca^{2+} from the intracellular stores (Alasmari et al., 2013a, Bedu-Addo, 2008, Bhaskar, 2008, Grimaldi, 2001, Ishida and Honda, 1993, Alasmari et al., 2013b). To cross the plasma membrane, allowing it to act on intracellular Ca^{2+} stores, 4AP must adopt its non-ionised form, permitting the drug to enter the cytoplasm (Stephens et al., 1994). It is therefore probable that its potency in mobilising Ca^{2+} and in stimulating hyperactivated motility will be enhanced at elevated pHo.

In the previous chapter (chapter 3) the dose-dependence of the effects of P4 (which activates CatSper) and 4AP (which mobilises stored Ca^{2+} in human sperm) on $[Ca^{2+}]_i$ and hyperactivated motility were investigated, 4AP proving to be a more effective modulator of sperm behaviour. In this chapter the effect of elevated pHo (and consequent intracellular alkalinisation) on these effects is investigated.

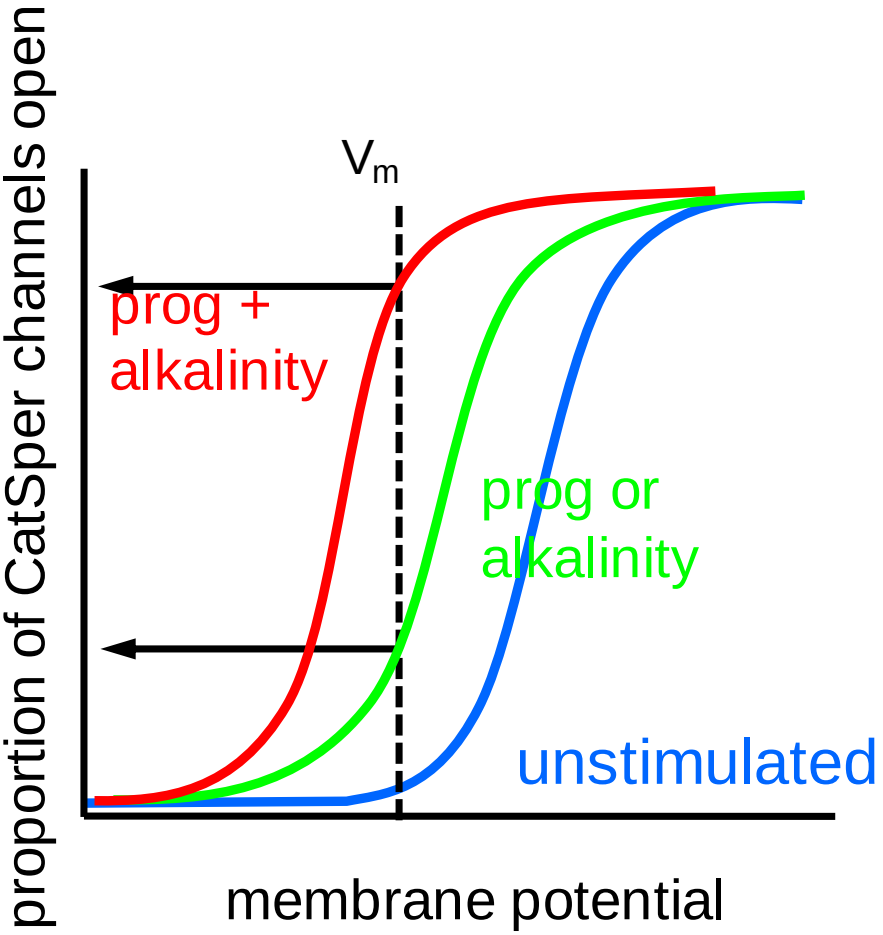

Figure 4.0: CatSper current induced by progesterone and high pH. At rest (blue), almost all channels are closed but agonists (progesterone and alkalinity) opens channels at more negative membrane potential by shifting the CatSper sensitivity to the left respectively. (adapted from (Publicover and Barratt, 2011a)

4.3 Materials and Methods

4.3.1 Materials

For the Materials section, see Chapter 2.1. 1

Progesterone (P4) and 4- aminopyridine (4AP) in pHo 7.4 and 8.5 saline respectively were used in this experiment.

4.3.2 Methods

4.3.2.1 Donor recruitment

Donor recruitment was conducted as described in Chapter 2.2.

4.3.2.2 Sperm cell preparation

The sperm cells were prepared as explained in chapter 2.4

4.3.2.3 Determination of the relationship between pHo and pHi in human sperm

The manipulation of the pHi in human sperm using pHo 6.0 – 9.0 range were performed using fluorescent pH-indicator BCECF-AM, (n = 5). It is a neutral lipophilic bis-carboxyfluorescein which can diffuse freely through the plasma membrane. On hydrolysis by esterases in the cells, BCECF is released and retained within the cytoplasm. The fluorescence intensity of BCECF is dependent upon the pH. See chapter 2.6.

4.3.2.4 Determination of pHi mediated changes on progesterone and 4-aminopyridine induced $[Ca^{2+}]_i$

The effect of pHi in progesterone and 4- aminopyridine responses on $[Ca^{2+}]_i$ were determined as reported in chapter 2.5 (P4, n = 8 and 4AP, n = 6).

4.3.2.5 To assess if calcium ion probes were saturated in high pHi and progesterone induced $[Ca^{2+}]_i$

To determine if the calcium ion probes were saturated in high pHi response to progesterone induced $[Ca^{2+}]_i$ were performed as in chapter 2.5 (0.1µMP4, n = 4 and 1µMP4, n = 8).

4.3.2.6 Determination of the effect of pHi on progesterone / 4 - aminopyridine induced hyperactivation

Assessment of the effect of pH, progesterone and 4-aminopyridine in high pH on hyperactivation were done as described in chapter 2.7 (pH, n = 34, P4, n = 21 and 4AP, n = 13).

4.3.2.7 Investigating the effect of progesterone and 4 aminopyridine on pHi

Determining the effect of calcium mobilising drugs on pHi were done as reported in chapter 2.6 (P4, n = 5 and 4AP, n = 5 at pHo 7.4 and n = 4 at pHo 8.5).

4.3.2.8 Determining whether effect of 4-aminopyridine on hyperactivation is due to pHi

To determine this, the effect of ammonium chloride (NH_4Cl) (increases the cytoplasmic pHi) on $[Ca^{2+}]_i$ and hyperactivation were carried out as reported in chapters 2.5 and 2.7 respectively. Effect of NH_4CL on; (i) pHi, (n = 5 at pHo 7.4 and n = 3 at pHo 8.5), (ii) $[Ca^{2+}]_i$, n = 6 and (iii) hyperactivation, (n = 9) respectively.

4.4 Results

4.4.1 Manipulation of pH

Assessment of pHi with BCECF-loaded cells was carried out as described in section 2.6. When cells were suspended in a range of pHo (6.0-9.0) there was a clear pH-dependence of the fluorescence ratio from the intracellular dye, showing that pHi was influenced by pHo. Upon addition of Triton-X-100, pHi equilibrated with pHo (Figure 4.1a). Using the fluorescence ratios recorded before (at pHo) and after (at pHi) cell permeabilisation it was possible to calibrate the BCECF fluorescence ratio (Figure 4.1b). There was a linear relationship between pHo and the pHi in human sperm (Figure 4.1c; R^2=0.9818). Using this approach it was shown that suspension of sperm in pHo=7.4 and pHo=8.5 resulted in pHi of 6.9 and 7.2 respectively (Figure 4.1d) and these were selected as appropriate values for subsequent experiments to determine; (a) the effect of alkalinisation on actions of progesterone and 4- aminopyridine on $[Ca^{2+}]_i$ and sperm motility and (b) the effect of progesterone and 4AP on pHi.

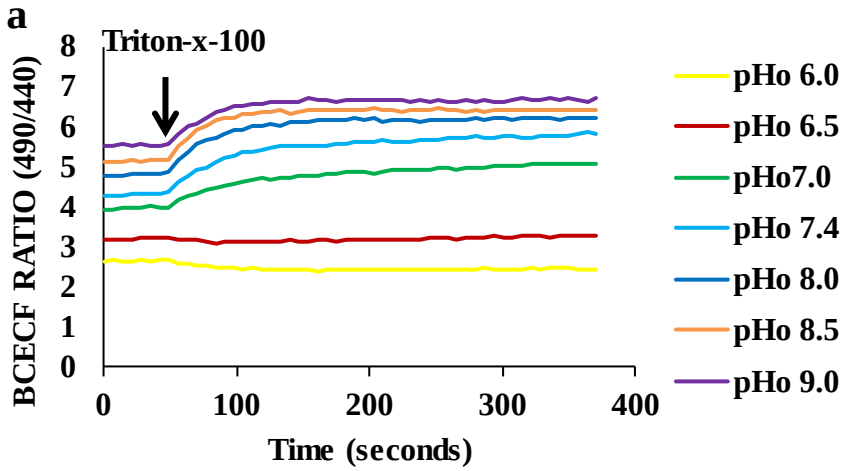

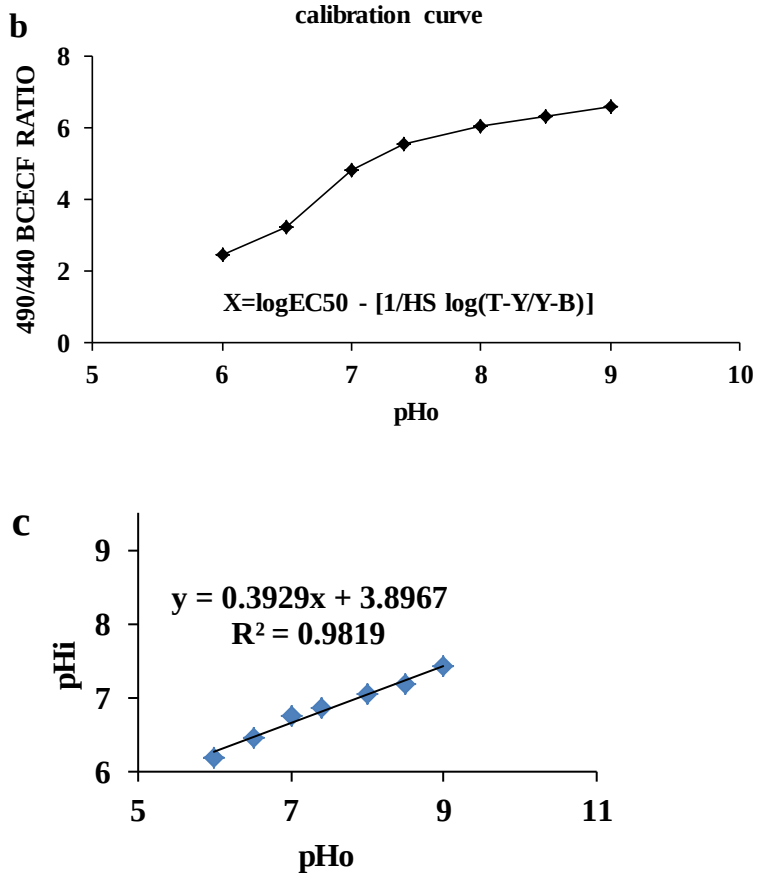

Figure 4.1: The calibration curve of human sperm fluorescence at various pHo. a –The BCECF fluorescence ratio increased with increasing pHo and on permeabilisation there was a further rise in the fluorescence ratio at pHo 7.0 – 9.0 respectively. b shows the calibration curve of BCECF fluorescence ratio and pHo. c shows extracellular pHo 7.4 and 8.5 produced intracellular pH 6.9 and 7.2 respectively

4.4.1.2 Resting calcium at pHo=7.4 and pHo=8.5

In alkalinising saline (pHo=8.5) resting $[Ca^{2+}]_i$ (fluorescence of Fluo4) was approximately 55% higher than in standard saline (***P < 0.001, n = 14, paired t - test; Figure 4.2). This effect was similar whether salines were buffered with 15 mM or 25 mM HEPES. However, when 4AP was added to saline buffered with 15 mM HEPES there was a clear rise in pHo and therefore experiments on the effects of 4AP and P4 used salines with 25 mM HEPES buffering.

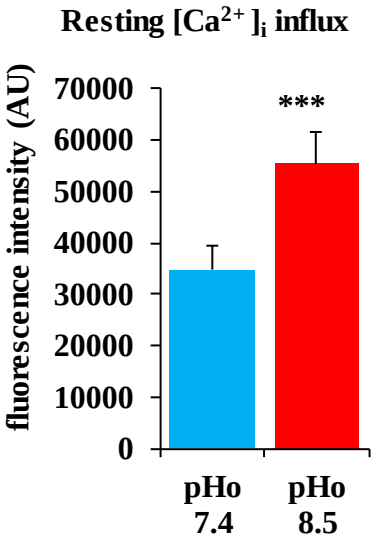

Figure 4.2: Alkalinisation significantly increased the mean basal $[Ca^{2+}]_i$ fluorescence intensity (fluo 4) (*P < 0.001, n =14).**

4.4.2 Effect of alkalinisation on P4-induced $[Ca^{2+}]_i$ responses in human sperm

Stimulation of cells suspended in saline pH 7.4 with P4 -induced a biphasic $[Ca^{2+}]_i$ response with a transient that lasted for ≈1.5 minutes followed by a sustained phase (Figure 4.3a). At pHo 8.5 a similar pattern was seen but the decay of the $[Ca^{2+}]_i$ transient was much slower (Figure 4.3b)

At both pH 7.4 and 8.5 the size of the $[Ca^{2+}]_i$ transient was dose-dependent over the range of concentrations used and saturated at 0.1 µM -1 µM (***P < 0.001, *P < 0.05, n=8). Surprisingly the maximum amplitude of the $[Ca^{2+}]_i$ transient at pHo=7.4 was slightly larger than at pHo=8.5 (approximately 69000 and 55000 respectively; Figure 4.3c) though this difference in transient amplitude was non- significant (P > 0.05, n = 8) (Figure 4.3c).

The sustained phase of the $[Ca^{2+}]_i$ response evoked by P4 (recorded 5 min after stimulation) was also dose-dependent (Figure 4.3d). The responses at pH 7.4 and 8.5 were of similar amplitude (≈19,000 units) at 1µM and both saturated at approximately 0.1 µM (Figure 4.3d).

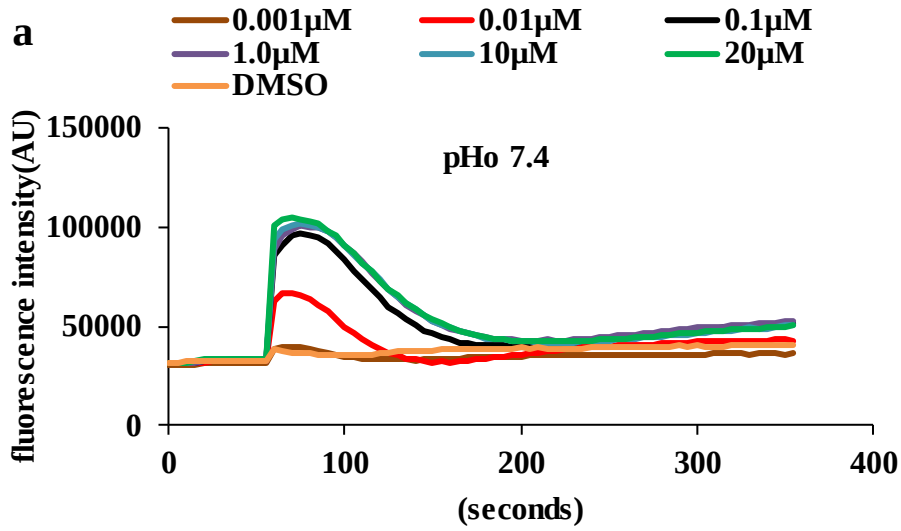

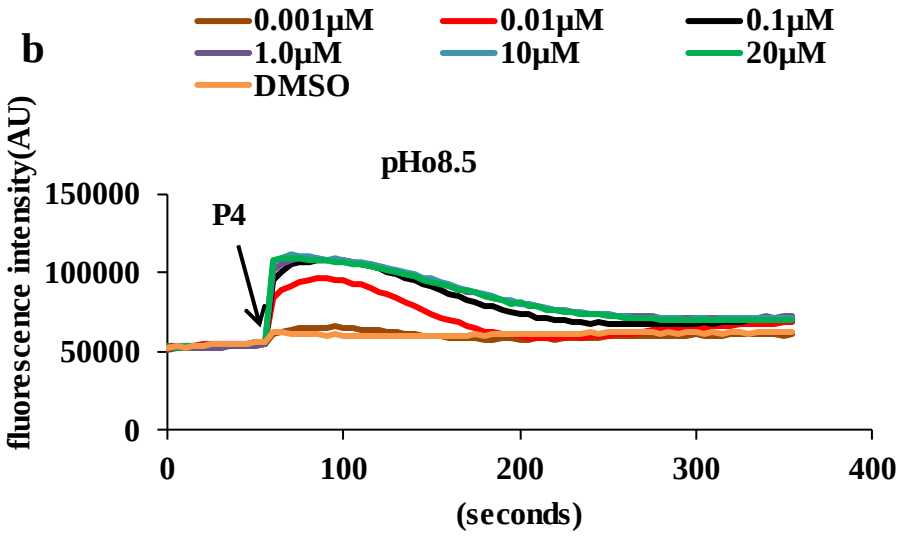
b
0.001µM
0.01µM
0.1µM
1.0µM
10µM
20µM
DMSO
pHo8.5
P4
fluorescence intensity(AU)
150000
100000
50000
0
0
100
200
300
400
(seconds)

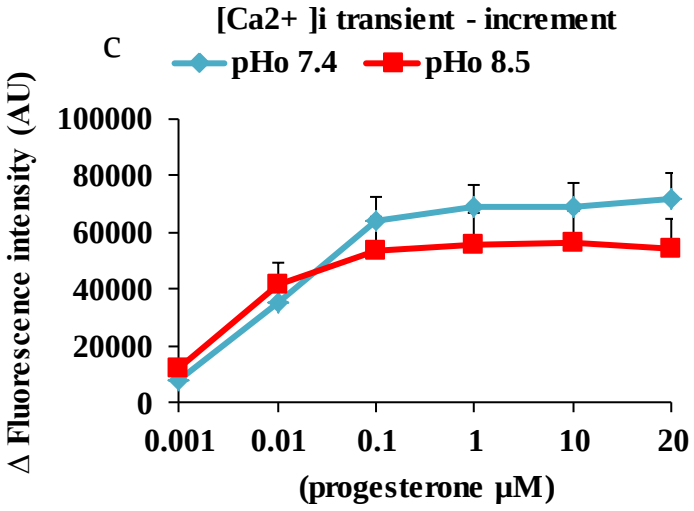
C
[Ca2+]i transient - increment
pHo 7.4
pHo 8.5
Δ Fluorescence intensity (AU)
100000
80000
60000
40000
20000
0
0.001
0.01
0.1
1
10
20
(progesterone µM)

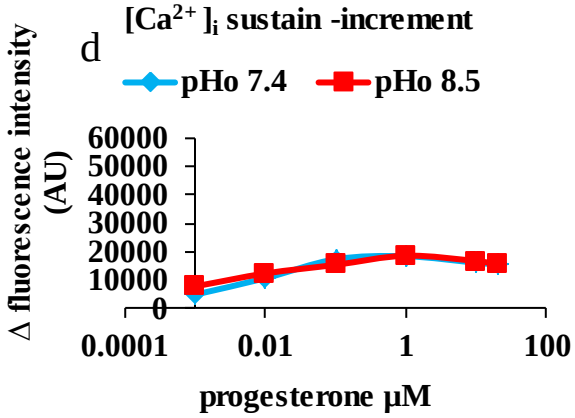

Figure 4.3: Effect of alkalinisation on P4 -induced $[Ca^{2+}]_i$. a and b - At both pHo 7.4 and 8.5 there was biphasic evoked $[Ca^{2+}]_i$ by P4 (n = 8). c and d show the dose - dependent transient and sustained response of P4 at pHo 7.4 and 8.5 respectively.

4.4.3 Use of alternative Ca^{2+} dyes to ascertain if fluo-4 probe was saturated in high pHi response to P4 -induced $[Ca^{2+}]_i$

The finding that the transient $[Ca^{2+}]_i$ increase induced by P4, which is believed to be primarily generated by activation of CatSper (Lishko et al, 2011; Strunker et al, 2011) was no greater at pHo =8.5 than that at pHo=7.4 was surprising (see introduction) and could possibly be an artefact due to saturation of the Fluo4 dye. Transient $[Ca^{2+}]_i$ responses to P4 were therefore assessed using two alternative dyes (the emission ratio dye fura-2 and the low affinity dye fluo5F).

In the fura-2 loaded sperm cells $[Ca^{2+}]$i was assessed using ratio of emission at 340 nM and 380 nM. The transient increase in this ratio upon stimulation with 1 uM P4 was greater at pHo=8.5 than at pHo=7.4 ($P = 0.03$, n = 6) (Figure 4.4a).

In the sperm cells loaded with fluo-5F probe, alkalinisation (pHo=8.5) did not change the size of the $[Ca^{2+}]_i$ increment induced by 0.1 µM (P = 0.53, n = 4,blue panel) or 1 µM (P = 0.61, n = 8, red panel) P4 (Figure 4.4b).

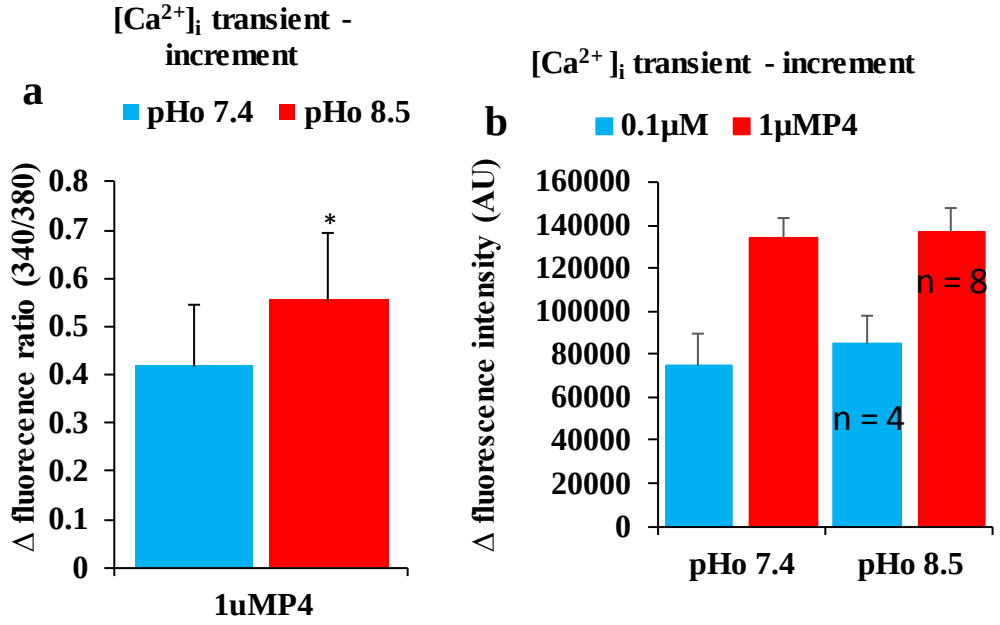

Figure 4.4: Effect of alternative Ca^{2+} dyes in response of high pHi on P4 induced $[Ca^{2+}]_i$. In a, P4 induced a higher transient Ca^{2+} response in high pH with fura-2 loaded sperm cells (n = 6). b shows no change in the effect of P4 in high pH on the transient response when sperm cells were loaded with fuo-5F dye (0.1µMP4, n = 4) and (1µMP4, n = 8).

4.4.4 Effect of alkalinisation on 4AP-induced $[Ca^{2+}]_i$ responses in human sperm

Stimulation of cells suspended in saline pH 7.4 or pH 8.5 with 4AP induced a biphasic $[Ca^{2+}]_i$ response with a transient that peaked within 30 s and decayed over a further 60-90 s followed by a sustained phase (Figure 4.5a). At pHo 8.5 a similar pattern was seen but the decay of the $[Ca^{2+}]_i$ transient was much slower and it was often difficult to differentiate the transient from the sustained phase (Figure 4.5b).

Over the range of concentrations used (200-5000 µM) both the transient peak and sustained $[Ca^{2+}]_i$ elevation (recorded 5 min after stimulation) were dose - dependent at both pH values (*P < 0.05,***P < 0.001, n = 6). At lower concentrations (0-2000 µM) the 4AP-induced transient appeared slightly larger at pHo=8.5 (red traces) but this difference was not significant (P > 0.05, n = 6, Figure 4.5c). The amplitude of the $[Ca^{2+}]$i transient saturated at ≈38,000 at both pHo=7.4 (blue traces) and pHo=8.5 (red traces) (Figure 4.5 c). In contrast, the sustained $[Ca^{2+}]$i increase (5 min after stimulation) was greater at pHo=8.5 (red traces) over the entire concentration range tested and the dose-dependence showed no sign of saturation at either pHo (Figure 4.5d).

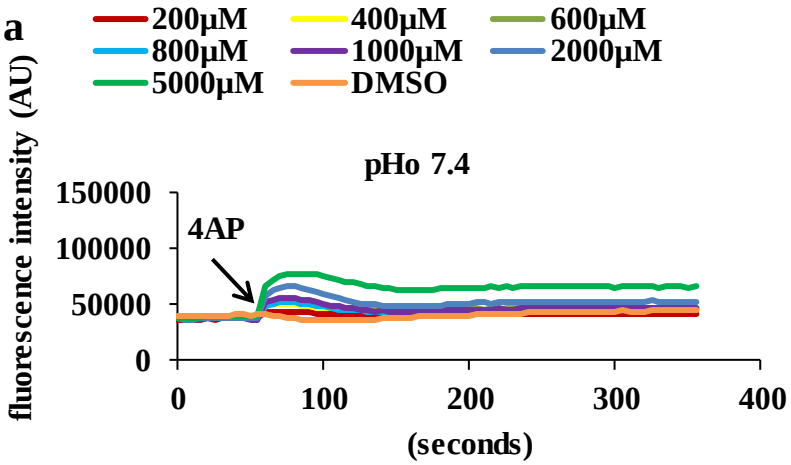
a
200µM
400µM
600µM
800µM
1000µM
2000µM
5000µM
DMSO
pHo 7.4
fluorescence intensity (AU)
150000
100000
50000
0
4AP
0
100
200
300
400
(seconds)

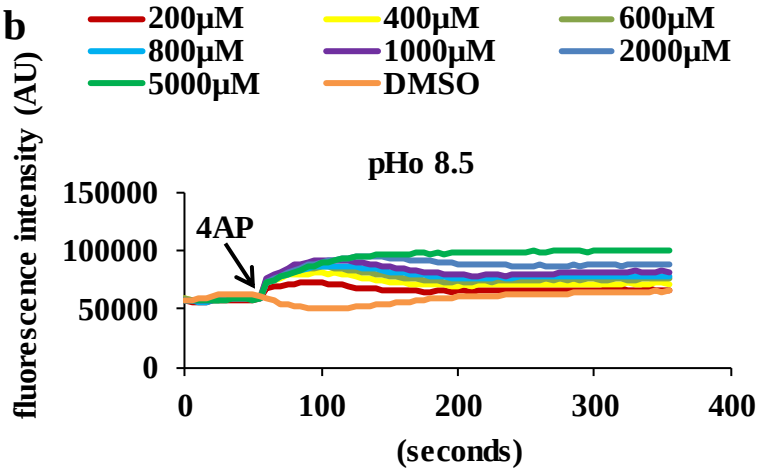
b
200µM
400µM
600µM
800µM
1000µM
2000µM
5000µM
DMSO
pHo 8.5
fluorescence intensity (AU)
150000
100000
50000
0
4AP
0
100
200
300
400
(seconds)

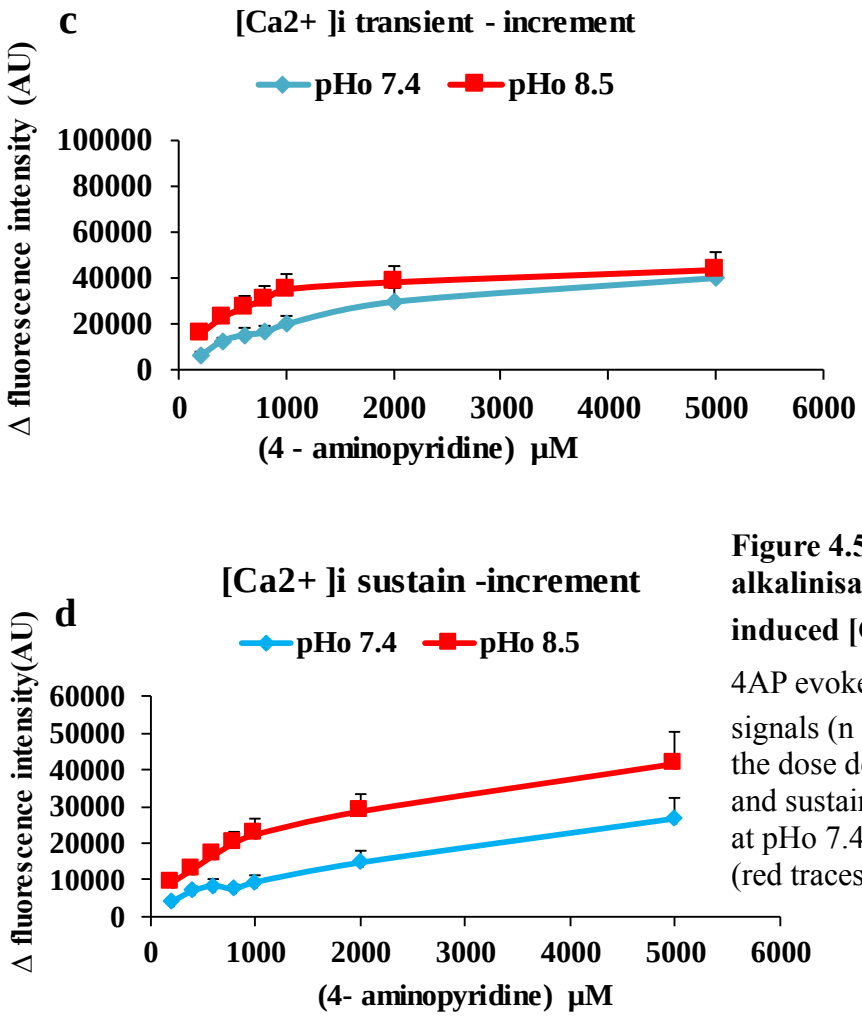

Figure 4.5: Effect of alkalinisation on 4AP - induced $[Ca^{2+}]_i$. a and b - 4AP evoked biphasic $[Ca^{2+}]_i$ signals (n = 6). c and d- show the dose dependent transient and sustained response of 4AP at pHo 7.4 (blue traces) and 8.5 (red traces) respectively.

4.4.5 Effect of progesterone and 4- aminopyridine on motility in human sperm at alkaline pH

4.4.5.1 pH and kinematic parameters of motility

Alkalinisation (pHo=8.5) significantly increased the level of hyperactivated motility compared that of cells at pHo=7.4. A pHo=7.4 (blue panel, Figure 4.6a) 1.75 ± 0.46 % of cells were assessed as hyperactivated by CASA but at pHo=8.5 (red panel, Figure 4.6a),

there was 6-fold increase to 10.53 ± 1.56 %t ($P = 1.06 \times 10^{-7}$, n = 34, paired t-test; Figure 4.6a). Alkalinisation significantly increased the basal curvilinear velocity (VCL; $P = 1.47 \times 10^{-8}$), amplitude lateral head displacement (ALH; $P=2.54 \times 10^{-10}$) and beat cross frequency (BCF; $P = 2.32 \times 10^{-5}$). Linearity (LIN) decreased from 60.1±1.2 to 58.0±1.5 % but this effect was not significant (P = 0.12; n = 34, paired t- test) (Figure 4.6b - e).

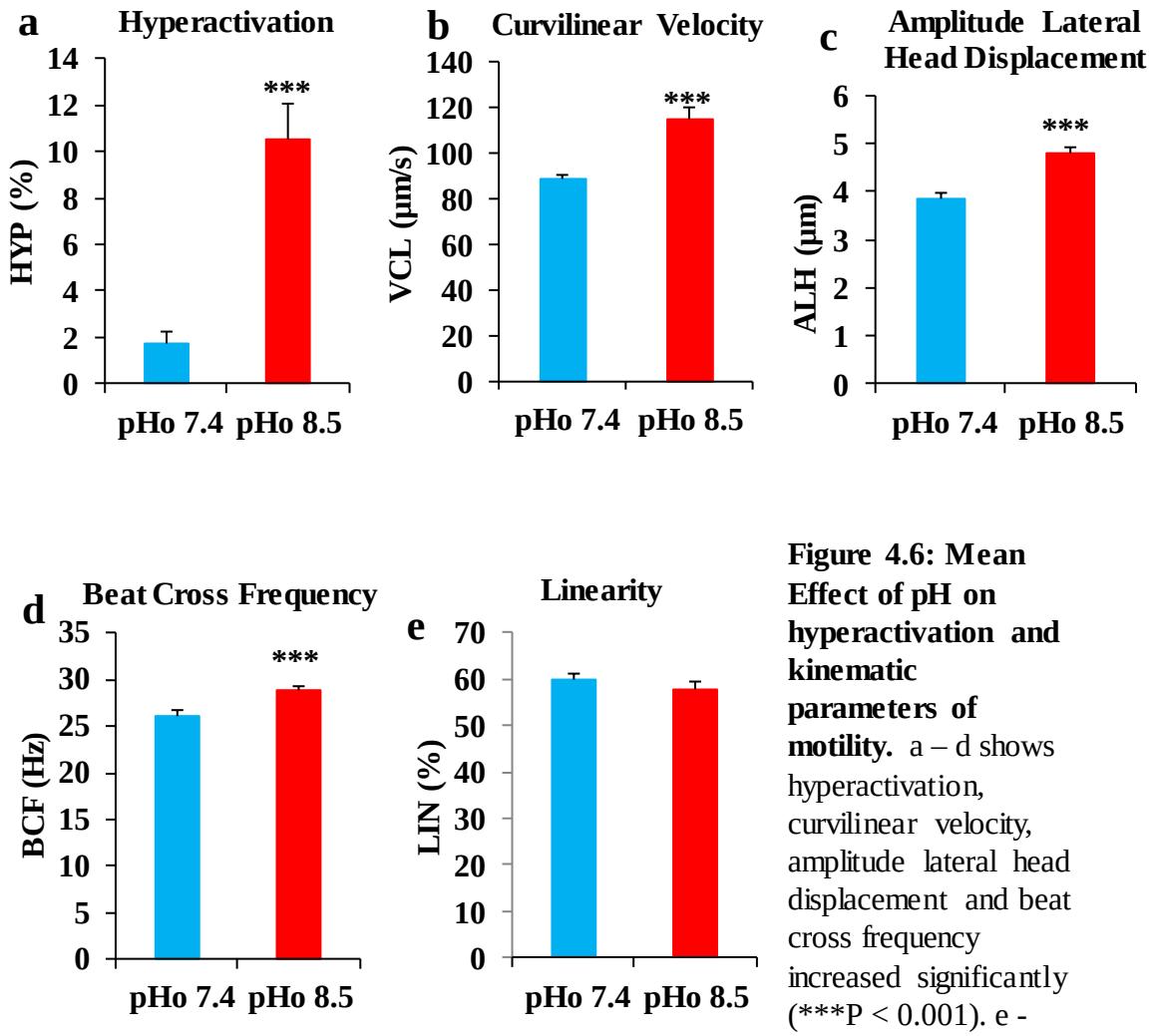

Figure 4.6: Mean Effect of pH on hyperactivation and kinematic parameters of motility. a – d shows hyperactivation, curvilinear velocity, amplitude lateral head displacement and beat cross frequency increased significantly (***P < 0.001). e - Linearity decreased non – significantly (P > 0.05) in pHi 7.2 (red panel) when compared with pHi 6.9 (blue panel) (n = 34).

Frequency distributions of the kinematic parameters measured by CASA, showed that alkalinisation shifted the VCL and BCF distributions to the right (decreasing the number of cells showing lower values of VCL and BCF) (Figure 4.7f, h). ALH modal value was not changed by alkalinisation but the distribution became more skewed with a long tail of high values. The distribution for LIN showed little change at the higher pH (Figure 4.7g, i).

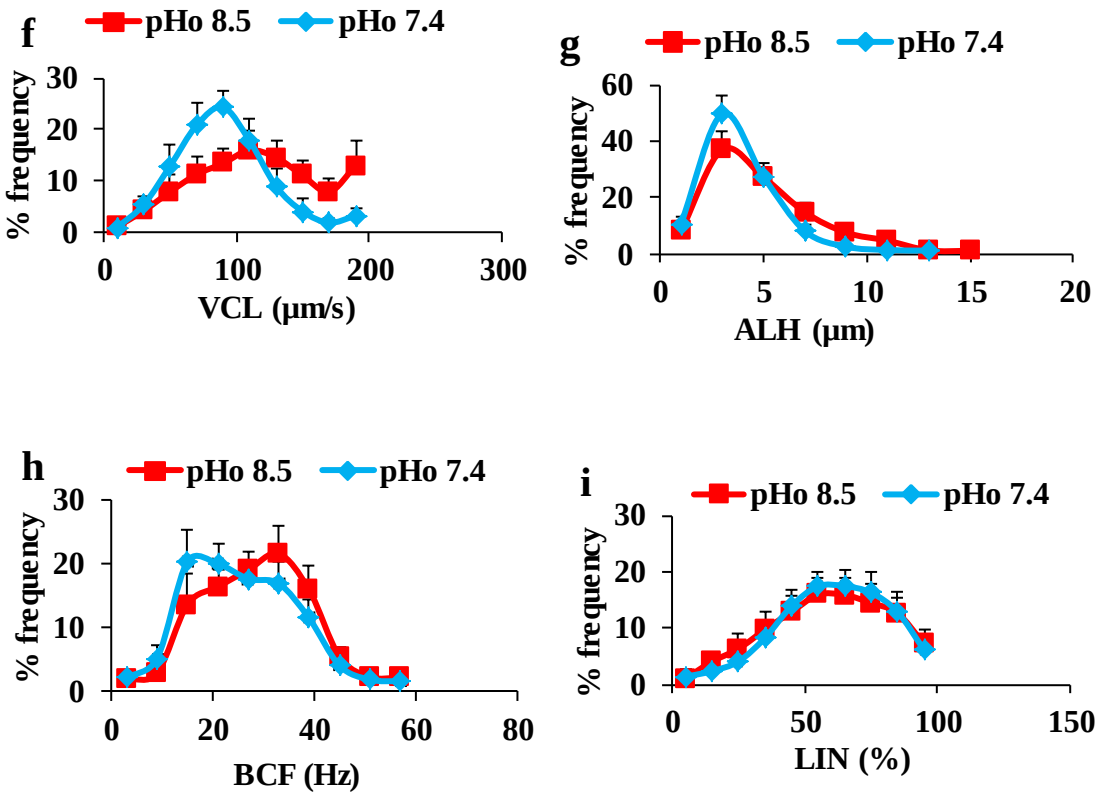

Figure 4.7: The frequency distribution of kinematic parameters induced in pH. F and h – High pH (red traces) increased the VCL and BCF distribution by shifting to the right. g – In high pH, there was small increase in number of cells with high ALH value due to slight shift to the right. i – Slight reduction in the percent of cells that have Linearity ≥ 50 compared to pH 7.4 (blue traces) (n = 34).

4.4.5.2 Progesterone and 4AP induced hyperactivation at alkaline pH

Cells were exposed to high pHo for 5 min before stimulation with P4 or 4AP. Induction of hyperactivation by P4 showed negligible sensitivity to alkalinisation. P4 induced hyperactivation at pHo=8.5 (red traces, Figure 4.8a) was ≤5% at all doses, showed no dose-dependence and was not significantly different to that at pHo=7.4 (blue traces; P > 0.05, n = 21) (Figure 4.8a).

Stimulation with 4AP at pHo=8.5 induced a dose-dependent increase in hyperactivation that significantly exceeded the effect of the drug at pHo=7.4 at every concentration tested (200-5000 µM; ***P < 0.001, **P < 0.01, n = 13) (Figure 4.8b). The dose effect curve for 4AP at pHo=8.5 appeared to have two phases with a large effect between 0 and 1 µM that was not apparent at pHo=7.4, and then a continuous but more gentle increase up to 5000 µM (Figure 4.8b).

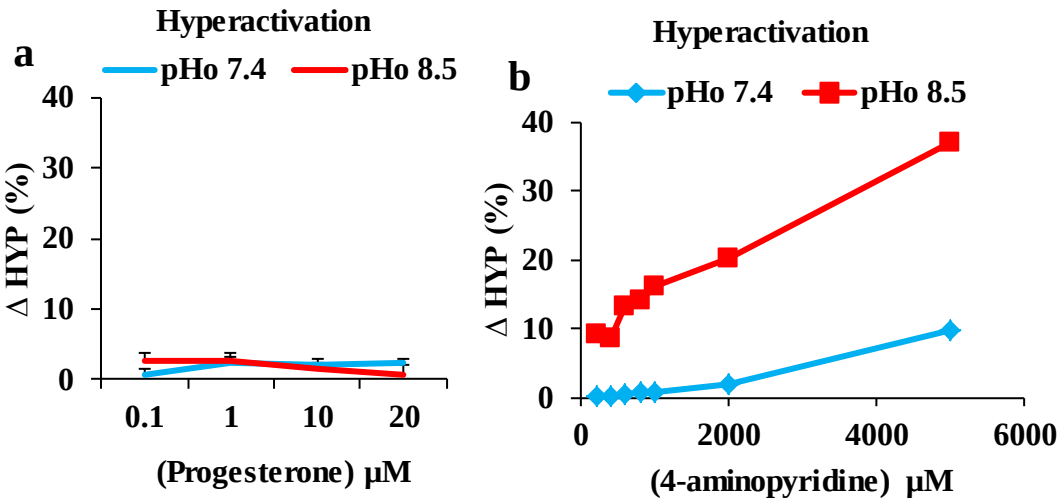

Figure 4.8: Effect of progesterone and 4 – aminopyridine response in high pHo on hyperactivation. a- p4 induced the same effect on hyperactivation at both pHo 7.4 (blue traces) and 8.5 (red traces) (n = 21). b- Hyperactivation is dose-dependent and potentiated in high pHo by 4AP (n = 13).

4.4.5.3 Effect of progesterone and 4AP on kinematic parameters of motility at alkaline pH

4.4.5.3.1 Curvilinear Velocity (VCL)

Alkalinisation failed to modify the effect of P4 on curvilinear velocity. As at pHo=7.4, there was no significant effect at any dose of P4 at pHo=8.5 (Figure 4.9a). At pHo=8.5 the effect of 4AP on VCL (red traces) was significantly enhanced (Figure 4.9b). VCL was significantly increased (compared to control) at all doses (**P < 0.01, *P < 0.05, n = 13) whereas at pHo=7.4 4AP increased VCL only at the highest doses (see section 3.4.3.2) (Figure 4.9b).

4AP shifted the VCL frequency curve to the right with more proportion of cells with VCL ≥ 170µm/s compared to the control pHi 6.9 (Figure 4.9c, d).

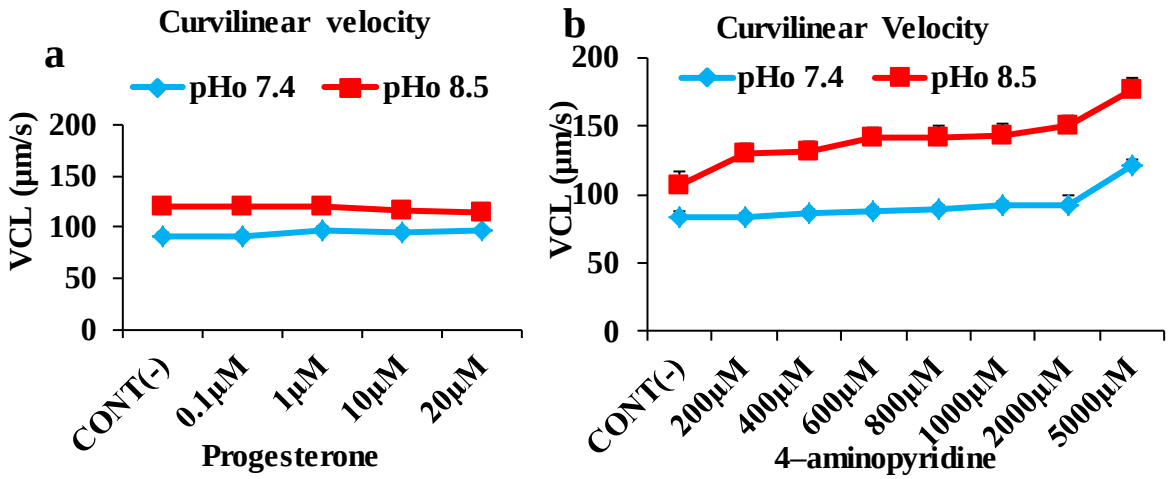

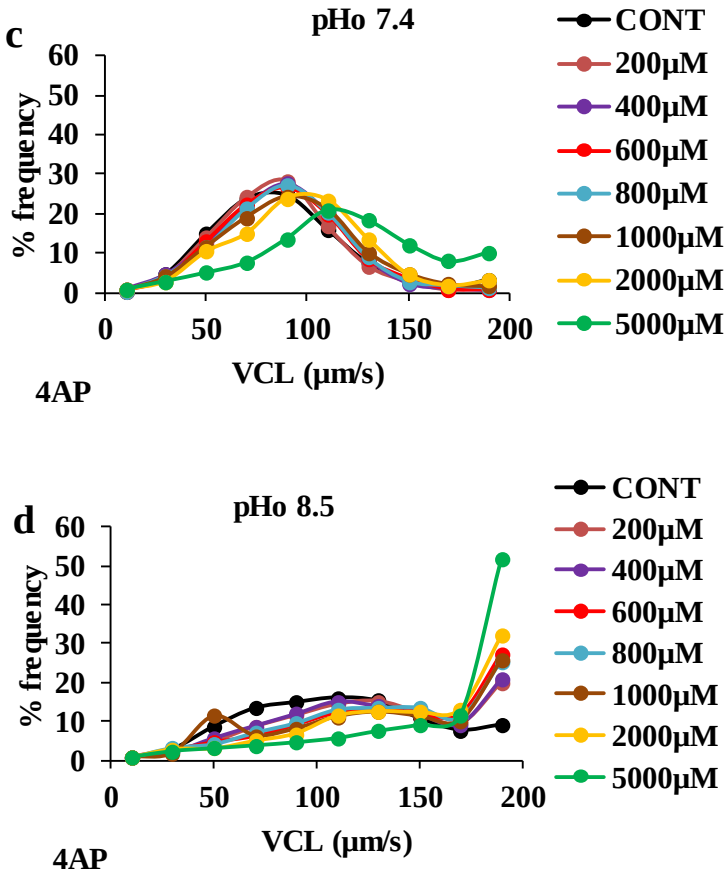

Figure 4.9: Effect of progesterone and 4 – aminopyridine on VCL in high pHo. a – There is no change in the effect of P4 on VCL at pHo 7.4 (blue traces) and 8.5 (red traces). b – VCL is increased significantly by 4AP across all doses at pHo 8.5 (red traces) compared to pHo 7.4 (blue traces) (***P < 0.001, n = 13). c and d – 4AP shifted VCL distribution to the right at pHo 8.5 increasing population with high VCL.

4.4.5.3.2 Amplitude lateral head displacement (ALH)

Alkalinisation failed to modify the effect of P4 on ALH. There was no clear dose-dependency over the dose range used (Figure 4.10 a). At pHo=8.5 the effect of 4AP on ALH (red traces) was significantly enhanced (Figure 4.10, panel b). ALH was significantly increased (compared to control) at all doses (***P < 0.001,**P < 0.01, n = 13) whereas at pHo=7.4 4AP increased ALH only at the highest doses (see section 3.4.3.2).

4AP shifted the distribution of ALH values to the right with a greater proportion of cells with ALH ≥7 µm compared to untreated cells. At the highest 4AP concentration (5000 µM) the ALH distribution appeared bimodal with a peak at 9 µm as well as a clear shoulder at ≈3 µm, the modal value in control cells (Figure 4.10 c, d).

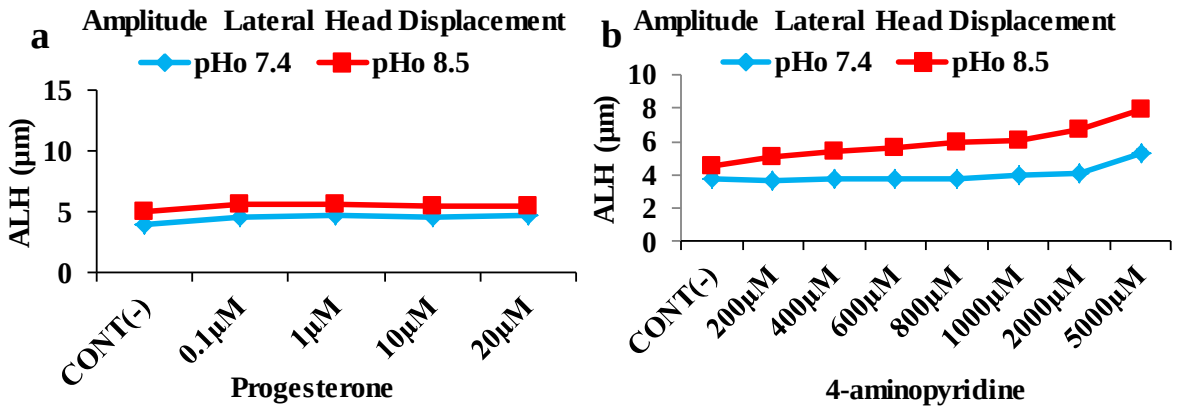

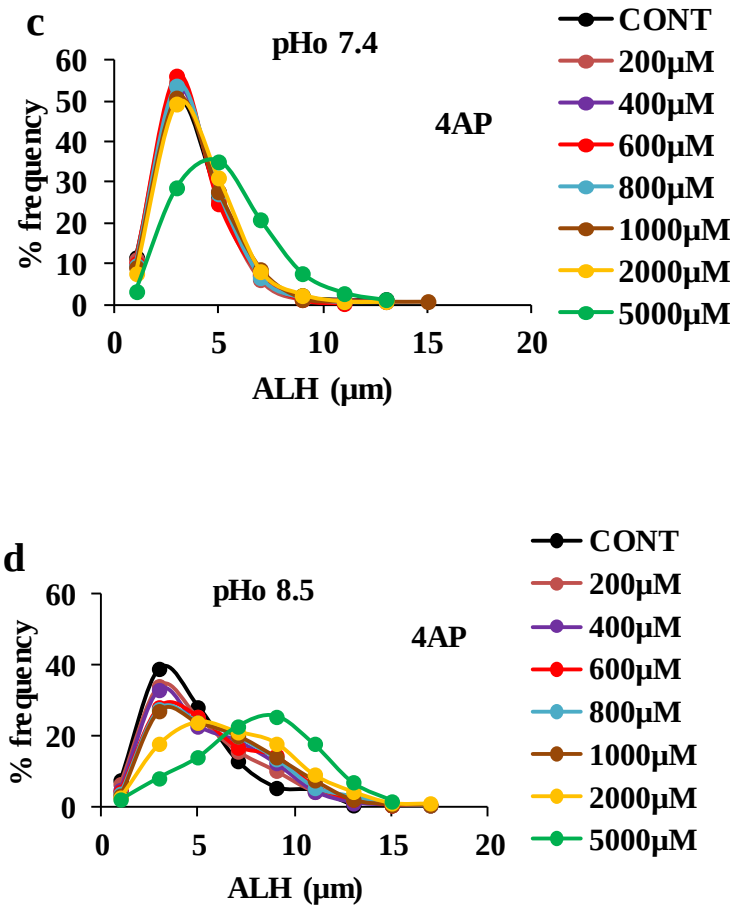

Figure 4.10: Effect of P4 and 4AP on ALH in high pHo. a – There is no change in the effect of P4 on ALH at pHo 7.4 (blue traces) and 8.5 (red traces) (n = 21). b – ALH is increased significantly by 4AP across all doses at pHo 8.5 (red traces) compared significantly (***P < 0.001,**P < 0.01, n = 13). c and d – At 5000 µM, 4AP shifted ALH distribution to the right at pHo 8.5 with bimodal values.

4.4.5.3.3 Beat cross frequency (BCF)

The effect of progesterone on the rate at which the sperm cell crosses the average path (BCF) was similar at pHo=8.5 to that at pHo=7.4 ($P > 0.05$, $n = 21$). Also, as at pHo=7.4, though BCF of progesterone-treated cells differed signifcantly from control ($P < 0.05$, $n = 21$) there was no significant dose-sensitivity ($P > 0.05$, n=21). (Figure 4.10 a).

Similarly to the effect of progesterone, the effect of 4AP on the BCF at pHo=8.5 was not significantly different from that at pHo=7.4 ($P > 0.05$, n=13).

The frequency distribution for BCF in the presence of progesterone at pHo=8.5 shifted to the left with the modal value clearly moving from 35 Hz to ≈20 Hz (Figure 4.11 c, d).

4AP (1000 – 5000µM) at pHo=8.5 acted similarly to BCF; shifted the BCF curve to the left and changed the modal value from 35 Hz to ≈20 Hz (Figure 4.11 e, f).

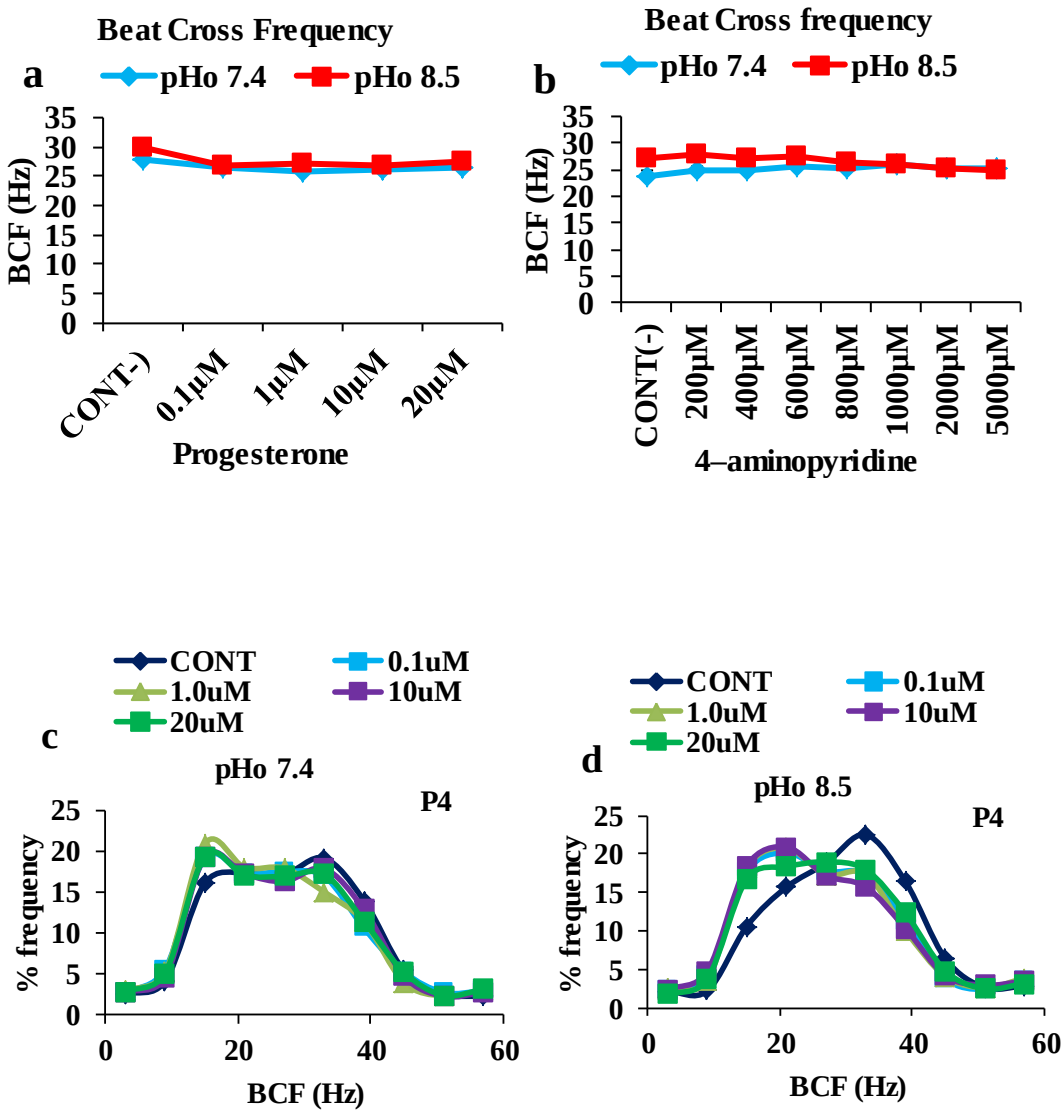

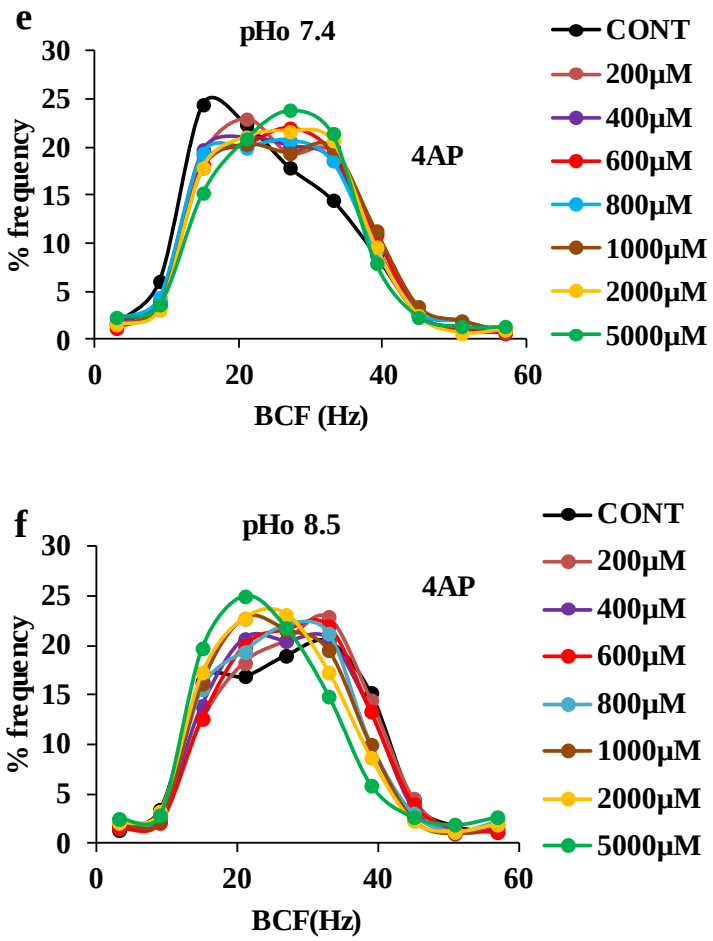

Figure 4.11: Effect of P4 and 4AP on BCF at both pHo 7.4 and 8.5. a and b – P4 and 4AP effect on BCF did not change in high pHo compared to pHo 7.4 ($P > 0.05$). c and d – In the frequency distribution, progesterone in high pHo shifted the BCF curve to left (n= 21). e and f – High [4AP] shifted the BCF curve to the left in high pHo 8.5 (n = 13).

4.4.5.3.4 Linearity (LIN)

The effect of P4 on the linearity of the sperm path (LIN) was similar at pHo=8.5 to that at pHo=7.4 ($P > 0.05$, n = 21). As at pHo=7.4, LIN of P4-treated cells at pHo=8.5 was significantly lower than that of the untreated control (***$P < 0.001$, n =21) (Figure 4.12 a), but there was no significant dose-dependent effect ($P > 0.05$, n =21).

Whereas 4AP when applied at pHo=7.4 had no significant effect on linearity compared to control, at pHo=8.5 there was a dose-dependent decrease in linearity (***P < 0.001, *P < 0.05, n = 13) (Figure 4.12 b). At pHo=8.5 P4, at all doses tested, shifted the frequency distribution for linearity to the left, similarly to at pHo=7.4 (Figure 4.12 c, d). 4AP at pHo 8.5 also shifted the distribution to the left, especially at higher doses of (2000 – 5000 µM) (Figure 4.12, panel e, f).

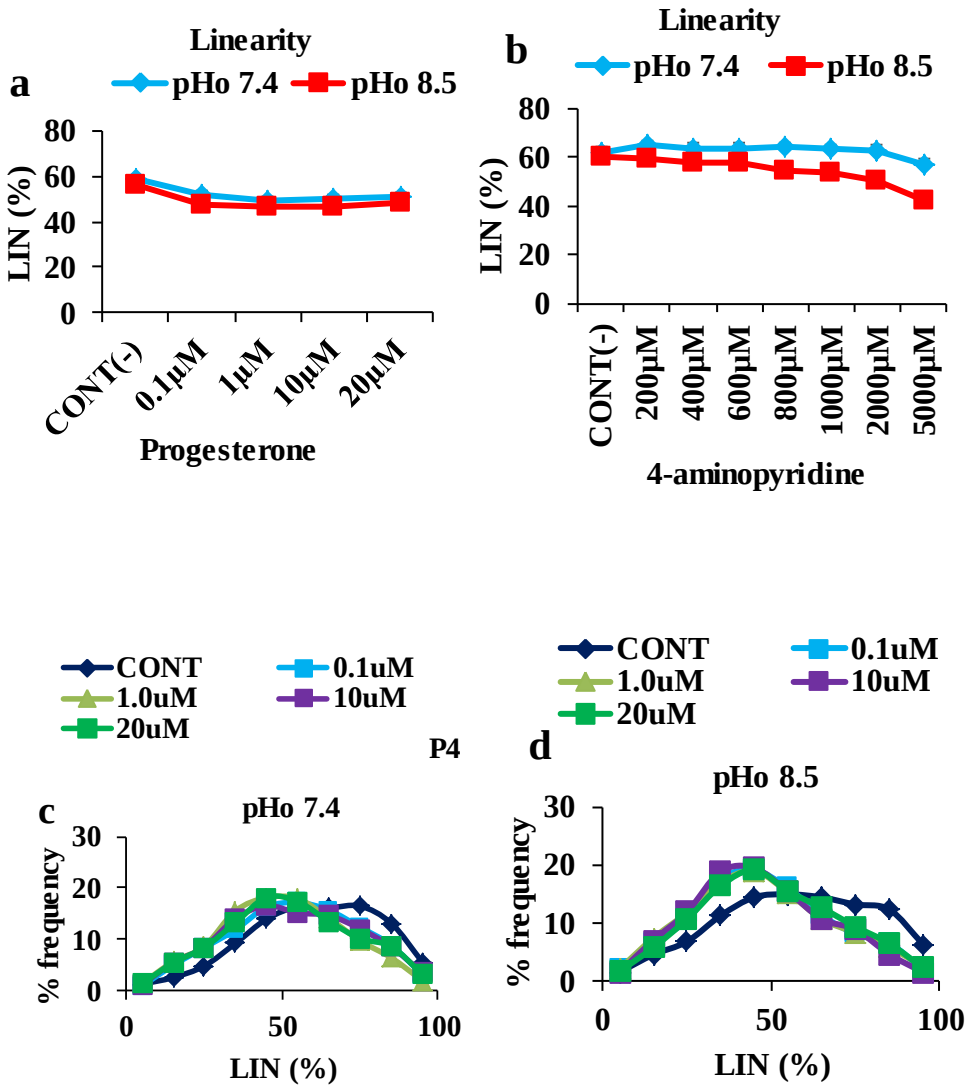

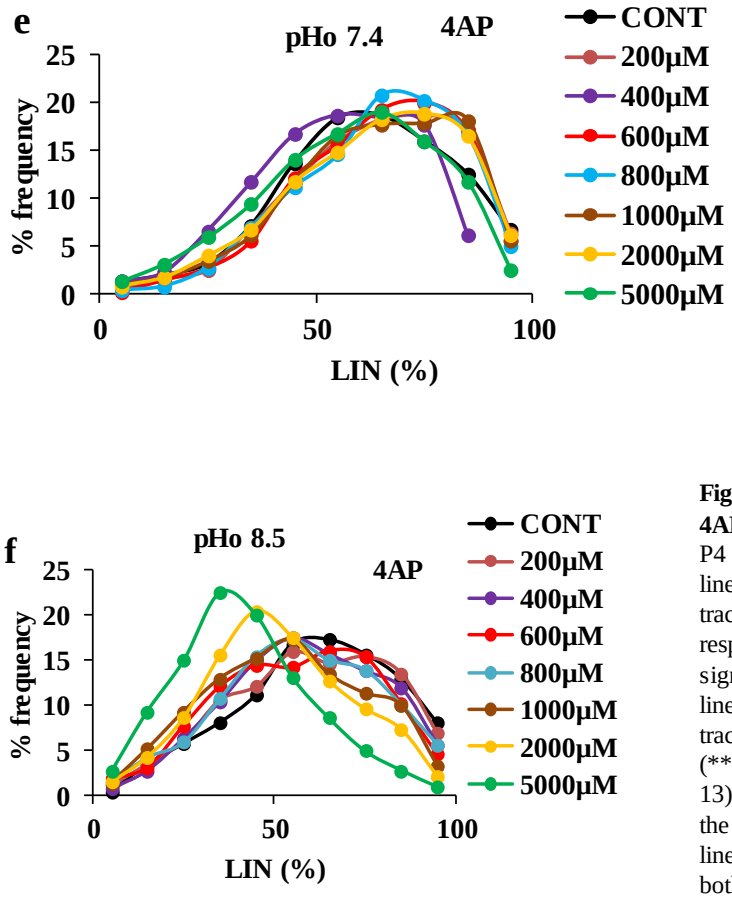

Figure 4.12: Effect of P4 and 4AP on Linearity in pHo. a – P4 did not change percent linearity at pHo 7.4 (blue traces) and pHo 8.5 (red traces) respectively (n = 21). b – 4AP significantly decreased the linearity in high pHo (red traces) compared to pHo 7.4 (***P < 0.001, *P < 0.05, n = 13). c and d show P4 shifted the frequency distribution of the linearity curve to the left at both pHo 7.4 and 8.5. e and f – At pHo 8.5, 4AP shifted the linearity curve to the left at higher doses of (2000 – 5000) µM compared to pHo 7.4.

4.4.6 Determining the effect of progesterone and 4AP on pHi

MSO and progesterone (1, 10, 20 µM) did not modify pHi at pHo=7.4 or pHo=8.5 (n =5; Figure 4.13a-c) but 2 mM 4AP elevated the pHi by 0.16 ± 0.05 (n = 5) and 0.52 ± 0.19 (n = 4) pH units when applied at pHo=7.4 and pHo=8.5 respectively (*P =0.04 and P = 0.07, paired t – test, light brown traces respectively) (Figure 4.13 a-c).

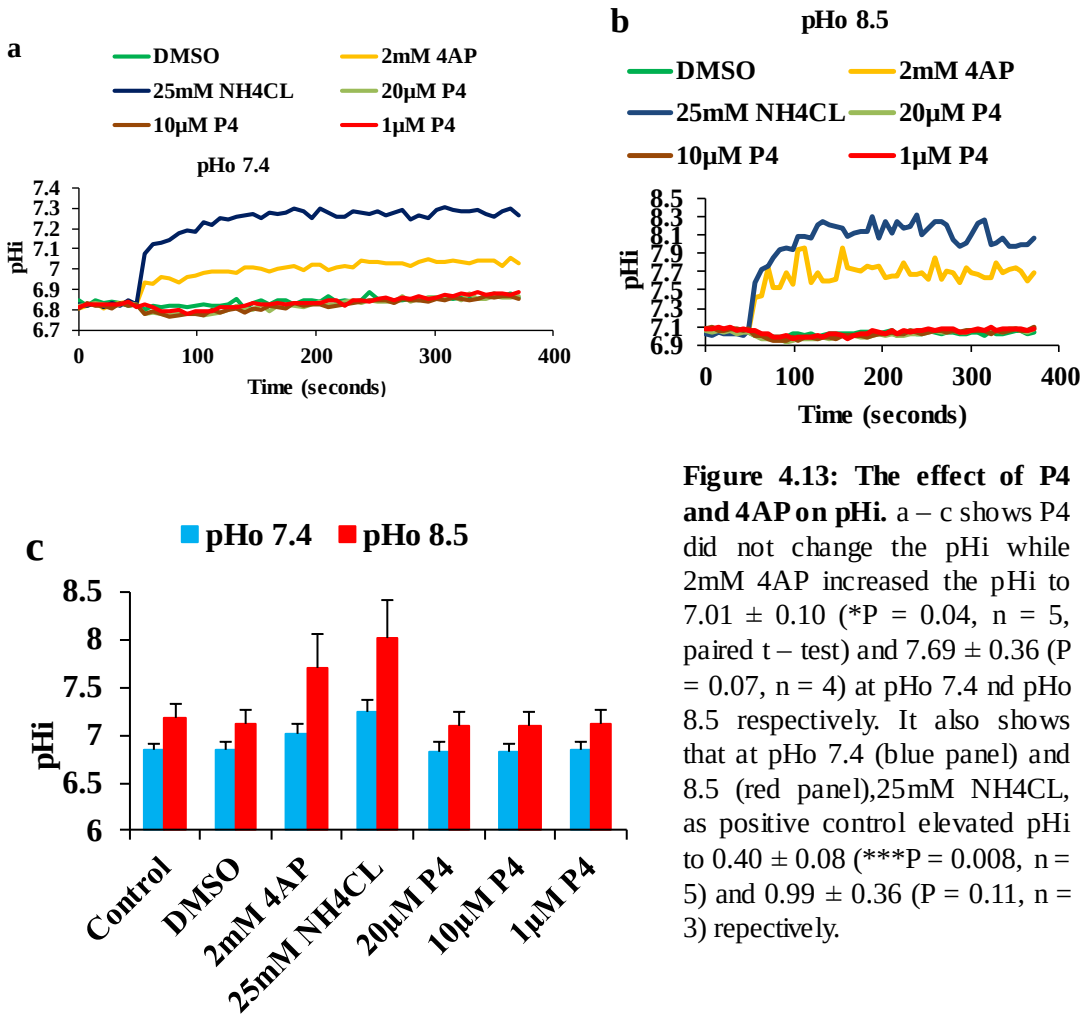

Figure 4.13: The effect of P4 and 4AP on pHi. a – c shows P4 did not change the pHi while 2mM 4AP increased the pHi to 7.01 ± 0.10 (*P = 0.04, n = 5, paired t – test) and 7.69 ± 0.36 (P = 0.07, n = 4) at pHo 7.4 nd pHo 8.5 respectively. It also shows that at pHo 7.4 (blue panel) and 8.5 (red panel),25mM NH4CL, as positive control elevated pHi to 0.40 ± 0.08 (***P = 0.008, n = 5) and 0.99 ± 0.36 (P = 0.11, n = 3) repectively.

4.4.6.1 Is the stimulation of hyperactivation by 2mM 4AP due to cytoplasmic alkalinisation?

Since 4AP significantly increased pHi, particularly in cells bathed in saline at pH 8.5, ammonium chloride (NH_4Cl; 25mM), was used to assess the effect of intracellular alkalinisation. 25 mM NH_4Cl elevated pHi by 0.40 ± 0.08 (n = 5) and 0.99 ± 0.36 (n =3) at

pHo=7.4 and pHo=8.5 respectively (***P = 0.008 and P = 0.11, paired t – test, deep blue traces, respectively) (Figure 4.13, panel a-c).

25mM NH_4Cl increased $[Ca^{2+}]_i$ to a level at least as great as 4AP at both pHo=7.4 and pHo=8.5 (Figure 4.14 d, e) but the ability of NH_4Cl to induce hyperactivation was negligible, whereas 4AP, applied in parallel experiments, was clearly effective (Figure 4.14 f), as described above (Figure 4.7 b).

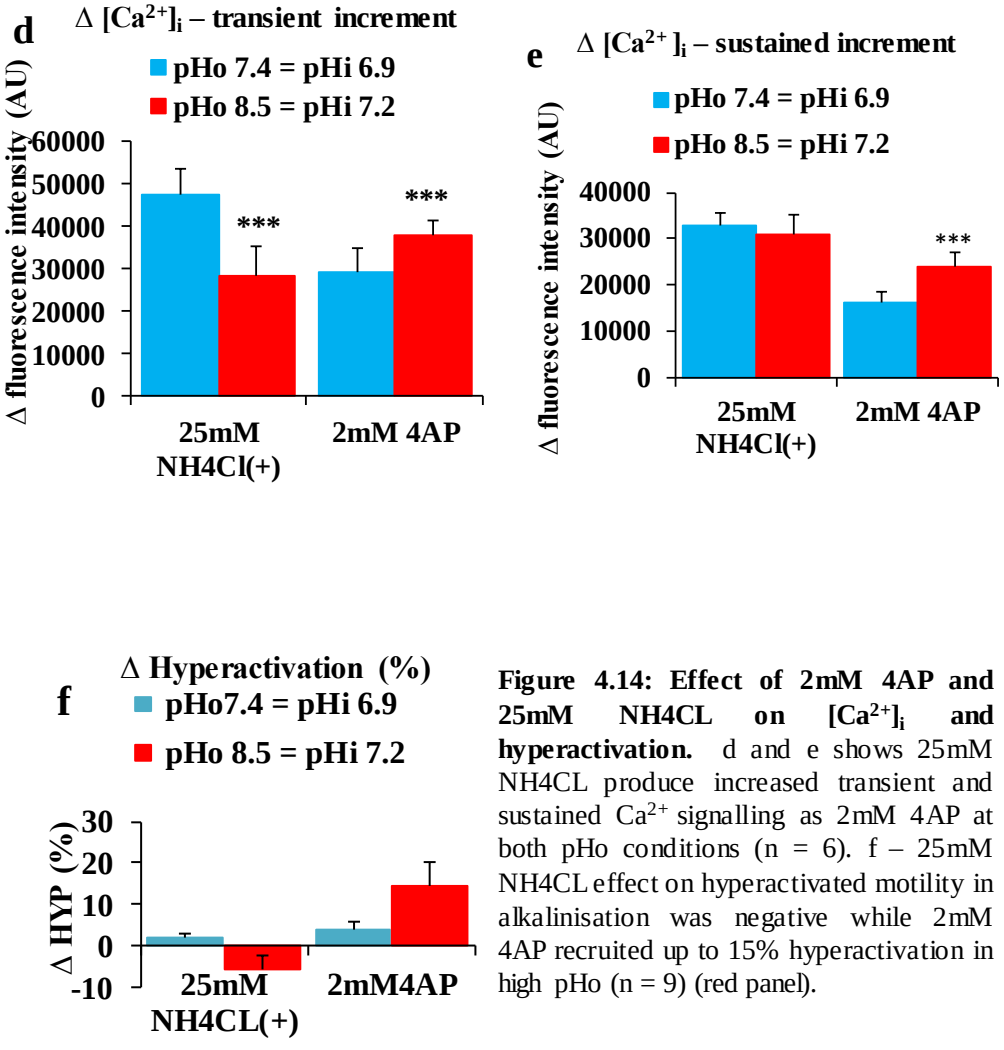

Figure 4.14: Effect of 2mM 4AP and 25mM NH4CL on $[Ca^{2+}]_i$ and hyperactivation. d and e shows 25mM NH4CL produce increased transient and sustained Ca^{2+} signalling as 2mM 4AP at both pHo conditions (n = 6). f – 25mM NH4CL effect on hyperactivated motility in alkalinisation was negative while 2mM 4AP recruited up to 15% hyperactivation in high pHo (n = 9) (red panel).

4.4.7 Relationship between $[Ca^{2+}]_i$ sustain and hyperactivation

Figure 4.15 shows the relationship between absolute fluorescence intensity (mean±sem) assessed during the sustained component of the $[Ca^{2+}]_i$ signal and percent sperm hyperactivation (mean±sem). The delay between agonist stimulation and CASA recording was such that motility assessment was made during the sustained component of the $[Ca^{2+}]_i$ response. Data for P4 (0.1, 1.0.10.20 µM) at pHo=7.4 and at pHo=8.5 and for 4AP (200, 400,600,800,1000,2000,5000 µM) at pHo=7.4 and at pHo=8.5 are all included. A 2nd order polynomial ($y = 9*10^{-9}x^2 - 0.0005x + 7.45$) gave a close fit to the data ($R^2 = 0.96$; Figure 4.15). The finding that for all data, under all conditions, the relationship between $[Ca^{2+}]_i$ and hyperactivation can be described by a single relationship suggests that hyperactivation is dependent on the level of $[Ca^{2+}]$i (as assessed by fluorimetry) but not the source.

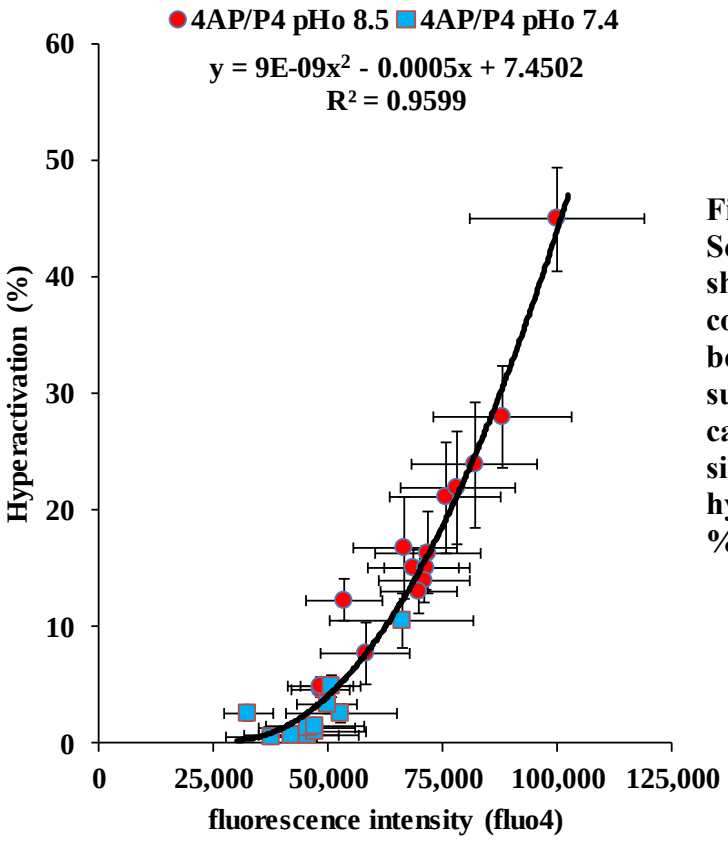

Figure 4.15: Scatter plot showing strong correlation between sustained calcium signalling and hyperactivation %.

4.5 Key findings

i. pHo affects the cytoplasmic pH of human sperm and differences in pHo as the sperm ascends the tract will affect pHi and therefore sperm function.

ii. High pHo (and consequently elevated pHi) increased resting $[Ca^{2+}]i$ and levels of hyperactivation.

iii. When progesterone was applied to sperm at high pHo (8.5) the amplitude and dose-dependence of the transient and sustained $[Ca^{2+}]i$ increments were similar to at pHo=7.4. The effects of pH and P4 were additive and not synergistic.

iv. When progesterone was applied to sperm at high pHo (8.5), the effect on hyperactivation, even at higher [progesterone] of 10 - 20μM, was not significantly enhanced over that observed at pHo=7.4. The effects of pH and P4 were additive and not synergistic.

v. High pHo enhanced the effect of 4AP on $[Ca^{2+}]i$ and hyperactivated motility. There was little if any change in the $[Ca^{2+}]i$ transient increment but there was a robust enhancement of the sustained $[Ca^{2+}]i$ increase and of hyperactivation.

vi. 4AP is a weak base and it increases pHi but NH_4Cl had a greater effect on pHi while failing to increase hyperactivation, confirming that the effect of 4AP does not merely reflect its intracellular alkalinising effect.

vii. The relationship between $[Ca^{2+}]_i$ and % hyperactivation in agonist-stimulated cells indicates that hyperactivated motility is dependent on the level of $[Ca^{2+}]i$ but not the source of $[Ca^{2+}]i$ entry.

4.6 Discussion

In this chapter the effects of elevated pH on the actions of progesterone and 4AP on $[Ca^{2+}]_i$ signalling and hyperactivated motility in human sperm were assessed.

4.6.1 Extracellular pH of the oviduct affects the intracellular pH of the human sperm

Manipulating pHo directly affected pHi (Figure 4.1, panel a,c) indicating that as the extracellular pH in the oviduct increases the cytoplasmic pH_i of human sperm will also increase, modulating activities of pH dependent processes, as described previously (Fraire-Zamora and Gonzalez-Martinez, 2004, Naz, 2014, Qi et al., 2007). The relationship between extracellular pH in the oviduct and intracellular pH in human sperm is pseudo-linear. In this study, using pHo 7.4 and 8.5 the determined corresponding pHi was 6.85 and 7.19 respectively. This agrees with (Hamamah et al., 1996, Lishko et al., 2012) but (Fraire-Zamora and Gonzalez-Martinez, 2004) concluded that pHo of 7.0 and 8.0 resulted in pHi values of of 6.59 and 6.9 in human sperm whereas (Naz, 2014), at pHo=7.4, measured a pHi of human sperm of 7.25 and 7.15 for mouse sperm. Clearly absolute values vary and this may depend on both the physiological status of the sperm and the technique used for pHi assessment, but clearly pHi of human sperm is sensitive to pHo.

4.6.2 Increased pHi enhanced resting $[Ca^{2+}]_i$

Increasing the pHo from 7.4 to pHo 8.5 clearly increased the resting $[Ca^{2+}]_i$. This suggests that CatSper is activated tonically in resting cells and is sensitive to pHi (Kirichok et al., 2006). In bovine and mouse sperm the activity of membrane Ca^{2+} channels was apparently stimulate by alkalinisation (Jin and Yang, 2016, Marquez and Suarez, 2007). Increased responsiveness of $[Ca^{2+}]_i$ to pH_i is associated with capacitation (Neri-Vidaurri Pdel et al., 2006) and may be crucial in controlling sperm activities (Nishigaki et al., 2014).

4.6.3 Progesterone and 4AP induced Ca^{2+} signals

The biphasic $[Ca^{2+}]_i$ elevation induced by P4 and 4AP in sperm bathed in standard (physiological) saline (pHo=7.4; see chapter 3) were also observed at when pHo was increased to 8.5. At pHo=8.5, the P4-induced $[Ca^{2+}]_i$ signals rose rapidly but decayed much more slowly. The response to 4AP appeared to rise more slowly than at pHo=7.4 and showed a great reduction in decay rate, with no decay at the highest concentrations. Though the extended response to 4AP may be due, in part, to store mobilisation (see below), it is likely that partial suppression of Ca^{2+}-clearance underlies the slow decay of the P4-induced transient. The plasma membrane Ca^{2+}-ATPase (PMCA) that exports Ca^{2+} from the sperm cytoplasm (section 1.7.3) co-transports one or two extracellular H^+ into the cell (Ruffin et al., 2014). The relative unavailability of H^+ at pHo=8.5 may have negatively affected PMCA activity and this may be responsible for the slower decay of the $[Ca^{2+}]_i$ signal under these conditions (Wennemuth et al., 2003).

4.6.4. Effect of pH on amplitude of responses to P4 and 4AP

When pHo was increased to 8.5 the amplitude of the P4-induced $[Ca^{2+}]$i transient was slightly smaller at the elevated pHo compared to the signal at pHo=7.4. This transient is CatSper mediated, which is regulated by both pHi and P4 and it was hypothesised the response to P4 might be enhanced by alkalinisation (Publicover and Barratt, 2011a). Furthermore, capacitation, which involves an increase in pH_i augments the transient phase of P4-induced Ca^{2+} entry (Lishko et al., 2011, Neri-Vidaurri Pdel et al., 2006, Strünker et al., 2011). One possible explanation for this finding is that the increase in resting $[Ca^{2+}]_i$ at elevated pHo (Figure 4.2) was such that, upon stimulation with P4, fluo4 saturated and was unable to report the $[Ca^{2+}]_i$ transient. To test this, response to P4 was assessed in cells loaded with fura-2 and fluo5F, which has a Ca^{2+}-affinity >7 times lower than fluo4. Using fluo5F there was no enhancement of the transient $[Ca^{2+}]_i$ response to P4 at pHo=8.5, suggesting that dye saturation was not an issue. Using the ratiometric dye fura-2 (which has a higher Ca^{2+}-affinity (Kd=140 nM) than fluo4 (Kd=345 nM)) the progesterone transient was slightly, but significantly, enhanced at pHo=8.5 (Figure 4.4). It therefore appears that the failure of elevated pHo to potentiate the P4-induced $[Ca^{2+}]_i$-transient is not an artefact caused by dye saturation but the conclusion that there is no effect of pH should be cautious.

The amplitude of the sustained P4-induced $[Ca^{2+}]_i$ signal (assessed 5 minutes after stimulation) was not affected by increased pHo. $[Ca^{2+}]_i$ at this point was ≈50% of that at the transient peak and is clearly not approaching saturation. Failure to observe synergistic enhancement by alkalinisation is perhaps not surprising since the sustained phase of the P4-induced $[Ca^{2+}]_i$ signal may be less dependent on CatSper and is potentially associated

with calcium induced calcium release (CICR) of stored Ca^{2+} followed by capacitative Ca^{2+} entry (Park et al., 2011, Qi et al., 2007).

The effect of 4AP on the $[Ca^{2+}]_i$ transient was not significantly enhanced at pHo=8.5 (Figure 4.5c) but the sustained $[Ca^{2+}]_i$ increase, measured 5 min after stimulation was significantly increased over the effect at pHo=7.4 (Figure 4.5d). The sustained effects of 4AP stimulation on $[Ca^{2+}]_i$ and motility appear to be at least partly dependent upon release of stored Ca^{2+} and activation of CCE (Alasmari et al., 2013b, Bedu-Addo, 2008) and this effect of enhanced pHo is therefore likely to be due to an increase in the concentration of the non-ionised form of 4AP, allowing entry into the sperm cytoplasm.

4.6.5 Spontaneous hyperactivation enhanced in pHi

Increasing pHo to 8.5 (and consequent effect on pHi) induced a 6-fold increase in the proportion of hyperactivated cells (Figure 4.6a) and, consistent with this observation, VCL, ALH and BCF were significantly enhanced and the frequency distributions for these variables were clearly shifted. LIN fell slightly but this effect was not significant. Since a rise in pHi will shift the activation curve of CatSper channels to more negative values (Kirichok et al., 2006, Lishko et al., 2011, Strünker et al., 2011); Figure 4.0), it appears likely that this reflects tonic activation of CatSper by intracellular alkalinisation. Such activity of CatSper may act directly on axonemal activity but may also trigger CICR of stored Ca^{2+}, which is implicated in human sperm hyperactivation (Alasmari et al., 2013b, Bedu-Addo, 2008). In bovine sperm elevation of pHi with NH_4Cl to activate CatSper, induced hyperactivation and similar results have been reported in mouse sperm (Chang and Suarez, 2011, Marquez and Suarez, 2007).

4.6.6 Progesterone effects on motility are not potentiated in high pH

Similarly to $[Ca^{2+}]_i$ responses, the effect of progesterone on hyperactivated motility at pHo=8.5 resembled that at pHo=7.4, being very small and dose independent over the concentration range used. Assessment of motility kinematics confirmed that P4 treatment slightly increased mean VCL and ALH and decreased BCF and LIN, similarly to the action seen at pHo=7.4. Frequency histograms for these variables showed shifts consistent with the small changes in mean value but the BCF curve was of interest in that the control distribution was a wide bell-shape with peak at 30 Hz and a smaller peak or shoulder at 15 Hz. Progesterone treatment appeared to shift cells from the 30 Hz to the 15 Hz class. This suggests the existence of two distinct motility classes in the population. However, since images were collected at 60 Hz (2x and 4x these class sizes) it is possible the observed peaks are a sampling artefact and further work with a higher video frame rate may be needed to resolve this. Thus the activation of CatSper by progesterone at increased pH was additive rather than synergistic, contrary to the effect reported by (Lishko et al., 2011) (Figure 4.0).

4.6.7 High pHi potentiates the effect of 4AP on motility

The effect of 4AP on hyperactivated motility was potentiated by intracellular alkalinisation. At pHo=8.5 the effects of the 4AP (1000-5000 µM) on mean VCL, ALH and LIN were all enhanced compared to pHo=7.4. Mean BCF showed little effect. The frequency distributions for these variables showed a strong rightward shift for VCL and ALH (particularly at 5000 µM) and a leftward shift for LIN.

4.6.8 pHi and stimulation of hyperactivation

Progesterone (1-20 µM) did not change the pHi but 2mM 4AP clearly increased pHi (more potently at pHo=8.5 than at pHo=7.4), which may induce Ca^{2+} entry through CatSper, leading to the potent stimulation of HA seen with this compound (Kirichok et al., 2006, Navarro et al., 2007); (Figure 4.13a-c). To determine if the effect of 4AP on hyperactivation is due to increased pHi we used 25mM NH_4Cl as a positive control for intracellular alkalinisation (Fraire-Zamora and Gonzalez-Martinez, 2004, Publicover et al., 2008). 25mM NH_4Cl elevated the pHi significantly more than 2 mM 4AP (both at pHo=7.4 and pHo=8.5, Figure 4.13a-c) and increased $[Ca^{2+}]_i$ as much as 4AP but failed to stimulate HA (Figure 4.14d-f). This indicates that the ability of 4AP to induce HA is not a reflection only of its effect on pHi, consistent with the reported action of the drug on store Ca^{2+} (Alasmari et al., 2013b).

4.6.9 Relationship between$[Ca^{2+}]_i$ sustained signalling and hyperactivated motility

The data reported here and in the previous chapter provide matched estimates of $[Ca^{2+}]_i$ (fluo4 fluorescence) and hyperactivated motility under a wide range of conditions, from control at pHo=7.4 to cells treated with 5 mM 4AP at pHo=8.5, when mean HA as assessed by CASA reached values of almost 40%. Figure 4.15 shows a scatter plot constructed using mean fluo4 fluorescence 5 min after stimulation (the approximate time at which CASA analysis was done) and mean HA for each condition tested. These data were collected over a period of months and there is clearly some 'noise' in the data, possibly due to differences between factors such as batch of BSA – leading to differences

in levels of capacitation. However, it appears that there is a relationship between $[Ca^{2+}]_i$ and % hyperactivated cells, suggesting that effect of the different treatments on motility is dependent primarily on $[Ca^{2+}]_i$ (whether derived by activation of CatSper or by store mobilisation) and not on other factors such as pH_i. Interestingly this suggests that the efficacy of store mobilisation in stimulating HA that was reported previously (Alasmari et al., 2013b) may be due to the ability of CCE to maintain elevated $[Ca^{2+}]_i$ for an extended period compared to CatSper activation, which rapidly decays. An anomaly to this relationship is the effect of alkalinisation with NH4Cl, which fails to induce HA to a level consistent with the effect on $[Ca^{2+}]_i$. This requires further investigation.

CHAPTER 5: EFFECT OF CATSPER BLOCKER ON pH AND PROGESTERONE INDUCED $[Ca^{2+}]_i$ SIGNALLING

5.1 Objective

CatSper activity is strongly regulated by pHi, thus manipulations that increase pHi may increase $[Ca^{2+}]_i$ by tonic activation of CatSper. Elevation of pHo caused a rise in pHi and a tonic increase in $[Ca^{2+}]_i$ (see chapter 4). The aim of the experiments described in this chapter was to use a new CatSper blocker to investigate whether resting $[Ca^{2+}]_i$ and the responses to stimulation with P4 at pHo=7.4 and 8.5 were similarly inhibited by pharmacological block of CatSper channels.

5.2 Introduction

CatSper, a specific ion channel found in the principal piece of humans, mice sperm is made up of CatSper 1 – 4 subunits each with six transmembrane segments (Quill et al., 2001, Ren et al., 2001) (see section 1.7.1). Entry of Ca^{2+} through activated CatSper channels is believed to induce hyperactivated motility in sperm (Carlson et al., 2005, Carlson et al., 2003, Qi et al., 2007, Ren et al., 2001), a vigorous side to side movement of the sperm head and uneven deep waveform of the flagellum that is essential for the sperm to ascend the female tract and penetrate the layers surrounding the oocyte (Qi et al., 2007). CatSper may also participate in guidance of the sperm by allowing calcium ion entry that induces the needed motility turns towards the egg (Eisenbach and Giojalas, 2006, Kaupp et al., 2008). It has been proposed that increased intracellular pH (pHi; which is crucial in regulating functions of many kinds of proteins (Boron, 2004) triggers hyperactivated motility through activation of CatSper channels (Kirichok et al., 2006). Progesterone also regulates CatSper function physiologically in humans and monkeys (Lishko et al., 2011, Smith et al., 2013, Strünker et al., 2011, Sumigama et al., 2015). (Tamburrino et al., 2015) showed that expression of CatSper 1 and localisation of the protein to the flagellar principal piece is correlated with both progressive motility and hyperactivation. Absence of CatSper 1 has been shown to strongly inhibit the hyperactivated motility in mouse (Carlson et al., 2003) whilst sperm from a man with natural mutation of CatSper 2 showed greatly reduced sperm motility (Smith et al., 2013).

Previously in chapter 4, resting $[Ca^{2+}]i$ and hyperactivation in sperm were shown to be enhanced in sperm incubated at high pHo (8.5), consistent with a activation of CatSper leading to Ca^{2+} influx and modulation of behaviour. However, (Alasmari et al., 2013a, Alasmari et al., 2013b) raised doubt on the role of CatSper in triggering hyperactivated

motility in human sperm, suggesting that mobilisation of stored Ca^{2+} was a more important factor, and (Sagare-Patil et al., 2012) reported that the effect of high concentration of progesterone on hyperactivation is not solely CatSper dependent. Therefore the work reported in this chapter seeks to use pharmacological block of CatSper to investigate the contribution of CatSper to these effects.

The CatSper blocker AR720-F1 is novel but a modified form of RU1968 (Renhack et al., 2017, unpublished). RU1968 is a ligand that interacts with sigma receptor for steroids and does not activate it. RU1968 was reported to hinder Ca^{2+} signals evoked by P4 and prostaglandin in human sperm (Schaefer et al., 2000).

5.3 Materials and Methods

5.3.1 Materials

For the Materials section, see Chapter 2.1. 1

Progesterone (P4) and CatSper inhibitor – AR720 –F1 (courtesy of Prof. Timo Strunker, Germany) at pH 7.4 and 8.5 were used in these experiments.

5.3.2 Methods

5.3.2.1 Donor recruitment

Donor recruitment was conducted as described in Chapter 2.2.

5.3.2.2 Sperm cell preparation

The sperm cells were prepared as explained in chapter 2.4

5.3.2.3 Measurement of $[Ca^{2+}]_i$ in fluorimeter

The $[Ca^{2+}]_i$ signalling induced by dose effect of AR720-F1 on 3µMP4 and bolus effect of 30µM AR720-F1 on (1,10,20)µM progesterone were determined as described in chapter 2.5 (n = 5).

5.4 Results

5.4.1 Dose - dependent effect of AR720-F1 on resting $[Ca^{2+}]_i$ signals

Exposing capacitated sperm cells loaded with fluo4 to the CatSper blocker AR720–F1 resulted to a dose dependent effect on resting $[Ca^{2+}]_i$ at both pHo=7.4 and pHo=8.5 (Figure 5.1a,b). At doses of ≤1 uM there was a small stimulatory effect that was more marked at pHo=8.5 but higher doses (up to 30 µM) AR720-F1 caused a rapid fall in $[Ca^{2+}]_i$ which was dose-dependent ($P < 0.01$, $^*P < 0.02$, n =5 at pHo=7.4 and 8.5 respectively) and was similar at the two pH values ($P>0.05$, n = 5, Figure 5.1c). When incubation with AR720-F1 was extended to 8 minutes, the effect at pHo =8.5 was greater than at pHo 7.4 (Figure 5.1d).

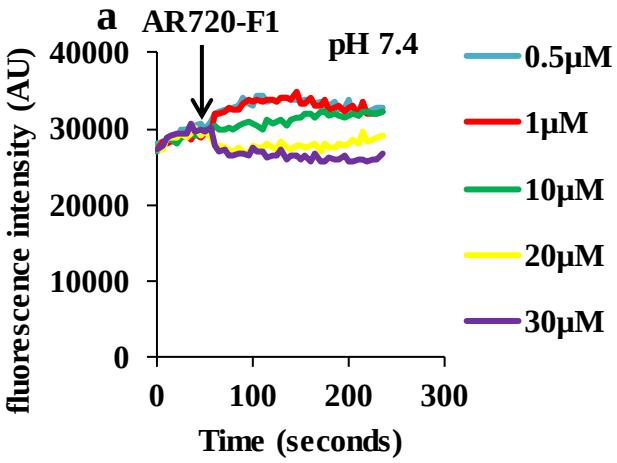

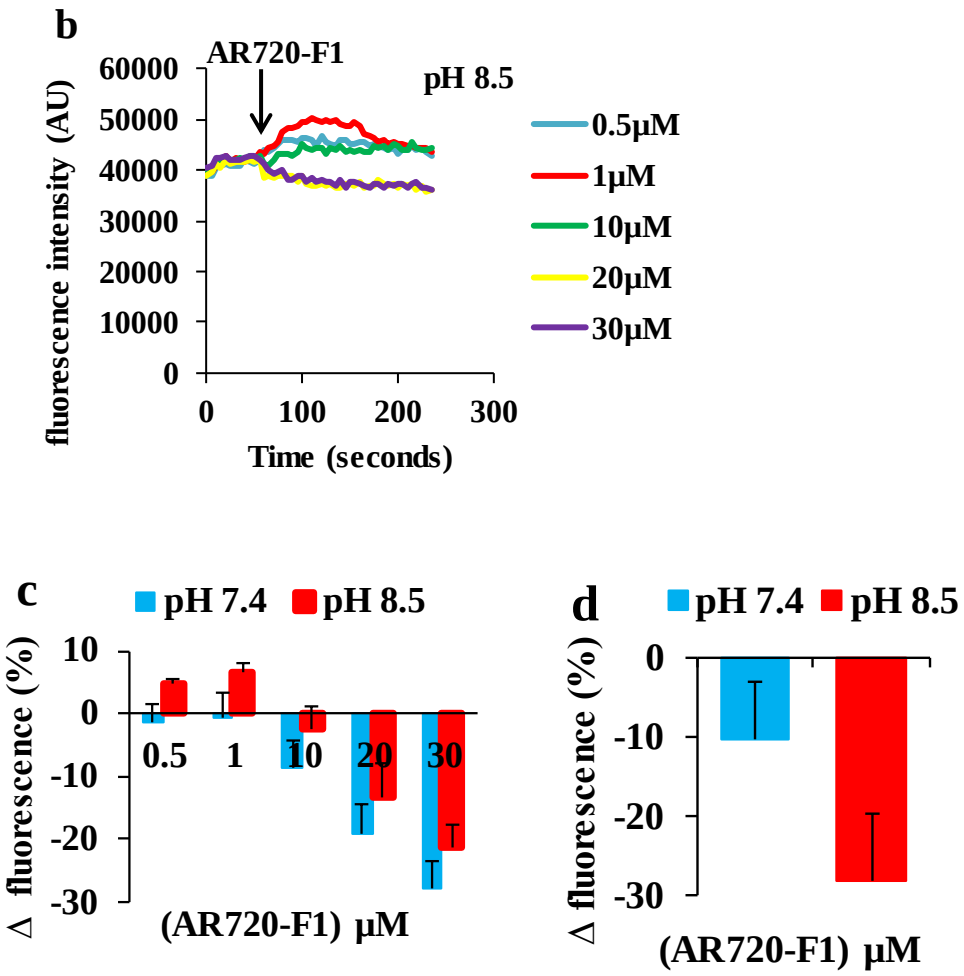

Figure 5.1: Mean effect of AR720-F1 on resting $[Ca^{2+}]_i$. a and b show dose effect of application of AR on resting $[Ca^{2+}]i$ at pHo = 7.4 (panel a) and pHo = 8.5 (panel b). c shows mean (±SEM;n=5)% change in fluo4 fluorescence at pHo=7.4 (blue) and pHo=8.5 (red). d shows the mean inhibitory effect at 460-510 seconds after application of 30µM AR in the absence of P4 at pHo 7.4 (blue) and 8.5 (red) (n = 5).

5.4.2 Effect of AR720-F1 on progesterone induced $[Ca^{2+}]_i$ signalling

When sperm were exposed first to AR-720-F1 then, after a delay of 3 min, treated with 3 uM progesterone, there was a clear inhibition of the progesterone-induced $[Ca^{2+}]_i$ signal at both pHo=7.4 and pHo=8.5 (Figure 5.2). Similarly to effects of the drug on resting $[Ca^{2+}]_i$, the transient was not inhibited by doses of ≤1 µM, but at greater concentrations there was a dose-dependent effect that achieved almost complete inhibition (>95%) at 30 µM (Figure 5.2a-c; ***P < 0.001). The effect of AR720-F1 on the sustained component of the progesterone-induced $[Ca^{2+}]_i$ response showed a similar dose-effect profile, but the drug was slightly less potent, inhibiting the $[Ca^{2+}]_i$ increase by ≈75% at 30µM (*P< 0.01; n=5; Figure 5.2d) Inhibition by AR720-F1 of both the transient and sustained components of the progesterone-induced $[Ca^{2+}]_i$ responses did not differ significantly between pHo=7.4 and pHo=8.5 (Figure 5.2c,d blue and red traces respectively).

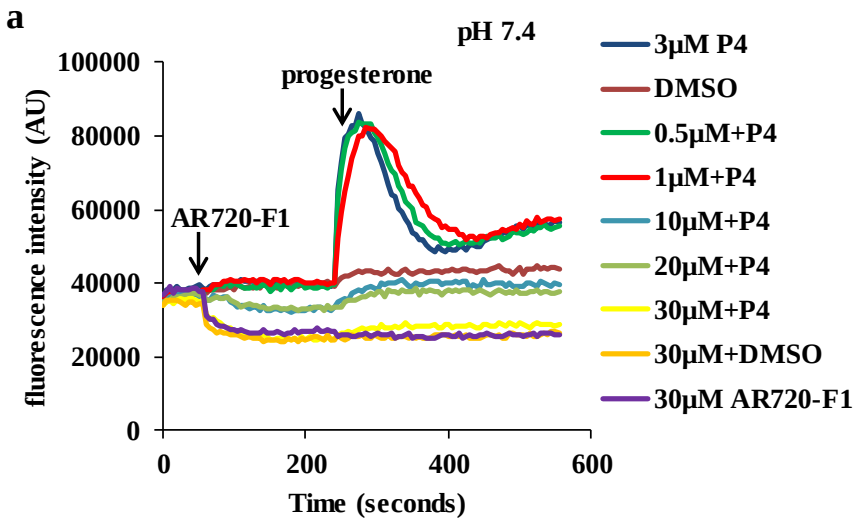

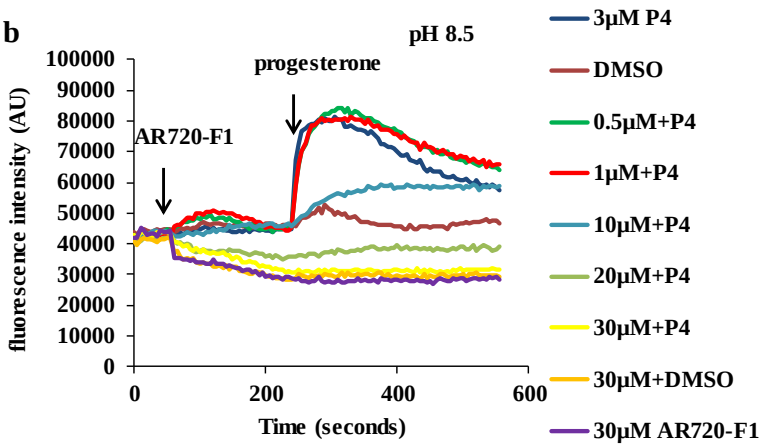

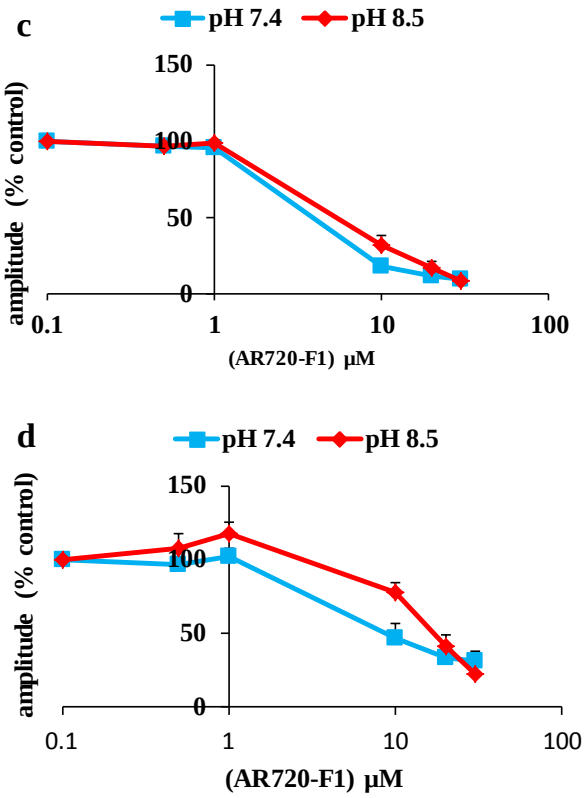

Figure 5.2: Effect of AR720-F1 on $[Ca^{2+}]_i$ signals induced by 3µM progesterone. a and b show examples of effect of pre-treatment with AR720-F1 on $[Ca^{2+}]_i$ responses to 3µM progesterone at pHo=7.4 (a) and pHo= 8.5 (b). First arrow shows time of addition of AR720-F1 and second arrow shows time of addition of progesterone. c and d show effect of pre-treatment with AR720-F1 on mean (±SEM; n=5) amplitude of $[Ca^{2+}]_i$ transient (c) and sustained $[Ca^{2+}]_i$ elevation (d), expressed as % of parallel control recording.

5.4.3 Can high concentrations of progesterone reverse the inhibitory effect of 30µM AR720-F1?

To investigate whether the inhibitory effect of AR720-F1 on the response to progesterone could be reversed by increase in the progesterone dose, the inhibitory effect was tested with 1 µM, 10 µM and 30 µM progesterone. Stimulation with 1 µM progesterone induced an immediate $[Ca^{2+}]_i$ transient (as decribed previously) that was similarly inhibited by 30 µM AR720-F1 at pHo=7.4 and pHo=8.5 ($P<0.001$, n=5; Figure 5.3a,b). Increasing the concentration of progesterone had negligible effects on the amplitude of the transient induced by progesterone at either value of pHo (Figure 5.3a,b,c)

As described above, the sustained component of the progesterone-induced $[Ca^{2+}]$i signal was inhibited by 30 µM AR720-F1 ($P< 0.01$, $P< 0.05$ at pHo=7.4 and 8.5 respectively, n = 5), but the effect was less pronounced than in the $[Ca^{2+}]$i transient (60-80% inhibition compared to more than 90% inhibition of the transient. It was also observed in this set of experiments that 30 µM AR720-F1 inhibited the sustained $[Ca^{2+}]$i signal at pHo=8.5 more potently than at pHo=7.4 ($P < 0.02$, n=5). Similarly to the $[Ca^{2+}]$i transient, increasing the concentraion of progesterone failed significantly to relieve the inhibitory effect of the drug (Figure 5.3d).

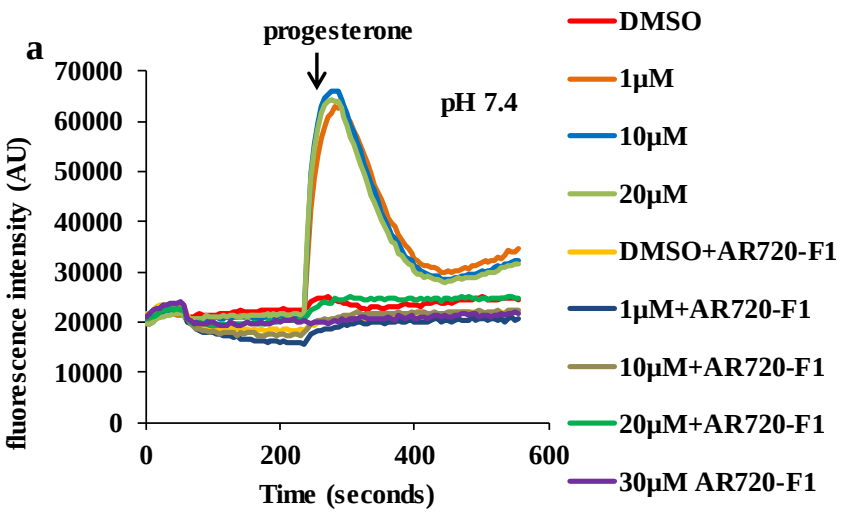
a
progesterone
pH 7.4
fluorescence intensity (AU)
70000
60000
50000
40000
30000
20000
10000
0
0
200
400
600
Time (seconds)
DMSO
1µM
10µM
20µM
DMSO+AR720-F1
1µM+AR720-F1
10µM+AR720-F1
20µM+AR720-F1
30µM AR720-F1

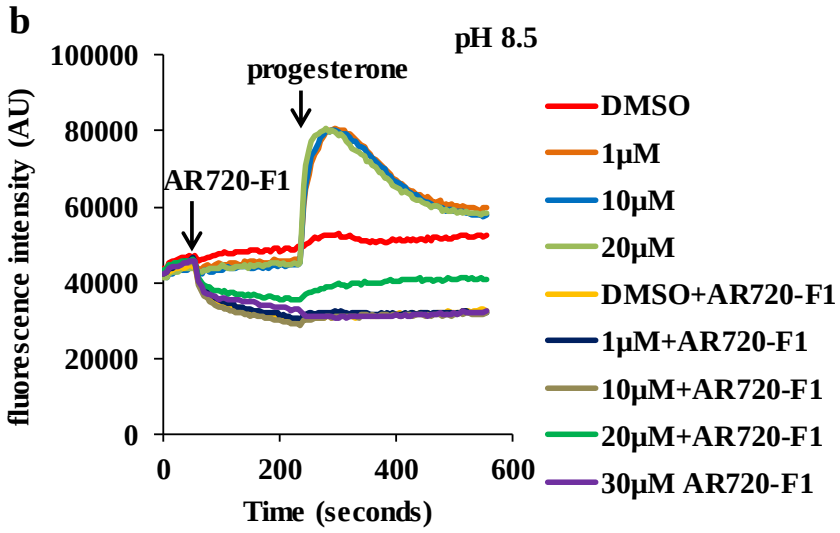
b
pH 8.5
progesterone
AR720-F1
fluorescence intensity (AU)
100000
80000
60000
40000
20000
0
0
200
400
600
Time (seconds)
DMSO
1µM
10µM
20µM
DMSO+AR720-F1
1µM+AR720-F1
10µM+AR720-F1
20µM+AR720-F1
30µM AR720-F1

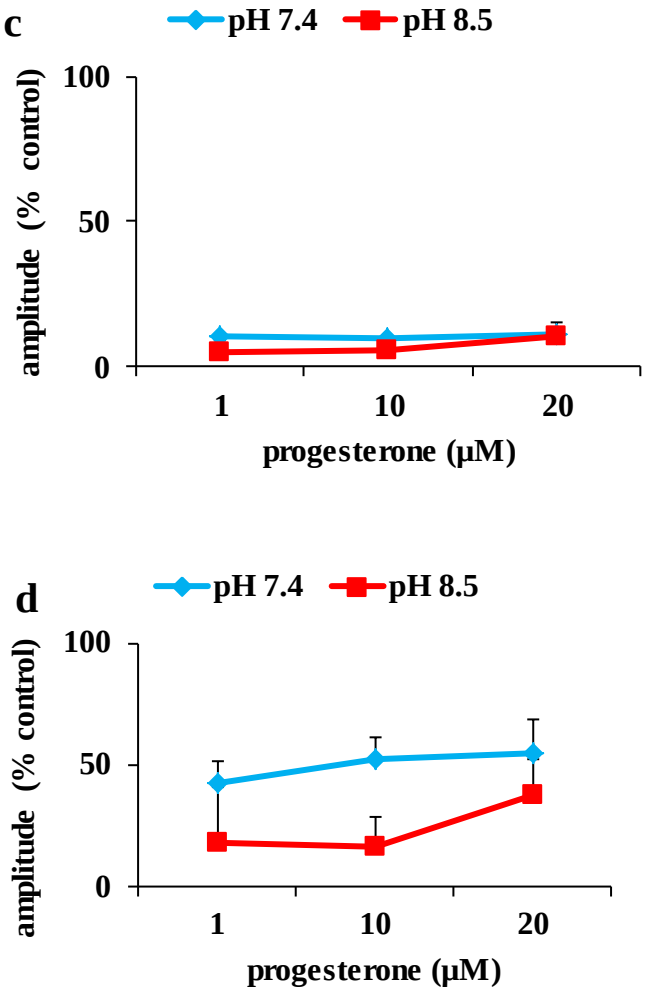

Figure 5.3: Effect of increasing [P4] on inhibitory response of 30µM AR720-F1 at both pH 7.4 and 8.5. a and b show $[Ca^{2+}]_i$ signals elicited by increasing [P4] in the absence and presence of AR720-F1 at both pH. c and d show that increasing [P4] did not change the percent inhibition of the Ca^{2+} transient and sustained signals at both pH 7.4 (blue trace) and 8.5 (red trace). The inhibitor was more effective on the increasing [P4] at pH 8.5 (red) and in the transient response (panel c, n = 5).

5.5 Key findings

i) CatSper channel contributed in the resting and progesterone induced $[Ca^{2+}]i$ responses at both pH 7.4 and 8.5 - the effect of CatSper block at pHo=8.5 was greater though this effect was not significant.

ii) Ca^{2+} flux through CatSper channels may be responsible for up to 30% of resting $[Ca^{2+}]_i$.

iii) Blockade of CatSper inhibited P4-induced transient and sustained responses by 90-95% and 65-70% respectively at both pH conditions.

iv) Increasing the concentrations of progesterone did not reverse the inhibitory effect of AR720-F1 on responses to P4 at either pH.

v) CatSper is recruited more in the transient phase and at high pH compared to the sustained phase and pH 7.4.

5.6 Discussion

In this chapter, we investigated the role of CatSper in progesterone induced calcium signalling by using AR720-F1 a pharmacological inhibitor of CatSper.

5.6.1 AR720-F1 produces a dose - dependent inhibitory effect on resting Ca^{2+} ion signalling at both pH 7.4 and 8.5

When AR720-F1 was applied to human sperm resting $[Ca^{2+}]_i$ rapidly fell at both pHo=7.4 and pHo=8.5, suggesting that open CatSper channels contribute to the determination of resting $[Ca^{2+}]_i$ dependent inhibition at both pH 7.4 and 8.5. Surprisingly, though alkalinisation would be expected to recruit CatSper and increase the contribution of the channel to the determination of resting $[Ca^{2+}]_i$ the effect of AR720-F1 was greater at pH 7.4 compared to pH 8.5 (Figure 5.1c). However, assessing the effect of 30µM AR720-F1 on resting $[Ca^{2+}]$i, at 460-510 seconds after application of AR720-F1 revealed an inhibitory effect greater at pH 8.5 compared to pH 7.4 (Figure 5.1d). This suggests that the dose dependent inhibitory signal may actually be greater at pH 8.5 rather than pH 7.4 with time.

5.6.2 Dose dependent inhibition by AR720-F1 on progesterone - induced $[Ca^{2+}]_i$ signalling at both pH 7.4 and 8.5

Concentrations of 10 - 30µM AR720-F1 induced a dose - dependent inhibition in the progesterone-induced $[Ca^{2+}]_i$ signal at both pH 7.4 and 8.5. The $[Ca^{2+}]_i$ transient was inhibited similarly at both pHo values, being reduced to only 5-10% of the control amplitude by 20-30 µM AR720-F1. This finding is consistent with previous report that the progesterone-induced transient is completely generated by (or dependent on) Ca^{2+}-influx through CatSper channels (Lishko et al., 2011, Strünker et al., 2011).

The effect of AR720-F1 on the sustained component of the signal was significant but less potent, 20-30µM reducing the amplitude by ≈70% percent at pHo=8.5 and ≈67% percent at pHo=7.4 respectively. These findings also replicate those described previously (Strünker et al., 2011) but whereas the CatSper blockers used previously tended, themselves, to raise $[Ca^{2+}]i$, making interpretation of this observation difficult, AR720-F1 appears not to have such side effect (Rennhack et al., 2017, unpublished) suggesting that, when CatSper is blocked, a small, non-CatSper sustained $[Ca^{2+}]_i$ mobilisation mechanism may still be recruited by progesterone.

5.6.3 Can high concentrations of progesterone reverse the inhibitory effect of 30µM AR720-F1?

Using a concentration of 30µM AR, which produced almost complete block of the $[Ca^{2+}]_i$ transient, we investigated whether the $[Ca^{2+}]_i$ response to progesterone could be rescued by use of higher concentrations (Figure 5.3). Increasing the dose of progesterone up to 20 uM had no effect on the blocking effect of AR720-F1 on either the $[Ca^{2+}]_i$ transient or the sustained $[Ca^{2+}]_i$ signal at either pH value. This effect of AR720-F1 might reflect irreversible binding with the receptor which is therefore not sensitive to increasing concentration of the agonist (Garret, 2010) but it is known that the effects of AR720-F1 on CatSper are rapidly reversed by washout (Rennhack et al., 2017, unpublished). The simplest interpretation of the observations reported here is therefore that AR720-F1 directly blocks the channel rather than interfering with binding of progesterone, though recent data on the mechanism of action of progesterone in human sperm (Miller et al., 2016) suggest that effects on other targets, such as the enzyme ABHD2, might have a similar effect.

CHAPTER 6: INTERACTING EFFECTS OF pH AND PROGESTERONE ON $[Ca^{2+}]_I$ OF HUMAN SPERM

6.1 Objective

The data obtained by fluorimetric recording of the effects of pHo and progesterone in $[Ca^{2+}]_i$ provide no information on the variation of responses of individual cells or the occurrence of more complex aspects of these response such as $[Ca^{2+}]_i$ oscillations. The aim of the experiments reported in this chapter was to observe single cell $[Ca^{2+}]_i$ responses to exposure to P4 and to changes in pHo. The ability to continuously perfuse cells also enables the application of more complex manipulations, such as changing pHo during recording.

6.2 Introduction

$[Ca^{2+}]_i$ signalling is critical for the regulation of sperm function (Baldi et al., 1998, Solzin et al., 2004). The sperm is equipped with a range of Ca^{2+}-signalling tools at the plasma membrane and in Ca^{2+} storage organelles of the neck/midpiece and head that enables it to control changes in $[Ca^{2+}]_i$ in response to cues detected in the female tract (Correia et al., 2015, De Blas et al., 2002, Ho and Suarez, 2003, Quill et al., 2001, Ren et al., 2001, Rossato et al., 2001). Progesterone, which is present at micromolar concentrations in the cumulus and follicular fluid (Harper et al., 2003, Sagare-Patil et al., 2012), is a key modulator of $[Ca^{2+}]_i$ changes in human sperm and the most intensively studied of these cues (Baldi et al., 1998). The physiological significance of the action of progesterone on $[Ca^{2+}]_i$ in human sperm was confirmed when the progesterone-induced $[Ca^{2+}]_i$ response was shown to be correlated with rate of fertilisation in IVF (Krausz, 1996). Consistent with the concentrations encountered by sperm in the female tract, the effect of progesterone on human sperm $[Ca^{2+}]_i$ is detectable at low nM concentrations and saturates at ≈1 μM (Harper et al., 2003, Lishko et al., 2011). In addition to the biphasic calcium signals evoked by progesterone and described in previous chapters, single cell imaging of progesterone-stimulated cells showed that a sub-population of sperm activated by progesterone showed $[Ca^{2+}]_i$ oscillations which are different in size and kinetics from the transient response (Bedu-Addo, 2008, Harper and Publicover, 2005, Kirkman-Brown et al., 2000). In human sperm, the progesterone induced waveforms emanate from the principal piece of the flagellum, where CatSper is the source of initial Ca^{2+} entry (Lishko et al., 2011, Strünker et al., 2011). Subsequent mobilisation of stored Ca^{2+} via CICR (ryanodine and/or IP_3 receptors) apparently amplifies and propagates this initial signal

(Olson et al., 2010). Bedu-Addo, 2008, Harper et al., 2004, demonstrated that maintenance of oscillations requires entry of Ca^{2+} into the cytosol which is needed in order to sustain the filling and emptying of the store.

In chapter 4 the fluorimetric method was used to investigate the influence on the 'population' $[Ca^{2+}]_i$ response evoked by progesterone of increased pH. In the current chapter, I investigate the interaction of pH and progesterone on Ca^{2+} signalling in single cells, including generation of oscillations, which cannot be detected in population recordings. This method involves perfusion of the recording chamber and pH and progesterone can therefore be changed during recording.

6.3 Materials and Methods

6.3.1 Materials

For the Materials section, see Chapter 2.1. 1

1μM Progesterone (P4) in pHo 7.4 and 8.5 saline respectively was used in these experiments (in all analysis n = 3).

6.3.2 Methods

6.3.2.1 Donor recruitment

Donor recruitment was conducted as described in Chapter 2.2.

6.3.2.2 Sperm cell preparation

The sperm cells were prepared as explained in chapter 2.4.

The assessment of Ca^{2+} responses was explained as in section 2.8.1.

Also because of the variation in the fluorescence signal between individual cells (probably a result of differences in loading efficiency of the AM-ester), all fluorescence intensity data reported in this chapter have normalised to the initial control recorded before stimulation and expressed as % change (see chapter 2 section 2.8.1). Thus a value of 0 indicates no change, 100% indicates that fluorescence intensity has increased 100% over control intensity and a negative value indicates that fluorescence intensity has fallen compared to control (Figure 2.4a).

6.3.2.3 Determination of the effect of alkalinisation on resting $[Ca^{2+}]i$ in human sperm

The effect of change in pH on resting $[Ca^{2+}]_i$ were determined as reported in chapter 2.8.1.

6.3.2.4 Assessing the effect of change in pH on progesterone induced $[Ca^{2+}]_i$ in human sperm

The effect of alkalinisation on progesterone induced $[Ca^{2+}]_i$ was determined as reported in chapter 2.8.1.

6.3.2.5 Measuring the dimensions of the oscillations at both pH 7.4 and 8.5

The amplitude and duration of the oscillations in the sustained phases at pH 7.4 and 8.5 were measured visually as reported in chapter 2.8.1.

6.4 Results

6.4.1 Effect of alkalinisation on resting $[Ca^{2+}]_i$

Figure 6.1a and c show a 'typical' single cell response to alkalinisation. Upon changing pHo from 7.4 to 8.5 there was a clear increase in $[Ca^{2+}]$ in 78% of cells (n=3 experiments, 285 cells), fluorescence peaking within 1.5 min at 121.17 ± 4.2 % above the level recorded at pHo=7.4 (n = 3 experiments, 223 cells; Figure 6.1a,b). $[Ca^{2+}]_i$ then decayed over the next 2 min and stabilised at 68.94 ± 3.18 % above control (pH 7.4) fluorescence (n=3 experiments, 223 cells) (Figure 6.1a,b). The transient and sustained components of the alkalinisation-induced $[Ca^{2+}]_i$ rise differed significantly ($P = 1.03 \times 10^{-32}$, n = 223).

Fig 6.1c shows pseudo colour images of fluo-4 fluorescence from a representative cell before (A), during (B) and after (C) exposure to pHo=8.5 .

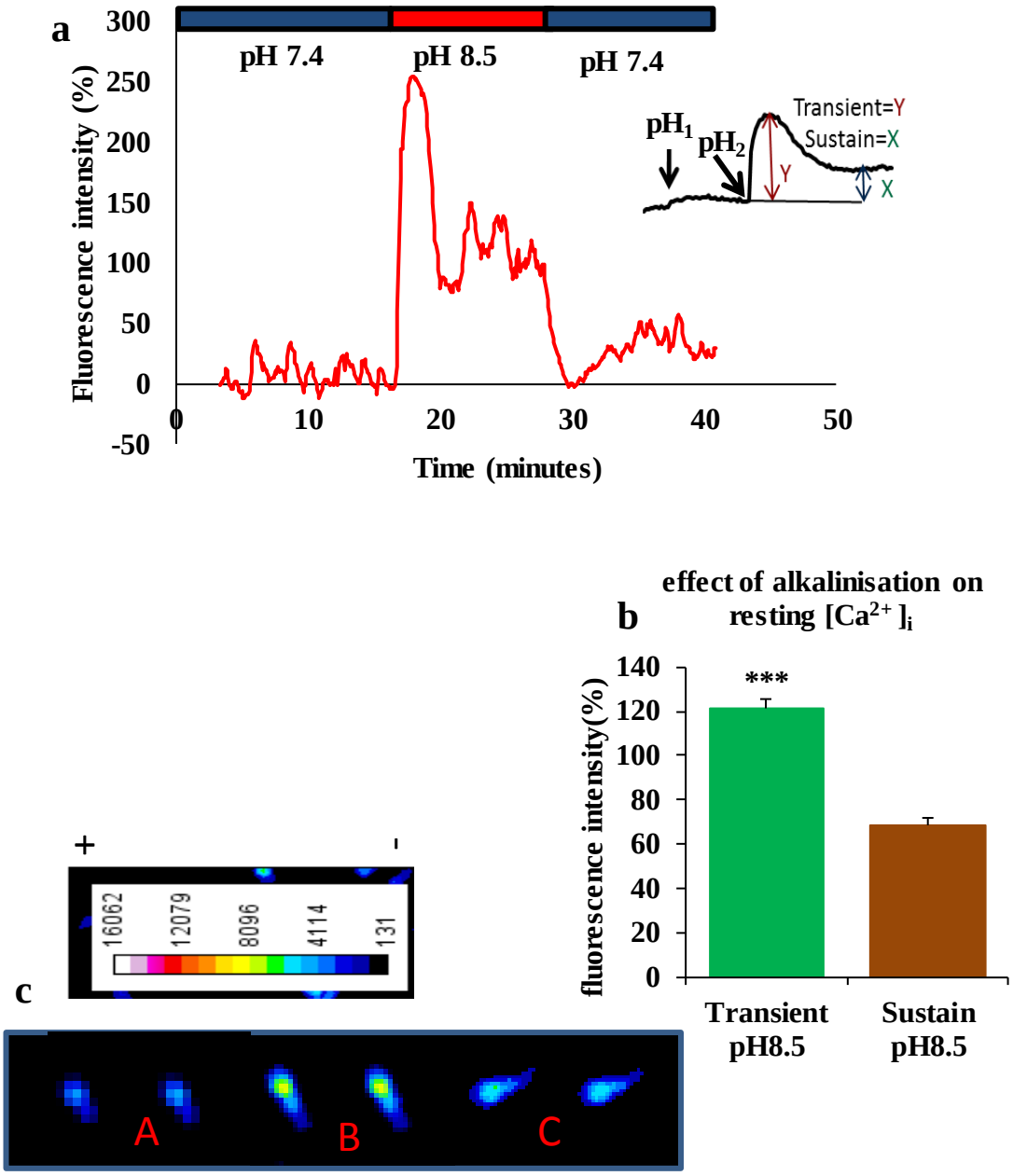

Figure 6.1: Effect of pH on resting $[Ca^{2+}]_i$. (a) Biphasic effect of alkalinisation on resting $[Ca^{2+}]_i$ in an individual cell.(b) Amplitude of transient and sustained $[Ca^{2+}]_i$ elevation induced by pHo=8.5. ($P < 0.001$, n = 223cells. Inset shows how values were calculated for each cell.) (c) Pseudo-colour images of Fluo-4 fluorescence in a typical sperm cell at various points in the experiment. Images in panel A are prior to treatment, panel B images are during alkalinisation and panel C are images during wash out.

6.4.2 pHo and $[Ca^{2+}]_i$ oscillations

Figure 6.2a-c shows examples of cells in which $[Ca^{2+}]_i$ oscillations were observed. Over three experiments 57/223 cells (25.5%) were spontaneously oscillating prior to alkalinisation (Figure 6.2a, 6.2d blue and green) and of these 32 (Figure 6.2d green) maintained this activity when pHo was increased to 8.5. In addition, 35 cells (16%) generated oscillations following the alkalinisation-induced $[Ca^{2+}]_i$ transient (Figure 6.2d red). To assess whether cells were more likely to generate oscillation under alkaline conditions the proportion of oscillating cells at each pH value was calculated for each of the three experiments, giving mean values of 24.4 ± 5.3 pHo=7.4 and 30.2 ± 0.8 at pHo=8.5 ($P>0.05$, n = 3; Figure 6.2e).

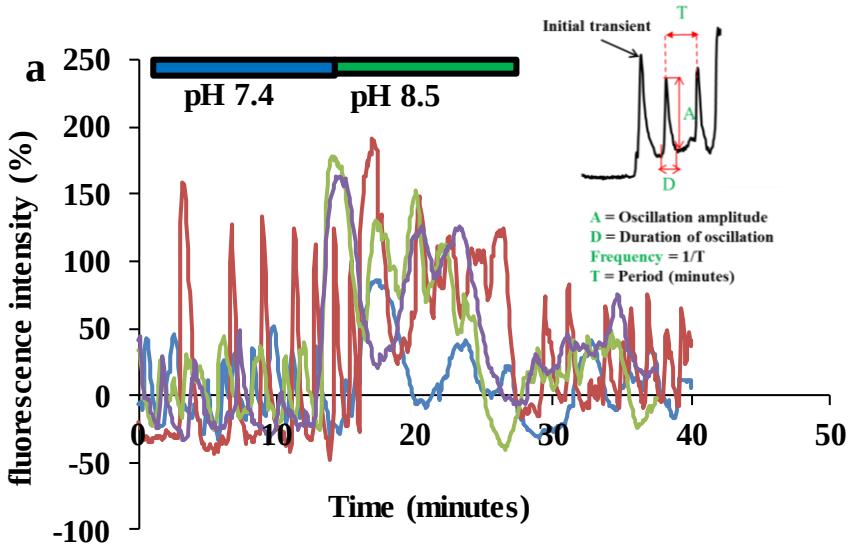

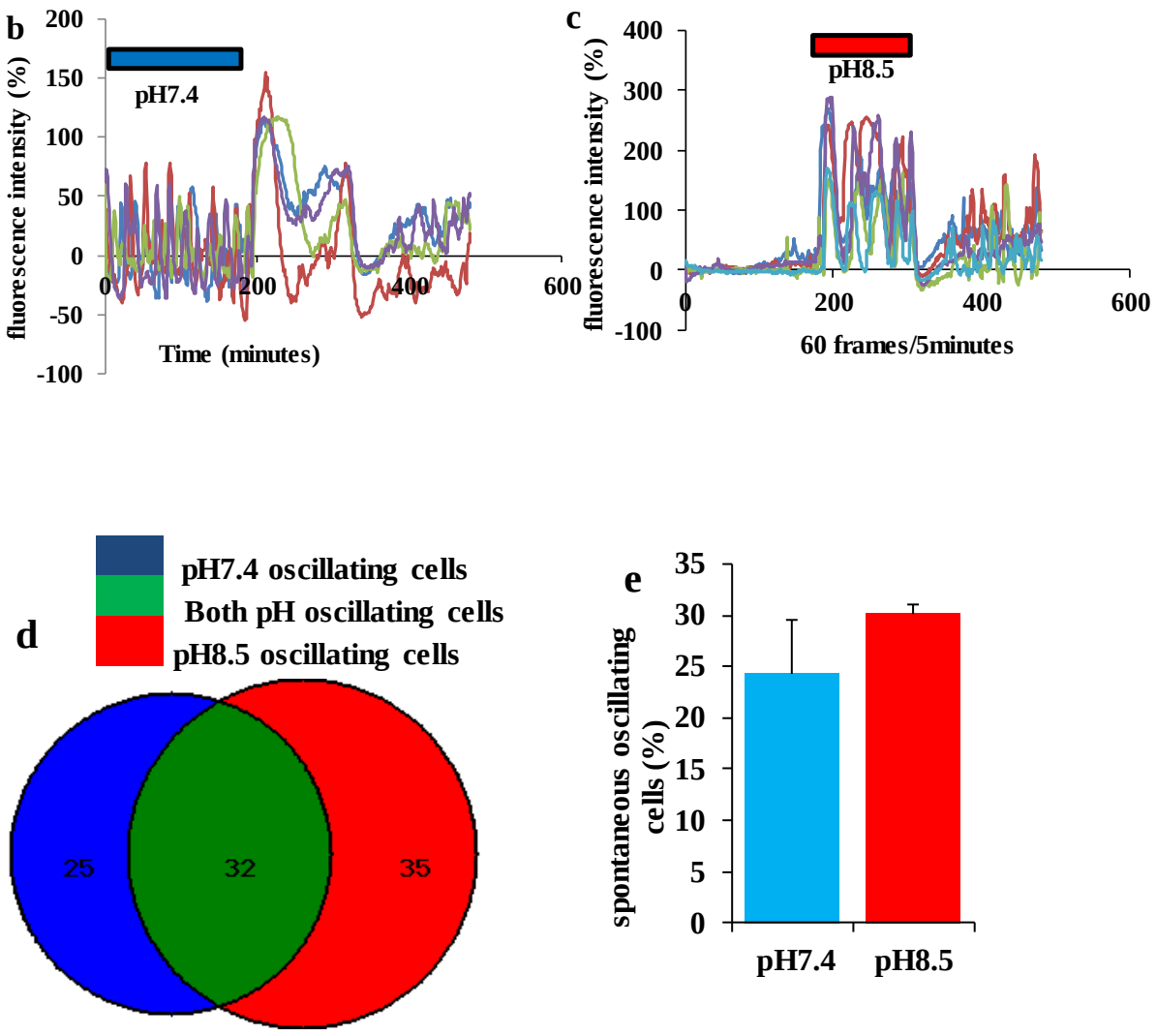

Figure 6.2: pH –induced $[Ca^{2+}]_i$ oscillations. a shows effect of changing pHo on occurrences of $[Ca^{2+}]_i$ oscillations in five cells. b shows the oscillations induced at pH 7.4 in four cells. c shows the pH 8.5 induced oscillations in five cells. d - the occurrence of oscillating cells before and after changing pHo (blue, green, red). e shows that alkalinisation increases the percentage of spontaneous oscillating cells non-significantly (P = 0.44, n =3, 223 cells). Inset shows the dimensions of an oscillation as calculated.

6.4.2.1 Frequency of $[Ca^{2+}]_i$ oscillations at pHo=7.4 and pHo=8.5

When all cells in which oscillations were observed were included in the calculation, the mean frequency of occurrence (oscillations.min^{-1}) at pHo=8.5 (0.44 ± 0.03. min^{-1}; n=67 cells) was significantly higher than at pHo=7.4 (0.35 ± 0.03. min^{-1}; 57 cells P=0.004; Figure 6.3a). When analysis was restricted to those cells in which oscillations were observed both at pHo=7.4 and at pHo=8.5 (Figure 6.2b green), the mean frequency of the Ca^{2+} oscillations was again significantly higher at pHo=8.5 (0.47 ± 0.04. min^{-1}) than at pHo=7.4 (0.34 ± 0.04. min^{-1}; P = 0.03, 35 cells) (Figure 6.3b).

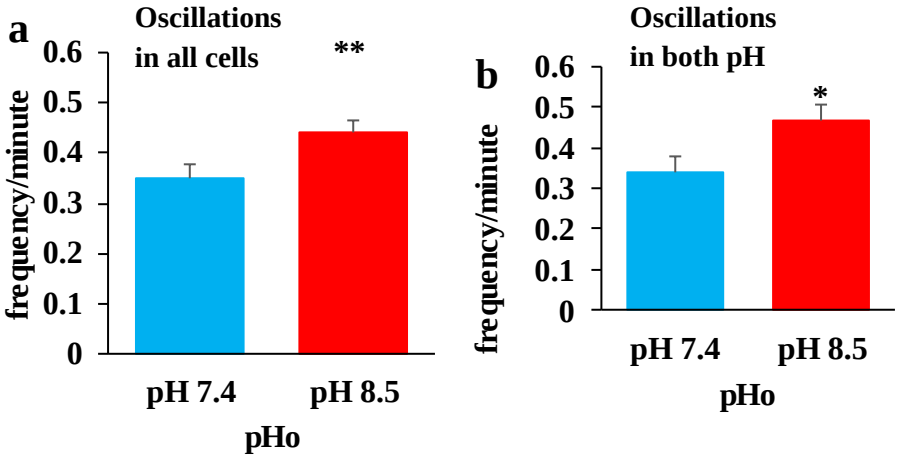

Figure 6.3: Mean frequency of Ca^{2+} oscillations induced by pH. a shows the rate of occurrences of spontaneous oscillations in pHo=7.4 (blue; n=57 cells) and pHo=8.5 (red; n=67 cells), calculated using all cells in which oscillations were observed. Rate was significantly higher at pHo=8.5 (P=0.004 ;). b shows the rate of occurrences of spontaneous oscillations in pHo=7.4 (blue) and pHo=8.5 (red) in those cells that oscillated under both conditions. Again rate was significantly higher at pHo=8.5 (P=0.03; n=35 cells).

6.4.2.2 Amplitude of $[Ca^{2+}]_i$ oscillations at pHo=7.4 and pHo=8.5

When all cells in which oscillations were observed were included in the calculation, the mean oscillation amplitude (% rise in Fluo4 fluorescence) at pHo=7.4 was 47.1 ± 2.4 (n=57 cells) whereas at pHo=8.5 this increased significantly to 63.9 ± 4.6 (Figure 6.4a; P = 0.0008, n=67 cells). When the analysis was restricted to those cells in which oscillations were observed both at pHo=7.4 and at pHo=8.5 (Figure 6.2b green), the mean amplitude at pHo=7.4 was 46.4 ± 3.2 which was increased to 55.4 ± 4.0 at pHo=8.5 respectively (NS; P = 0.07, n=35 cells from 3 experiments; Figure 6.4b).

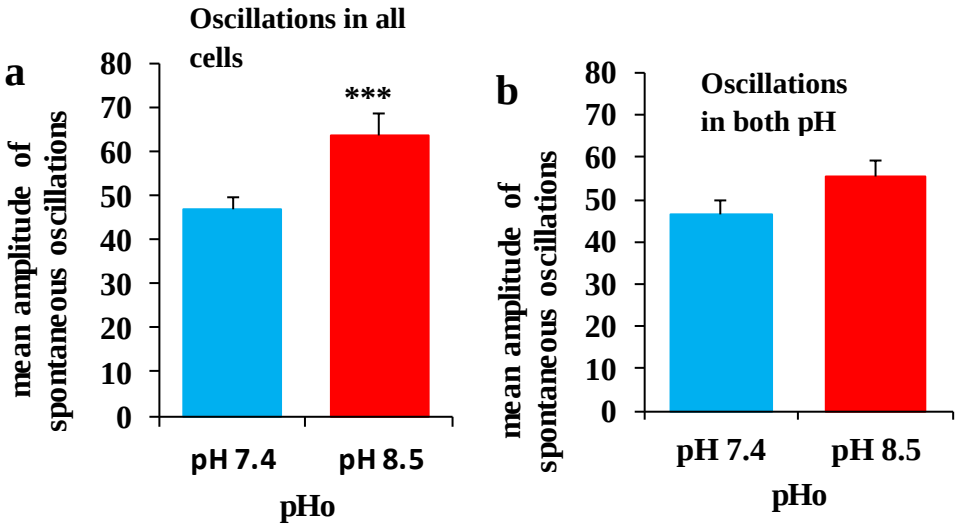

Figure 6.4: The mean amplitude of pH - induced oscillations. a shows the amplitude of $[Ca^{2+}]$i oscillations in pHo=7.4 (blue) and pHo=8.5 (red), calculated using all cells in which oscillations were observed. Amplitude was significantly greater at pHo=8.5 (P<0.001). b shows the amplitude oscillations in pHo=7.4 (blue) and pHo=8.5 (red) in those cells that oscillated under both conditions. Alkalinisation did not significantly increase the mean amplitude of oscillations (P = 0.07, n=35 cells).

6.4.2.3 Duration of $[Ca^{2+}]_i$ oscillations at pHo=7.4 and pHo=8.5

When all cells in which oscillations were observed were included in the calculation, the mean duration of Ca^{2+} oscillations at pHo=8.5 was 2.17 ± 0.13 min (Figure 6.5a red; n= 67 cells), which was significantly longer than at pHo=7.4 (1.63 ± 0.07) (Figure 6.5a blue) (P = 0.002). When analysis was restricted to those cells in which oscillations were observed both at pHo=7.4 and at pHo=8.5 the mean duration was again significantly longer at pHo= 8.5 (2.07 ± 0.16; Figure 6.5b; red) than at pHo=7.4 (1.59 ± 0.10) (Figure 6.5b; blue; P = 0.009, n=57 cells).

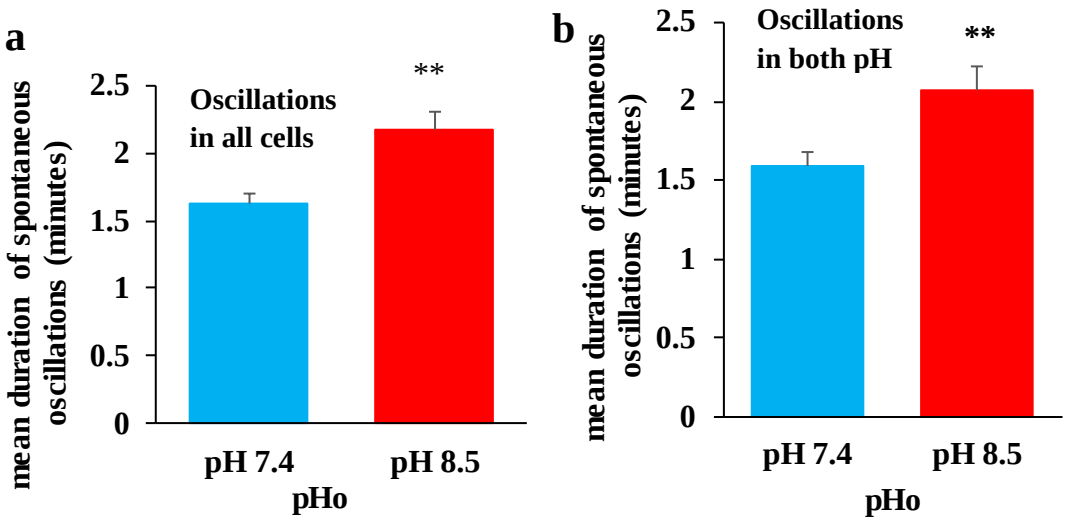

Figure 6.5: The mean duration of pH - induced $[Ca^{2+}]_i$ oscillations. a - On average, the spontaneous oscillations last longer in pH 8.5 (red panel) than in pH 7.4 (blue panel). b - In individual cells, the duration of spontaneous oscillations occurring in both pH (7.4 and 8.5) is significantly higher at pH 8.5 (red panel) when compared with pH 7.4 (blue panel) for the 3 days analysis**.**

6.5.1 Interacting effects of pH and progesterone on $[Ca^{2+}]_i$

Figure 6.6 shows an example of a single cell $[Ca^{2+}]_i$ response to P4 followed by manipulation of pHo. In this cell, application of progesterone at pHo=7.4 induced a biphasic Ca^{2+} signal that rose quickly to peak within 0.5 min (Figure 6.6a; purple bar begins) and then decayed over a period of ≈ 1min to a plateau of 111.24 ± 4.2 %. Subsequent increase of pHo to 8.5 (in the continued presence of progesterone; fig 6.6a; brown bar) induced a further $[Ca^{2+}]_i$ transient rise that peaked within 1 minute then decayed over 1.84 minutes and stabilised at a new, higher plateau level of 204.32 ± 5.34 % (Figure 6.6, panel a (red traces)). When pHo was returned to 7.4 (Figure 6.6a; second sky blue bar) $[Ca^{2+}]_i$ fell rapidly then stabilised at a level similar to that seen when first stimulated with progesterone The percentage of cells that responded to progesterone as pH changes from 7.4 to 8.5 was determined to be 88 % (n=3, 298 cells).

Figure 6.6b shows pseudo colour images of fluo-4 fluorescence from a representative cell before (A) during P4 treatment (B) during alkalinisation with P4 (C) and after return to pH 7.4 (D)

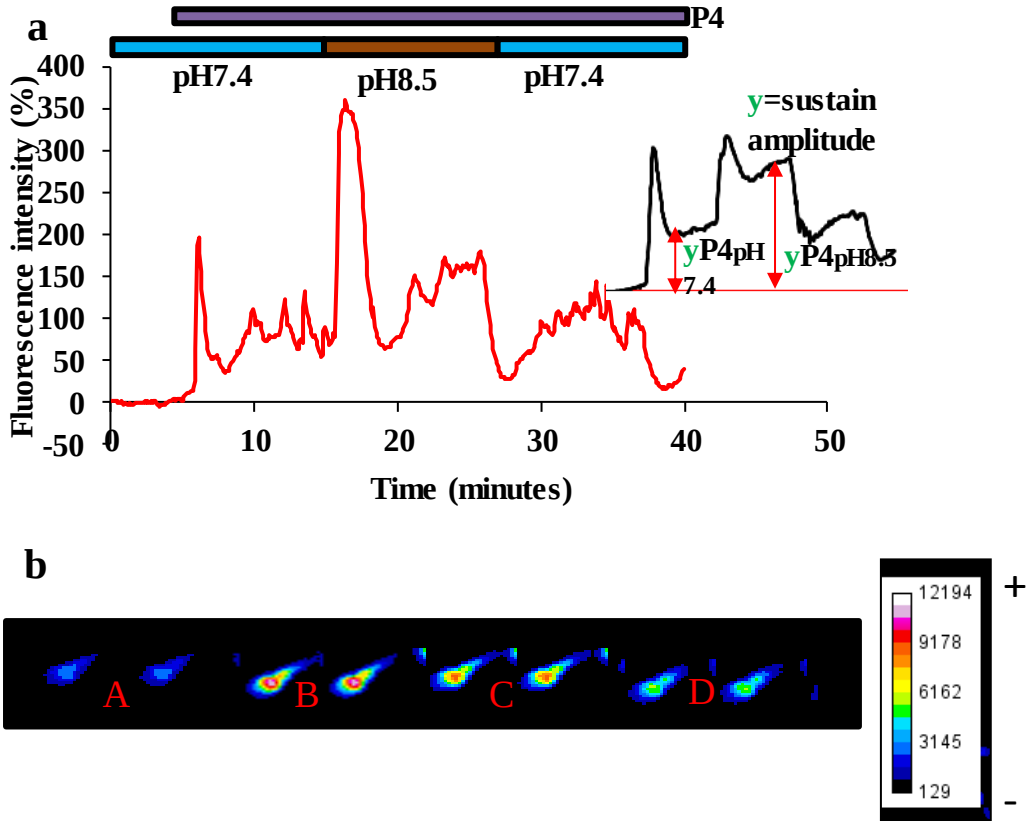

Figure 6.6: Effect of pH on progesterone -induced intracellular $[Ca^{2+}]_i$. a - $[Ca^{2+}]_i$ spike revealing the effect of pH on P4 -induced intracellular $[Ca^{2+}]_i$ (n =3, 263 cells). b shows The pseudo-colour images of Fl-4 fluorescence in a typical sperm cell at various points in the experiment. Images in panel A are prior to treatment, panel B images are during P4 treatment, panel C are images during alkalinisation with P4 treatment and panel D images are treatment with P4 after return to pH7.4. Inset shows sustain as calculated in this experiment.

6.5.2 Mean $[Ca^{2+}]_i$ sustain response

Elevation of pHo from 7.4 to 8.5 during the sustained phase of the P4-induced Ca^{2+} response significantly increased $[Ca^{2+}]_i$, (93.08 ± 3.72 %; Figure 6.6a and 6.7a; $P=1.6x10^{-71}$,n=263 cells). Plotting of the single cell amplitude distribution for normalised fluorescence recorded during the sustained phase of the response to P4 at pHo=7.4, gave a skewed bell shaped distribution (Figure 6.7b; blue plot). When pHo was increased to 8.5 the entire distribution was shifted to the right (Figure 6.7b; red plot). To investigate whether sensitivity of individual cells to P4 and to alkalinisation were correlated, the amplitude of the increments in normalised fluorescence induced by P4 and by alkalinisation were calculated for each cell and plotted as a scattergram. There was no significant relationship between the responses to the two stimuli and, despite considerable variation, it appeared that the response to alkalinisation was essentially independent of the preceding effect of stimulation with P4 (Figure 6.7c). To verify if there is synergism between P4 and pH, plotting of the single cell amplitude distribution for normalised fluorescence of sustained phase in the presence (red) and absence of P4 at pHo=8.5 (blue) , gave a slight shift to the right (Figure 6.7d).

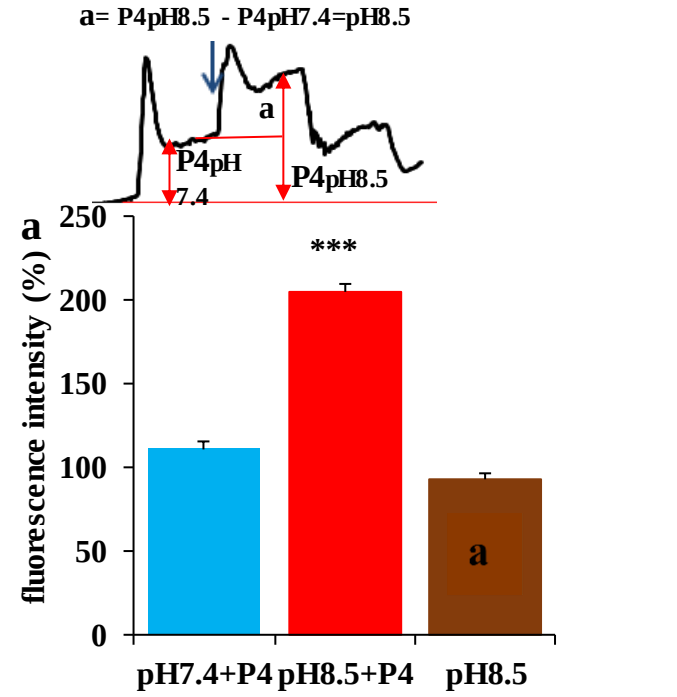
a= P4pH8.5 - P4pH7.4=pH8.5
a
P4pH 7.4
P4pH8.5
a
***
fluorescence intensity (%)
250
200
150
100
50
0
a
pH7.4+P4
pH8.5+P4
pH8.5

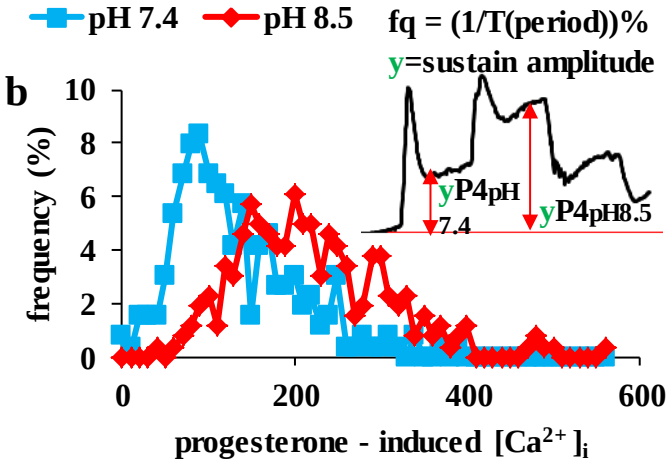
pH 7.4
pH 8.5
fq = (1/T(period))%
y=sustain amplitude
b
frequency (%)
10
8
6
4
2
0
yP4pH 7.4
yP4pH8.5
0
200
400
600
progesterone - induced [Ca2+]i

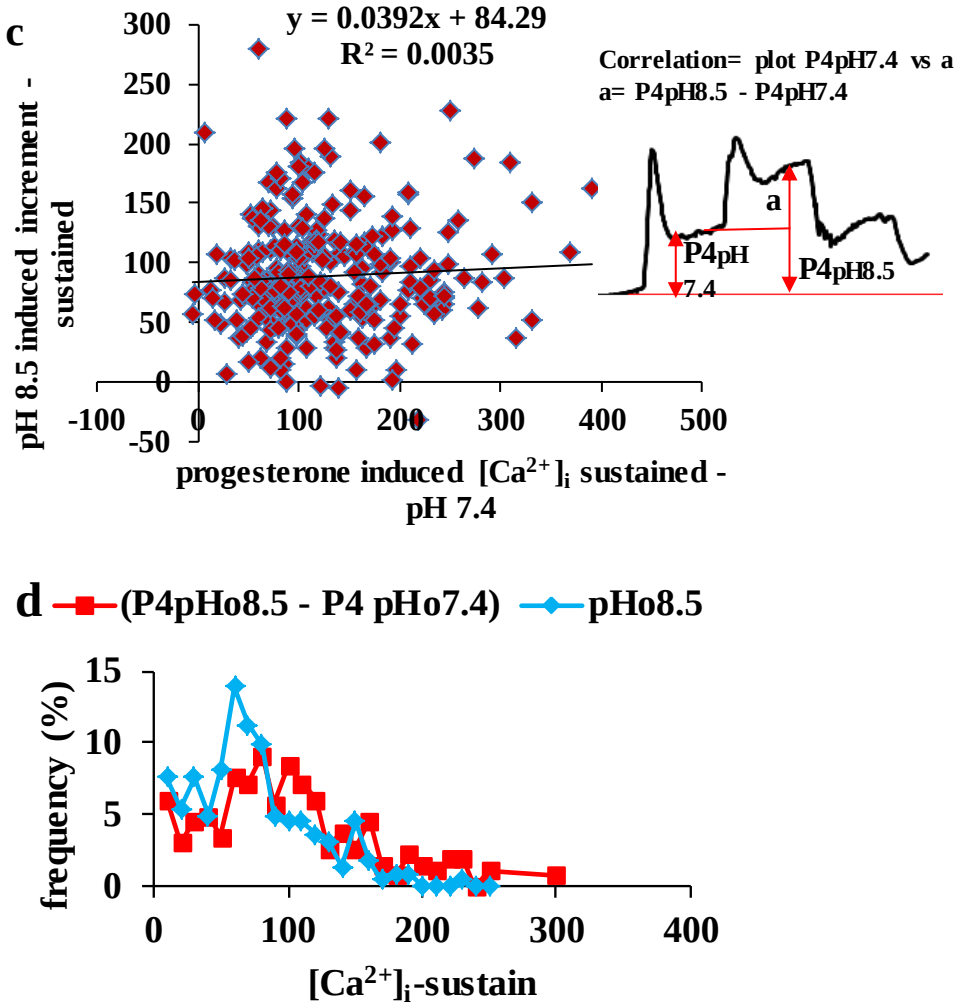

Figure 6.7: Progesterone induced Ca^{2+} sustained response in high pH. a shows amplitude of resting [Ca^{2+}] in the presence of P4 (sustained response-blue) and after elevation of pHo to 8.5 (red) – alkalinisation significantly increased the resting [Ca^{2+}]i (**P<0.01, n = 3,). Brown bar shows the mean increment induced by alkalinisation. b: - Alkalinisation shifted the amplitude P4 - induced sustained to the right and reduced the percent rate of occurrence. c- shows relationship between resting [Ca^{2+}] in the presence of P4 (sustained response) and increment induced by subsequent alkalinisation (pHo=8.5). The effect of alkalinisation is largely independent of the elevation of $[Ca^{2+}]_i$ induced by P4 (n=268 cells). d- There is slight shift to the right by pHo8.5 sustain response in the presence of P4 (red) compared to pHo in the absence of P4 (blue).Insets show what is measured and plotted in each panel.

6.5.3 Effect of alkalinisation on Progesterone induced $[Ca^{2+}]_i$ oscillations

Figure 6.8a-c show different oscillations induced by P4 at different pH conditions. In 106/263 (40.3%) of cells exposed to P4, the initial stimulation with progesterone induced the generation of $[Ca^{2+}]_i$ oscillations, superimposed on the sustained $[Ca^{2+}]_i$ plateau (Figure 6.8a; Figure 6.8d; blue and green). Of these 106 oscillating cells, 73 continued to oscillate when pHo was increased from 7.4 to 8.5 (Figure 6.8a,d; green). In addition, a further 31 cells which were 'quiet' during exposure to P4 at pHo=7.4 generated $[Ca^{2+}]_i$ oscillations upon elevation of pHo from 7.4 to to 8.5 (Figure 6.8c,d red), making a total of 104/263 (39.5%) oscillating in the presence of P4 at pHo=8.5, similarly to at pH 7.4 (Figure 6.8e).

To assess whether alkalinisation affected the characteristics of $[Ca^{2+}]_i$ oscillations in cells exposed to P4, I next assessed their frequency and also their amplitude and duration under each condition.

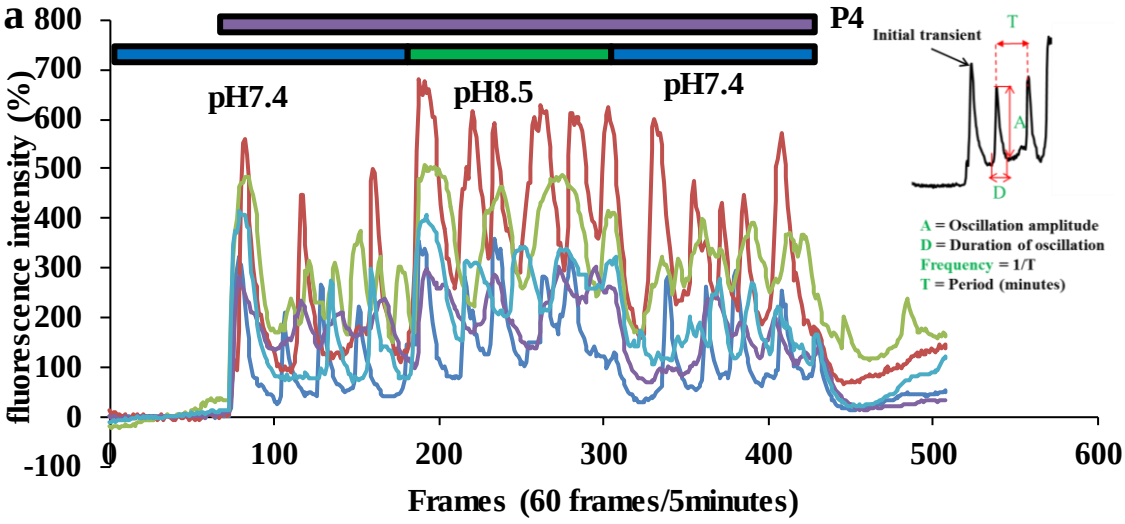

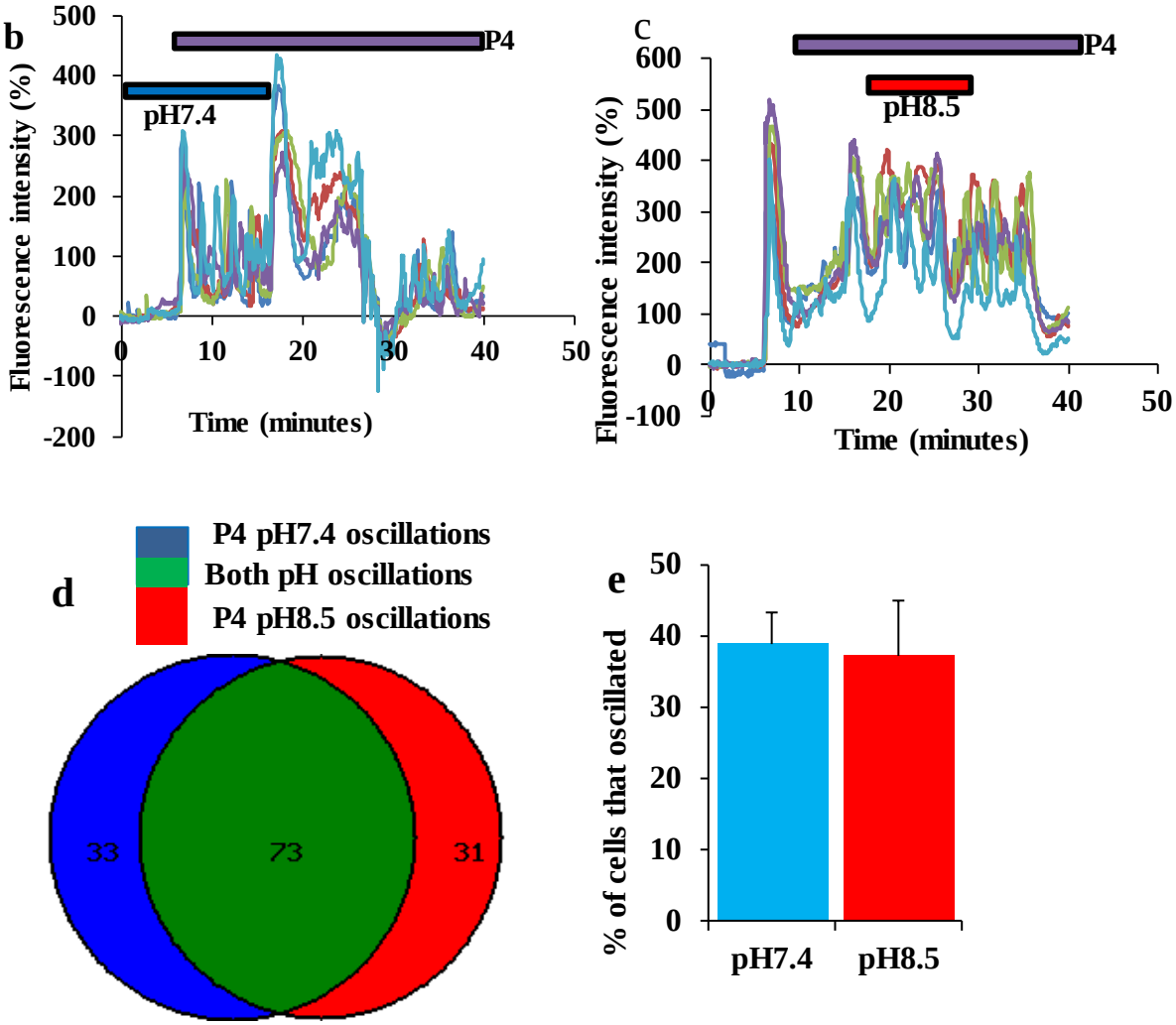

Figure 6.8: Progesterone induced oscillations in alkalinisation. a shows oscillatory spikes induced by P4 modulated $[Ca^{2+}]_i$ at both pH 7.4 and 8.5 in five individual cells. b, c shows oscillating cells at pH 7.4 and 8.5 respectively. d shows distribution of oscillations in individual cells before and after changing pHo (blue, green, red). e – Alkalinisation did not change the percentage of oscillating cells.

6.5.3.1. Frequency of progesterone induced $[Ca^{2+}]_i$ oscillations at pHo=7.4 and pHo=8.5

When all cells in which oscillations occurred were included in the calculation, the mean frequency of oscillation (rate.min^{-1}) at pHo=8.5 (0.44 ± 0.02) (was slightly lower than but not significantly different from that at pHo=7.4 (0.51 ± 0.02) (Figure 6.9a; P= 0.06, n =3). When analysis was restricted to those cells in which oscillations were observed both at pHo=7.4 and at pHo=8.5 the mean frequency of the Ca^{2+} oscillations was again slightly lower at pHo=8.5 (0.47 ± 0.03) than at pHo=7.4 (0.53 ± 0.03) but again this difference was not significant, (Figure 6.9b).

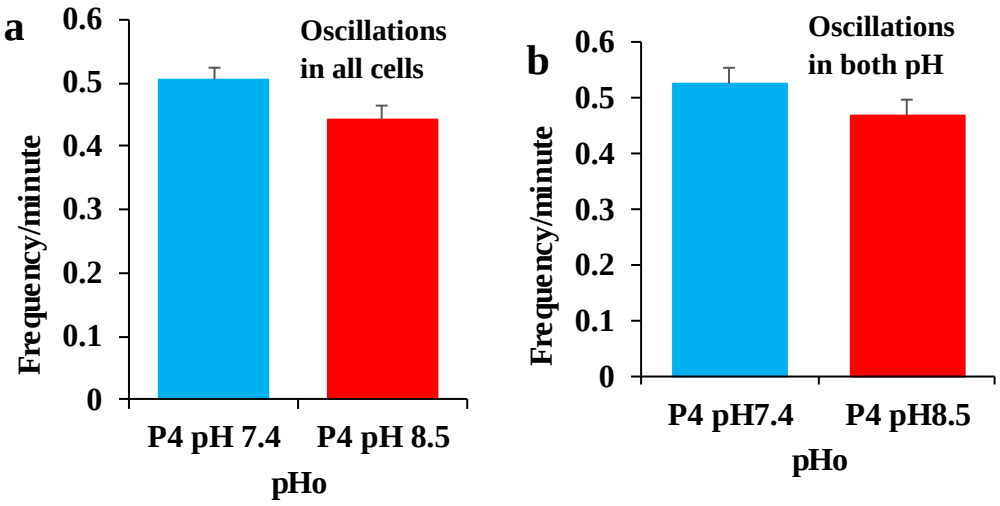

Figure 6.9: The mean frequency of oscillations induced by P4 at pH 7.4 and 8.5. a - Change in pHo did not affect the rate of oscillation in all oscillating cells. b - In individual cells where oscillations occurred at both pH (7.4 and 8.5). Alkalinisation did not change the frequency of oscillation (n = 3, 268 cells) and there was no significance change in each case (P > 0.05).

6.5.3.2 Amplitudes of progesterone induced $[Ca^{2+}]_i$ oscillations at pHo=7.4 and pHo=8.5

When all cells in which oscillations occurred were included in the calculation, there was no significant difference in the mean amplitude of Ca^{2+} oscillations at pHo=7.4 and pHo=8.5 (Figure 6.10a; P=0.44, n=3). When the analysis was restricted to those cells in which oscillations were observed both at pHo=7.4 and at pHo=8.5 again the mean amplitude was similar at pHo=7.4 and pHo=8.5 ((Figure 6.10b; P=0.92, n = 3).

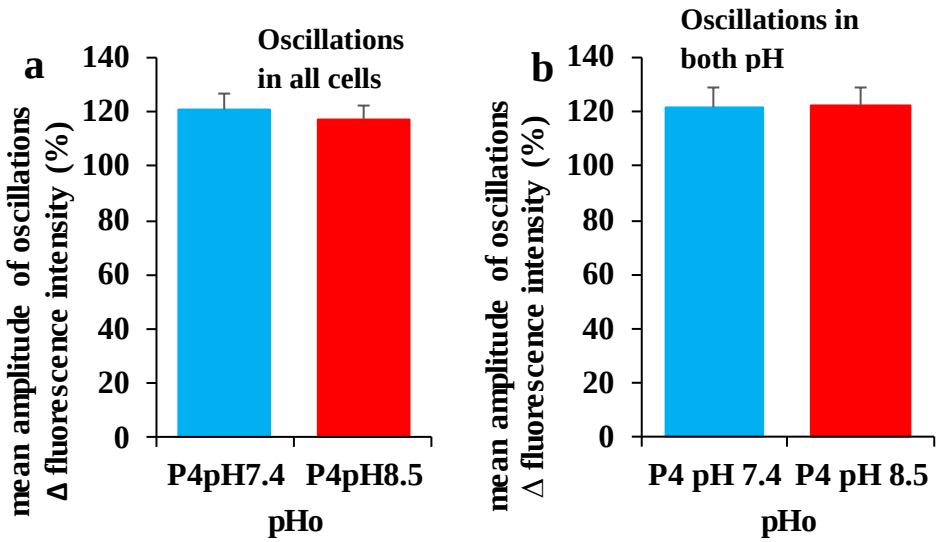

Figure 6.10; The mean amplitude of oscillations produced by progesterone at pH 7.4 and 8.5. a - Change in pHo did not change the amplitude in all oscillating cells. b shows individual cells where oscillations occurred in both pH (7.4 and 8.5) there were no change in the amplitude of oscillations in alkalinisation. There was no significant difference at pH 8.5 (red panel) compared to control pH 7.4 (blue panel) (n =3, 268 cells) (panel a, b).

6.5.3.3 Duration of progesterone induced $[Ca^{2+}]_i$ oscillations at pHo=7.4 and pHo=8.5

When all cells in which oscillations were observed were included in the calculation, the mean duration of Ca^{2+} oscillations was significantly greater at pHo=8.5 (2.47 ± 0.11) than at pHo=7.4 (1.46 ± 0.04) (Figure 6.11a; P= $3.6*10^{-14}$, n =3). When the analysis was restricted to those cells in which oscillations were observed both at pHo=7.4 and at pHo=8.5 a similar pattern was seen. At pHo=7.4 mean duration was 1.45 ± 0.05 min but after elevation of pHo to 8.5 this increased to 2.29 ± 0.11 (Figure 6.11b; P=$4*10^{-11}$, n = 3).

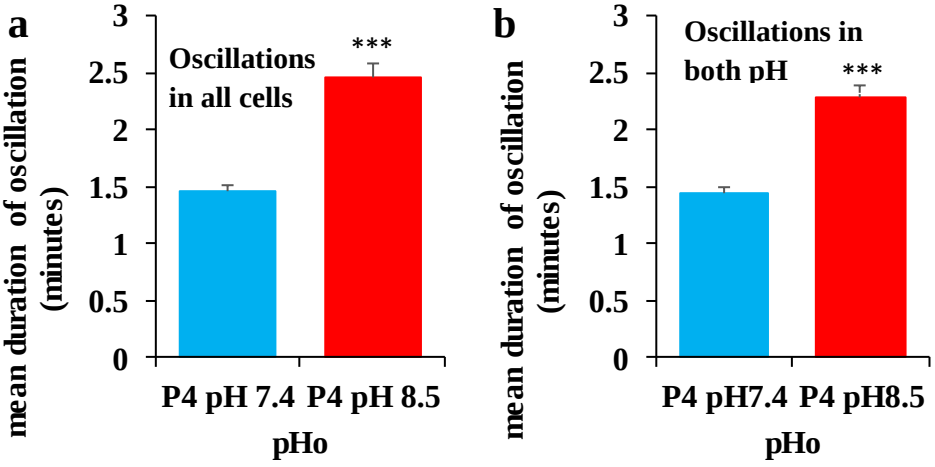

Figure 6.11: The mean duration of oscillations induced by progesterone with change in pHo. a - The duration of oscillations in all oscillating cells was significantly greater in pH 8.5 (red panel) than in pH 7.4 (blue panel). b shows the duration of oscillations that occurred in cells that oscillated at both pH (7.4 and 8.5) was significantly higher in pH 8.5 (red panel) than pH 7.4 (blue panel) (***P < 0.001, 268 cells).

6.6 Key findings

(i) Consistent with population analysis, increasing the pHo from 7.4 to 8.5 elevated (i) resting $[Ca^{2+}]_i$ -consistent with tonic activation of CatSper and (ii) the the sustained $[Ca^{2+}]_i$ response of cells already exposed to progesterone.

(ii) The Effect of combined stimulation with high pHo and progesterone appeared to be additive and not synergistic since the increment in $[Ca^{2+}]_i$ caused by application of alkalinisation to cells already stimulated with P4 was independent of the amplitude of the preceding response to P4.

(iii) Spontaneous $[Ca^{2+}]_i$ oscillations occurred at both pH conditions. At high pHo the amplitude, duration and frequency of the oscillations was increased but there was no change in the number of oscillating cells.

(iv) Changing the pHo from 7.4 to 8.5 in cells already exposed to progesterone did not affect oscillation amplitude or frequency or change proportion of oscillating cells but increased the duration of oscillations.

(v) The increase in duration of oscillations at high pH may reflect inhibition of calcium clearance mechanisms.

6.7 Discussion

6.7.1 Alkalinisation elevated the resting $[Ca^{2+}]_i$

Consistent with the higher resting $[Ca^{2+}]_i$ measured in cell populations suspended in saline at pH of 8.5, Increase of pHo from 7.4 to 8.5 caused a rapid increase in resting $[Ca^{2+}]_i$ signal that peaked at >100% above the level at pHo=7.4 then stabilised at a lower plateau level. This observation confirms the importance of pH in determining influx of Ca^{2+} into human sperm and indicates that the observed effect of extracellular alkalinisation on pHi (see chapter 4) is sufficient to cause tonic activation of CatSper and set $[Ca^{2+}]_i$ at a new, higher level.

When pHo was increased from 7.4 to 8.5 in cells that had already been exposed to progesterone the resting $[Ca^{2+}]_i$ increased by 93%, compared to a rise of 69% when pHo was increased in the absence of P4. These values are significantly different ($P=1.7x10^{-06}$,paired t-test, see Figure 6.7d) suggesting some level of synergistic interaction of P4 and pH as suggested by (Lishko et al., 2011, Strünker et al., 2011). However, plotting of the relationship between the P4-induced sustained $[Ca^{2+}]_i$ signal (increment in resting $[Ca^{2+}]_i$ induced by P4) and the increment in $[Ca^{2+}]_i$ induced by subsequent increase of pHo from 7.4 to 8.5, revealed no relationship – the response to alkalinisation was similar in cells that responded strongly to P4 and those that gave a negligible response.

6.7.2 Alkalinisation and $[Ca^{2+}]_i$ oscillations

When cells were at pHo=7.4 spontaneous $[Ca^{2+}]_i$ oscillations occurred in ≈25% of sperm and this was not significantly altered by elevation of pHo to 8.5. However, alkalinisation did increase the amplitude, duration and rate at which oscillations occurred. Oscillations induced by treatment with P4 at pHo=7.4 were larger than those occurring spontaneously (≈120% compared to ≈50%, P = 5.4 x 10-17, n = 3). When pHo was increased to 8.5 there was no significant effect on either the proportion of oscillating cells (35-40%) or their rate of occurrence, but the duration was greatly increased, similarly to spontaneous oscillations, from ≈1.5 to ≈2.5 minutes.

The mechanisms underlying generation of $[Ca^{2+}]_i$ oscillations are not clear and therefore these effects of alkalinisation, though interesting, are not easy to interpret. It was shown previously that generation of oscillations in human sperm requires a minimal level of Ca^{2+} entry at the plasma membrane (Bedu-Addo, 2008, Harper et al., 2004), which may then mobilise stored Ca^{2+}. Similarly, in heart muscle, calcium oscillations are associated with calcium induced calcium released mechanism initiated by entry of $[Ca^{2+}]o$ (Bers, 2002) or store operated Ca^{2+} entry (Miyazaki, 1995). $[Ca^{2+}]_i$ oscillations generated by P4 in human sperm were reported to involve CICR mediated by ryanodine receptors (Bedu-Addo, 2008). CatSper, the primary route for Ca^{2+} entry at the plasma membrane of sperm, is activated by increased intracellular pH (Navarro et al., 2007, Xia and Ren, 2009b) and thus the alterations in oscillation characteristics may reflect this enhanced Ca^{2+} influx, though it is surprising that the proportion of oscillating cells was not increased.

The most striking effect of alkalinisation was on the duration of the oscillations (Figures 6.5 and 6.11) This may be due to reduced rates of Ca^{2+} clearance by the plasma membrane Ca^{2+}ATPase, due to unavailability of extracellular H^{+} (Wennemuth et al., 2003). However. it is notable that examination of oscillations at pHo=8.5 suggests that their longer duration is not only due to slow Ca^{2+} clearance but also involves a slower or stepped rising phase.

CHAPTER 7: THE EFFECT OF $[Ca^{2+}]_i$ MOBILISING DRUGS AND pH ON SPERM BEHAVIOUR

7.1 Objective

Sperm can show a number of motility patterns or 'behaviours'. Switching between behaviours has been observed in cells swimming in vitro and may be functionally important during navigation of the female tract, probably being regulated by changes in $[Ca^{2+}]_i$. Having characterised the effects on $[Ca^{2+}]_i$ and on motility of cell populations of elevated pHo and of stimuli that target CatSper and Ca^{2+} stores, the aim of the experiments reported in this chapter was to observe the effects of these manipulations on sperm behaviour.

7.2 Introduction

Human sperm motility is dependent on the beating of the flagellum, which enables the cell to progress from the vagina to the site of fertilisation in the oviduct (Suarez and Pacey, 2006). In freshly ejaculated sperm the flagella waveform is symmetrical and bends are shallow, generating progressive, 'activated' motility (Suarez, 2008). At some points of the journey in the female tract, a proportion of the sperm adopts a more erratic behaviour with asymmetric flagella waveforms and deeper bending which generate vigorous side to side movement of the head (which can be progressive or non-progressive in low viscosity medium) and is referred to as 'hyperactivated' motility. The sperm switch between progressive and non-progressive types of hyperactivation and between hyperactivated and activated motility (Mortimer and Swan, 1995). Armon and Eisenbach, (2011) suggested that progesterone acts as a chemoattractant to human sperm and the stimulation of sperm by progesterone in the oviduct evoked progressive motility up the progesterone concentration gradient towards the oocyte but when the sperm starts to swim away from the oocyte, down the progesterone (chemoattractant) gradient, it switches to the vigorous head movement and flagella whiplash pattern to generate a change in direction.

To assess the pattern of sperm movement the position of the sperm head is often used since it is easier to detect and moves more slowly than the flagellum. Computer assisted sperm analysis (CASA) tracks the sperm head in a series of video frames and 'draws' the trajectory made of the sperm head. CASA analysis of sperm movement relies on the assumption that movement of the head reflects the beating pattern of the tail, and measures characteristic features in the track traced by the sperm head. These include velocity (curvilinear velocity (VCL μm/s), average path velocity (VAP) and straight line velocity (VSL)), amplitude of head displacement either side of the sperm's path (ALH), rate at

which the sperm head crosses the average path (BCF) and degree of deviation from a straight line (LIN) (Mortimer, 2000).

In the previous chapters we saw that; alkalinisation, progesterone and 4AP induce elevated $[Ca^{2+}]_i$ and affect motility, potency of 4AP being enhanced by alkalinisation. Ca^{2+} plays a central role in the regulation of hyperactivation since the switch in sperm motility pattern is dependent on increase in $[Ca^{2+}]_i$ (Suarez, 2008) , but mobilisation of stored Ca^{2+} may be particularly important for transition to hyperactivated motility (Alasmari et al., 2013b, Bedu-Addo, 2008). The peaks of P4 induced $[Ca^{2+}]_i$ oscillations, when stored Ca^{2+} is believed to be mobilised by CICR, are associated with increased flagella bending (Harper 2004). Therefore, in this work, I collected extended high-speed (60 Hz) video recordings of single cells that were exposed to:

- high pHo (8.5)
- agonists of CatSper: (P4, follicular fluid, which contains P4 and other endogenous molecules that regulate sperm function through $[Ca^{2+}]_i$ (Baldi et al., 1998, De Jonge, 2005, Fujinoki et al., 2015, O'Gorman et al., 2013) (FF))
- agonists of Ca^{2+} stores: 4AP, thimerosal (activates IP_3/Ry receptors; (Bultynck et al., 2004, Tanaka and Tashjian, 1994) (Tm)), in order to investigate their effect on the behaviour of human sperm, including occurrence and frequency switching between different motility types.

7.3 Materials and Methods

7.3.1 Materials

For the Materials section, see Chapter 2.1

0.3µM P4, 2mM 4AP, 1µM Tm, 1% FF and control (no agonist) in pHo 7.4 (25 mM Hepes saline) and 8.5 saline respectively were used in these experiments (See Table 1.0 for replicates).

7.3.2 Methods

7.3.2.1 Donor recruitment

Donor recruitment was conducted as described in Chapter 2.2.

7.3.2.2 Sperm cell preparation

The sperm cells were prepared as explained in chapter 2.4

7.3.2.3 Acquisition of images on the effect of pH and calcium mobilising drugs on motility behaviour in human sperm

The acquisition of images was done as reported in chapter 2.9.

7.3.2.4 Sperm tracking of the motility behaviours induced by pH and Ca^{2+} mobilising drugs

The Metamorph machine was used to generate trajectory tracks and corresponding excel data as reported in chapter 2.9

7.3.2.4.1 Experimental protocol

Freely swimming cells were recorded continuously for 3 min. After the initial examination of the tracks and studying the behaviour of cells on videos, 4 different categories of motility were defined - T1, T2, T3 and T4 (see results for further detail). Since most cells

changed behaviour several times during the recording period, each 3 min video/track was considered in 180, 1 s segments, each segment being categorised as behaviour T1, T2, T3 or T4. From these data, the proportion of time spent by each cell in each behaviour, the duration of each period consistent motility (dwell time) and the rate at which motility changed (motility switching) could be calculated. The behaviour of 15-21 cells was studied in this way for each of 10 different conditions, control, and in the presence of P4, FF, 4AP, thimerosol, each at pHo=7.4 and at pHo=8.5 (Table 1.0).

Table 1.0: Breakdown of 3minute videos showing human sperm behavior stimulated by Ca^{2+} mobilizing drugs at pH7.4 and 8.5

Treatment	pH 7.4 Number of videos captured (n)	pH 8.5 Number of videos captured (n)
Control	18	18
0.3µM P4	18	15
1% FF	17	19
1µM Tm	19	16
2mM 4AP	21	20

7.4 Results

7.4.1 Motility types

In order to investigate the effects of each drug on motility patterns, single cells were followed and images acquired over a period of 180 seconds (Table 1). These videos showed great variation in motility but patterns could be classified into four types (T1-T4) (Figure 7.1 a-d):

Type1 (T1) – (not hyperactivated) – a progressive motility type with limited lateral movement of the head (Figure 7.1; panel a) produced by symmetric flagella movements (Figure7.2b, sky-blue arrow). Cells showing this behaviour sometimes followed a curving track such that they described large circles or ovoid (Figure 7.2a). Type2 (T2) – (transitional hyperactivated) – in tracks of T2 motility lateral movements were clearly greater than in T1 (T2=7μm, T1 = 2μm). Tracks could be progressive (T2 'straight') or included sudden turns (T2 'folded') but many cells continuously turned producing star shaped tracks (Figure 7.3; panel a – d). Examination of the videos of T2 motility showed moderate, asymmetric flagella bending and sometimes stronger bending that was restricted to the proximal flagellum (Figure 7.3; panel e, red arrow) and (Figure 7.3; panel f, red arrow). Type3 (T3) – (hyperactivated) – tracks of T3 motility showed more pronounced lateral movement than T2 (T3=8μm, T2=7μm)) and were star-shaped or highly folded (straight portions interspersed with tight turns) so that the cell was non-progressive (Figure 7.4; panel a – d). Examination of videos showed deep, whiplash bending of the principal piece producing strong side to side movement of head (Figure 7.4; panel e and f, yellow arrows) and

Type4 (T4) (hyperactivated/arrested) – this type of motility was characterised by tight bending of the midpiece producing a J-shape or coil. Cells were arrested for up to 20

seconds in this state and 'twitched' whilst remaining stationary (Figure 7.5; panel a) or else generated bending only in the region of the flagellum behind the tight anterior bend, resulting in poor forward movement (Figure 7.5; panel b, brown arrow).

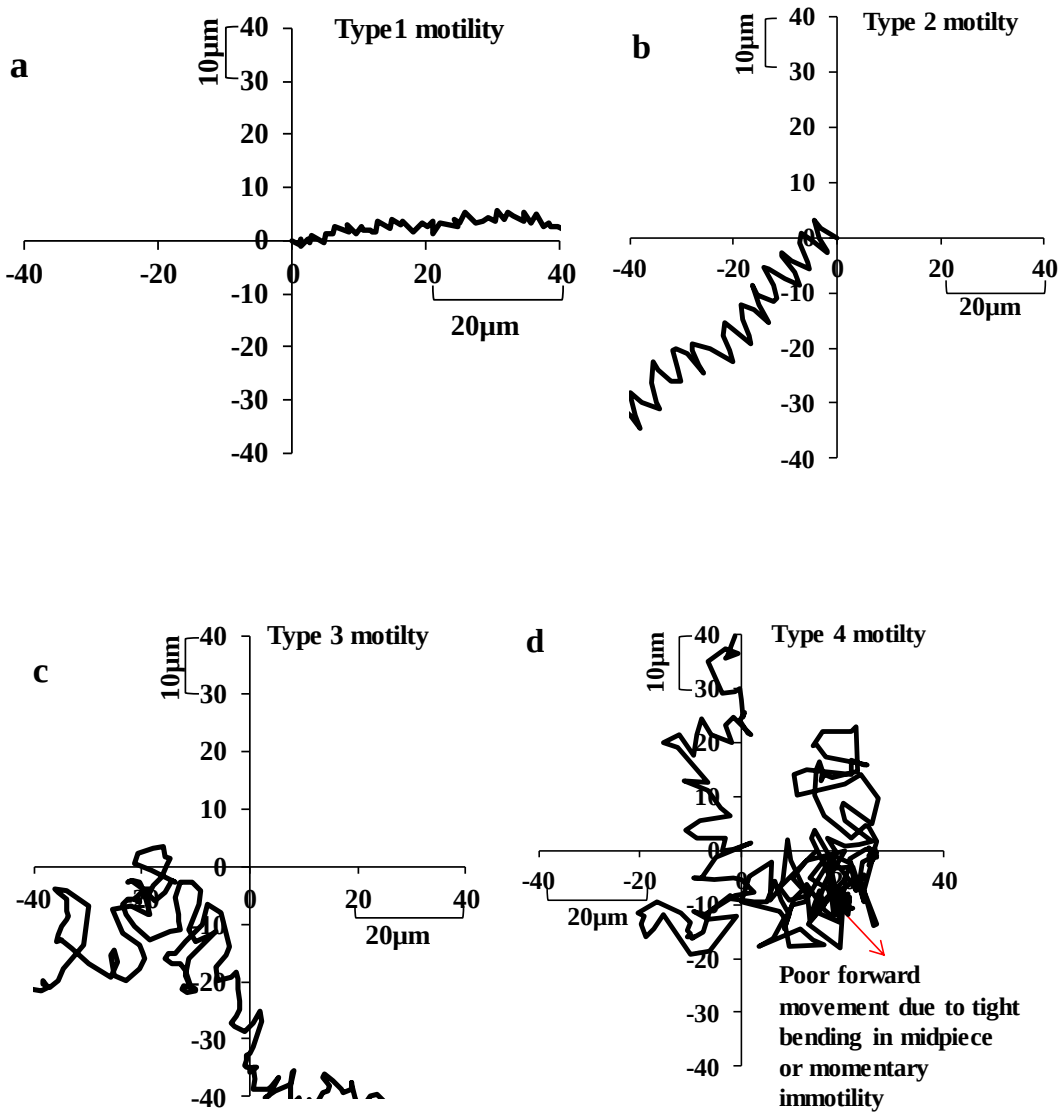

Figure 7.1: Motility types observed.
a - At both pH conditions, in the absence and presence of drugs, single cell was followed using the microscope stage and image recorded on video for 3 minutes in each treatment. 4 categories of assessed motility was assigned motility type; (a) Type1 – (not hyperactivated). (b) Type2 – (Less hyperactivated). (c) Type3 – Highly hyperactivated and (d) Type4 – Cell can freeze or move with great difficulty with deep bending near the neck. Red arrow shows constrained movement.

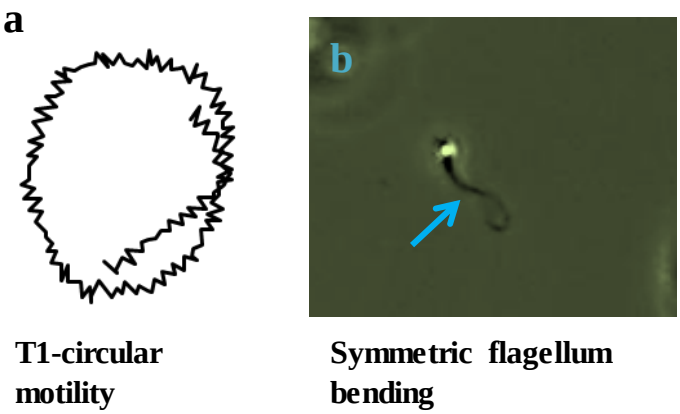

Figure 7.2: Type1 – motility and symmetric flagella bending. a show a non-hyperactivated circular motility type (panel a).b shows T1- type is associated with symmetric flagellum bending (sky blue arrow, panel b).

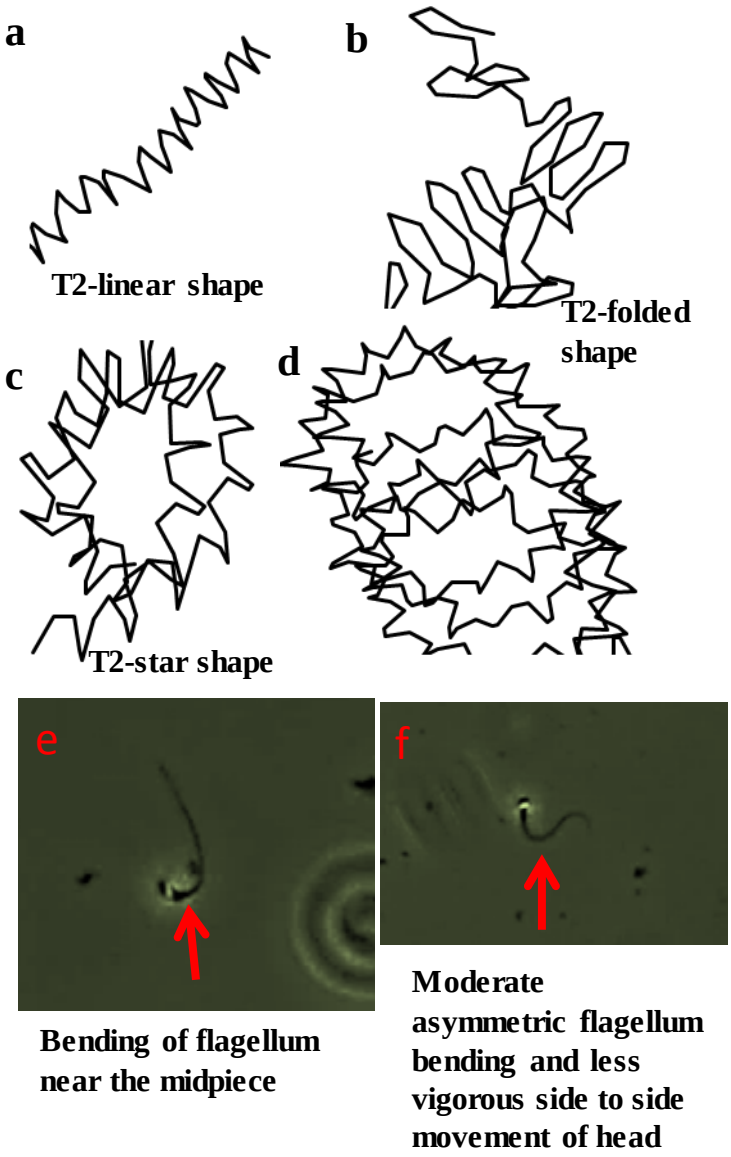

Figure 7.3: Type2-motility with less erratic lateral head movement (less hyperactivated). a – d show the star, cluster, folded and linear shapes of T2 motility type. T2 motility is generated when there is bending of the proximal region of the principal piece without propagation of the wave across the tail (panel e, red arrow) and moderate asymmetric flagellum bending with less erratic lateral movement of sperm head (panel f, red arrow).

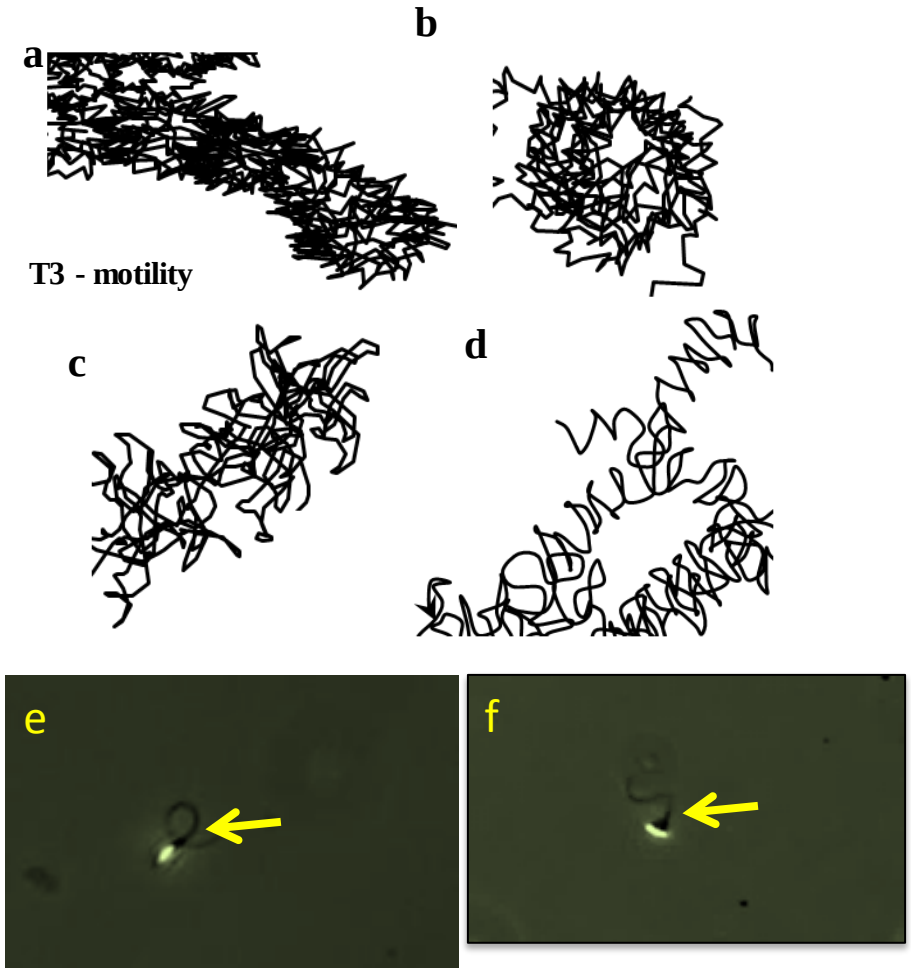

Figure 7.4: Type3 motility with erratic bending of tail and head (highly hyperactivated). a – d show T3 motility type has highly clustered pattern (panel a-d). e and f show T3 is associated with continuous deep flagellum bending and uncontrollable movement of sperm head over a small area (panel e, f, yellow arrows)

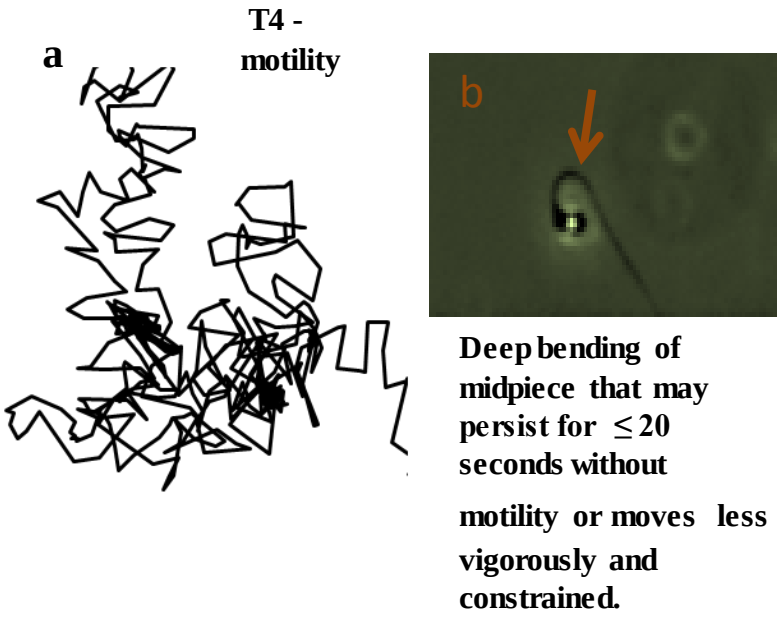

Figure 7.5: T4- Hyperactivated/arrested motility type. a shows the traces of type 4 motility. b shows sperm with deep bending of midpiece that sometimes freezes or is constrained in movement. Though the flagellum bending is always deep (panel b, brown arrow), the movement is not vigorous.

7.4.2 Proportion of time spent in each motility type

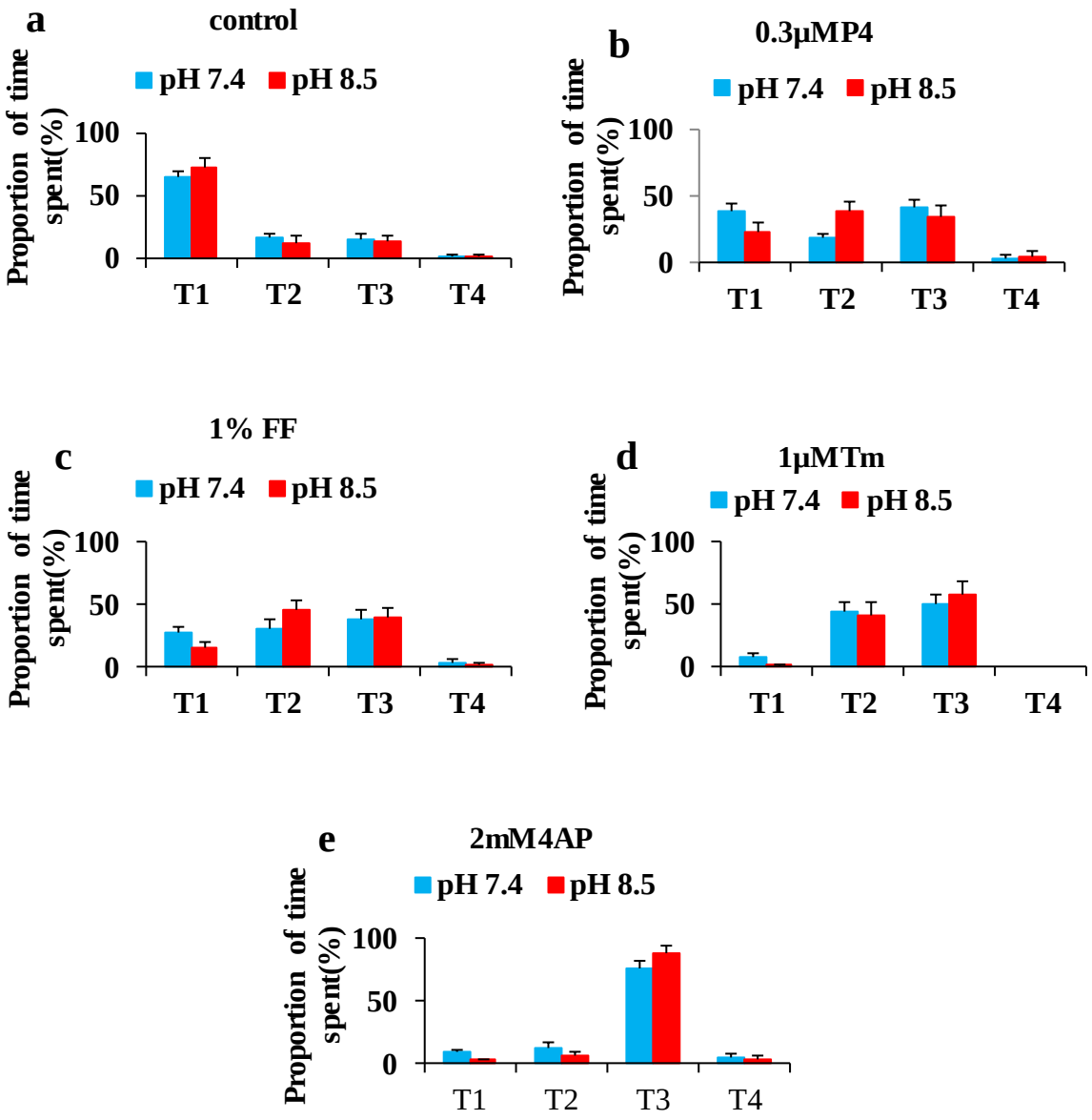

Figure 7.6: Proportion of time spent in each motility type at both pH 7.4 and 8.5. a shows that in the absence of drugs the highest percent of time was spent in T1 motility . b – d show that in the presence of drugs the percent time spent in T2 and T3 motility type increased while the T1 type decreased compared to control. However, in panel d Tm did not switch into T4 type while 4AP spent most percent time in T3 in panel e. (b-d) The proportion of time spent in motility types T2 and T3 increased with alkalinisation in drug responses.

Analysis of the proportion of time spent in each motility type showed that under control conditions cells spent 65-70% of the time displaying T1-type (non-hyperactivated) motility. All of the stimuli used here reduced the proportion of time spent in type T1 and increased T2-T4, but this effect was strongest with 4AP where cells spent >90% of the recorded time in T3 or T4. Thimerosal also strongly affected behaviour, but motility type adopted was either T2 or T3, T4 never being observed. Stimulation with P4 and FF also had clear effects (Figure 7.6b,c) but these were more modest, cells spending 30% of the time in T1 in the presence of P4 and only 30-40% in T3. Distribution of time spent between the motility categories was largely similar for pHo=7.4 and 8.5 but the higher pH tended to increase the proportion of time spent in hyperactivate-type motility patterns.

7.4.3 Does visual assessment of tracks and behaviour identify significantly different motility types?

As T2, T3 and T4 represent different degree of hyperactivated motility, to calculate % hyperactivation for each cell studied the total time spent in these behaviours was expressed as a percentage of the total tracking time of 180 seconds ((T2+T3+T4 ÷ 180) *100). A mean value for % hyperactivation was then calculated for each of the ten conditions used in this study (see Table 1) both using assessment of tracking data and using Figures for hyperactivation (sort7) from CASA assessments carried out in parallel using the same samples. Plotting of the data as a scattergram showed a strong positive correlation between the two methods (R^2=0.8) (Figure 7.7), confirming that the method used here categorised motility similarly to the widely used CASA criteria.

Using a tracking application that calculates kinematics from sperm tracks (similarly to CASA) see Figure 2.6.1), the mean VCL was calculated for each of the four motility types under control (unstimulated) conditions at pHo=7.4 and at pHo =.5. (n=3, cells switching between motility types and not stuck to the slide were selected for the analysis) There was a clear increase in VCL between TI and T2, both at pHo=7.4 and 8.5 ($P = 8.6x10^{-34}$ at pHo7.4, $P=1.2x10^{-15}$ at pHo8.5, paired t-test), and a smaller difference between T2 and T3. Assessment of motility in cells exhibiting T4 type motility gave lower values for VCL. Interestingly, in all four categories of motility mean VCL was slightly greater for cell in alkalinising medium (*P < 0.05,***P < 0.001, Holm-Bonferroni) (Figure 7.8).

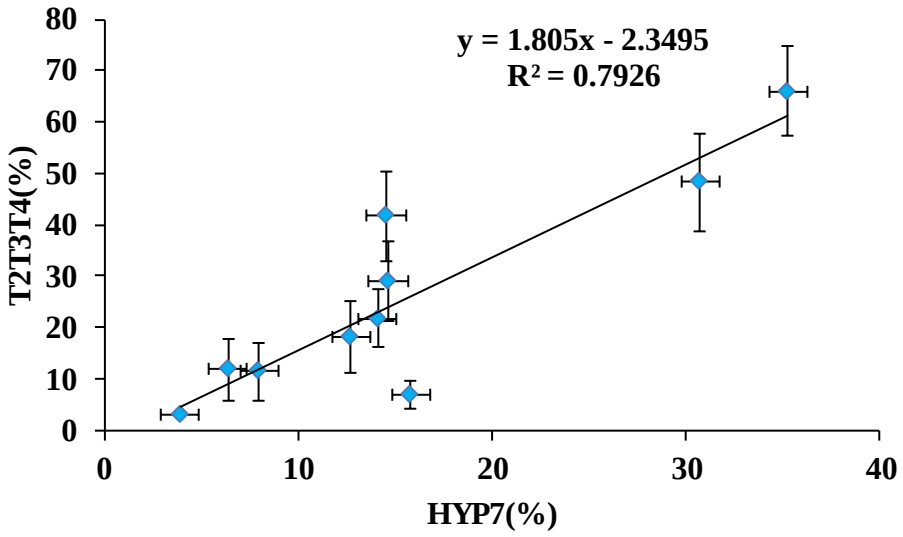

Figure 7.7: Correlation between the hyperactivation in tracked cells and CASA.

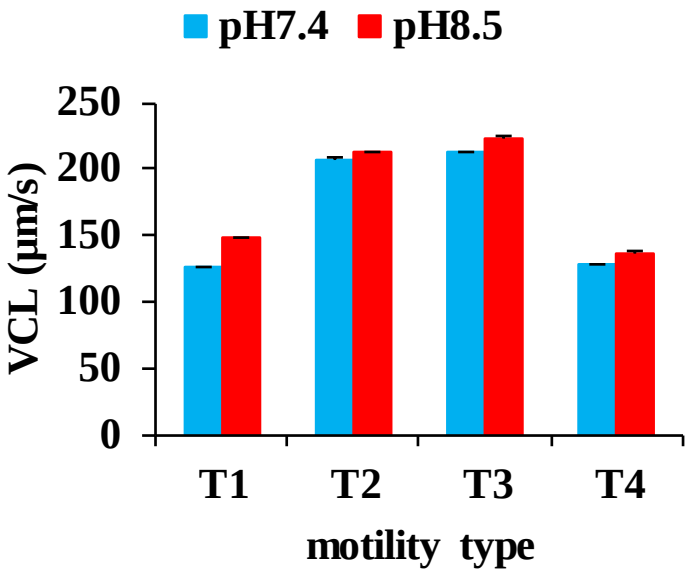

Figure 7.8: The mean VCL increase as the cell switches from non –hyperactivated to hyperactivated motility types.

7.4.4 Switching between motility types

Analysis of the motility of freely swimming cells under control conditions showed that abruptly 'switching' between motility types was a common event. The behaviour of individual cells varied markedly, some switching behaviour regularly between all motility types 1 to 4, or in bursts, whereas others would maintain the same motility type for the entire 180 s of recording (Figure 7.9a-g).

7.4.4.1 Rate of motility switching

Many cells switched between motility types several times during the 180 seconds of a recording (Figure 7.9a,c). The rate of transition of non-treated (control) cells was 6.5±0.8 and 4.1±1.1 transitions/min at pHo=7.4 (Figure 7.10 blue) and 8.5 (Figure 7.10 red) respectively (mean of 18 cells; p=0.14). Treating cells with P4 (0.3µM) had little effect on

the rate of transitions. At pHo=8.5 the rate of transitions in the presence of 1% FF appeared to be lower than in control cells but this effect was not significant (Table 2, Figure 7.10). However, when cells were exposed to 1µM Tm or 2mM 4AP (Ca^{2+} store mobilisers and potent inducers of hyperactivation) the rate of transitions was significantly reduced compared to control at both pHo=7.4 and 8.5. For all the agonists used in this study, the rate of transition between motility types was lower at pHo=8.5 than at pHo=7.4 (Figure 7.10), but this effect was significant only in the presence of 4AP and 1% FF (P=0.002, P=0.005, Table 2, Figure 7.10).

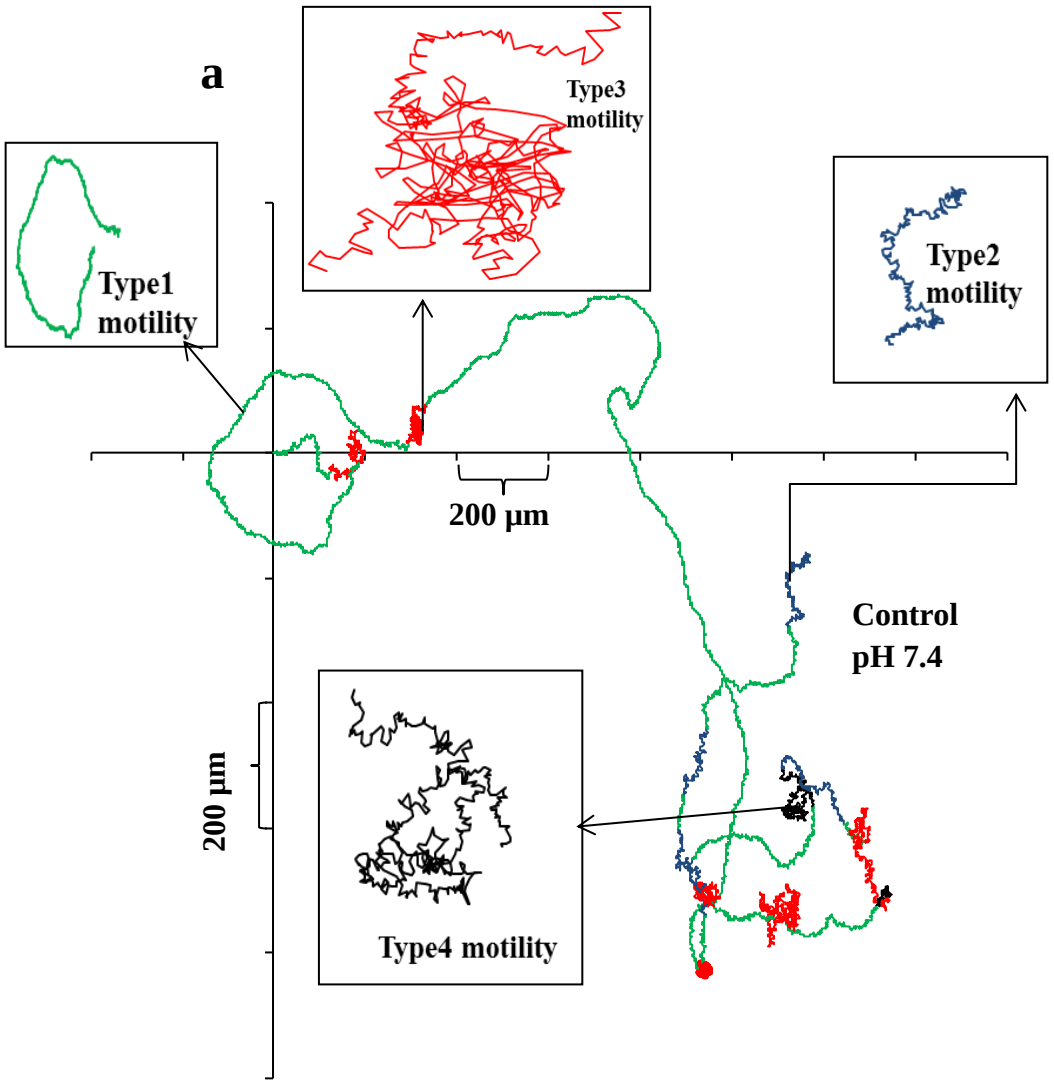

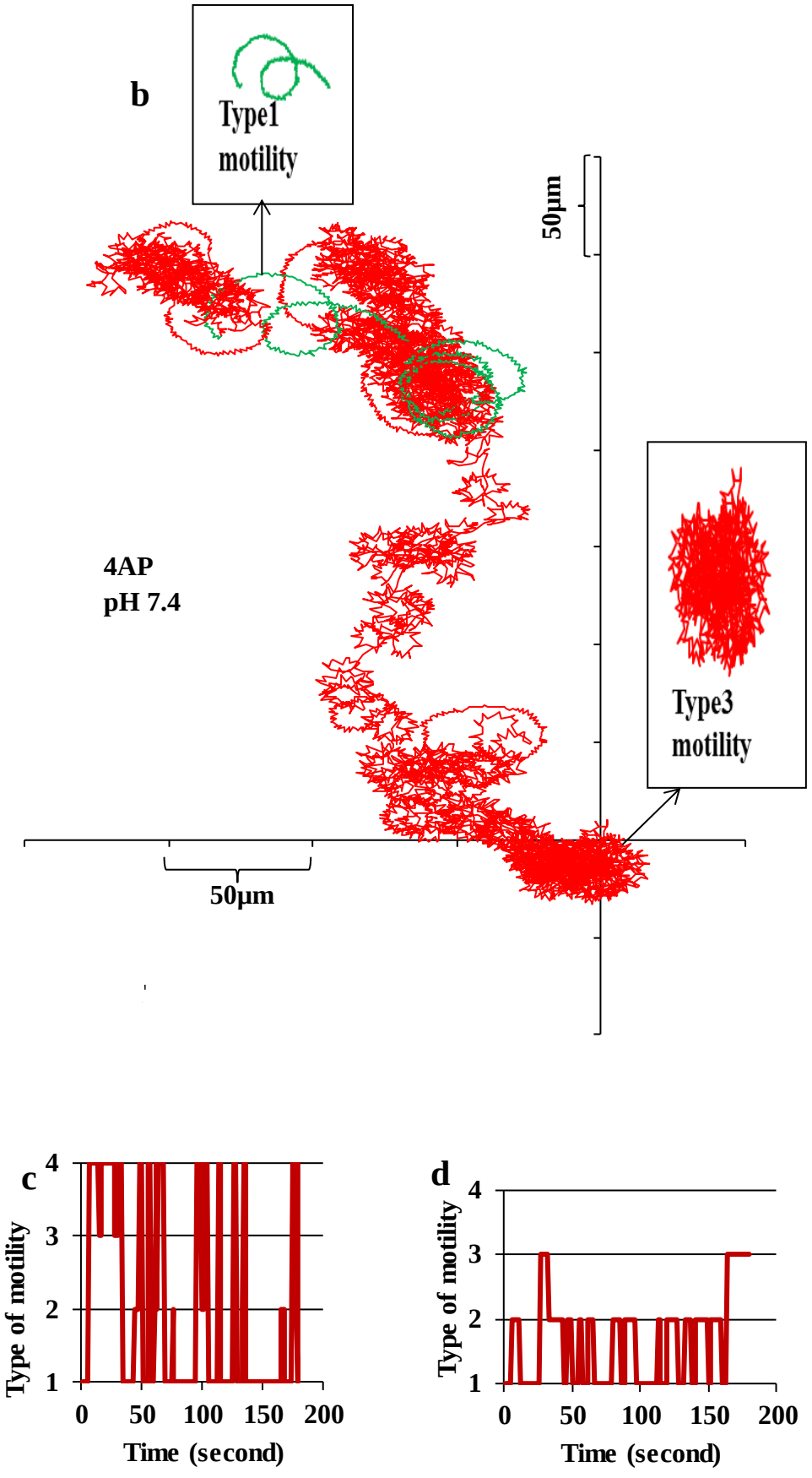
b
Type1
motility
50µm
4AP
pH 7.4
Type3
motility
50µm
c
Type of motility
4
3
2
1
0
50
100
150
200
Time (second)
d
Type of motility
4
3
2
1
0
50
100
150
200
Time (second)

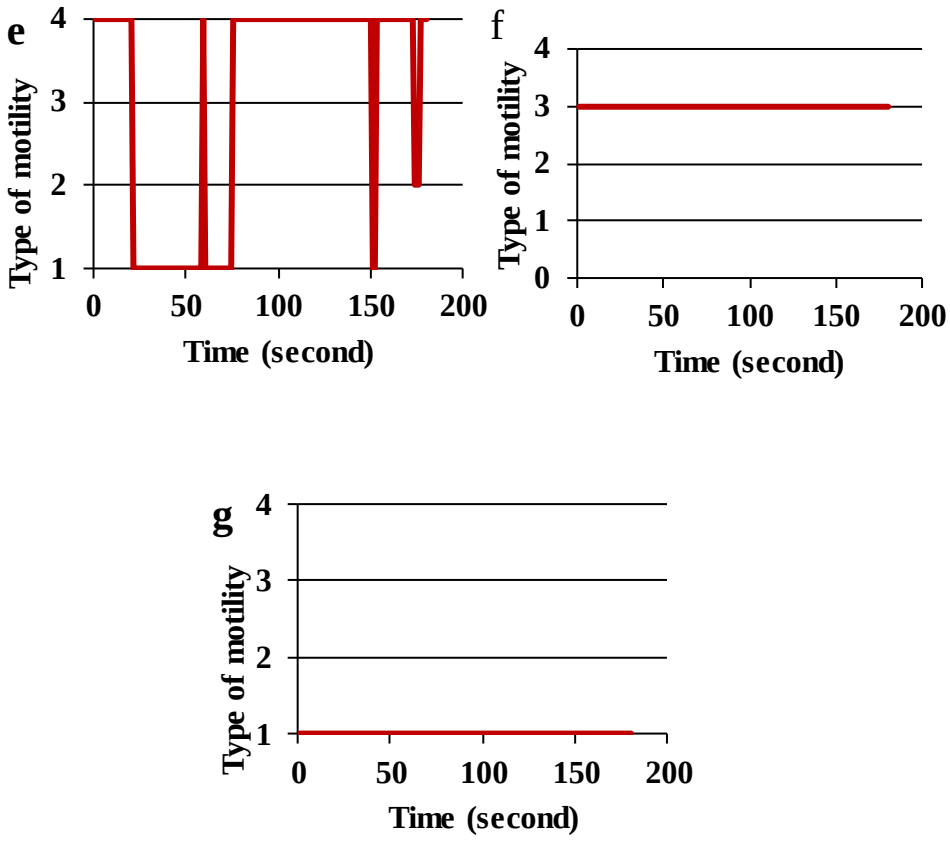

Figure 7.9: Switching between motility types observed in the absence and presence of Ca^{2+} mobilising drugs at pHo 7.4 and 8.5. At both pH conditions, in the absence and presence of drugs, single cell was followed moving the microscope stage and image recorded on video for 3 minutes in each treatment. a, b – shows switching between motility types in two cells exposed to control and 4AP at pHo 7.4, respectively. In absence of drugs there was more switching between motility types T1,T2,T3 and T4 compared to 4AP effect with switching only between T3 and T1. In analysis of the 180,1second segments, c, d shows more frequent switching between motility types. e – There was less switching between motility types while f, g – typical of 4AP and control, there was only T3 and T1 types respectively.

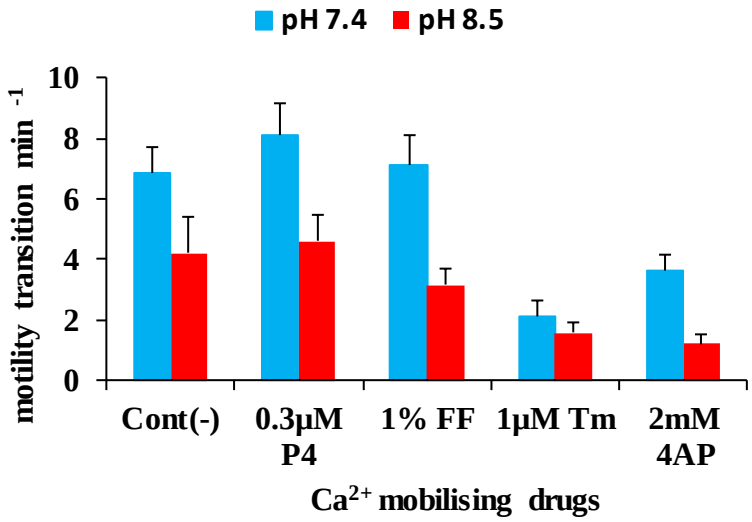

Figure 7.10: The motility transition rates induced by $[Ca^{2+}]_i$ mobilising drugs in alkalinisation. The rate of transition decreased with alkalinisation in all treatments. The rate of transition was lowest in the 4AP and Tm at both pH 7.4 (blue panel) and 8.5 (red panel).

Table 2.0: – Transition rate of cells treated with drugs at pH 7.4 and 8.5 with the statistical difference to non-treated cells and in alkalinisation

Drug	Average transitions (180 seconds)		Transition/min		p-value for transition rate		
	pH 7.4	pH 8.5	pH 7.4	pH 8.5	pH7.4 (a)	pH 8.5 (b)	pH (c)
Control	20.61	12.67	6.87	4.22	-	-	0.14
0.3µM P4	24.33	13.8	8.11	4.6	0.74	0.81	0.06
(1%) FF	21.29	9.47	7.10	3.16	0.86	0.81	0.005
1µM Tm	6.63	4.69	2.1	1.56	0.0001	0.14	0.35
2mM 4AP	10.91	3.6	3.64	1.2	0.006	0.05	0.002

a and b – Statistic; transition rate of cells treated with drugs compared to control at pH 7.4 and 8.5 respectively . c – Statistic; transition rate at pH 8.5 compared to pH 7.4.

7.4.4.2 Duration of time (dwell time) in each motility pattern

Under control conditions, the mean time spent before switching to another behaviour (dwell time) was greatest for T1 (13s at pHo=7.4 and 23 s at pHo=8.5; Figure 7.11a) and became progressively shorter at the more hyperactivated behaviours (T2,T3,T4; Figure 7.11 panel a). However, when any of the agonists was present this pattern was reversed, with dwell times in T1 becoming shorter and time spent in more hyperactivated behaviours increasing, this pattern is most prominent with the hyperactivating agonists 4AP and Tm (Figure 7.11d, e). Since under every condition tested, the rate of transition between behaviours was slower at pHo=8.5 than 7.4 (see 7.4.5.1 above), the mean dwell between behavioural switches must be longer at under these conditions. When this was analysed further it was found, both under control conditions and in the presence of agonists, that dwell time at pHo=8.5 exceeded that at pHo=7.4 for every motility type except for one instance (T4 in the presence of 4AP (Figure 7.11e)). Thus the effect of increased pHo is an overall decrease in the rate of behavioural switching rather than a selective prolongation of periods of any specific motility type.

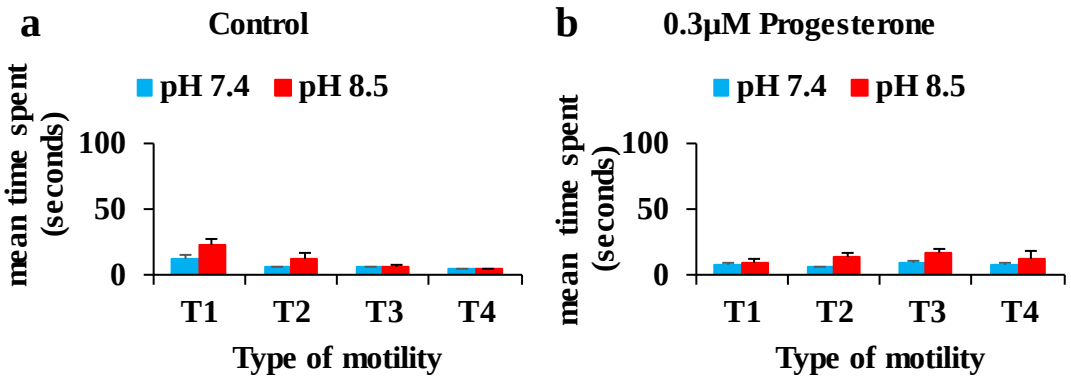

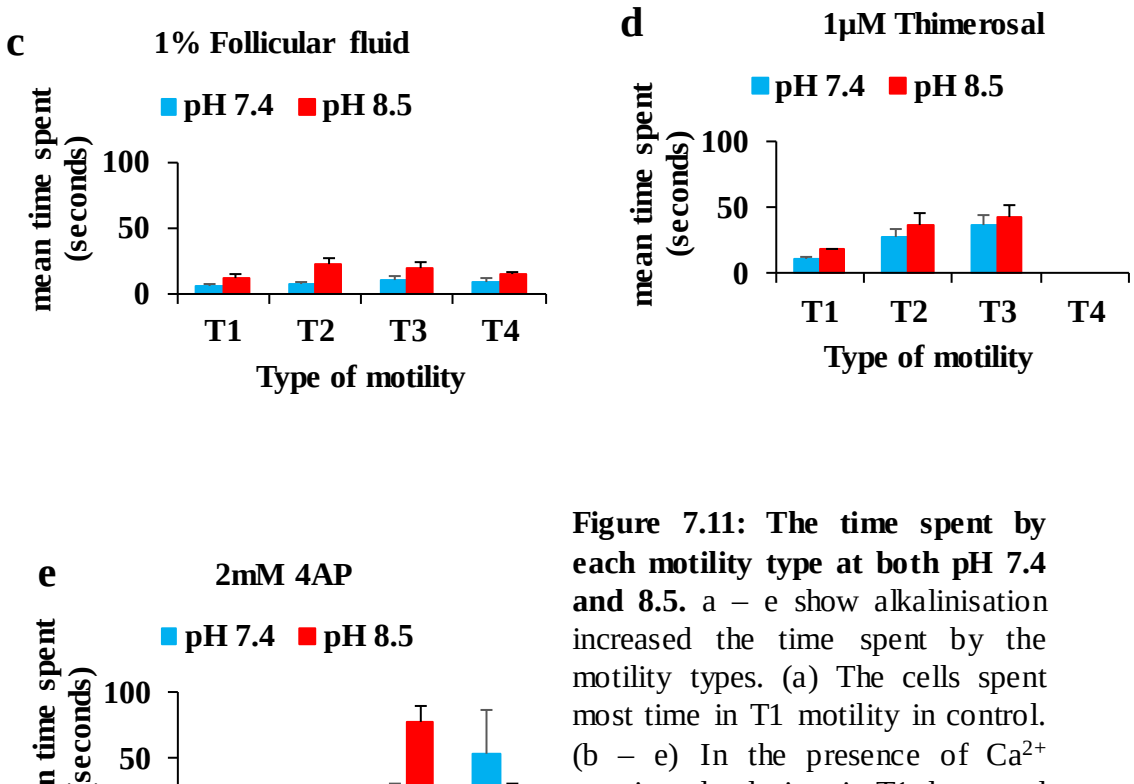

Figure 7.11: The time spent by each motility type at both pH 7.4 and 8.5. a – e show alkalinisation increased the time spent by the motility types. (a) The cells spent most time in T1 motility in control. (b – e) In the presence of Ca^{2+} agonists, dwelt time in T1 decreased but increased in T2, T3, and T4 (hyperactivated) motility types. The duration of time spent in hyperactivated motility increased in this order P4<FF<Tm<4AP. d – T4 motility type was not observed in Tm stimulation but occurred highest in 4AP than other drugs as shown in panel e.

7.5 key findings

i) Four motility types; T1(non-hyperactivated), and T2, T3, T4 (hyperactivated) were identified by observation of sperm tracks and of flagellar activity.

ii) There was good correlation between levels of hyperactivaed behaviour assessed by visual analysis of individual and by population (CASA) analysis of cells from the same aliquot.

iii) Sperm repeatedly switched between the motility types in both the unstimulated and drug treated conditions.

iv) At pH 7.4 and 8.5, the unstimulated sperm cells (control) showed mostly the non-hyperactivated motility type and

v) In the presence of Ca^{2+}-mobilising drugs and high pHo sperm exhibited more of the hyperactivated behaviours, especially with 4AP and Tm treatment (mobilisation of stored Ca^{2+}), where the dwell time in these hyperactivated behaviours increased while the transition rates decreased compared to the control. The T4 (arrested) motility type occurred more in 4AP treatment and was not observed in Tm treated cells.

vi) Effects of P4 and FF on hyperactivated behaviour were moderate.

7.6 Discussion

7.6.1 Motility types and associated flagellum bending observed in sperm behaviour

Using visual assessment of sperm tracks, combined with examination of the videos from which the tracks were derived, four different motility types, T1- non hyperactivated and T2,T3,T4 – hyperactivated were defined in single cell tracking of sperm behaviour modulated by pH and Ca^{2+} agonists. Flagellar bending was symmetrical in the non-hyperactivated T1 motility type but asymmetric, erratic flagellar beating and vigorous side to side movements of the sperm head occurred in T2 and T3. The T4 motility type was characterised by 'freezing' of the anterior flagellum in a J shape associated with less vigorous bending of the distal flagellum, which periodically arrested completely. The tight, arrested bend in the anterior flagellum has been described previously and is believed to be associated with very high levels of $[Ca^{2+}]_i$ (Pereira et al., 2017, Ho et al., 2002, Lindemann and Goltz, 1988). This suggests that the T4 type may be due to very high concentration of Ca^{2+} in the cytosol, a type of over-hyperactivation which thereby hinders movement.

7.6.2 Correlation between CASA and visual analysis on hyperactivation

Since *in vivo* studies of sperm motility in human is not feasible, drugs that can modify $[Ca^{2+}]_i$ homeostasis were used to investigate the regulation of hyperactivated motility of human sperm. Population analysis using CASA (which assesses motility over ≈500 ms) and extended 'visual' analysis of individual cells analysis as described above, showed a strong correlation. Using the tracking application to analyse VCL showed an increase in

VCL as the motility type's transit from T1-non hyperactivated to hyperactivated motility types T2, T3, and T4 at both pH values. (Mortimer, 2000) reported that in hyperactivated cells there is increase in VCL. Analysis of the kinematic parameters (ALH, LIN, and STR) of tracked cells with the tracking buffer calibration application and with a large sample of cells will be required for further understanding.

7.6.3 Switching between motility types

Examination of the behaviour of freely swimming sperm over an extended period (seconds-minutes) showed that most cells abruptly changed their behaviour (Mortimer and Swan, 1995). Using the four motility types described above, the characteristics of behavioural switching, in control and agonist-stimulated cells, were analysed.

In the absence of stimulation, the cells spent the most time in the T1 motility type. Increasing pHo from 7.4 to 8.5 had little effect on the behaviours recorded in the absence of agonist stimulation. However, in the presence of agonists, particularly upon treatment with 4AP and Tm, cell behaviour switched away from T1 to more hyperactivated-type behaviours, as might be expected from the CASA data described previously. T1 comprised less than 10% of total duration in cells exposed to Tm and 4AP. In addition, the time spent between motility transitions (dwell time) increased and the rate of switching consequently fell, particularly at pHo=8.5. Interestingly motility type T4, where cells formed a hook and sometimes arrested completely (apparently due to excessive $[Ca^{2+}]_i$ – see above), was relatively common in 4AP-stimulated cells but was never seen in cells treated with Tm, which also had a lower proportion of time spent in T3 than 4AP-stimulated cells. This may reflect the fact that Tm should act only to release stored Ca^{2+} whereas 4AP alkalinises the cytoplasm and will also activate CatSper.

Clearly both alkalinisation and (more particularly) stimulation with agonists of $[Ca^{2+}]_i$ signalling modify the complex behavioural patterns of human sperm. One possibility is that behaviour is regulated by $[Ca^{2+}]_i$ and thus ongoing changes in $[Ca^{2+}]_i$, such as oscillations, cause continuous changes in observed behaviour. P4, alkalinisation and other stimuli such as $NO^{\cdot}$ induce $[Ca^{2+}]_i$ oscillations due to release of Ca^{2+} from the stores (Harper et al., 2004, Machado-Oliveira et al., 2008), and in immobilised cells with the peaks of these $[Ca^{2+}]_i$ signals correlate with flagellar bending (Harper et al., 2004). The observation that stimulation with 4AP and Tm, which directly mobilise stored Ca^{2+}, both increase hyperactivated motility and reduce switching is consistent with this idea, but the direct recording of $[Ca^{2+}]_i$ in free swimming cells is needed to test this idea.

CHAPTER 8: General Discussion

Recent data suggest that in humans, as in other mammals, the ability of sperm to achieve hyperactivated motility is essential for male infertility (reviewed in (Hildebrand et al., 2010). Since hyperactivation is strongly dependent on $[Ca^{2+}]_i$ signalling (Suarez, 2008), one possibility is that in (at least some) men where sperm fail to hyperactivate adequately, this is due to a genetic disorder which affects expression or function of CatSper (Smith et al., 2013), as has been demonstrated in the CatSper-null mouse (Carlson et al., 2003, Ren et al., 2001). If the failure of CatSper function can cause failure of hyperactivation then the CatSper channel may be a good target to prevent conception (Aitken, 2002, Carlson et al., 2009, Zhang and Gopalakrishnan, 2005). Though CatSper is apparently crucial for hyperactivation, in sperm of mice, bull and humans, release of Ca^{2+} from stores is also able to induce this type of motility (Alasmari et al., 2013b, Gu et al., 2004, Ho and Suarez, 2001, Marquez and Suarez, 2007). In fact, in human sperm, it was observed that specific activation of CatSper increased penetration into viscous medium but not hyperactivation and it was suggested that the role of CatSper in hyperactivation might be as a trigger for release of stored Ca^{2+} (Alasmari et al., 2013b).

To investigate how activity of Ca^{2+} signalling components in human sperm regulate transitions between different types of motility, the effects of P4 (a CatSper agonist which is present in the female tract, reaching concentrations of >10 micromolar around the oocyte (Sagare-Patil et al., 2012, Tamburrino et al., 2014) and 4AP (a potent activator of human sperm hyperactivation (Gu et al., 2004) which mobilises stored Ca^{2+} (Bedu-Addo, 2008, Grimaldi, 2001) were used to investigate modulation of $[Ca^{2+}]_i$ and hyperactivation (chapter 3). Also, as the sperm cells swim up the oviduct the pHo increases which is likely to affect the activity of CatSper. At the height of

fertility in humans, the pH can increase up to 9.0 (reviewed in (Lishko et al., 2012) therefore investigated the effects of increased pHo on pHi and on the effects of P4 and 4AP on Ca^{2+} and motility (chapters 4 and 6), and also used a novel CatSper antagonist to investigate the significance of CatSper activity in the effects of elevated pHo (chapter 5). Lastly, since changes in $[Ca^{2+}]_i$ are likely to underlie the behavioural 'switching' that is observed when human sperm are observed for more than a few seconds (Lefievre et al., 2012), the effects on long terms patterns of behaviour of manipulation of CatSper (P4 and pH) and Ca^{2+} stores (4AP and Tm) were investigated (chapter 7).

Is there synergism between P4 and pH induced Ca^{2+} response?

Since P4 and intracellular alkalinisation both activate CatSper channels by shifting the voltage sensitivity of CatSper to more negative values, it would be predicted that their effects on $[Ca^{2+}]_i$ may be synergistic (Lishko et al., 2011). Therefore, having established that, under the conditions used here, elevation of pHo caused a predictable rise in pHi, I investigated the interaction between pHo and P4 mediated $[Ca^{2+}]_i$ responses. Surprisingly, the maximum $[Ca^{2+}]_i$ (fluo4 fluorescence) at the transient peak was similar at both pHo=7.4 and 8.5 and the $[Ca^{2+}]$i transient amplitude (increment in fluorescence) was smaller at pHo=8.5. Since resting $[Ca^{2+}]_i$ is higher at pHo=8.5 this might reflect saturation of Fluo 4 at very high levels of $[Ca^{2+}]_i$. This was investigated by using fura 2 (higher affinity dye than fluo4 but ratiometric) and fluo5F (7-fold lower Ca^{2+}-affinity than fluo4). Using fluo5F, no effect of pHo on the P4-induced Ca^{2+}-transient amplitude could be detected but with fura2 the response at pHo=8.5 appeared larger.

In population assays (Fluostar) the P4 induced sustained $[Ca^{2+}]$i rise (increment in fluorescence) and the associated increase in hyperactivation were similar at pHo=7.4 and pHo=8.5 (chapter 4;section 4.4.2,Figure 4.3d, and section 4.4.5.2, 4.7a)). However, when the response to

increasing pHo was investigated in imaging experiments (where pHo could be varied while recording), the alkalinisation-induced rise in fluo4 fluorescence was greater in the presence of P4 than in its absence (Figure 6.7d). However, surprisingly there was no correlation found between the amplitude of the sustained effect of P4 at pHo =7.4 and the subsequent increment in fluorescence when pHo was increased to 8.5 (section 6.5.2, Figure 6.7c,) – cells that are virtually insensitive to P4 respond as well to alkalinisation as those that are strongly stimulated. On balance, these findings suggest that alkalinisation had no significant synergistic interaction with the response to P4 and that the effect of these two stimuli on $[Ca^{2+}]_i$ are largely additive.

What is the relationship between $[Ca^{2+}]_i$ and hyperactivation?

An increase in intracellular calcium concentration is required for the hyperactivation of spermatozoa (Lishko et al., 2012, Suarez, 2008). The data obtained in this study include an large number of conditions which were imposed in order to manipulate $[Ca^{2+}]_i$ and at which both fluorescence of fluo4 and hyperactivation were assessed (control at pH7.4 and 8.5, P4 [4 concentrations] at pH7.4 and 8.5 and 4AP [7 concentrations] at pH7.4 and 8.5). Therefore, a scattergram was constructed showing hyperactivation as a function of fluo4 fluorescence recorded 5 min after stimulation (to reflect the time at which motility was assessed). The resulting plot appears to show a continuous relationship between $[Ca^{2+}]_i$ and hyperactivation (Figure4.13). This is particularly interesting since the effect on motility of P4, 4AP, pH or combinations of these appears to depend not on the source/localisation of mobilised Ca^{2+} as suggested previously (Alasmari et al., 2013b) but to be determined primarily by $[Ca^{2+}]_i$ (as measured fluorimetrically), irrespective of the source. The large difference between the effects of P4 and 4AP on motility may there be due to the fact that elevation of $[Ca^{2+}]_i$ by 4AP is sustained

much better than that induced by P4 (Figure 4.3, 4.5), possibly due to release by 4AP of stored Ca^{2+} and activation of SOCs (Lefievre et al., 2012). If this is correct then stored Ca^{2+} release strongly and persistently activates hyperactivation because of the consequent capacitative Ca^{2+} influx.

How does cytoplasmic alkalinisation modulate $[Ca^{2+}]_i$ and hyperactivation?

When human sperm were exposed to increased pHo (8.5, which raised pHi from 6.9 to 7.2) there were clear effects on both hyperactivation which was increased 6-fold; section 4.4.5.1(Figure 4.6a and $[Ca^{2+}]_i$ (fluo4 fluorescence), section 4.4.1.2 (Figure 4.2). Reporting of $[Ca^{2+}]_i$ by fluo4 might be affected directly by manipulation of pHi, since many Ca^{2+}-reported dyes lose sensitivity at low pH. However, most dyes are relatively insensitive to alkaline pH and (Lattanzio, 1990), reported that, at pH $\geq$7.0, fluo3 (which is closely related to fluo4) is largely insensitive to pH changes (Figure 4.4c). Thus the changes in fluorescence that occur at or in response to pHo=8.5 will be due entirely or primarily to changes in $[Ca^{2+}]_i$.

When intracellular pHi increases it is expected that CatSper is activated, allowing influx of Ca^{2+}, which may lead to hyperactivated motility (Darszon et al., 2011, Lishko and Kirichok, 2010). Using a pharmacological blocker of CatSper that has little effect on resting $[Ca^{2+}]_i$, I investigated the contribution of CatSper to pH-mediated $[Ca^{2+}]_i$ elevation. Interestingly, data from these experiments suggested that CatSper contributed only 30% of the rise in $[Ca^{2+}]_i$ caused by alkalinisation. Clearly, this should be interpreted cautiously since pharmacological data can be misleading, but this suggests that increased tonic elevation of pHi may have effects other than CatSper activation, such as mobilisation of stored Ca^{2+} or inhibition of Ca^{2+}-clearance

mechanisms (Wennemuth et al., 2003). This is consistent with the observations described in chapter 4, that frequency, amplitude and duration of $[Ca^{2+}]_i$ oscillations was greater at pHo=8.5 than at 7.4.

4AP both mobilises stored Ca^{2+} and also raises pH_i. In bovine and mouse sperm, alkalinising the cytoplasm with NH_4Cl, a weak base, is associated with increased pHi and hyperactivation (Chang and Suarez, 2011, Marquez and Suarez, 2007). I, therefore, used 25 mM NH_4Cl to assess whether a similar effect of cytoplasmic alkalinisation on $[Ca^{2+}]_i$ and hyperactivation occurred in human sperm. Though the increase in pH_i induced by NH_4Cl was approximately double that seen with 2 mM 4AP (Figure 4.12a-f), the effects on $[Ca^{2+}]_i$ was similar and the increase in hyperactivation induced by NH_4Cl was negligible. Furthermore, though cytoplasmic alkalinisation with NH_4Cl was equivalent to the effect of raising pHo to 8.5, extracellular alkalinisation was far more potent in inducing hyperactivation (Figure 4.6a). This suggests that increased pHo has effects that are not only through raising pHi.

Finally, it should be noted that data from experiments on de-membranated animal sperm suggest that an increase in pHi may directly affect the axoneme, increasing flagellar bending and hyperactivation (Brokaw, 1987, Brokaw and Kamiya, 1987, Ho et al., 2002). However, examination of the data from skinned bovine sperm suggest that such effect occur as pH_i exceeds 7.5, above the levels of pHi occurring with pH=8.5 saline or 4AP

How do the Calcium mobilising drugs regulate sperm motility?

Having characterised the effects of P4, 4AP and pHo on $[Ca^{2+}]_i$ and hyperactivation, I investigated their effects on switching of sperm between different behaviours. In the absence of drugs, sperm tracked for 3 min spent most of their time in Type 1, non-hyperactivated motility, both at pHo=7.4 and pHo=8.5 (section 7.4.2), though switching to hyperactivated type motility, for just a few seconds, occurred regularly.

When treated with P4 or FF (containing approximately 300 nM P4), the proportion of hyperactivated motility particularly the T2, T3 motility types increased moderately. However, when cells were treated with 4AP or Tm (which have been shown to be potent activators of hyperactivation, apparently due to Ca^{2+}-store mobilisation) there was a marked increase in time spent in hyperactivate-type behaviours and a great drop in the rate at which sperm switched behaviours. In particular, cells became 'stuck' in motility T3 with average 'dwell-time' in this behaviour of approximately a minute before switching. In addition, the occurrence of T4 motility (where the sperm forms a tight non-propagating bend in the proximal flagellum) became much more common in 4AP-treated cells. T4 motility type is ascribed to high $[Ca^{2+}]$i. This may be explained in an additional ability of 4AP to increase cytoplasmic pHi, inducing Ca^{2+} influx through CatSper as well as mobilising stored Ca^{2+}.

Clearly, modulation of $[Ca^{2+}]_i$ in human sperm moderates not only the type of behaviours exhibited but also the tendency to change. $[Ca^{2+}]_i$ in human sperm cells, even in the absence of stimulation, is unstable and shows regular fluctuations and spikes (which may be organised into oscillations; fig 6.2). Though it seems unlikely that the complex pattern of behavioural switching described here is a simple reflection of this rise and fall of $[Ca^{2+}]_i$, it seems likely that spatio-

temporal patterns of $[Ca^{2+}]_i$ in the sperm are crucial and monitoring of $[Ca^{2+}]_i$ in free-swimming sperm must be key next step.

Sperm dysfunction, particularly affecting sperm motility, is one of the primary causes of infertility. Studies on hyperactivation, regulated by $[Ca^{2+}]$i through CatSper and/or stores provide us with information on; how sperm works naturally, possible pharmacological targets and improving the technology of artificial assistance for conception (Publicover et al., 2007, Barratt et al., 2011). Using a combination of population and single cell techniques to investigate the effects on the cell of targeted Ca^{2+} mobilisers (4AP and Tm), natural stimulants (progesterone, follicular fluid) and manipulation of extracellular pH within the range found naturally in the oviduct has provided valuable information on the mechanisms by which $[Ca^{2+}]_i$ is regulated in human sperm, how it can be manipulated and the effects these Ca^{2+} signals on the motility of the cell. These data will inform future studies on techniques for manipulation of sperm function for improvement of fertilisation *in vitro*. The data generated in this work show that human sperm may regulate hyperactivated motility in high pHi by recruiting both CatSper and non-CatSper dependent $[Ca^{2+}]$i responses and that high pHo may inhibit the plasma membrane calcium ATPase (PMCA) – calcium ion/ proton ion (Ca^{2+}/H^{+}) pumps thereby decreasing the calcium clearance from the cytoplasm (Wennemuth et al., 2003, and Ruffin et al., 2014). Progesterone responses are dependent on CatSper dependent perhaps with downstream effects such as CICR, but these appear to rapidly down regulate with little sustained response under the conditions used here. 4AP potently stimulated hyperactivation, apparently because it induced a much more significant sustained $[Ca^{2+}]_i$ rise. This may be due to the occurrence of capacitative Ca^{2+} entry upon store mobilisation, which will not occur in cells where only CatSper has been activated by progesterone. Moreover high pHi potently enhanced 4AP efficiency (Ca^{2+} - sustained response is robust and potentiated in high pH). Targeting of sperm Ca^{2+} stores may provide a powerful tool

for manipulating sperm behaviour, even in cells with impaired CatSper function, increasing the chances of fertilisation.

8.1 Limitations of the work

This work is limited by the variability in donors (we do not determine their fertility status), sperm samples, batch of BSA (bovine serum albumin) that aid capacitation, temperature differences due to season, equipment and experimental bias.

8.2 Future work

(i) To extend the progesterone dose effect on $[Ca^{2+}]i$ and hyperactivation down to pico molar concentrations (chemoattractant concentration) since it plateaus at up to 20 µM P4.

(ii) Use of higher frame rate video to verify the existence of two distinct motility classes of sperm population with BCF at 30 Hz and 15 Hz respectively.

(iii) To use the CatSper inhibitor on 4AP induced response on $[Ca^{2+}]_i$ and hyperactivation in order to confirm that 4AP stimulation of hyperactivation is not only due to effects on cytoplasmic pH and CatSper activation.

(iv) NH_4Cl increased cytoplasmic pHi and induced $[Ca^{2+}]i$ changes but did not induce hyperactivation. It will be interesting to know how pHi interacted with human sperm and evoked $[Ca^{2+}]i$ change that did not regulate behaviour.

(v) Monitoring the level of $[Ca^{2+}]_i$ in the free swimming sperm cells will help to explain the complex pattern of switching in motility observed in this work.

APPENDIX 1: MEDIA PREPARATION

Supplemented Earle's Balanced Salt solution (sEBSS)

Sodium Dihydrogen phosphate (NaH_2PO_4)…….. (1.0167 mM)

Potassium Chloride (KCl)…….. (5.4 mM)

Magnessium Sulphate heptahydrate ($MgSO_4.7H_2O$)……. (0.811 mM)

Glucose ($C_6H_{12}O_6$)…….. (5.5 mM)

Sodium Pyruvate (C3H3NaO3)…… (2.5mM)

Sodium Lactate LD ($CH_3CH(OH)COONa$……...(19.0mM)

Sodium Bicarbonate ($NaHCO_3$)…… (25.0mM)

HEPES ($C_8H_{18}N_2O_4S$)…… (15mM)

Calcium Chloride dihydrate ($CaCl.2H_2O$)…… (1.8mM)

Sodium Chloride (NaCl)……. (≈116.4 mM)

Sodium Chloride was used to adjust the Osmolarity to 291 -294 mOsm (OSMOMETER, Type M, 10/25µLl, Camlab, www.camlab.co.uk, Löser, which is always calibrated with $H_2O(0)$, 300 and 900 mosm/Kg H_20 calibration standards) SEBSS is adjusted to pH 7.4 with 1M HCl and 1M NaOH and subsequently under sterilised environment, poured into 100ml volumes of glass bottles and stored at 4°C. 0.3% Bovine serum albumin (BSA) was added on the day of experiment.

In order to prepare saline at pH 8.5, HEPES was replaced with 25mM TAPS N-Tris (hydroxymethyl) methyl-3-aminopropanesulfonic acid ($C_7H_{17}NO.S$). To prepare the saline for pH calibration curve, 15 mM ADA [N – [2 –Acetamido] – 2 – iminodiacetic acid] for pH6.0 and 6.5, 15mM Hepes for pH 7.0, 7.4 and 8.0, 25mM TAPS for pH8.5 and 9.0 were used to maintain the required pH. All pH was adjusted with the pH meter.

APPENDIX 11: RESEARCH PUBLICATIONS

Abstract

Interaction of progesterone and pH in regulation of hyperactivated motility in human spermatozoa. Society for Reproduction and Fertility Annual Conference (20 – 22 July, 2015) at St. Catherine's College, Oxford.

Effect of pHi on regulation of hyperactivated motility in human spermatozoa. Society for Reproduction and Fertility Annual Conference (11 – 13 July, 2016) at the University of Winchester, UK

REFERENCES

2010. Spermatogenesis physiology. *Encyclopedia Britannica.* http: //www.britannica.com.

AITKEN, R. J. 2002. Immunocontraceptive vaccines for human use. *Journal of Reproductive Immunology,* 57**,** 273-287.

AITKEN, R. J. & MCLAUGHLIN, E. A. 2007. Molecular mechanisms of sperm capacitation: progesterone-induced secondary calcium oscillations reflect the attainment of a capacitated state. *Society Reproduction and Fertility Supplement,* 63**,** 273-293.

AITKEN, R. J. & NIXON, B. 2013. Sperm capacitation: a distant landscape glimpsed but unexplored. *Molecular Human Reproduction,* 19(12), 785-793

ALASMARI, W., BARRATT, C. L. R., PUBLICOVER, S. J., WHALLEY, K. M., FOSTER, E., KAY, V., MARTINS DA SILVA, S. & OXENHAM, S. K. 2013a. The clinical significance of calcium-signalling pathways mediating human sperm hyperactivation. *Human Reproduction,* 28**,** 866-876.

ALASMARI, W., COSTELLO, S., CORREIA, J., OXENHAM, S. K., MORRIS, J., FERNANDES, L., RAMALHO-SANTOS, J., KIRKMAN-BROWN, J., MICHELANGELI, F., PUBLICOVER, S. & BARRATT, C. L. R. 2013b. Ca2+ signals generated by catsper and ca2+ stores regulate different behaviors in human sperm. *Journal of Biological Chemistry,* 288**,** 6248-6258.

AQUILA, S. & DE AMICIS, F. 2014. Steroid receptors and their ligands: effects on male gamete functions. *Experimental Cell Research,* 328**,** 303-313.

ARMON, L. & EISENBACH, M. 2011. Behavioral mechanism during human sperm chemotaxis: involvement of hyperactivation. *PloS one,* 6**,** e28359.

ARNDT, L., CASTONGUAY, J., ARLT, E., MEYER, D., HASSAN, S., BORTH, H., ZIERLER, S., WENNEMUTH, G., BREIT, A., BIEL, M., WAHL-SCHOTT, C., GUDERMANN, T., KLUGBAUER, N. & BOEKHOFF, I. 2014. NAADP and the two-pore channel protein 1 participate in the acrosome reaction in mammalian spermatozoa. *Molecular Biology of the Cell,* 25**,** 948-964.

AUSTIN,C.R. 1951. Observations on the penetration of the sperm in the mammalian cell. *Australian Journal of Scientific Research,* (B) 4, 581-596.

BAIBAKOV, B., BOGGS, N.A., YAUGER, B., BAIBAKOV, G., DEAN, J. 2012. Human sperm bind to the N-terminal domain of ZP2 in humanized zonae pellucidae in transgenic mice. *Journal of Cell Biology,* 197(7), 897-905.

AVELLA, M.A., BAIBAKOV**,** B., DEAN, J. 2014. A single domain of the ZP2 zona pellucida protein mediates gamete recognition in mice and humans. *Journal of Cell Biology,*205(6), 801-809.

BAJPAI, M. & DONCEL, G. 2003. Involvement of tyrosine kinase and cAMP-dependent kinase cross-talk in the regulation of human sperm motility. *Reproduction,* 126**,** 183-195.

BALDI, E., LUCONI, M., BONACCORSI, L. & FORTI, G. 1998. Nongenomic effects of progesterone on spermatozoa: mechanisms of signal transduction and clinical implications. *Frontiers in Bioscience,* 3**,** D1051-9.

BALDI, E., LUCONI, M., BONACCORSI, L. & FORTI, G. 2002. Signal transduction pathways in human spermatozoa. *Journal of Reproductive Immunology,* 53**,** 121 - 131.

BALDI, E., LUCONI, M., MURATORI, M., MARCHIANI, S., TAMBURRINO, L. & FORTI, G. 2009. Nongenomic activation of spermatozoa by steroid hormones: Facts and fictions. *Molecular and Cellular Endocrinology,* 308**,** 39-46.

BARFIELD, J. P., YEUNG, C. H. & COOPER, T. G. 2005. Characterization of potassium channels involved in volume regulation of human spermatozoa. *Molecular Human Reproduction,* 11**,** 891-897.

BARÓN, L., FARA, K., ZAPATA-CARMONA, H., ZUÑIGA, L., KONG, M., SIGNORELLI, J., DÍAZ, E. S. & MORALES, P. 2016. Participation of protein kinases and phosphatases in the progesterone-induced acrosome reaction and calcium influx in human spermatozoa. *Andrology***,** 4, 1073-1083.

Barratt, C. L. R., Mansell1, S., Beaton, C., Tardif, S & Oxenham, S. K. 2011. Diagnostic tools in male infertility—the question of sperm dysfunction. *Asian Journal of Andrology,* 13, 53–58.

BEDU-ADDO, K., BARRATT, C. L. R., KIRKMAN-BROWN, J. C. & PUBLICOVER, S. J. 2007. Patterns of [Ca2+]i mobilization and cell response in human spermatozoa exposed to progesterone. *Developmental Biology,* 302**,** 324-332.

BEDU-ADDO, K., COSTELLO,S., HARPER,C., MACHADO-OLIVEIRA,G., LEFIEVRE, L., FORD, C., BARRATT, C. & PUBLICOVER, S. 2008. Mobilisation of stored calcium in the neck region of human sperm - a mechanism for regulation of flagellar activity. *International Journal of Developmental Biology,* 52**,** 615-626.

BERRIDGE, M. J., BOOTMAN, M. D. & RODERICK, H. L. 2003. Calcium signalling: dynamics, homeostasis and remodelling. *Natural Review of Molecular Cell Biology,* 4**,** 517-29.

BERS, D. M. 2002. Sarcoplasmic reticulum Ca release in intact ventricular myocytes. *Frontiers of Bioscience,* 7**,** d1697-711.

BHASKAR, A., SUBBANNA, P. K., ARASAN, S., RAJAPATHY, J., RAO, J. P. & SUBRAMANI,S. 2008. 4-Aminopyridine-induced contacture in frog ventricle is due to calcium released from intracellular stores. *Indian Journal of Physiological pharmacology,* 52**,** 366-374.

BIANCHI, E., DOE, B., GOULDING, D. & WRIGHT, G. J. 2014. Juno is the egg Izumo receptor and is essential for mammalian fertilization. *Nature,* 508**,** 483-487.

BILLINGTON, R. A., HARPER, C., BELLOMO, E. A., PUBLICOVER, S., BARRATT, C. L. R. & GENAZZANI, A. A. 2006. Characterization of cyclic adenine dinucleotide phosphate ribose levels in human spermatozoa. *Fertility and Sterility,* 86**,** 891-898.

BLOMBERG JENSEN, M. & PUBLICOVER, S. J. 2012. Progesterone and CatSper dependency. *International journal of andrology,* 35**,** 631-632.

BORON, W. F. 2004. Regulation of intracellular pH. *Advanced Physiological Education,* 28**,** 160-179.

BORYSHPOLETS, S., PÉREZ-CEREZALES, S. & EISENBACH, M. 2015. Behavioral mechanism of human sperm in thermotaxis: a role for hyperactivation. *Human Reproduction,* 30**,** 884-892.

BRENKER, C., GOODWIN, N., WEYAND, I., KASHIKAR, N. D., NARUSE, M., KRAHLING, M., MULLER, A., KAUPP, U. B. & STRUNKER, T. 2012. The CatSper channel: a polymodal chemosensor in human sperm. *European Molecular Biology Organisation Journal,* 31**,** 1654-1665.

BROKAW, C. J. 1987. Regulation of sperm flagellar motility by calcium and cAMP-dependent phosphorylation. *Journal of Cellular Biochemistry,* 35**,** 175-84.

BROKAW, C. J. & KAMIYA, R. 1987. Bending patterns of Chlamydomonas flagella: IV. Mutants with defects in inner and outer dynein arms indicate differences in dynein arm function. *Cell Motility and the Cytoskeleton,* 8**,** 68-75.

BROWN, S. G., PUBLICOVER, S. J., MANSELL, S. A., LISHKO, P. V., WILLIAMS, H. L., RAMALINGAM, M., WILSON, S. M., BARRATT, C. L., SUTTON, K. A. & DA SILVA, S. M. 2016. Depolarization of sperm membrane potential is a common feature of men with subfertility and is associated with low fertilization rate at IVF. *Human Reproduction,* 31**,** 1147-1157.

BUFFONE, M. G., HIROHASHI, N. & GERTON, G. L. 2014. Unresolved questions concerning mammalian sperm acrosomal exocytosis. *Biology of Reproduction*. 90(5):112,1-8

BULTYNCK, G., SZLUFCIK, K., KASRI, NAEL N., ASSEFA, Z., CALLEWAERT, G., MISSIAEN, L., PARYS, JAN B. & DE SMEDT, H. 2004. Thimerosal stimulates Ca^{2+} flux through inositol 1,4,5-trisphosphate receptor type 1, but not type 3, via modulation of an isoform-specific Ca^{2+}-dependent intramolecular interaction. *Biochemical Journal,* 381**,** 87-96.

BURTON, K. A. & MCKNIGHT, G. S. 2007. PKA, germ cells, and fertility. *Physiology (Bethesda),* 22**,** 40-6.

CARLSON, A., QUILL, T., WESTENBROEK, R., SCHUH, S., HILLE, B. & BABCOCK, D. 2005. Identical phenotypes of CatSper1 and CatSper2 null sperm. *Journal of Biological Chemistry,* 280**,** 32238 - 32244.

CARLSON, A., WESTENBROEK, R., QUILL, T., REN, D., CLAPHAM, D., HILLE, B., GARBERS, D. & BABCOCK, D. 2003. CatSper1 required for evoked Ca2+ entry and control of flagellar function in sperm. *Proceedings of National Academy of Sciences of the United states of America,* 100**,** 14864 - 14868.

CARLSON, A. E., BURNETT, L. A., DEL CAMINO, D., QUILL, T. A., HILLE, B., CHONG, J. A., MORAN, M. M. & BABCOCK, D. F. 2009. Pharmacological targeting of native CatSper channels reveals a required role in maintenance of sperm hyperactivation. *PLoS One,* 4**,** e6844.

CHANG, M.C. 1951. Fertilizing capacity of spermatozoa deposited in the fallopian tubes. *Nature,* 168, 697-698.

CHANG, H. & SUAREZ, S. S. 2011. Two distinct Ca2+ signaling pathways modulate sperm flagellar beating patterns in mice. *Biology of Reproduction,* 85**,** 296-305.

CHÁVEZ, J. C., FERREIRA GREGORIO, J., BUTLER, A., TREVIÑO, C. L., DARSZON, A., SALKOFF, L. & SANTI, C. M. 2014. SLO3 K+ channels control calcium entry through CatSper channels in sperm. *Journal of Biological Chemistry*, 289(46), 32266-32275

CHIU, P. C. N., LAM, K. K. W., WONG, R. C. W. & YEUNG, W. S. B. 2014. The identity of zona pellucida receptor on spermatozoa: An unresolved issue in developmental biology. *Seminars in Cell & Developmental Biology*, 30, 86-95

CHUNG, J.-J., SHIM, S.-H., EVERLEY, ROBERT A., GYGI, STEVEN P., ZHUANG, X. & CLAPHAM, DAVID E. 2014. Structurally distinct Ca2+ signaling domains of sperm flagella orchestrate tyrosine phosphorylation and motility. *Cell,* 157**,** 808-822.

COOPER, T.G. 2011. The epididymis, cytoplasmic droplets and male fertility. *Asian Journal of Andrology,* 13(1), 130-138.

COOPER, T. G. & YEUNG, C. 2007. Sperm maturation in the human epididymis. *In:* De Jonge, C. J. B., C. L. R. (ed.) *The Sperm Cell Production,Maturation, Fertilization, Regeneration.* First edition ed. pp. 72-107. UK: Cambridge University Press.

CORREIA, J., MICHELANGELI, F. & PUBLICOVER, S. 2015. Regulation and roles of Ca2+ stores in human sperm. *Reproduction,* 150**,** R65-76.

COSTELLO, S., MICHELANGELI, F., NASH, K., LEFIEVRE, L., MORRIS, J., MACHADO-OLIVEIRA, G., BARRATT, C., KIRKMAN-BROWN, J. & PUBLICOVER, S. 2009. Ca2+-stores in sperm: their identities and functions. *Reproduction (Cambridge, England),* 138**,** 425-437.

DARSZON, A., NISHIGAKI, T., BELTRAN, C. & TREVIÑO, C. L. 2011. Calcium channels in the development, maturation, and function of spermatozoa. *Physiological reviews,* 91**,** 1305-1355.

DE BLAS, G., MICHAUT, M., TREVINO, C. L., TOMES, C. N., YUNES, R., DARSZON, A. & MAYORGA, L. S. 2002. The intraacrosomal calcium pool plays a direct role in acrosomal exocytosis. *Journal of Biological Chemistry,* 277**,** 49326-49331.

DE JONGE, C. 2005. Biological basis for human capacitation. *Human Reproduction Update,* 11**,** 205-14.

DECOURSEY, T. E. 2013. Voltage-gated proton channels: *Molecular Biology, Physiology, and Pathophysiology of the HV Family*. *Physiology Review,* 93, 599-652.

DEY, S., ROY, D., MAJUMDER, G. C. & BHATTACHARYYA, D. 2014. Extracellular regulation of sperm transmembrane adenylyl cyclase by a forward motility stimulating protein. *PLoS ONE,* 9.

DUN, M., MITCHELL, L., AITKEN, R. J. & NIXON, B. 2010. Sperm–zona pellucida interaction: molecular mechanisms and the potential for contraceptive intervention. *In:* Habenicht, U.-F. & Aitken, R. J. (eds.) *Fertility Control.* 198, pp. 139-178. Springer Berlin Heidelberg.

EDDY, E. M. 2007. The scaffold role of the fibrous sheath. *Society of Reproduction and fertility Supplement,* 65, 45-62.

EGGERT-KRUSE, W., KOHLER, A., ROHR, G. & RUNNEBAUM, B. 1993. The pH as an important determinant of sperm-mucus interaction. *Fertility and Sterility,* 59**,** 617-28.

EISENBACH, M. 1999. Sperm chemotaxis. *Reviews of Reproduction,* 4**,** 56-66.

EISENBACH, M. & GIOJALAS, L. C. 2006. Sperm guidance in mammals [mdash] an unpaved road to the egg. *Natural Review of Molecular Cell Biology,* 7**,** 276-285.

ESPINO, J., MEDIERO, M., LOZANO, G. M., BEJARANO, I., ORTIZ, A., GARCIA, J. F., PARIENTE, J. A. & RODRIGUEZ, A. B. 2009. Reduced levels of intracellular calcium releasing in spermatozoa from asthenozoospermic patients. *Reproductive Bioliogy and Endocrinology,* 7**,** 11.

ESPOSITO, G., JAISWAL, B. S., XIE, F., KRAJNC-FRANKEN, M. A., ROBBEN, T. J., STRIK, A. M., KUIL, C., PHILIPSEN, R. L., VAN DUIN, M., CONTI, M. & GOSSEN, J. A. 2004. Mice deficient for soluble adenylyl cyclase are infertile because of a severe sperm-motility defect. *Proceedings of National Academy of Sciences of the United States of America,* 101**,** 2993-2998.

FENG, M., GRICE, D. M., FADDY, H. M., NGUYEN, N., LEITCH, S., WANG, Y., MUEND, S., KENNY, P. A., SUKUMAR, S., ROBERTS-THOMSON, S. J., MONTEITH, G. R. & RAO, R. 2010. Store-independent activation of Orai1 by SPCA2 in mammary tumors. *Cell,* 143**,** 84-98.

FRAIRE-ZAMORA, J. & GONZALEZ-MARTINEZ, M. 2004. Effect of intracellular pH on depolarization-evoked calcium influx in human sperm. *American Journal of Physiology Cell Physiology,* 287**,** C1688 - 1696.

FREITAS, M. J., VIJAYARAGHAVAN, S. & FARDILHA, M. 2017. Signaling mechanisms in mammalian sperm motility†. *Biology of Reproduction,* 96**,** 2-12.

FUJINOKI, M., TAKEI, G. & KON, H. 2015. Non-genomic regulation and disruption of spermatozoal in vitro hyperactivation by oviductal hormones. *The Journal of Physiological Sciences***,** 1-6.

GADELLA, B. M. V., P. E. 2006. Regulation of capacitation. *In:* De Jonge, C. J. B., C. L. R. (ed.) *The sperm cell: Production, Maturation, Fertilization, Regeneration* . pp 134-169. UK: Cambridge University Press.

GAKAMSKY, A., ARMON, L. & EISENBACH, M. 2009. Behavioral response of human spermatozoa to a concentration jump of chemoattractants or intracellular cyclic nucleotides. *Human Reproduction,* 24**,** 1152-63.

GARRET, R. H. A. G., C.M. 2010. Enzymes – kinetics and specificity. *Biochemistry: Chapter 13- part 11 Protein Dynamics.* pp 407-455. BROOKS/COLE CENGAGE Learning, Canada.

GRIMALDI, M., ATZORI,M.,RAY,P., AND ALKON,D.L. 2001. Mobilization of calcium from intracellular stores, potentiation of neurotransmitter-induced calcium transients, and capacitative calcium entry by 4-aminopyridine. *The Journal of Neuroscience,* 21**,** 3135-3143.

GU, Y., KIRKMAN-BROWN, J. C., KORCHEV, Y., BARRATT, C. L. R. & PUBLICOVER, S. J. 2004. Multi-state, 4-aminopyridine-sensitive ion channels in human spermatozoa. *Developmental Biology,* 274**,** 308-317.

GUPTA, S. K. & BHANDARI, B. 2011. Acrosome reaction: relevance of zona pellucida glycoproteins. *Asian Journal of Andrology,* 13**,** 97-105.

HAMAMAH, S., MAGNOUX, E., ROYERE, D., BARTHELEMY, C., DACHEUX, J. L. & GATTI, J. L. 1996. Internal pH of human spermatozoa: effect of ions, human follicular fluid and progesterone. *Molecular Human Reproduction,* 2**,** 219-24.

HARAYAMA, H. 2013. Roles of intracellular cyclic AMP signal transduction in the capacitation and subsequent hyperactivation of mouse and boar spermatozoa. *Journal of Reproduction and Development,* 59**,** 421-30.

HARPER, C. V., BARRATT, C. L. R. & PUBLICOVER, S. J. 2004. stimulation of human spermatozoa with progesterone gradients to simulate approach to the oocyte: induction of [Ca2+]i oscillations and cyclical transitions in flagellar beating. *Journal of Biological Chemistry,* 279**,** 46315-46325.

HARPER, C. V., KIRKMAN-BROWN, J. C., BARRATT, C. L. R. & PUBLICOVER, S. J. 2003. Encoding of progesterone stimulus intensity by intracellular [Ca2+] ([Ca2+]i) in human spermatozoa. *Biochemical Journal,* 372**,** 407-417.

HARPER, C. V. & PUBLICOVER, S. J. 2005. Reassessing the role of progesterone in fertilization—compartmentalized calcium signalling in human spermatozoa? *Human Reproduction,* 20**,** 2675-2680.

HESS, K. C., JONES, B. H., MARQUEZ, B., CHEN, Y., ORD, T. S., KAMENETSKY, M., MIYAMOTO, C., ZIPPIN, J. H., KOPF, G. S., SUAREZ, S. S., LEVIN, L. R., WILLIAMS, C. J., BUCK, J. & MOSS, S. B. 2005. The "soluble" adenylyl cyclase in sperm mediates multiple signaling events required for fertilization. *Developmental Cell,* 9**,** 249-259.

HILDEBRAND, M. S., AVENARIUS, M. R., FELLOUS, M., ZHANG, Y., MEYER, N. C., AUER, J., SERRES, C., KAHRIZI, K., NAJMABADI, H., BECKMANN, J. S. & SMITH, R. J. H. 2010. Genetic male infertility and mutation of CatSper ion channels. *European Journal of Human Genetics,* 18**,** 1178-1184.

HINO, T., MURO, Y., TAMURA-NAKANO, M., OKABE, M., TATENO, H.,

YANAGIMACHI, R. 2016. the behavior and acrosomal status of mouse spermatozoa in vitro, and within the oviduct during fertilization after natural mating. *Biology of Reproduction,* 95(3):50, 1-11.

HO, H. C., GRANISH, K. A. & SUAREZ, S. S. 2002. Hyperactivated motility of bull sperm is triggered at the axoneme by Ca2+ and not cAMP. *Developmental Biology,* 250**,** 208-217.

HO, H. C. & SUAREZ, S. S. 2001. An inositol 1,4,5-trisphosphate receptor-gated intracellular Ca(2+) store is involved in regulating sperm hyperactivated motility. *Biology of Reproduction,* 65**,** 1606-1615.

HO, H. C. & SUAREZ, S. S. 2003. Characterization of the intracellular calcium store at the base of the sperm flagellum that regulates hyperactivated motility. *Biology of Reproduction,* 68**,** 1590-1596.

HO, K., WOLFF, C. & SUAREZ, S. 2009. CatSper-null mutant spermatozoa are unable to ascend beyond the oviductal reservori. *Reproduction Fertilility and Development,* 21**,** 345 - 350.

ICKOWICZ, D., FINKELSTEIN, M. & BREITBART, H. 2012. Mechanism of sperm capacitation and the acrosome reaction: role of protein kinases. *Asian journal of andrology,* 14**,** 816-821.

IJIRI, T. W., MAHBUB HASAN, A. K. M. & SATO, K.-I. 2012. protein-tyrosine kinase signaling in the biological functions associated with sperm. *Journal of Signal Transduction,* 2012**,** 2018.

INABA, K. 2011. Sperm flagella: comparative and phylogenetic perspectives of protein components. *Molecular Human Reproduction,* 17**,** 524-538.

ISHIDA, Y. & HONDA, H. 1993. Inhibitory action of 4-aminopyridine on Ca(2+)-ATPase of the mammalian sarcoplasmic reticulum. *Journal of Biological Chemistry,* 268**,** 4021-4024.

JAISWAL, D., SINGH, V., DWIVEDI, U. S., TRIVEDI, S. & SINGH, K. 2014. Chromosome microarray analysis: a case report of infertile brothers with CatSper gene deletion. *Gene,* 542**,** 263-265.

JIMENEZ-GONZALEZ, C., MICHELANGELI, F., HARPER, C. V., BARRATT, C. L. R. & PUBLICOVER, S. J. 2006. Calcium signalling in human spermatozoa: a specialized 'toolkit' of channels, transporters and stores. *Human Reproduction Update,* 12**,** 253-267.

JIN, M., FUJIWARA, E., KAKIUCHI, Y., OKABE, M., SATOUH, Y., BABA, S. A., CHIBA, K., & HIROHASHI, N. 2011. Most fertilizing mouse spermatozoa begin their acrosome reaction before contact with the zona pellucida during in vitro fertilization. *Proceedings of the National Academy of Sciences*, 108(12), 4892-4896.

JIN, S.K. & YANG, W.X. 2017. Factors and pathways involved in capacitation: how are they regulated? *Oncotarget,* 8(2), 3600-3627.

JOHNSON, M. H. A. E., B.J. 2007. Coitus and Fertilization. Essential Reproduction: Chapter 9 – pp 168 – 187. Sixth edition. UK, Blackwell Publishing.

KAUPP, U. B., KASHIKAR, N. D. & WEYAND, I. 2008. Mechanisms of sperm chemotaxis. *Annu Rev Physiol,* 70**,** 93-117.

KAY, V. & ROBERTSON, L. 1998. Hyperactivated motility of human spermatozoa: a review of physiological function and application in assisted reproduction. *Human Reproduction Update,* 4**,** 776-786.

KILIC, F., KASHIKAR, N. D., SCHMIDT, R., ALVAREZ, L., DAI, L., WEYAND, I., WIESNER, B., GOODWIN, N., HAGEN, V. & KAUPP, U. B. 2009. Caged progesterone: a new tool for studying rapid nongenomic actions of progesterone. *Journal of the American Chemical Society,* 131**,** 4027-4030.

KIRICHOK, Y., NAVARRO, B. & CLAPHAM, D. E. 2006. Whole-cell patch-clamp measurements of spermatozoa reveal an alkaline-activated Ca2+ channel. *Nature,* 439**,** 737-740.

KIRKMAN-BROWN, J. C., BARRATT, C. L. R. & PUBLICOVER, S. J. 2004. Slow calcium oscillations in human spermatozoa. *Biochemical Journal,* 378**,** 827-832.

KIRKMAN-BROWN, J. C., BRAY, C., STEWART, P. M., BARRATT, C. L. R. & PUBLICOVER, S. J. 2000. Biphasic Elevation of [Ca2+]i in Individual Human Spermatozoa Exposed to Progesterone. *Developmental Biology,* 222**,** 326-335.

KRAUSZ, C. C., BONACCORSI, L., MAGGIO, P., LUCONI, M., CRISCUOLI, L., FUZZI, B., PELLEGRINI, S., FORTI, G., BALDI, E. 1996. Two functional assays of sperm responsiveness to progesterone and their predictive values in *in-vitro* fertilization. *Human Reproduction,* 11**,** 1661-1667

LATTANZIO, F., A. 1990. The effects of pH and temperature on fluorescent calcium indicators as determined with chelex-100 and EDTA buffer systems. *Biochemical and Biophysical Research Communications,* 171**,** 102-108.

LAWSON, C., DORVAL, V., GOUPIL, S. & LECLERC, P. 2007. Identification and localisation of SERCA 2 isoforms in mammalian sperm. *Molecular Human Reproduction,* 13**,** 307-316.

LEFIÈVRE, L., CONNER, S.J., SALPEKAR, A., OLUFOWOBI, O., ASHTON, P., PAVLOVIC, B., LENTON, W., AFNAN, M., BREWIS, I.A., MONK, M., HUGHES, D.C., BARRATT, C.L. 2004**.** Four zona pellucida glycoproteins are expressed in the human. *Human Reproduction,* 19, 1580-1586.

LEFIEVRE, L., NASH, K., MANSELL, S., COSTELLO, S., PUNT, E., CORREIA, J., MORRIS, J., KIRKMAN-BROWN, J., WILSON, S. M., BARRATT, C. L. & PUBLICOVER, S. 2012. 2-APB-potentiated channels amplify CatSper-induced Ca(2+) signals in human sperm. *Biochemical Journal,* 448**,** 189-200.

LINDEMANN, C. B. & GOLTZ, J. S. 1988. Calcium regulation of flagellar curvature and swimming pattern in triton X-100--extracted rat sperm. *Cell Motility and the Cytoskeleton,* 10**,** 420-431.

LISHKO, P., CLAPHAM, D. E., NAVARRO, B. & KIRICHOK, Y. 2013. Sperm Patch-Clamp. *In:* Wallace, F. M. (ed.) *Methods in Enzymology.* Chapter Four – 525, 59-83. Academic Press.

LISHKO, P. V., BOTCHKINA, I. L., FEDORENKO, A. & KIRICHOK, Y. 2010. Acid extrusion from human spermatozoa is mediated by flagellar voltage-gated proton channel. *Cell,* 140**,** 327-337.

LISHKO, P. V., BOTCHKINA, I. L. & KIRICHOK, Y. 2011. Progesterone activates the principal Ca2+ channel of human sperm. *Nature,* 471**,** 387-391.

LISHKO, P. V. & KIRICHOK, Y. 2010. The role of Hv1 and CatSper channels in sperm activation. *The Journal of Physiology,* 588**,** 4667-4672.

LISHKO, P. V., KIRICHOK, Y., REN, D., NAVARRO, B., CHUNG, J. J. & CLAPHAM, D. E. 2012. The control of male fertility by spermatozoan ion channels. *Annual review of physiology,* 74**,** 453-475.

LÓPEZ-GONZÁLEZ, I., TORRES-RODRÍGUEZ, P., SÁNCHEZ-CARRANZA, O., SOLÍS-LÓPEZ, A., SANTI, C. M., DARSZON, A. & TREVIÑO, C. L. 2014. Membrane hyperpolarization during human sperm capacitation. *Molecular Human Reproduction,* 20**,** 619-629.

LOPEZ-TORRES, A. S. & CHIRINOS, M. 2017. Modulation of human sperm capacitation by progesterone, estradiol, and luteinizing hormone. *Reproductive Sciences,* 24**,** 193-201.

LOSEL, R. & WEHLING, M. 2003. Nongenomic actions of steroid hormones. *Nature Reviews, Molocular Cell Biology,* 4**,** 46-56.

LUCONI, M., CANTINI, G., BALDI, E. & FORTI, G. 2011. Role of a-kinase anchoring proteins (AKAPs) in reproduction. *Frontiers in Bioscience (Landmark Ed),* 16**,** 1315-3130.

LUCONI, M., FRANCAVILLA, F., PORAZZI, I., MACEROLA, B., FORTI, G. & BALDI, E. 2004. Human spermatozoa as a model for studying membrane receptors mediating rapid nongenomic effects of progesterone and estrogens. *Steroids,* 69**,** 553-559.

MA, F., WU, D., DENG, L., SECREST, P., ZHAO, J., VARKI, N., LINDHEIM, S. & GAGNEUX, P. 2012. Sialidases on mammalian sperm mediate deciduous sialylation during capacitation. *Journal of Biological Chemistry,* 287**,** 38073-38079.

MAAS, D. H., STOREY, B. T. & MASTROIANNI, L., JR. 1977. Hydrogen ion and carbon dioxide content of the oviductal fluid of the rhesus monkey (Macaca mulatta). *Fertility and Sterility,* 28**,** 981-985.

MACHADO-OLIVEIRA, G., LEFIÈVRE, L., FORD, C., HERRERO, M. B., BARRATT, C., CONNOLLY, T. J., NASH, K., MORALES-GARCIA, A., KIRKMAN-BROWN, J. & PUBLICOVER, S. 2008. Mobilisation of Ca2+ stores and flagellar regulation in human sperm by S-nitrosylation: a role for NO synthesised in the female reproductive tract. *Development,* 135**,** 3677-3686.

MANNOWETZ, N., NAIDOO, N. M., CHOO, S. A. S., SMITH, J. F. & LISHKO, P. V. 2013. Slo1 is the principal potassium channel of human spermatozoa. *Elife,* 2**,** 19.

MANSELL, S. A., PUBLICOVER, S. J., BARRATT, C. L. R. & WILSON, S. M. 2014. Patch clamp studies of human sperm under physiological ionic conditions reveal three functionally and pharmacologically distinct cation channels. *Molecular Human Reproduction,* 20(5), 392-408.

MARÍN-BRIGGILER, C. I., JHA, K. N., CHERTIHIN, O., BUFFONE, M. G., HERR, J. C., VAZQUEZ-LEVIN, M. H. & VISCONTI, P. E. 2005. Evidence of the presence of

calcium/calmodulin-dependent protein kinase IV in human sperm and its involvement in motility regulation. *Journal of Cell Science,* 118**,** 2013-2022.

MARQUEZ, B., IGNOTZ, G. & SUAREZ, S. 2007. Contributions of extracellular and intracellular Ca2+ to regulation of sperm motility: Release of intracellular stores can hyperactivate CatSper1 and CatSper2 null sperm. *Developmental Biology,* 303**,** 214 - 221.

MARQUEZ, B. & SUAREZ, S. S. 2007. Bovine sperm hyperactivation is promoted by alkaline-stimulated Ca2+ influx. *Biology of Reproduction,* 76**,** 660-665.

MICHELANGELI, F. & EAST, J. M. 2011. A diversity of SERCA Ca2+ pump inhibitors. *Biochemical Society Transactions,* 39**,** 789-97.

MIKI, K. & CLAPHAM, DAVID E. 2013. Rheotaxis guides mammalian sperm. *Current Biology,* 23**,** 443-452.

MILLER, D. & OSTERMEIER, G.C. 2006. Spermatozoal RNA: Why is it there and what does it do? *Gynaecology Obstetrics & Fertility*, 34(9), 840-846.

MILLER, M. R., MANNOWETZ, N., IAVARONE, A. T., SAFAVI, R., GRACHEVA, E. O., SMITH, J. F., HILL, R. Z., BAUTISTA, D. M., KIRICHOK, Y. & LISHKO, P. V. 2016. Unconventional endocannabinoid signaling governs sperm activation via sex hormone progesterone. *Science.* 352(6285),555-559.

MILLER, M. R., MANSELL,S.A.,MEYERS,S.A.,LISHKO,P.V. 2015. Flagellar ion channels of sperm: similarities and differences between species. *cell Calcium,* 58**,** 105-113.

MIYAZAKI, S. 1995. Inositol trisphosphate receptor mediated spatiotemporal calcium signalling. *Current Opinion in Cell Biology,* 7**,** 190-6.

MIZUNO, K., SHIBA, K., OKAI, M., TAKAHASHI, Y., SHITAKA, Y., OIWA, K., TANOKURA, M. & INABA, K. 2012. Calaxin drives sperm chemotaxis by Ca2+-mediated direct modulation of a dynein motor. *Proceedings of the National Academy of Sciences,* 109**,** 20497-20502.

MORTIMER, S. T. 1997. A critical review of the physiological importance and analysis of sperm movement in mammals. *Human reproduction update,* 3**,** 403-439.

MORTIMER, S. T. 2000. CASA—Practical aspects. *Journal of Andrology,* 21**,** 515-524.

MORTIMER, S. T. & SWAN, M. A. 1995. Variable kinematics of capacitating human spermatozoa. *Human Reproduction,* 10**,** 3178-82.

NAKANO, I., KOBAYASHI,T.,YOSHIMURA,M.,& SHINGYOJI,C. 2003. Central pair-linked regulation of microtubule sliding by calcium in flagellar axonemes. *Journal of Cell Science* 116**,** 1627 – 36.

NASH, K., LEFIEVRE, L., PERALTA-ARIAS, R., MORRIS, J., MORALES-GARCIA, A., CONNOLLY, T., COSTELLO, S., KIRKMAN-BROWN, J. C. & PUBLICOVER, S. J. 2010. Techniques for imaging Ca2+ signaling in human sperm. *Journal of visualized experiments,* (40), e1996, 1-4.

NAVARRO, B., KIRICHOK, Y., CHUNG, J. J. & CLAPHAM, D. E. 2008. Ion channels that control fertility in mammalian spermatozoa. *International Journal of Developmental Biology,* 52**,** 607-613.

NAVARRO, B., KIRICHOK, Y. & CLAPHAM, D. E. 2007. KSper, a pH-sensitive K+ current that controls sperm membrane potential. *Proceedings of the National Academy of Sciences,* 104**,** 7688-7692.

NAZ, R. K. 2014. The effect of curcumin on intracellular pH (pHi), membrane hyperpolarization and sperm motility. *Journal of Reproduction and Infertility,* 15**,** 62-70.

NAZ, R. K. & RAJESH, P. B. 2004. Role of tyrosine phosphorylation in sperm capacitation/acrosome reaction. *Reproductive Biology and Endocrinology,* 2**,** 75.

NERI-VIDAURRI PDEL, C., TORRES-FLORES, V. & GONZALEZ-MARTINEZ, M. T. 2006. A remarkable increase in the pHi sensitivity of voltage-dependent calcium channels occurs in human sperm incubated in capacitating conditions. *Biochemical and Biophysical Research Communications,* 343**,** 105-9.

NISHIGAKI, T., JOSE, O., GONZALEZ-COTA, A. L., ROMERO, F., TREVINO, C. L. & DARSZON, A. 2014. Intracellular pH in sperm physiology. *Biochemical and Biophysical Research Communications,* 450**,** 1149-58.

NOGUCHI, T., FUJINOKI, M., KITAZAWA, M. & INABA, N. 2008. Regulation of hyperactivation of hamster spermatozoa by progesterone. *Reproductive Medicine and Biology,* 7**,** 63-74.

NOLAN, M. A., BABCOCK, D. F., WENNEMUTH, G., BROWN, W., BURTON, K. A. & MCKNIGHT, G. S. 2004. Sperm-specific protein kinase A catalytic subunit Calpha2 orchestrates cAMP signaling for male fertility. *Proceedings of National Academy of Sciences of the United States of America,* 101**,** 13483-8.

NOMURA, M., YOSHIDA,M., MORISAWA,M. 2004. Calmodulin/calmodulin-dependent protein kinase II mediates SAAF –induced motility activation of ascidian sperm. *Cell Motility and Cytoskeleton,* 59**,** 28-37.

O'GORMAN, A., WALLACE, M., COTTELL, E., GIBNEY, M. J., MCAULIFFE, F. M., WINGFIELD, M. & BRENNAN, L. 2013. Metabolic profiling of human follicular fluid identifies potential biomarkers of oocyte developmental competence. *Reproduction,* 146**,** 389-95.

OKABE, M. 2013. The cell biology of mammalian fertilization. *Development,* 140**,** 4471-4479.

OLSON, S., SUAREZ, S. & FAUCI, L. 2010. A model of CatSper channel mediated calcium dynamics in mammalian spermatozoa. *Bulletin of Mathematical Biology,* 72**,** 1925-1946.

PARK, K.-H., KIM, B.-J., KANG, J., NAM, T.-S., LIM, J. M., KIM, H. T., PARK, J. K., KIM, Y. G., CHAE, S.-W. & KIM, U.-H. 2011. *Ca2+ signaling tools acquired from prostasomes are required for progesterone-induced sperm motility*. *Science signaling, 4(173), ra31*.

PEREIRA, R., SA, R., BARROS, A. & SOUSA, M. 2017. Major regulatory mechanisms involved in sperm motility. *Asian Journal of Andrology,* 19**,** 5-14.

PUBLICOVER, S. & BARRATT, C. 2011a. Reproductive biology: Progesterone's gateway into sperm. *Nature,* 471**,** 313-314.

PUBLICOVER, S., HARPER, C. V. & BARRATT, C. 2007. [Ca2+]i signalling in sperm making the most of what you've got. *Nature Cell Biology,* 9**,** 235-242.

PUBLICOVER, S. J. & BARRATT, C. L. R. 2011b. Sperm motility: things are moving in the lab! *Molecular Human Reproduction,* 17**,** 453-456.

PUBLICOVER, S. J., GIOJALAS, L. C., TEVES, M. E., DE OLIVEIRA, G. S., GARCIA, A. A., BARRATT, C. L. & HARPER, C. V. 2008. Ca2+ signalling in the control of motility and guidance in mammalian sperm. *Frontiers in Bioscience,* 13**,** 5623-37.

QI, H., MORAN, M. M., NAVARRO, B., CHONG, J. A., KRAPIVINSKY, G., KRAPIVINSKY, L., KIRICHOK, Y., RAMSEY, I. S., QUILL, T. A. & CLAPHAM, D. E. 2007. All four CatSper ion channel proteins are required for male fertility and sperm cell hyperactivated motility. *Proceedings of the National Academy of Sciences,* 104**,** 1219-1223.

QUILL, T., SUGDEN, S., ROSSI, K., DOOLITTLE, L., HAMMER, R. & GARBERS, D. 2003. Hyperactivated sperm motility driven by CatSper2 is required for fertilization. *Proceedings of the National Academy of Sciences of the United States of America,* 100**,** 14869 - 14874.

QUILL, T. A., REN, D., CLAPHAM, D. E. & GARBERS, D. L. 2001. A voltage-gated ion channel expressed specifically in spermatozoa. *Proceedings of the National Academy of Sciences,* 98**,** 12527-12531.

REN, D., NAVARRO, B., PEREZ, G., JACKSON, A. C., HSU, S., SHI, Q., TILLY, J. L. & CLAPHAM, D. E. 2001. A sperm ion channel required for sperm motility and male fertility. *Nature,* 413**,** 603-609.

REN, D. A. X., JINGSHENG 2010. Calcium signaling through catsper channels in mammalian fertilization. *Physiology,* 25, 165-175

ROMAROWSKI, A., SÁNCHEZ-CÁRDENAS, C., RAMÍREZ-GÓMEZ, H. V., PUGA MOLINA, L. D. C., TREVIÑO, C. L., HERNÁNDEZ CRUZ, A., DARSZON, A. I. & BUFFONE, M. G. 2016. A specific transitory increase in intracellular calcium induced by progesterone promotes acrosomal exocytosis in mouse sperm. *Biology of Reproduction*,94(3):63, 1-12

ROSSATO, M., DI VIRGILIO, F., RIZZUTO, R., GALEAZZI, C. & FORESTA, C. 2001. Intracellular calcium store depletion and acrosome reaction in human spermatozoa: role of calcium and plasma membrane potential. *Molecular Human Reproduction,* 7**,** 119-28.

RUFFIN, V. A., SALAMEH, A. I., BORON, W. F. & PARKER, M. D. 2014. Intracellular pH regulation by acid-base transporters in mammalian neurons. *Frontiers in physiology, 5(43), 1-11*

SAGARE-PATIL, V., GALVANKAR, M., SATIYA, M., BHANDARI, B., GUPTA, S. K. & MODI, D. 2012. Differential concentration and time dependent effects of progesterone on kinase activity, hyperactivation and acrosome reaction in human spermatozoa. *International Journal of Andrology,* 35**,** 633-644.

SAGARE-PATIL, V. & MODI, D. 2016. Identification of motility-associated progesterone-responsive differentially phosphorylated proteins. *Reproduction, Fertility and Development,* 29(6), 1115-1129.

SÁNCHEZ-TUSIE, A. A., VASUDEVAN, S. R., CHURCHILL, G. C., NISHIGAKI, T. & TREVIÑO, C. L. 2014. Characterization of NAADP-mediated calcium signaling in human spermatozoa. *Biochemical and Biophysical Research Communications,* 443**,** 531-536.

SANTI, C. M., MARTÍNEZ-LÓPEZ, P., DE LA VEGA-BELTRÁN, J. L., BUTLER, A., ALISIO, A., DARSZON, A. & SALKOFF, L. 2010. The SLO3 sperm-specific potassium channel plays a vital role in male fertility. *Federation of European Biochemical Societies Letters,* 584**,** 1041-1046.

SATI, L., CAYLI, S., DELPIANO, E., SAKKAS, D. & HUSZAR, G. 2014. The pattern of tyrosine phosphorylation in human sperm in response to binding to zona pellucida or hyaluronic acid. *Reproductive Sciences,* 21**,** 573-581.

SATOUH, Y., INOUE, N., IKAWA, M. & OKABE, M. 2012. Visualization of the moment of mouse sperm–egg fusion and dynamic localization of IZUMO1. *Journal of Cell Science,* 125**,** 4985-4990.

SCHAEFER, M., HABENICHT, U. F., BRAUTIGAM, M. & GUDERMANN, T. 2000. Steroidal sigma receptor ligands affect signaling pathways in human spermatozoa. *Biology of Reproduction,* 63**,** 57-63.

SCHIFFER, C., MULLER, A., EGEBERG, D. L., ALVAREZ, L., BRENKER, C., REHFELD, A., FREDERIKSEN, H., WASCHLE, B., KAUPP, U. B., BALBACH, M., WACHTEN, D., SKAKKEBAEK, N. E., ALMSTRUP, K. & STRUNKER, T. 2014. Direct action of endocrine disrupting chemicals on human sperm. *European Molecular Biology Organisation Reports,* 15**,** 758-65.

SCHLINGMANN, K., MICHAUT, M. A., MCELWEE, J. L., WOLFF, C. A., TRAVIS, A. J. & TURNER, R. M. 2007. Calmodulin and CaMKII in the sperm principal piece: evidence for a motility-related calcium/calmodulin pathway. *Journal of Andrology,* 28**,** 706-716.

SEIFERT, R., FLICK, M., BÖNIGK, W., ALVAREZ, L., TRÖTSCHEL, C., POETSCH, A., MÜLLER, A., GOODWIN, N., PELZER, P., KASHIKAR, N. D., KREMMER, E., JIKELI, J., TIMMERMANN, B., KUHL, H., FRIDMAN, D., WINDLER, F., KAUPP, U. B. & STRÜNKER, T. 2015. *The CatSper channel controls chemosensation in sea urchin sperm*. *European Molecular Biology Organisations Journal,* 34(3), 379-392

SERVIN-VENCES, M. R., TATSU, Y., ANDO, H., GUERRERO, A., YUMOTO, N., DARSZON, A. & NISHIGAKI, T. 2012. A caged progesterone analog alters intracellular Ca2+ and flagellar bending in human sperm. *Reproduction (Cambridge, England),* 144**,** 101-109.

SHERWOOD, L. 2013. The reproductive system. *Introduction to human physiology,* International edition, chapter 20- pp. 773-834. Brooks/Cole CENGAGE Learning, United States

SHIBA, K. & INABA, K. 2014. Distinct roles of soluble and transmembrane adenylyl cyclases in the regulation of flagellar motility in Ciona sperm. *International Journal of Molecular Sciences,* 15(8)**,** 13192-131208.

SIGNORELLI, J., DIAZ, E. & MORALES, P. 2012. Kinases, phosphatases and proteases during sperm capacitation. *Cell and Tissue Research,* 349**,** 765-782.

SILVERTHORN, D. U. & JOHNSON, B. R. 2013. Reproduction and development. *Human physiology :* an integrated approach, chapter 26- pp. 850-888. Pearson, Boston ; London.

SINGH, A. P. & RAJENDER, S. 2015. CatSper channel, sperm function and male fertility. *Reproductive BioMedicine Online,* 30**,** 28-38.

SKALHEGG, B. S., HUANG, Y., SU, T., IDZERDA, R. L., MCKNIGHT, G. S. & BURTON, K. A. 2002. Mutation of the C alpha subunit of PKA leads to growth retardation and sperm dysfunction. *Molecular Endocrinology,* 16**,** 630-9.

SMITH, E. F. 2002. Regulation of flagellar dynein by calcium and a role for an axonemal calmodulin and calmodulin-dependent kinase. *Molecular Biology of the cell,* 13**,** 3303-3313.

SMITH, J. F., SYRITSYNA, O., FELLOUS, M., SERRES, C., MANNOWETZ, N., KIRICHOK, Y. & LISHKO, P. V. 2013. Disruption of the principal, progesterone-activated sperm Ca2+ channel in a CatSper2-deficient infertile patient. *Proceedings of National Academy of Sciences of the United States of America,* 110**,** 6823-6828.

SMITH, K. J., FELTS, P. A. & JOHN, G. R. 2000. Effects of 4-aminopyridine on demyelinated axons, synapses and muscle tension. *Brain,* 123 (1)**,** 171-184.

SOLZIN, J., HELBIG, A., VAN, Q., BROWN, J. E., HILDEBRAND, E., WEYAND, I. & KAUPP, U. B. 2004. Revisiting the role of H+ in chemotactic signaling of sperm. *Journal of General Physiology,* 124**,** 115-124.

SOSA, C. M., PAVAROTTI, M. A., ZANETTI, M. N., ZOPPINO, F. C. M., DE BLAS, G. A. & MAYORGA, L. S. 2015. Kinetics of human sperm acrosomal exocytosis. *Molecular Human Reproduction,* 21**,** 244-254.

SOSA, C. M., ZANETTI, M. N., POCOGNONI, C. A. & MAYORGA, L. S. 2016. Acrosomal swelling is triggered by cAMP downstream the opening of store-operated calcium channels during acrosomal exocytosis in human sperm. *Biology of Reproduction*,94(3):57,1-9

STARR, C. A. M., B 2012. Reproductive systems. *Human biology: development and ageing,* chapter 17- 351-374. Brooks/Cole CENGAGE Learning, Canada.

STEPHENS, G. J., GARRATT, J. C., ROBERTSON, B. & OWEN, D. G. 1994. On the mechanism of 4-aminopyridine action on the cloned mouse brain potassium channel mKv1.1. *Journal of Physiology,* 477 (2)**,** 187-196.

STRÜNKER, T., GOODWIN, N., BRENKER, C., KASHIKAR, N. D., WEYAND, I., SEIFERT, R. & KAUPP, U. B. 2011. The CatSper channel mediates progesterone-induced Ca2+ influx in human sperm. *Nature,* 471**,** 382-386.

SUAREZ, S. S. 2008. Control of hyperactivation in sperm. *Human Reproduction Update,* 14**,** 647-657.

SUAREZ, S. S. & PACEY, A. A. 2006. Sperm transport in the female reproductive tract. *Human Reproduction Update,* 12**,** 23-37.

SUGIYAMA, H. & CHANDLER, D. E. 2014. Sperm guidance to the egg finds calcium at the helm. *Protoplasma,* 251**,** 461-75.

SUMIGAMA, S., MANSELL, S., MILLER, M., LISHKO, P. V., CHERR, G. N., MEYERS, S. A. & TOLLNER, T. 2015. Progesterone accelerates the completion of sperm capacitation and activates CatSper channel in spermatozoa from the rhesus macaque. *Biology of Reproduction,* 93(6):130, 1-11.

SUTOVSKY, P. M., G. 2006. Mammalian spermatogenesis and sperm structure anatomical and compartmental analysis. *In:* De Jonge, C. J. B., C. L. R. (ed.) *The sperm cell: Production, Maturation, Fertilization, Regeneration.* pp 1-30. UK: Cambrigde University Press.

TAMBURRINO, L., MARCHIANI, S., MINETTI, F., FORTI, G., MURATORI, M. & BALDI, E. 2014. The CatSper calcium channel in human sperm: relation with motility and involvement in progesterone-induced acrosome reaction. *Human Reproduction*, 29(3), 418-428.

TAMBURRINO, L., MARCHIANI, S., VICINI, E., MUCIACCIA, B., CAMBI, M., PELLEGRINI, S., FORTI, G., MURATORI, M. & BALDI, E. 2015. Quantification of CatSper1 expression in human spermatozoa and relation to functional parameters. *Human Reproduction*, 30(7), 1532-1544.

TANAKA, Y. & TASHJIAN, A. H. 1994. Thimerosal potentiates Ca2+ release mediated by both the inositol 1,4,5-trisphosphate and the ryanodine receptors in sea urchin eggs. Implications for mechanistic studies on Ca2+ signaling. *Journal of Biological Chemistry*, 269**,** 11247-11253.

TANG, Q.-Y., ZHANG, Z., XIA, X.-M. & LINGLE, C. J. 2010. Block of mouse Slo1 and Slo3 K+ channels by CTX, IbTX, TEA, 4-AP and quinidine. *Channels*, 4**,** 22-41.

TATENO, H., KRAPF, D., HINO, T., SÁNCHEZ-CÁRDENAS, C., DARSZON, A., YANAGIMACHI, R. & VISCONTI, P. E. 2013. Ca2+ ionophore A23187 can make mouse spermatozoa capable of fertilizing in vitro without activation of cAMP-dependent phosphorylation pathways. *Proceedings of the National Academy of Sciences*, 110**,** 18543-18548.

TAVARES, R. S., MANSELL, S., BARRATT, C. L. R., WILSON, S. M., PUBLICOVER, S. J. & RAMALHO-SANTOS, J. 2013. p,p′-DDE activates CatSper and

compromises human sperm function at environmentally relevant concentrations. *Human Reproduction,* 28**,** 3167-3177.

TEVES, M. E., BARBANO, F., GUIDOBALDI, H. A., SANCHEZ, R., MISKA, W. & GIOJALAS, L. C. 2006. Progesterone at the picomolar range is a chemoattractant for mammalian spermatozoa. *Fertility and Sterility,* 86**,** 745-749.

TEVES, M. E., GUIDOBALDI, H. A., UÑATES, D. R., SANCHEZ, R., MISKA, W., PUBLICOVER, S. J., MORALES GARCIA, A. A. & GIOJALAS, L. C. 2009. Molecular mechanism for human sperm chemotaxis mediated by progesterone. *PLoS ONE,* 4**,** e8211.

TURNER, R. M. 2005. Moving to the beat: a review of mammalian sperm motility regulation. *Reproduction, Fertility and Development,* 18**,** 25-38.

VARNER, D. D. 2015. Odyssey of the spermatozoon. *Asian Journal of Andrology,* 17**,** 522-528.

VISCONTI, P. 2009a. Understanding the molecular basis of sperm capacitation through kinase design. *Proceedings of the National Academy of Sciences of the United States of America,* 106**,** 667 - 668.

VISCONTI, P. E. 2009b. Understanding the molecular basis of sperm capacitation through kinase design. *Proceedings of the National Academy of Sciences,* 106**,** 667-668.

WANG, D., KING, S. M., QUILL, T. A., DOOLITTLE, L. K. & GARBERS, D. L. 2003. A new sperm-specific Na+/H+ Exchanger required for sperm motility and fertility. *Nature Cell Biology,* 5**,** 1117-1122.

WANG, Y., STORENG, R., DALE, P. O., ABYHOLM, T. & TANBO, T. 2001. Effects of follicular fluid and steroid hormones on chemotaxis and motility of human spermatozoa in vitro. *Gynecological Endocrinology,* 15**,** 286-292.

WENNEMUTH, G., BABCOCK, D. F. & HILLE, B. 2003. Calcium clearance mechanisms of mouse sperm. *Journal of General Physiology,* 122**,** 115-128.

WILLIAMS, H. L., MANSELL, S., ALASMARI, W., BROWN, S. G., WILSON, S. M., SUTTON, K. A., MILLER, M. R., LISHKO, P. V., BARRATT, C. L. R., PUBLICOVER, S. J. & MARTINS DA SILVA, S. 2015. Specific loss of CatSper function is sufficient to compromise fertilizing capacity of human spermatozoa. *Human Reproduction*, 30(12),2737-2746.

WOO, A. L., JAMES, P. F. & LINGREL, J. B. 2002. Roles of the Na,K-ATPase α4 isoform and the Na+/H+ exchanger in sperm motility. *Molecular Reproduction and Development,* 62**,** 348-356.

WU, Z. Z., LI, D. P., CHEN, S. R. & PAN, H. L. 2009. Aminopyridines potentiate synaptic and neuromuscular transmission by targeting the voltage-activated calcium channel beta subunit. *Journal of Bioliogical Chemistry*, 284**,** 36453-36461.

XIA, J., REIGADA, D., MITCHELL, C. & REN, D. 2007. CATSPER channel-mediated Ca2+ entry into mouse sperm triggers a tail-to-head propagation. *Biology of Reproduction,* 77**,** 551 - 559.

XIA, J. & REN, D. 2009a. The BSA-induced Ca(2+) influx during sperm capacitation is CATSPER channel-dependent. *Reproductive Biology and Endocrinology,* 7(119), 1-9

XIA, J. & REN, D. 2009b. Egg-coat proteins activate calcium entry into mouse sperm via CATSPER channels. *Biology of Reproduction,* 80**,** 1092 - 1098.

XIE, F., GARCIA, M. A., CARLSON, A. E., SCHUH, S. M., BABCOCK, D. F., JAISWAL, B. S., GOSSEN, J. A., ESPOSITO, G., VAN DUIN, M. & CONTI, M. 2006. Soluble adenylyl cyclase (sAC) is indispensable for sperm function and fertilization. *Developmental Biology,* 296**,** 353-362.

ZHANG, D. & GOPALAKRISHNAN, M. 2005. Sperm ion channels: molecular targets for the next generation of contraceptive medicines? *Journal of Andrology,* 26**,** 643-653.

ZHOU, J., CHEN, L., LI, J., LI, H., HONG, Z., XIE, M., CHEN, S. & YAO, B. 2015. The Semen pH Affects Sperm Motility and Capacitation. *PLOS ONE,* 10**,** e0132974.